Investigation of the mechanism of 4E-BP Caf20 eIF4E-Independent Repression of mRNA Translation

A thesis submitted to the University of Manchester for the degree of Doctor of Philosophy (PhD) in the Faculty of Biology, Medicine and Health

2020

Ebelechukwu C. Nwokoye (Mmeka)

School of Biological Sciences

Division of Molecular and Cellular Systems

List of Contents

Final word count (excluding references and Appendices): 51,792

List of Figures

List of Tables

List of Appendices

List of Abbreviations

3'UTRs	3' untranslated regions
40S	Small ribosome subunits
4E: FLAG	ratio of eIF4E to FLAG
4E-BPs	eIF4E-binding proteins
4E-DEP	eIF4E-Dependent
4E-IND	eIF4E-independent
5'UTR	5' untranslated region
60S	large ribosome subunit
ANOVA	Analysis of variance
A-site	Aminoacyl site
BE	beads elution
BMH	Bismaleimidehexane
bp	base pairs
BRE	Bruno response element
Caf20	Cap Associated Factor 20
cAMP	cyclic adenosine monophosphate
carb	carbenicillin
CIA	cytosolic Fe-S protein assembly
CK2	casein kinase 2
CP	central protuberance
CPE	cytoplasm polyadenylation element
DC	decoding centre
ddH_2O	Double distilled water
DEPC	Diethylpro carbonate
Dhh1	Dead-box RNA helicase
DSS	disuccinimidylsuberate
E. coli	*Escherichia coli*
eEFs	eukaryotic elongation factors
EF-Tu	elongation factor Tu
eIF2.GTP.Met-tRNA$_i$	eIF2-ternary complex
eIF2αP	phosphorylated eIF2α
eIFs	eukaryotic initiation factors
EP	empty vector plasmid
eRFs	eukaryotic release factors
E-site	exit site or tunnel
FLAG tag	Full length Affinity gel tag
FRAP kinase	FKBP-12-rapamycin-associated protein kinase
GAP	GTPase accelerating protein
Gcn2	General control non-depressible 2
Gcn4	General control non-depressible 4
GDF	GDI displacement factor
GDI	GDP dissociation inhibitor
GEF	Guanine nucleotide exchange factor
GO	Gene ontology
HF	High Fidelity
IAM	Iodoacetamide
IP	Immunoprecipitation
IP_{low}	Low salt buffer for immunoprecipitation wash steps
IRESs	Internal ribosome entry sites
KO	knock out
L	Input load
LB	*Luria-Bertani*
LiAc/TE	Lithium Acetate/TE

M	Marker
M^7Gppp	7-methylguanosine
Mad2	Mediator complex 2
MAP	Mitogen-activated protein
MAPK	Mitogen activated protein kinase
MBS	m-maleimidobenzoyl-N-hydroxysuccinimide ester
Met-$tRNA_i$	initiator methionyl tRNA
Mnk1/Mnk2	Mitogen-activated (MAP) kinase signal integrating kinases 1 or 2
MPN	Mpr1, Pad1, amino-terminal
mRNA	messenger RNA
MS	Mass spectrometry
mTOR	Mammalian target of rapamycin
mTORCs	mTOR complexes 1 and 2
NHS	N-hydroxysuccinimide
NTD	N-terminal domain
OD	Optical density
ORF	Open reading frame
P	Pellet
P/M	polysome to monosome ratio
PABP/ Pab1	Poly (A) binding protein
p-bodies	Processing bodies
pCaf20-FLAG	*Caf20-FLAG* plasmid
pCaf20m2-FLAG	*Caf20m2-FLAG* plasmid
PCR	Polymerase chain reaction
PCI	Protosome, COP9 signalosome, eIF3
PE	peptide elute
PEG	polyethylene glycol
PHG	Pseudohyphal growth
pI	isoelectric points
PIC	43S preinitiation complex
PKA	Protein kinase A,
polyA	3'-polyadenine
Post-TCs	Post-termination complexes
PP1	protein phosphatase
PPIase	Peptidylprolyl-cis/trans-isomerase
P-site	Peptidyl site
PSK1/PSK2	PAS Kinase 1/2
PTC	peptidyl-transferase centre
qPCR	quantitative real-time polymerase chain reaction
qRT-PCR	quantitative real-time reverse transcription polymerase chain reaction
RAS	Rat sarcoma,
Ras2/cAMP-PKA	RAS GTPase with cyclic adenosine monophosphate to activate protein kinase A
RIP-Seq	RNA-binding protein immunoprecipitation and next generation sequencing
RNA	Ribonucleic acid
rpm	revolutions per minute
RPs	ribosomal proteins
rRNAs	ribosomal RNAs
RSLC	Rapid Separation Liquid Chromatography
RT-PCR	Reverse transcription polymerase chain reaction
S	Supernatant
S. cerevisiae	*Saccharomyces cerevisiae*
SCD/SCGE	Synthetic complete dextrose or glycerol/ethanol
SD/SGE	synthetic dextrose or glycerol/ethanol
SDM	Site Directed Mutagenesis

SDS PAGE	Sodium dodecyl sulfate polyacrylamide gel electrophoresis
Ser^{51}	Serine residue
SGD	Saccharomyces genome database
SNF	Sucrose nonfermentable
SRPK	SR protein kinase
TAE	Tris/Acetate/EDTA
TAP tag	Tandem Affinity purification tag
TBS	Tris Buffered saline
TBST	Tris buffered Saline Tween
TCA	Trichloroacetic acid
Tcep	Tris (2-carboxyethyl) phosphine
TOR	Target of rapamycin
tRNA	transfer RNA
uORF	upstream ORF
WCE	Whole cell extract
wt	wildtype
YPD/YPGE	Yeast peptone dextrose or glycerol/ethanol
[MYC]	Chromosome integrated Caf20-9MYC tag
[TAP]	Chromosome integrated Caf20-TAP tag
-ve control	Negative control
°	Degree
μ	Micro (prefix)
α	Alpha (prefix subunit)
β	Beta (prefix subunit)
γ	Gamma (subunit)
Δ	Delta (deletion)
δ	Delta (subunit)
ε	Epsilon (subunit)

Abstract

The University of Manchester

Ebelechukwu Cecilia Nwokoye

PhD Molecular Biology

Investigation of the mechanism of 4E-BP Caf20 eIF4E-Independent Repression of mRNA Translation

2020

The translation factor, eIF4F is a complex made up of the eIF4E, eIF4G and eIF4A. The eIF4F is a major determinant in mRNA selection for recruitment of ribosomes for protein synthesis initiation. eIF4E recognises and binds the 5' cap. On actively translating mRNAs, eIF4G associates with eIF4E leading to increased synthesis of the encoded proteins. However, eIF4E-eIF4G interactions are regulated across all eukaryotes by a group of inhibitory binding proteins called the 4E-BPs that can displace eIF4G from eIF4E and repress translation. In yeast, Caf20 and Eap1 are the two 4E-BPs identified that associate with eIF4E and inhibit translation. Prior studies in Graham Pavitt's lab identified a new role for Caf20, whereby it was shown to interact with ribosomes and specific mRNAs independently of its binding to eIF4E. The research presented in this thesis describes an investigation of the elements of Caf20 important of its association with eIF4E, the ribosome and itself; and mechanisms of Caf20 interaction with other proteins.

By a combination of systematic mutagenesis and immunoprecipitation experiments it was shown that Caf20 requires a short motif within its amino terminal region (NTD) to interact with eIF4E. In contrast Caf20 requires multiple elements driven largely by an extended region of the N-terminus to interact with the ribosome. By using a double tagging and immunoprecipitation approach, it was demonstrated that Caf20 interacts with its binding partners as a monomer rather than a homodimer or other higher order complex. *In vivo* crosslinking of whole cell extracts and polysome enriched fractions combined with western blotting identified some specific proteins including a novel approximately 10 KDa Caf20-interacting protein. Mass-spectrometry provided some candidates of which ribosomal proteins, Rps5, Rps24, Rps27, Rpl10, Rpl27 and Rpl30 of the small and large subunits were identified. The crosslinked ribosomal proteins are located around the interface of the 40S and 60S subunits. Results from different phenotypic characterisations for Caf20 indicated that it affects cell growth when there is a switch from glucose medium to respiratory medium, especially at low temperatures (16°C). Caf20 was found not to be a target of the TOR pathway, but Caf20 presence did increase strain sensitivity to clioquinol drug and excess $CuSO_4$ treatments. *CAF20* deletion in three RP-TAP strains was found to have synthetic growth defects when two strains (Rpl27-TAP and Rps27B-TAP) were grown at different temperatures. Mild phenotypes identified in this study all appear to be largely explained by the eIF4E-Caf20 interaction rather than the novel Caf20-ribosome interaction. In summary, this study broadens our understanding of how Caf20 binds to the ribosome.

Keywords: Caf20, 4E-BP, eIF4E, mRNA, Translation initiation, Regulation, ribosome

Declaration

I declare that no portion of the work referred to in the thesis has been submitted in support of an application for another degree or qualification of this or any other university or other institute of learning.

Copyright Statement

Dedicated to my late father, Mr Longinus Chukwujekwu Mmeka

"Though you are far away, I am here living out your dreams"

Acknowledgements

A lot of people have contributed in one way or the other for the successful completion of this PhD studies. I want to first of all acknowledge my supervisor, Prof Graham Pavitt for his great support. I have never had a wonderful supervisor-student relationship like I did in this PhD study. It was more like a father-daughter relationship. I appreciate your patience, encouragement and guidance which helped me to achieve this success. I am very grateful to my spiritual director at Holy Name Catholic Chaplaincy, Jean Marsh, for her counselling and support that kept me balanced both spiritually and mentally to go through the rigors of the PhD journey. I also want to appreciate my advisor, Dr. Anil Day, whose advice at my first year planning meeting set my mind toward what PhD work entails. I am also grateful to my PhD Tutor, Dr. Minsung Kim who facilitated in an immense way to ensure successful completion of my PhD studies. I am indebted to Prof Chris Grant and Prof Mark Ashe for their constructive feedbacks during my lab meetings.

I also want to appreciate all the members of Graham Pavitt's lab especially Chris Kershaw, Martin Jennings, Fidel Peacock and Robert Crawford who helped me during the course of this PhD studies. I am specifically grateful to Robert for his assistance in creating the Gene ontology (GO) classification used in this thesis. I will not forget our lab ladies group – Ateeka, Eemann, Margherita, Priya and Catherina including those who have left, Jennifer Lui, and the Malaysian ladies (Sarah, Hidayah and Fadilah) for their friendship and support.

I am so indebted to my family both nuclear and extended for the support they rendered to me. I am particularly grateful to my mum, for taking care of my daughter from her six months of age, all through the first to third year of my PhD. I am also grateful to my husband who had been my biggest support throughout this PhD journey in both hard and happy times. I cannot quantify the love and support showered on me by my siblings, Chinelo, Tochukwu, Ogochukwu and Ifeoma. I promise to be there for you guys when you need me. I also acknowledge my in-laws for checking on me from time to time. I would not forget my treasure daughter, Mmachukwu Nwokoye for her companionship and keeping us busy outside PhD work.

Finally, I want to thank my sponsors, Tertiary Education Trust Fund (TETFund), Nigeria for sponsoring this PhD and giving me the opportunity to study abroad.

Communications

1. **Ebelechukwu C. Nwokoye** and Graham D. Pavitt. **Insight into eIF4E-independent translational regulation by the yeast 4E-BP Caf20. A poster** presented at Cold Spring Harbor Laboratory Translation Conference, New York, USA, 4th - 8th September, 2018

2. **Ebelechukwu C. Nwokoye** and Graham D. Pavitt. **The role of 4E-BP Caf20 in eIF4E-Independent Translation initiation regulation in yeast.** A poster presented at Translation UK 2018 at the University of Manchester, UK; 5th -6th July, 2018.

3. **Ebelechukwu C. Nwokoye** and Graham D. Pavitt. **eIF4E-independent interactions of the yeast 4E-BP Caf20 with translating ribosomes.** Molecular and Cellular Function Postgraduate Showcase, AV Hill Atrium, FBMH, University of Manchester, UK; 22nd Nov. 2017

4. **Ebelechukwu C. Mmeka** and Graham D. Pavitt. **eIF4E-Independent interactions of the yeast Caf20 with translating ribosome.** A poster presented at Translation UK Conference, University of Nottingham, UK. 6th-7th July, 2017.

5. **Ebelechukwu C. Mmeka** and Graham D. Pavitt. **Investigating eIF4E-independent Translation repression by yeast 4E BP Caf20**. A talk presented at the Doctoral Academy PhD Conference, Whitworth Hall, University of Manchester, 16th May, 2017

6. **Ebelechukwu C. Mmeka** and Graham D. Pavitt. **Understanding the Mechanism of eIF4E-Independent Translation repression by yeast 4E BP**. 2nd Year Poster presentation at the School of Biology (SBS) Launch Symposium, Faculty of Biology, Medicine and Health on the 9th Jan, 2017.

7. **Mmeka, Ebelechukwu C**., Peacock Fidel J, Pavitt, Graham D. **Investigating the mechanism of eIF4E-independent translational control by the yeast 4E-BP Caf20.** A Poster presentation at the Translation UK 2016, University of Reading, Surrey. UK. July 2017.

Chapter 1

Introduction

1.1 General introduction

Understanding the exact regulatory mechanisms and signal pathways are very important to our knowledge of the mechanisms of life. The central dogma in molecular biology established that information encoded in the form of nucleotides are used to synthesise messenger RNAs (mRNAs) through the process of transcription and the information on the mRNA used to synthesize proteins in the ribosome through the process of translation. Protein synthesis is the product of ribonucleic acid (RNA) translation mediated through the recruitment of the ribosome to messenger RNA (mRNA) and in the cytoplasm of eukaryotic cells requires at least twelve different eukaryotic initiation factors (eIFs) as well as eukaryotic elongation factors (eEFs) that facilitate synthesis of the polypeptide chain and eukaryotic release factors (eRFs) that recognise a stop codon and facilitate release of the formed polypeptide from the ribosome. During mRNA synthesis, a 7-methylguanosine (M^7Gppp) cap and a poly (A) tail is added to the 5'end and 3' end respectively of the pre-mRNA to protect the mRNA from degradation and enable ribosome attachment during protein translation. The mature mRNA with translatable reading frame is released into the cytoplasm after the introns are removed from the mRNA. Introns are cleaved from the mRNA to protect it from degradation to avoid nonsense codon that leads to incorrect protein or abrupt termination of protein synthesis. Ribosomal RNAs (rRNAs) and transfer RNAs (tRNAs) which are molecular structures that aid in protein synthesis are also produced during transcription. The rRNA are transcribed as 2 long precursor molecules into 4 rRNAs that form a major component of the ribosome. The tRNA on the other hand are transcribed, processed and released into the cytoplasm where they are charged with different amino acids. Each tRNA recognizes and carries one particular amino acid specified by its anticodon. The tRNA interacts with the mRNA through complementary base pairing between the triplet codes, (codon) of the mRNA and the anticodon on the tRNA. A special initiator tRNA, Met-$tRNA_i$ carries an initiator residue, methionine (that has been formylated in case of prokaryotes), recognises the initiation codon (AUG) that marks the beginning of the open reading frame (ORF) on the mRNA and initiates the start of polypeptide chain formation in the ribosome.

The introduction covers an overview of the current view of the ribosome, mechanism of protein synthesis initiation and its regulatory mechanisms and then reviews interesting regulatory evidences of 4E-BP Caf20 leading to this study.

1.2. The eukaryotic ribosome structure

Ribosomes are special non-membrane-bound organelles, complex in nature and function in translating information encoded on the mRNAs into proteins. They are in the cytoplasm or peripheral to the endoplasmic reticulum. All ribosomes are made up of two subunits called large and small which dissociates when the ribosome is not synthesizing protein and rejoins during translation. Each subunit is comprised of dedicated ribosomal proteins and rRNAs. The rRNAs have sequence complementarity to regions of mRNA with which it can associate with. The mRNA binds at the cleft situated between the head and the body of the small subunit (Fig 1.1A). The ribosome has three binding sites for tRNA: the acceptor or A-site is responsible to accept the approaching aminoacyl tRNA which must be matched to the mRNA sequence in the decoding centre (DC) (Fig 1.1A), the peptidyl-transferase or P-site holds the peptidyl-tRNA attached to the forming polypeptide chain. This contains the peptidyl-transferase centre (PTC) where peptide bonds are formed between the amino acids linked to the A-site and P-site bound tRNAs. Peptide bond formation transfers the growing chain to the A-site tRNA, while the deacylated tRNA in the P site can subsequently move to the adjacent exit or E-site (Fig 1.1A and B) before it is released from the ribosome. The growing polypeptide chain exits through a dedicated tunnel in the large subunit (Schmeing and Ramakrishnan, 2009). The crystal structures of the ribosome has been studied widely in the prokaryotes and eukaryotes and comparisons of both organisms has been deciphered in relation to translation initiation, termination and regulation (Ben-Shem et al., 2011; Ben-Shem et al., 2010; Jenner et al., 2012; Passmore et al., 2007; Schmeing and Ramakrishnan, 2009).

Eukaryotic ribosome has a sedimentation coefficient of 80S and with a minimal of ~3.3 MD (yeast and plant), is roughly 40% larger than its bacterial counterpart (70S) (Ben-Shem et al., 2010). The eukaryotic large ribosome subunit, 60S, consists of 3 ribosomal RNAs (rRNAs): 5S, 5.8S and 25S and 46 proteins. The small subunit (40S) has only one rRNA (18S) and contains 33 proteins (**Fig 1.1**). The human 80S ribosome proteins are very similar to that of the yeast, but some of the rRNA expansion segments (ES) differ such that human ribosomes are larger than those of yeast. Each ribosome has a single copy of each specific protein except for the P-stalk proteins that function to assist in binding translation elongation factors. A ‘ratchetlike’ movement in the ribosome subunits facilitates movement or translocation of the ribosome along the

mRNA by one codon at a time. Viewing the *Saccharomyces cerevisiae* 80S ribosome at 4.15 Å, Ben-Shem et al. (2010) reported that the 60S moves in a clockwise rotation at angle 15.5° to the tRNA while the 40S head moves at 4° -5° in an anticlockwise direction when compared with the 'non-ratchetlike' prokaryote ribosome (**Fig 1.1C** and **D**). Upon ratcheting, there are structural alterations observed within the protuberance 5S rRNA and the functional protein bridge sites such as the bridge B2a formed from the helix, h44 of the 18S and H69 of the 25S rRNA. This results in conformational changes between the head and mRNA-tRNA complex that creates a steric block between the P-site and E-site.

The mRNA entry and exit tunnel differ from that of prokaryotes in respect of how they interact with the mRNA and initiation factors on the 40S ribosome (**Fig 1.1E and F**). The entry tunnel shows an open conformation that moves further from the body without rRNA-protein interaction unlike in prokaryotes with closed helix (h16) and presence of rRNA protein interaction between the h16 and ribosomal proteins S3, S4 and S5 (Ben-Shem et al., 2010). The binding of the eIF1 and eIF1A to the 40S subunit induces the h16 to adopt a closed orientation and facilitate the scanning process as well sustain the open state of the entry site of the mRNA (Passmore et al., 2007). The exit site or tunnel (E-site) of the mRNA is more complex when compared with the prokaryotes, there is an interaction between the E-site, S5 and S28e. ES7of the 18S rRNA forms part of the mRNA exit channel (**Fig 1.1E-I**). Also, there is a strong interaction between the entry and exit channels of the mRNA maintained by S0-S2 protein interactions (Ben-Shem et al., 2010).

Advancement in the crystal structure resolutions of the ribosome has revealed the complexities in the expansion segments of rRNAs and addition of more protein moieties. Upon further improvement in resolution and observation of the eukaryotic yeast ribosome at 3.0 Å (40S ratcheting at 9° and the 60S rotating at 10.5°) (**Fig 1.1E-I**), Ben-Shem et al. (2011) identified extra elements of the rRNA expansion segments (ES) and almost all the ribosomal proteins including Stm1. The concentrations of which the concentrations and densities of the elements at the L1 stalk, P-stalk and the surroundings of the central protuberance (CP) were reported as well as more proteins bridges (helices), eB12 and eB13 of L19e and L24e respectively which were interacting with the small ribosome (40S) at the solvent sides (**Fig 1.1E-I**). A new nomenclature was proposed for naming the ribosome proteins in bacteria, archaea and eukaryotes (Jenner et al., 2012).

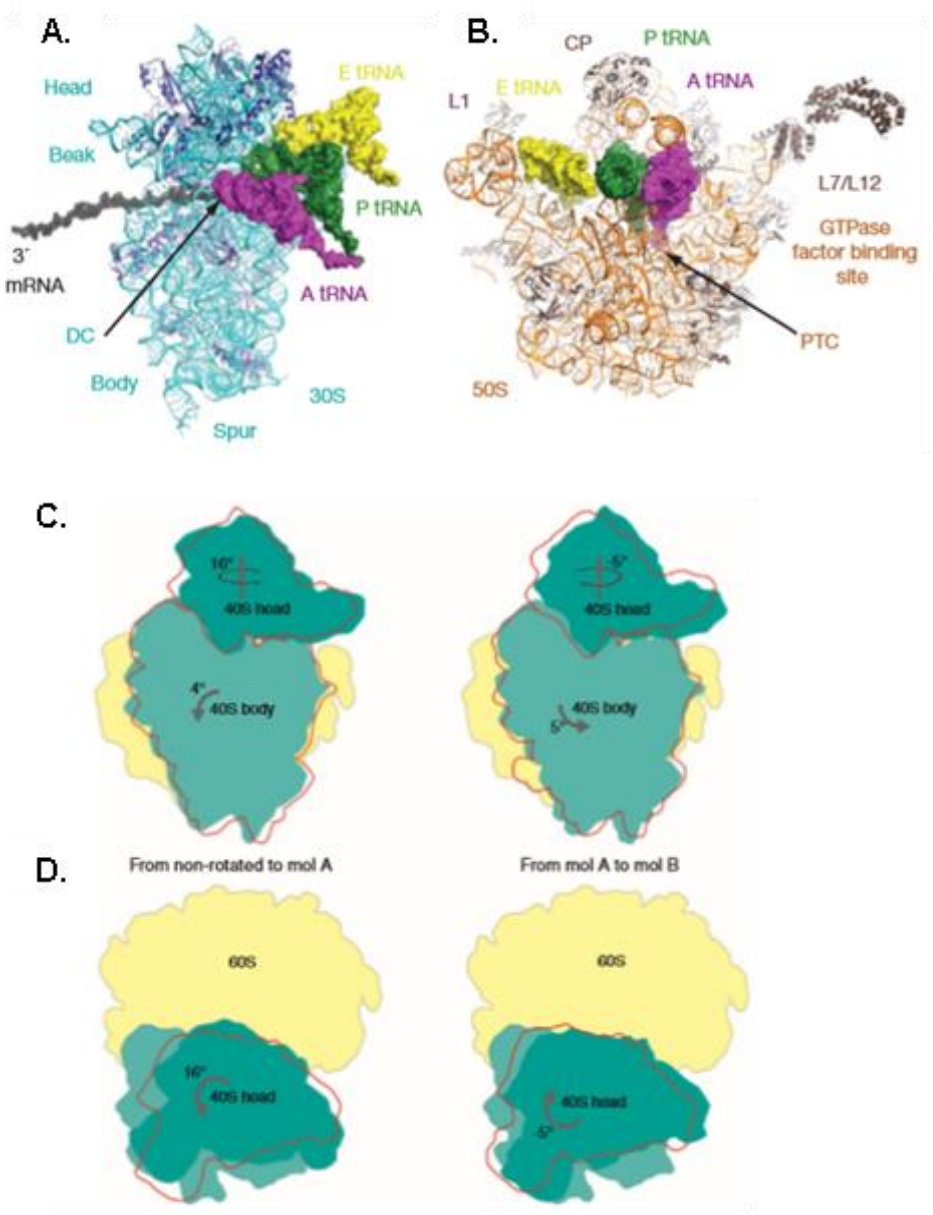
A.
Head
Beak
E tRNA
P tRNA
A tRNA
3'
mRNA
DC
Body
30S
Spur
B.
CP
P tRNA
L1
E tRNA
A tRNA
L7/L12
GTPase
factor binding
site
PTC
50S
C.
16°
40S head
4°
40S body
5°
40S head
5°
40S body
From non-rotated to mol A
From mol A to mol B
D.
60S
16°
40S head
60S
-5°
40S head

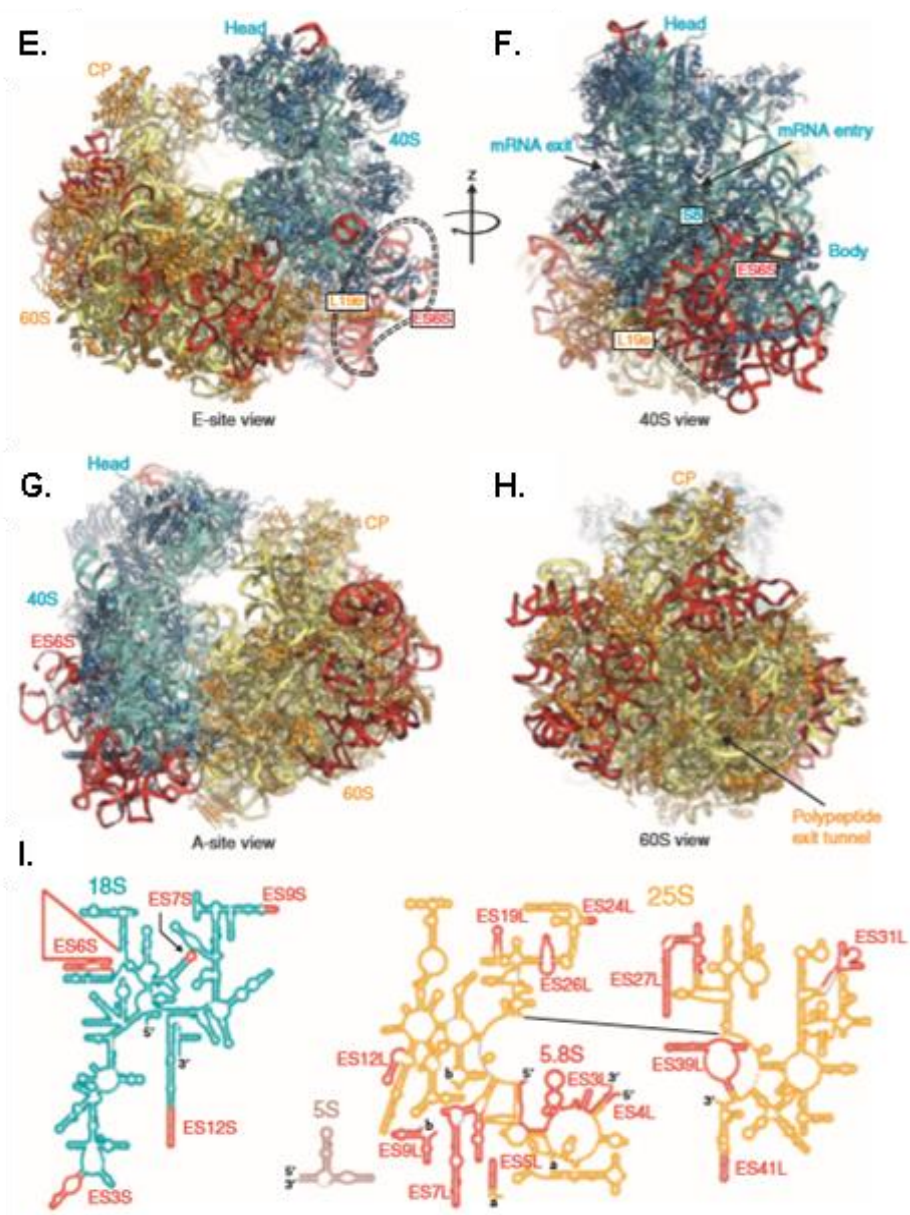
E.
Head
CP
40S
60S
E-site view
F.
Head
mRNA exit
mRNA entry
Body
40S view
G.
Head
CP
40S
ES6S
60S
A-site view
H.
CP
Polypeptide
exit tunnel
60S view
I.
18S
ES7S
ES9S
ES6S
ES12S
ES3S
25S
ES19L
ES24L
ES31L
ES26L
ES27L
ES12L
5.8S
ES39L
ES3L
ES4L
5S
ES9L
ES5L
ES7L
ES41L

Figure 1.1 Architecture of the ribosome. A-B. View of 30S and 50S subunits of prokaryote with mRNA and A-P-E-site tRNAs. The structure of the L7/L12 arm is visible. **C-D**. Swivelling states of the 80S ribosome. Typical representation of rotation in two resolutions (4.15 Å and 3.0 Å) from non-ratcheting state to molecule A and from molecule A to molecule B. view from the solvent side of 40S (**C**) and from the top of the 80S (**D**). The arrow indicates the movement route. **E**-**H**. Views from the E-site, small subunit side, A-site and large subunit side of crystal structure of the *S. cerevisiae* 80S ribosome**. F**, **G** and **H** were twisted 908, 1808 and 2708 around the z-axis with respect to **E**. mRNA entry and exit tunnels and polypeptide exit tunnel are indicated. The 40S subunit is represented in cyan with blue proteins and the 60S subunit in yellow with orange proteins. The eukaryote expansion segments (ES) are shown in red. Visibly, most of the ES are located on the surface of the ribosome dense into two clusters. **I.** secondary structure image of 18S rRNA in blue, 5S rRNA in brown, 5.8rRNA in dark red and 25S rRNA in yellow with their ES. Adapted from Protein Data Bank's crystal structures for 4V7R and 4V88 (Ben-Shem et al., 2011; Ben-Shem et al., 2010; Jenner et al., 2012; Schmeing and Ramakrishnan, 2009).

1.2.1 mRNA-specific regulation - Specialization in ribosomes and gene expression regulation.

More evidences have shown that ribosomes are not homogenous but rather heterogeneous in nature in respect to their structural and functional features between ribosomes isolated from the same population (Crawford and Pavitt, 2019; Mauro and Edelman, 2007). The ribosome complexity can be seen through its association of sub-stoichiometric RNA-binding proteins to promote interactions with specific mRNA. This in turn interacts with different protein that bind with the polysomes and monosome complexes (Crawford and Pavitt, 2019). Protein-protein interactions are maintained in the ribosome by a scaffolding WD40 domain contained in the Asc1 of the small subunit. WD40 domain is widespread in eukaryotes and through this domain, Asc1 interacts with eIFs such as eIF3 contributing to the formation of pre-initiation complexes (des Georges et al., 2015). The domain can bind the polysomes and with a variety of other proteins such as Scp160, Sro9, Gis2, etc. (Opitz et al., 2017). Each of the RNA-binding protein leads the ribosomes to translate a specific set of mRNAs, crating diversity in ribosome composition and function. Under nutrient-rich conditions, Asc1 is required for efficient translation of highly translated short open reading frame (ORF) (Thompson et al., 2016).

Ribosomes are heterogeneous macromolecular structures. Many of the yeast ribosomal proteins are encoded by two paralogous genes (isoforms) (Planta and Mager, 1998), as a result of genome duplications enabling ribosomes to differ in their core subunit composition as well as in association of peripheral RNA-binding proteins. Differences in the expression, localisation and function of these paralogous ribosomal

proteins is been documented for the past 25 years and recent evidence of structural differences between ribosomes has only begun to emerge due to improved mass spectrometry analysis (review in (Crawford and Pavitt, 2019)).. More evidence of stoichiometric differences between eukaryotic ribosomal proteins has been reported (Shi et al., 2017) which faults previous works that portrayed ribosomes as having a uniform or homogeneous conformation (Ben-Shem et al., 2011; Ben-Shem et al., 2010). Paralogues of many core ribosomal proteins and rRNAs may show differences in stoichiometry when modified by addition of methyl or phosphoryl groups. Though there are no much of specialized ribosomes in the cells as majority are undistinguishable, those that become specialised are important in responses to environmental stress.

Yeast genome was duplicated over 2 million years ago which brought about loss of gene or modifications in the duplicated gene. 59 out of the 80 ribosomal proteins exists in paralogue pair and are expressed as 'a' and 'b' forms of paralogous genes (Planta and Mager, 1998). Though most of these paralogous pairs vary by one or a few amino acids, the continual co-existence of both pairs in the cell shows differences in function and expression at different levels (Kulak et al., 2014). Recent studies showed a more complex relationship between paralogous pairs. A study of Rps27a and Rps27b found that cell lacking Rps27a exhibit ribosomal assembly defects and deficiencies in rRNA processing despite growing at the wildtype rate, demonstrating that growth rate does not really reflect functionality (Baudin-Baillieu et al., 1997). High-throughput screens have suggested more subtle differences between duplicated ribosomal protein genes, including specific defects in sporulation, actin organisation and bud-site selection (Komili et al., 2007). A well-researched functional specificity of duplicated ribosome paralogs is the yeast protein Ash1. The Ash1 localizes specifically to the daughter cell where it acts to suppress matting-type switching during cell division. Protein localization is obtained by *ASH1* mRNA localization through a well-characterized translation and translation regulation. Studies have shown that mutation in *ASH1* mRNA that disrupt its translation hinder bud-tip anchoring, as does inhibition of translation resulting in a mislocalization of mRNA throughout the emerging daughter cell (Irie et al., 2002). Loc1 (a nuclear protein) and Puf6 (a member of pumilio family) are part of the factors required for the localization of *ASH1* mRNA and in ribosomal assembly (Harnpicharnchai et al., 2001; Nissan et al., 2002) as well as translational repression of *ASH1* mRNA (Gu et al., 2004; Komili et al., 2007). Another study revealed that paralogous specific effects of some duplicated ribosomal proteins and transcriptional

and phenotypic profiling which shows differences between the specific functional roles of paralogous ribosomes beyond effects on mRNA localization indicating complex specialization of ribosomal proteins for specific cellular process. Another similar study revealed specialisation in paralogous ribosomal proteins Rpl8a and Rpl8b to stress hen the carbon source was changed from glucose to glycerol. Genetic analysis to support the evidence revealed divergent function for the paralogous pair as the pair can complement each other during growth on glucose but not glycerol (Sun et al., 2018).

In addition to specialisation of paralogous pair, some ribosomal proteins are non-essential for normal ribosome function but their deletion can specialize ribosome to translate certain mRNA substrates. Heterogeneous ribosomes can be generated through removal of subunits which differs in application to addition of RNA-binding proteins to achieve a similar goal, but seems to be important for translational control in changing conditions (Briggs and Dinman, 2017; Crawford and Pavitt, 2019). There are also differential stoichiometry among core ribosomal proteins. Polysome profiling in combination with mass spectrometry has demonstrated that the relative amounts of different ribosomal proteins vary across the ribosome fractions (monosomes and polysomes) in yeast and mammalian cells. These polysome profile ratios can also vary based on the stress applied to the cells (Slavov et al., 2015). Similar work in mammalian cells revealed differential stoichiometry among uL1, eL38 and eS25 in the polysomes with heavily translated mRNAs (Shi et al., 2017). Some of these ribosomal proteins associate with certain subset of mRNA, uL1are enriched for association for transcripts with extracellular matrix organisation as well as alcohol metabolic and other functions; eS25 are highly enriched in transcripts with cell cycle, vesicle-mediated transport and organelle fission functions (Shi et al., 2017). Direct interactions of these ribosomal proteins with mRNAs may be responsible for such effects, as both uL1 and eS25 bind are needed for IRES-mediated translation (review from (Crawford and Pavitt, 2019)).

Apart from sub-stoichiometric association of ribosomal proteins, modification in rRNAs are important for IRES-mediated translation. Changes in rRNA pseudouridylation results in a specific defect in the translation of some IRES-containing mRNAs. In mammals like mice that are hypomorphic for dyskerin (which is an enzyme that converts rRNA uridine to pseudouridine), general cap-dependent translation is not impaired. However, translation of IRES-containing mRNAs including the tumour suppressors, p27 and p58 is altered (Bellodi et al., 2010a; Bellodi et al., 2010b; Montanaro et al., 2010). As a result, these mice have a higher chance to develop cancer.

Importantly, ribosomes that lack pseudouridine modifications show a direct deficiency in binding to IRES elements (Jack et al., 2011; Xue and Barna, 2012). All these evidences of specialized ribosomes and gene expression regulation support the existence of a ribosome code. .

1.3 Protein initiation synthesis in eukaryotic cells.

Protein synthesis is a cyclical event and a dynamic process of mRNA translation involving the ribosome in conjunction with the eIF2.GTP.Met-tRNAi ternary complex being recruited to the mRNA and requires at least eleven different eIFs as well as elongation factors (eEFs) and amino-acylated tRNAs that facilitate synthesis of the polypeptide chain, followed by the release factors (eRFs) that recognise a stop codon and facilitate release of the formed polypeptide from the ribosome (Jackson et al., 2010). An active dividing haploid yeast cell growing in a rich medium has around 200,000 ribosomes and synthesizes up to 13,000 proteins per second (von der Haar, 2008). The rate of synthesis of each protein being dependent on the abundance of mRNA transcripts and the efficiency of ribosome recruitment, AUG recognition and the rate of elongation along its ORF (Blank et al., 2017). Because the mechanism of translation initiation is most relevant to the topic of this thesis, this is discussed in the stages outlined below. Some of the translation factors and their functions are shown in **Table 1.1** and the scheme is outlined in **Figure 1.2.**

1.3.1 Formation of 43S complex

The translation initiation phase begins following the recycling of the post-termination complexes (Post-TCs). The Post-TC is made up of the 80S competent ribosome, the bound mRNA and termination anticodon tRNA bound at the peptidyl site (P-site) and an eRF1. Under low concentrations of Mg^{2+}, eIF3 detaches from the 80S ribosome and in conjunction with the eIF1 and eIF1A dissociates the ribosomes into its component free large (60S) and small (40S) ribosome subunits. The eIF3, eIF1 and eIF1A immediately bind to the 40S ribosome after recycling to prevent premature re-joining of the 60S subunit, see step **1** of **Fig 1.2** (Jackson *et al.*, 2010). eIF6 is another protein that can help to prevent re-association of ribosome subunits (Klinge *et al.*, 2011).

Following the dissociation of ribosome into component 40S and 60S subunits, the second step in the translation initiation process is the eukaryotic initiation factor 2

(eIF2)-ternary complex formation. The eIF2-ternary complex is made up of eIF2.GTP with the initiator tRNA (eIF2.GTP.Met-tRNA$_i$). The eIF2 is a G-protein that delivers initiator-methionyl tRNA, (Met-tRNA$_i$) to the P-site of the ribosome with bound GTP (Dever et al., 2016; Hinnebusch and Lorsch, 2012; Jackson et al., 2010). The eIF2.GTP complex is not stable until it is bound by tRNA charged with an amino acid, Met (Met-tRNA$_i^{Met}$) to form a ternary complex (Dever et al., 2016; Pavitt and Proud, 2009). Its G-protein cycle is regulated by two proteins, eIF5 and eIF2B. eIF5 functions as both GTPase accelerating protein (GAP) and GDP dissociation inhibitor (GDI) by limiting the amount of GDP released in order to prevent spontaneous nucleotide exchange by eIF2B and also maintain eIF2 in its inactive form (Jennings and Pavitt, 2010a, b). eIF2B on the other hand, is a decameric guanine nucleotide exchange factor (GEF) that catalyses the substitution of GDP for GTP and has been reported to have two copies each of 5 subunits (α, β, γ, δ, ε) (Gordiyenko et al., 2014; Jackson et al., 2010; Kashiwagi et al., 2016; Pavitt and Proud, 2009; Wortham et al., 2014). It has been shown that eIF2B serves as GDF (GDI displacement factor) by recruiting eIF2 from eIF2.GDP/eIF5 complexes before the GEF activity and that eIF2B binds to the eIF2.GDP through its γ subunit (Jennings and Pavitt, 2014; Jennings *et al.*, 2013). The crystal structure of the eIF2B of *S. pombe* shows a core (comprising a pair of each α, β, and δ subunits) with two γ catalytic arm domains on top and ε subunits at the bottom of each arm (Kashiwagi et al., 2016). Also the structures of eIF2/eIF2B complexes have been elucidated (Adomavicius et al., 2019). The eIF2.GTP.Met-tRNA$_i$ and eIF5 are recruited together to the ribosome (Jennings et al., 2017). The joining of the eIF2.GTP.Met-tRNA$_i$/eIF5 to the 40S ribosome alongside with the eIFs 1, 1A and 3 constitute the 43S complex that is required for optimum fidelity in the start codon selection (See step **2** and **7** of **Fig 1.2**).

Some molecular structural architecture has been proposed for the 43S complex. The 40S subunit consists of a head, a platform and a body, with the mRNA-binding channel wrapping around the neck (Schuler *et al.*, 2006) and the 5-lobed eIF3 is placed by the side facing the solvent (des Georges et al., 2015; Hinnebusch, 2006; Llacer et al., 2015; Siridechadilok et al., 2005). The proteasome, COP9 signalosome, eIF3 and Mpr1, Pad1, amino-terminal (PCI/MPN) subunits function as backbone with direct interactions with eIF1 (Aylett et al., 2015) and eIF4G (at eIF3c, d and e subunits) (LeFebvre et al., 2006; Villa et al., 2013). Within the 43S complex the Met-tRNA$_i^{Met}$ was shown to be deeply inserted into the P-site of the 40S (des Georges et al., 2015; Llacer et al., 2015). The eIF1 binds to the interface between the Met-tRNA$_i^{Met}$ and the platform (Lomakin

et al., 2003). eIF1A structural binding domain resides inside the aminoacyl site (A-site) forming a link over the mRNA channel, whereas its N- and C-terminal tails lengthens into the P-site (Yu *et al.,* 2009). The binding of eIF1 and eIF1A to the ribosome causes a conformational change by opening the mRNA entrance point between the body and the head and hence the formation of a new head-body connection on the solvent side between the entrance (Hussain et al., 2014; Passmore et al., 2007).

eIF4F is proposed to bind on the solvent side of the 43S complex, maybe between the PCI/MPN core and the eIF3b-eIF3i-eIF3g module (des Georges et al., 2015). The eIF3b-eIF3i-eIF3g module is implicated to be involved in scanning (Chiu et al., 2010; Cuchalova et al., 2010; des Georges et al., 2015; Elantak et al., 2010) and also facilitate mRNA entry into the ribosome and its positioning during the scanning process (des Georges et al., 2015)

1.3.2 Messenger RNA selection and attachment of 43S complex

Majority of 5’ capped mRNA are efficiently translated because their start codons are situated in a favourable context and have reduced amount of secondary structures (De Benedetti and Harris, 1999). The 5' UTR of the mRNA may possess secondary structure that can impede the attachment of 43S complex. Structure is dissolved through the help of eIF4F and eIF4B which unwinds the 5' cap-proximal end region of mRNA and prepares it for attachment of the ribosome. The eIF4F comprises three subunits: the eIF4E, a 24 KDa protein with a concave surface that binds the 5' cap, eIF4A (a DEAD-box RNA helicase) and eIF4G, a scaffolding factor of that binds eIF4E, eIF4A, poly (A)-binding protein (PABP) and eIF3 (Jackson et al., 2010; Pestova et al., 2007). A part of the eIF4G engulfs the N-terminal region of the eIF4E inducing a structural change that increases eIF4E's affinity for the cap (Gross et al., 2003; von der Haar et al., 2004). The eIF4B and Ded1 promotes the helicase activity of the eIF4A by preventing mRNA re-annealing and promoting one directional movement of the eIF4A (Gupta et al., 2018; Marintchev et al., 2009). The 4A anchors itself on the 5' end cap to resume mRNA unwinding in every progressive cycle therefore keeping the 5' region ever ready for translation (LeFebvre et al., 2006). The eIF1 and eIF1A induces the open latch conformation for the attachment of the 43S complex (Jackson et al., 2010; Passmore et al., 2007). The recruitment of the 43S complex to the mRNA is achieved through mRNA 5’ cap-eIF4E-eIF4G-eIF3 interactions for all nuclear encoded mRNAs. This constitute the 48S preinitiation complex (PIC) (steps **3, 4, 8** of **Fig 1.2**).

1.3.3 Ribosome scanning of mRNA 5'UTR and recognition of initiation Codon

After the attachment of the 43S complex to the mRNA, the mRNA 5'UTR unwinds allowing the 43S complex to scan every nucleotide of the mRNA downstream of the cap to the initiation codon via codon/anticodon interaction (step **5** of **Fig 1.2)** between the AUG of the mRNA and the anticodon of the Met-tRNA$_i^{Met}$ (Cigan *et al.*, 1988; Jackson *et al.*, 2010; Kozak, 1993, 1995). The scanning requires ATP whose amount is dependent on the degree of secondary structures of the mRNA 5' (Jackson, 1991; Svitkin *et al.*, 2001).

To ensure fidelity in the selection of initiation codon, the AUG must be in the optimum context of - GCC(A/G)CC**AUG**G, (with a purine at the -3 and a G at +4 position relative to the A of the AUG codon) (Kozak, 1991). eIF1 helps in maintaining this by preventing the selection of non-AUG triplets or AUG codons with poor context (Pestova et al., 1998). In yeast cells, eIF1 has been implicated to be the major determinant in AUG context selection (Donahue, 2000). The joining of the 48S complexes with the AUG codon at the P-site shows the beginning of the ORF on the mRNA. The commitment of ribosome to the initiation codon is facilitated by eIF5, an eIF2-specific GAP (discussed in section 1.3.1 above). The eIF5 binds to the eIF2's β and γ subunits to induce the GTPase activity of eIF2's β–subunit (Algire et al., 2005; Paulin et al., 2001). eIF1 also helps to prevent premature hydrolysis of eIF2-bound GTP. The pairing of mRNA AUG codon-tRNA anticodon base pairing results in the displacement of eIF1 (Maag et al., 2005). Hydrolysis of GTP reduces the eIF2-ternary complex by lowering eIF2 affinity for Met-tRNA$_i^{met}$ and eIF2-GDP/eIF5 complexes are released from the ribosome before the eIF2B recycles the eIF2 (step **7** of **Fig 1.2**) for the next round of initiation (Pestova *et al.*, 2007).

1.3.4 Ribosomal subunit joining

eIF5B is a ribosome-dependent GTPase that helps the joining of 60S subunits (step **6**, **Fig 1.2**) together with eIF1A to the 48S subunits to form the 80S elongation-competent ribosome (Pestova *et al*., 2000). eIF5B's hydrolysis of GTP enables its release from the assembled 80S competent ribosome. The eIF5B has the ability to partially displace eIF2-GDP from 40S subunit. eIF1A persists longer and interacts with eIF5B on the 40S and is required during the joining of the 60S ribosome and in subsequent GTP hydrolysis of

eIF5B to GDP +Pi and fully displaced in the presence of 60S subunit. eIF1A is released alongside with the eIF5B (Acker *et al.*, 2006; Acker *et al*., 2009).

Different translation factors recruited during protein synthesis must be present to initiate translation in eukaryotes. Some other initiation factors such as eIF2A, eIF2D and eIF6 have been identified (Table 1). For example eIF2D in the absence of GTP promotes tRNA binding to the P-site (Dmitriev *et al*., 2010). eIF5A is a translation factor essential in elongation process by preventing ribosome stalling during the synthesis of subset of nascent proteins including those with long stretches of proline (Doerfel *et al*., 2013). A group of some mRNAs (about 5-10% of total) do not depend on 5' M^7Gppp (7-methylguanosine) cap to facilitate ribosome binding (Ingolia et al., 2011). They initiate translation by promoting the binding of 40S ribosomes to a conserved internal site known as the internal ribosome entry sites, IRESs (**Fig 1.2**). These are common among viruses, including the picornavirus family (Pestova *et al*., 1996) and are found in some cellular mRNAs (Jackson, 2013).

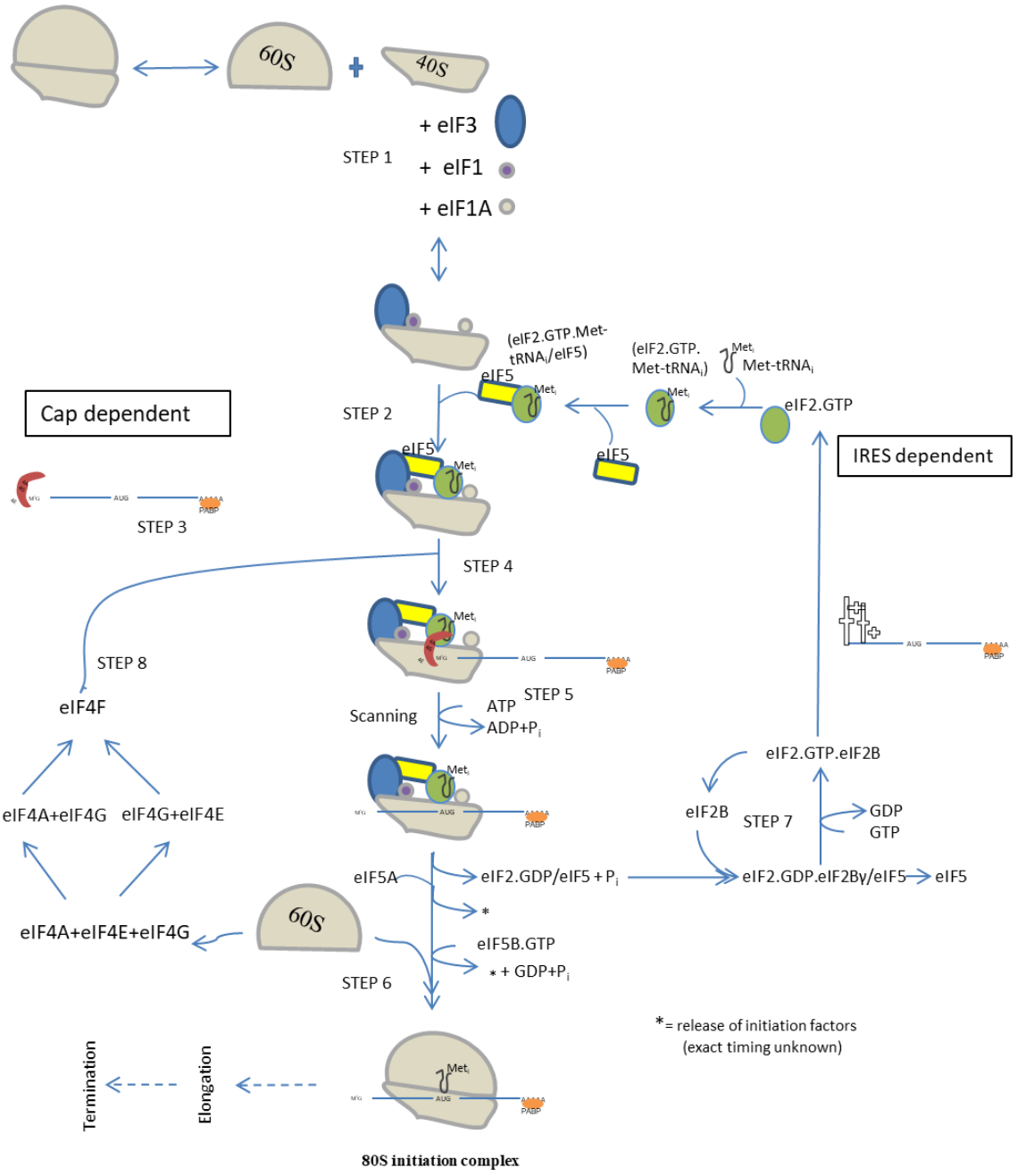

Figure 1.2 Pathway of eukaryotic translation. This cartoon diagram of protein synthesis from initiation to termination depicts two possible initiation mechanisms (M^7G-cap-dependent scanning and IRES-dependent internal). The established pathway of eukaryotic initiation shown is grouped into eight steps (1-8). The first step is the recycling if post-termination complexes to yield separated 40S and 60S ribosomal subunits and initiation factors 1, 1A and 3 (**1**); formation 43S preinitiation complexes by joining of eIF2 ternary complex (**2**); mRNA activation through unwinding of the mRNA cap region by eIF4F and eIF4B (**3**); attachment of 43S preinitiation complexes to the mRNA (**4**); scanning of the mRNA cap from 5'-3' by the 43S complexes, establishment of initiation codon-anticodon pairing and formation of 48S preinitiation complexes (**5**); partial displacement of eIF1and hydrolysis of eIF2- bound GTP by eIF5 and joining of 60S ribosomal subunit to 48S complexes to form elongation-competent 80S initiation complex and alongside displacement of eIF2-GDP and other factors (eIF1, eIF3, eIF4F, eIF5) by eIF5B (**6**); recycling of eIF2 by eIF2B (**7**); recycling of eIF4F (**8**). Also shown are how the ribosomes, methionyl-tRNA, mRNA and ATP/GTP interact; how the initiation factors interact; scanning in cap-dependent binding; not

shown are the detailed illustration of IRES-directed scanning and translation factors for elongation and termination. Adapted from Jackson *et al* (2010); Merrick (2010); Hershey *et al* (2012); Llacer *et al* (2015); des Georges *et al* (2015)

Table 1.1 Different initiation, elongation and release factors and other proteins important in the translation process

Factor	Importance	No of subunits	Source
eIF1	Ensure the right selection of initiation codon; promotes the competent scanning activity, the attachment of the eIF2-GTP-Met-tRNA$^{met}_{i}$ ternary complex to the 40S ribosome and prevent premature hydrolysis of the eIF2-GTP by the eIF5.	1	Jackson et al. (2010)
eIF1A	Promote the binding of eIF2-GTP-Met-tRNA$^{met}_{i}$ to the 40S ribosome and assist eIF1 in performing its duties.	1	Jackson et al. (2010)
eIF2	A Met-tRNA$^{Met}_{i}$ transporter; forms part of eIF2-GTP-ternary complex and enhance eIF2-GTP-Met-tRNA$^{met}_{i}$ ribosome recruitment	3 (α, β, γ)	Jackson et al. (2010)
eIF2A	Facilitate the binding of tRNA$^{met}_{i}$ to the 40S ribosome subunit.	1	Komar et al. (2005); Ventoso et al. (2006)
eIF2B	A G-protein that promote recycling of eIF2-GDP to eIF2-GTP	5	Hershey et al. (2012); Jackson et al. (2010)
eIF2D	which in absence of GTP promotes tRNA binding to the P-site	1	Dmitriev et al. (2010)
eIF3	Binds to the 40S ribosome, promote the attachment of the eIF2 ternary complex to the 40S ribosome and help in dissociation of the 80S into its subunits.	up to 13	Jackson et al. (2010)
eIF4A	4AI and 4AII isoforms. ATP-dependent RNA helicase that promote translation by unwinding the 5'UTR of the mRNA	1	Jackson et al. (2010)
eIF4B	An RNA-binding protein that binds to the eIF4A and to the mRNA and promote the helicase activity of eIF4A	1	Jackson et al. (2010)
eIF4E	Recognises and binds the m7Gppp cap	1	Richter and Sonenberg (2005); Sonenberg et al. (1978)
eIF4F	This complex recognises the cap and promotes the binding of 43S ribosome to the cap for the scanning process.	3	Gingras et al. (1999b); Sonenberg (1988)
eIF4G	(4GI and 4GII isoforms) Binds to the eIF4E, eIF4A, eIF3, SLIP1 and the PABP; promote the translation of the mRNA and eIF4A helicase activity	1	Jackson et al. (2010)
eIF4H	An RNA binding protein that promotes the unwinding activity of eIF4A and show homolog to a segment of eIF4B.	1	Jackson et al. (2010)
eIF5	A GTPase-activating protein that promote the dissociation of bounded eIF2 TC through hydrolysis of eIF2-GTP to eIF2-GDP	1	Hershey et al. (2012)
eIF5A	Essential in elongation process by preventing ribosome stalling during the synthesis of subset of nascent proteins with long stretches of proline	1	Doerfel et al. (2013)
eIF5B	A ribosome-dependent GTPase that facilitate the binding of the 43S preinitiation complex to the 60S ribosome	1	Jackson et al. (2010)
eIF6	Help to prevent the premature re-association of 60S with 40S subunits	1	Jackson et al. (2010); Klinge et al. (2011)
eEF1	A complex composed of eEF1A, aminoacyl tRNA, and eEF1B complex (comprised eEF1Bα, eEF1Bγ and eEF1Bδ). Binds and delivers aminoacyl tRNA to the growing ribosome through GDP-GTP exchange.	4	Li et al. (2013)
eEF2	Promotes GTP-dependent translocation of the nascent polypeptide chain from A-site to P-site of the ribosome	1	Kaul et al. (2011)

eRF1	Identifies all stop codons and transfer the signal from the mRNA stop codon occupying the A-site of the ribosome to the peptidyl transferase centre, inducing the hydrolysis of peptidyl-tRNA.	1	Inge-Vechtomov et al. (2003)
eRF3	A GTPase that stimulate the release of peptide chain by eRF1 through hydrolysis of GTP in eRF1.eRF3.GTP ternary complex.	1	des Georges et al. (2014)
PABP	Binds directly to the 3' poly A tail of the mRNA, to eIF4G and release factor eRF3; also enhance the binding of eIF4F to the cap.	1	Jackson et al. (2010)
DHX29	A protein that provide helicase activity during scanning	1	Parsyan et al. (2009)
DDX3	Provides helicase activity during scanning process	1	Lai et al. (2008)
Dhh1	Dead-box RNA helicase, a decapping activator	1	Park et al. (2006)

1.4 Regulation of translation initiation

Cells do not express all their encoded genes all of the time. While some genes are redundant or silenced, others which are synthesized and made it to the cytoplasm are subjected to various forms of regulation. Translation initiation is the most widely studied phase of protein synthesis control and offers an effective avenue to manipulate gene expression. Translation efficiencies in all eukaryotic cells are regulated at the step of binding the 43S complexes (40S ribosome and its factors) to the 5' end of the mRNA (Gingras et al., 1999b). This in turn is dependent on the competitive ability of the mRNA concerned forming an initiation complex with the limited pool of free ribosomes available at the time (Tuxworth *et al.*, 2004). As detailed in the scheme in **Fig 1.3**, regulation of translation initiation can be achieved via at least two separate paths (shown in dotted lines); first through the regulation of the activities of eIF2 ternary complexes and secondly at mRNA selection through the 5' mRNA cap complexes; eIF4F (made up of eIF4E, eIF4G, eIF4A) and the poly A binding proteins (Pab1) (Jackson et al., 2010; Mathews et al., 2007; Merrick, 2010).

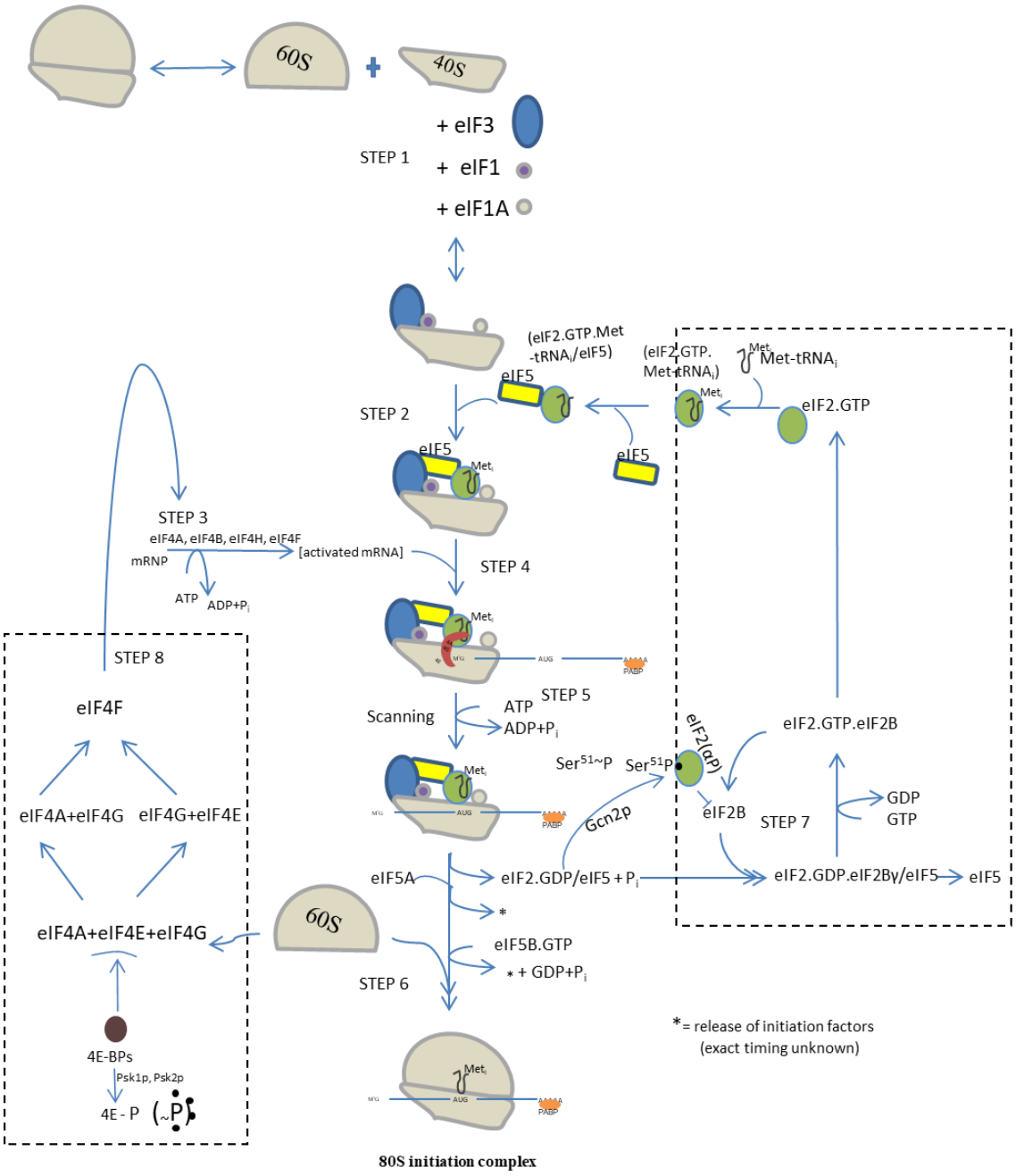

Figure 1.3. Model of the recognized pathway of eukaryotic translation initiation primed with regions of translation initiation control.
The recognized pathway of eukaryotic initiation is divided into eight steps (1-8). Different manipulations in the regulation of translation initiation can be applied along the pathways marked in broken lines. Phosphorylation of αsubunit of the eIF2 (right side) by the Gcn2p Kinase through a conserved Serine residue (Ser^{51}) in the N-terminus of the α subunit. The phosphorylated eIF2 (αP) has a high affinity for eIF2B and regulates its activities. Also on the left, is the regulation by the 4E-BPs whose activities is also being repressed through phosphorylation of conserved residues in the binding motifs. An example from yeast is the phosphorylation by PAS kinase (Psk1p and Psk2p) in sugar flux. Adapted from Merrick (2010); Pavitt and Proud (2009); Jackson *et al*. (2010); Jennings and Pavitt (2014); Rutter *et al*. (2002).

1.4.1 Regulation via eIF2

Translation initiation is controlled by regulating the activity off eIF2. The eIF2-ternary complex (TC) is made up of eIF2.GTP with the initiator tRNA (eIF2.GTP.Met-$tRNA_i$). The amount of the eIF2 ternary complex available for translation initiation is regulated by the eIF2B (with GEF and GDF functions) and eIF5 (with GAP and GDI activities) through the phosphorylation of the eIF2α subunit (**Figure 1.4**). The eIF2.GTP complex is not stable until it is bound by tRNA charged with an amino acid, Met (Met-$tRNA_i^{Met}$) to form a ternary complex (TC) (Dever et al., 2016; Pavitt and Proud, 2009). Met-tRNAi has a ~10 times greater positive interaction affinity for eIF2-GTP over eIF2-GDP (Kapp and Lorsch, 2004). Hydrolysis of eIF2-GTP and Pi release during AUG codon recognition, enables of loss of eIF2-GDP from translation initiating ribosomes (Algire et al., 2005). The eIF2-GDP must be changed to an active eIF2-GTP for continued active translation initiation. Reactivation of eIF2 depends on eIF2B (Pavitt, 2005). eIF2B is a decameric guanine nucleotide exchange factor (GEF) that catalyses the substitution of GDP for GTP and has been reported to have two copies each of 5 subunits (α, β, γ, δ, ε) (Gordiyenko et al., 2014; Jackson et al., 2010; Kashiwagi et al., 2016; Pavitt and Proud, 2009; Wortham et al., 2014). eIF2 colocalizes with eIF2B bodies in yeast (Campbell et al., 2005). It has been shown that eIF2B serves as GDF (GDI displacement factor) by recruiting eIF2 from eIF2.GDP/eIF5 complexes before the GEF activity and that eIF2B binds to the eIF2.GDP through its γ subunit (Jennings and Pavitt, 2014; Jennings *et al.*, 2013). A family of eIF2α kinases when activated are responsible for the phosphorylation of eIF2α subunit at a conserved residue (Ser^{51}) in the N-terminal domain of α subunit. Phosphorylation is typically induced when the cell is subjected to a stress condition (such as amino acid starvation as shown in **Fig 1.4**) (Jennings et al., 2017). The eIF2B and eIF5 can compete in an antagonistic manner to regulate the activities of eIF2. The phosphorylated eIF2α (eIF2αP) has high affinity for eIF2B and blocks eIF2B GEF recycle of eIF2-GDP to eIF2-GTP thereby destabilizing the levels of eIF2-ternary complex formation. The kinase that catalyses the phosphorylation of eIF2α in yeast is the Gcn2 (General control non-depressible 2) (Hinnebusch and Lorsch, 2012; Pavitt and Proud, 2009; Pavitt and Ron, 2012).

eIF5 on the other hand functions as both GTPase accelerating protein (GAP) and GDP dissociation inhibitor (GDI) by limiting the amount of GDP released in order to prevent spontaneous nucleotide exchange by eIF2B and also maintain eIF2 in its inactive form (Jennings and Pavitt, 2010a, b) (**Fig 1.4**). The eIF2.GTP.Met-$tRNA_i$ and

eIF5 are recruited together to the ribosome (Jennings et al., 2017). The joining of the eIF2.GTP.Met-tRNA$_i$/eIF5 to the 40S ribosome alongside with the eIFs 1, 1A and 3 constitute the 43S complex that is required for optimum fidelity in the start codon selection. The eIF2β subunit has also been reported to assist in control the recycling of eIF2 by interacting with eIF5 to prevent untimely release of GDP from the eIF2γ (Jennings et al., 2016).

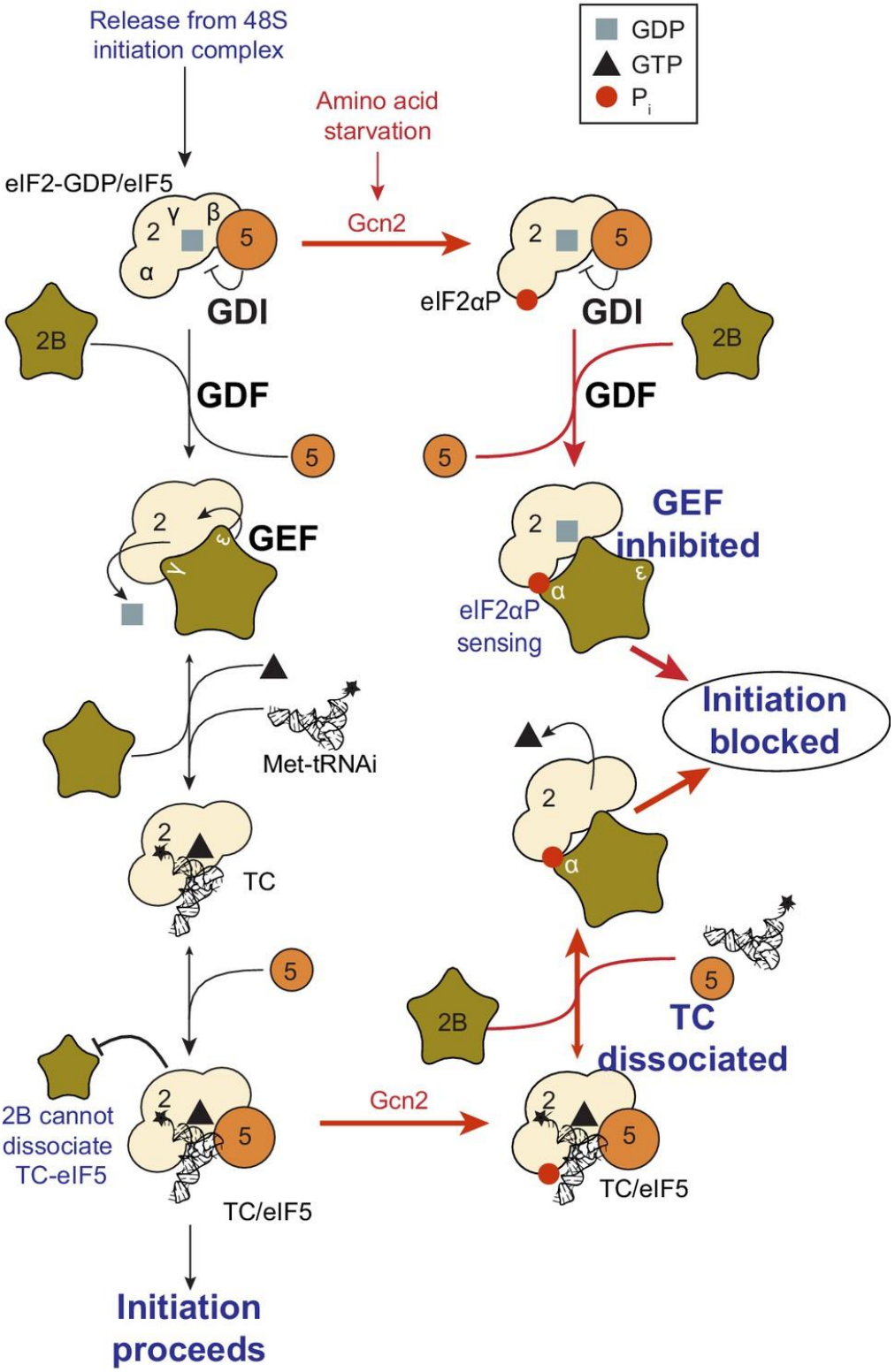

Figure 1.4 Regulation of eIF2 via eIF2B and eIF5. A model of interactions between eIF2, eIF2B, eIF5 and Met-tRNAi to produce eIF2-TC/eIF5 complexes and their inhibition by eIF2 (αP) (Jennings et al., 2017).

A classic example of Gcn2 phosphorylation is the translation regulation of *GCN4* translation (**Figure 1.5**). The *GCN4* protein (Gcn4) is a transcription factor of over 30 amino acid biosynthetic genes that is switched on in stressed cells or cells that are under nutrient starvation such as amino acids or vitamins starvation (Hinnebusch, 2005). The *GCN4* mRNA leader sequence has four upstream AUGs (uORF1, uORF2, uORF3 and uORF4), which according to the scanning model should be selected before the initiation codon of the Gcn4 open reading frame (ORF) (**Figure 1.5**). Translational reinitiation following termination at a short upstream ORF (uORF) helps to regulate *GCN4* expression. At the stop codon, only the 60S but not the 40S subunit dissociates from mRNA in an incomplete ribosome recycling reaction. This retained small subunit then resumes scanning downstream and recruits the Met-tRNAi^{met} in a form of a ternary complex with eIF2-GTP (TC) along the way to be able to "re-initiate" again at a next AUG start site (Valasek, 2012). It has been reported that the ability of some uORFs to retain 40S subunit on the same mRNA molecule after it has terminated translation at the uORF's termination codon depends on (a) cis-acting mRNA elements surrounding a given uORF, (b) the amount of time needed for the uORF translation which is determined by the length of a short uORF and the rates of translation elongation and lastly (c) on various translation initiation factors (review from (Hinnebusch, 2005; Valasek, 2012)). The ORF length or the ribosome transit time increases the likelihood that these factors are released (Rajkowitsch et al., 2004). After translation of the first reinitiation (REI)-permissive uORF1, a sizeable number of 40S subunit does not dissociate from the *GCN4* mRNA and instead resumes scanning downstream.

Reinitiation downstream following translation of uORF4 is not effective. In order to reinitiate on any of the downstream uORFs or on the main GCN4 ORF, these re-scanning subunits have to first acquire the ternary complex. Such that under normal nutrient sufficient (rich media growth) conditions (**Fig 1.5**, steps 3a and 4a), translation of the uORFs restricts the expression of *GCN4.* This is due to the intracellular levels of the ternary complex are high, so most of re-scanning ribosomes pick up before reaching the AUG start codon of the inhibitory (REI-nonpermissive) uORF4, at which they reinitiate. This uORF does not allow resumption of scanning of post-termination 40S

ribosomes and thus blocks further reinitiation. However, under amino acid deprivation, the amount of eIF2 ternary complexes is reduced drastically through phosphorylation of eIF2 caused by GCN2 kinase (Gcn2), which inhibits recycling of eIF2-GDP to eIF2-GTP by eIF2B. When the ternary complexes are limited, the uORF reinitiation process is altered in such a way that uORF4 could be bypassed by ribosomes and this in turn overcomes the normal barrier to *GCN4* translation created by the uORFs. Ribosomes that skip uORF4 translation may translate the *GCN4* ORF downstream. The elevated Gcn4 produced (up to a ten-fold increase) induces the transcription of stress proteins and amino acid biosynthetic enzymes, which make amino acids from available carbon and nitrogen sources to overcome the perceived amino acid limitation, thereby allowing resumed growth (Hinnebusch, 2005; Valasek, 2012). A similar mechanism operates on many stress-responsive mammalian mRNAs, including *ATF4* and *ATF5* (Palam et al., 2011; Vattem and Wek, 2004).

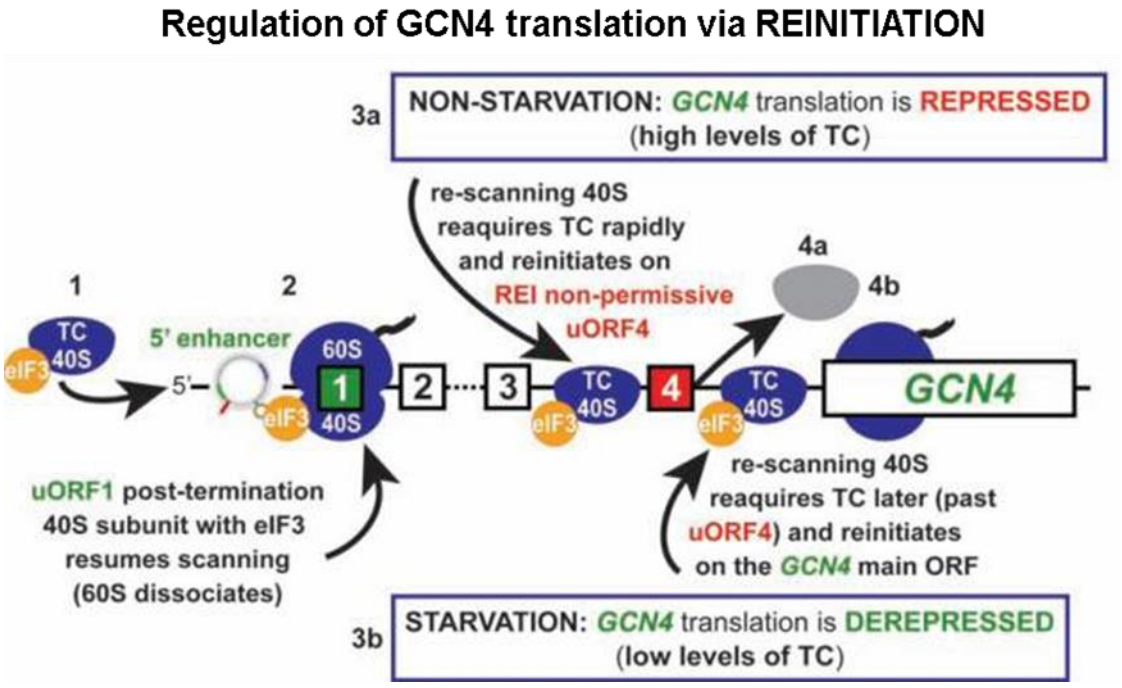

Figure 1.5 Mechanism of GCN4 mRNA translation control. Diagrammatic representation of the GCN4 mRNA leader showing distribution of the 4 short uORFs (REI-permissive uORF1 shown in green and the REI-non-permissive indicated in red), the uORF1 cis-acting elements (5'-enhancer), the 40S and 80S-bound ribosome and the illustration of the mechanism of GCN4 translation regulation. The 3a and 4a steps (GCN4-expression repressed) occur under non-starvation conditions with abundant TC levels, whereas the 3b and 4b steps (GCN4-expression derepressed) takes place under starvation condition (Valasek, 2012).

1.4.2 Regulation of mRNA selection via eIF4E binding proteins

A second regulatory mechanism operates at the mRNA recognition and selection stage. It is this mode of control that is directly relevant to my studies. The competitive ability of the mRNA in forming an initiation complex with the limited pool of free ribosomes available is dependent on both *cis*-acting and *trans*-acting factors inherent to the mRNA. The cis-acting elements in the 5'-UTR of the mRNA include the M^7Gppp 5' cap, the presence of AUG codons upstream of the coding region (as in the example of *GCN4* described above*)* and stable secondary structures produced by G: C base pairing within the mRNA leader sequence (Kozak, 1992, 1999). The trans–acting proteins or factors include the eukaryotic initiation factor 4F (eIF4F) complexes and their regulatory proteins.

Translation is initiated by the association of the mRNA with eIF4F complex (section 1.3.2). The eIF4F functions by the assembly of its components and its affinity for the 5' mRNA cap (Gingras et al., 1999b; Raught and Gingras, 1999). As the eIF4E binds to the m7Gppp cap, eIF4A helicase activities facilitate the binding of the 43S preinitiation complexes to the mRNA by lowering the level of secondary structures of the 5'-UTR. The interaction between eIF4E and eIF4G is one main determinant of the efficiency of an mRNAs translation. eIF4G coordinates the interactions between translation initiation factors (Prevot et al., 2003) such that in steady state, they remain bound with eIF4E as part of the eIF4F complex and recruit the 43S ribosomal subunit (Kozak, 2002). eIF4G has two isoforms in both mammals (called eIF4GI and eIF4GII) and in yeast, (called eIF4G1 and eIF4G2, encoded by *TIF4631* and *TIF4632* genes respectively sharing about 51% sequence similarity) (Goyer et al., 1993). However, a family of proteins called the eIF4E-binding proteins (4E-BPs) regulate eIF4F assembly by inhibiting the activities of eIF4E and consequently the amount of eIF4F complexes synthesized. 4E-BPs show amino acid homology with eIF4G (at the eIF4E-binding site) and compete with them for a share to interact with the eIF4E binding site (Altmann et al., 1997; Mader et al., 1995). The 4E-BPs are described in more detail in section 1.5.

Apart from the significant roles of the mRNA cap and translation factors on mRNA recognition and selection, the 3'-polyadenine (polyA) tail and Poly (A) binding protein (PABP, Pab1 in yeast) on the other end of the mRNA have also proved to have a profound impact on eukaryotic translation initiation (Prevot et al., 2003; Sachs, 2000). PolyA tail and PABP have been reported to aid in the joining of the large ribosomal

subunit (Searfoss et al., 2001); in the formation of the closed loop complex with additional function of promoting translation initiation and termination; in recruiting and recycling of ribosomes and in the stability of the mRNA (Mangus et al., 2003; Richter and Sonenberg, 2005). A typical depiction of the closed loop complex with eIF4E, eIF4G, poly A tail and poly A binding protein, PABP bound to the mRNA and also the separate 4E-BP/eIF4E/mRNA complex is shown in **Fig 1.6**.

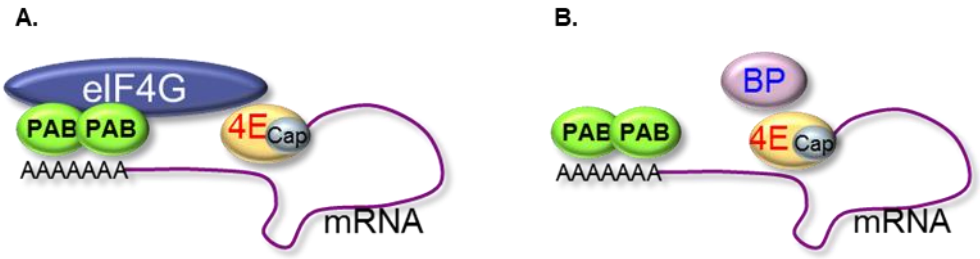

Figure 1.6 The mRNA closed loop complex interaction with the 4E-BP. A diagram showing the closed loop complex with eIF4E, eIF4G and PABP bound to the mRNA; the interaction of eIF4G and the 4E-BPs, Caf20 and Eap1p competing for a share on eIF4E binding site**. A.** With eIF4G binding to eIF4E, closed loop complex is established, ribosome can be recruited enabling enhanced translation. **B.** With one of the 4E-BPs bound, no eIF4G or ribosome recruitment and translation is blocked. Adapted from (Castelli et al., 2015; Costello et al., 2015)

1.5 eIF4E and its inhibitory proteins (4E-BPs)

1.5.1 Overview of 4E-BPs and mechanisms of repression

4E-BPs function as effectors of signalling pathways involved in cell growth and development, cellular stress, tumour repression, synaptic plasticity, neuronal balance which can have effect on memory acuity and dysregulation in autism spectrum disorders (Bidinosti et al., 2010; Gingras et al., 2001; Gingras et al., 1999b; Gkogkas et al., 2013; Martineau et al., 2013; Mothe-Satney et al., 2000; Richter and Sonenberg, 2005; Tuxworth et al., 2004). In most actively translated mRNA, the eIF4E is usually in complex with the scaffolding protein eIF4G as part of the eIF4F complex (Gross et al., 2003), Fig. 1.4A. A binding motif enabling eIF4E interaction of approximately 15 amino acids is shared between eIF4G and 4E-BP proteins (Mader et al., 1995). Hence 4E-BPs compete with eIF4G in binding to eIF4E where they consequently inhibit the translation of the bound mRNA (Richter and Sonenberg, 2005). The 4E-BPs (in yeast and metazoans) share a common conserved (canonical) motif YXXXXLΦ (**Fig 1.9A**,

where Y is tyrosine; Φ can be any hydrophobic amino acid such as Met, Leu or Phe; X is any amino acid, L is Leucine) (Altmann et al., 1997; Mader et al., 1995).

Several types of 4E-BPs have been identified in different organisms which differ in whether they can be untethered or tethered to target mRNAs through specific mRNA sequences. Initially, all 4E-BPs were believed to be untethered where the 4E-BP binds directly with the eIF4E without recourse to associate with any sequence on the mRNA or RNA binding proteins. More recent evidence shows that some of the 4E-BPs can be tethered by binding to various sequence or structural elements prior to targeting eIF4E. Tethered 4E-BPs include CPEB-Maskin (in *Xenopus*) and Cup (in *Drosophila*) (Richter and Sonenberg, 2005). The cytoplasmic polyadenylation protein, CPEB can recognise and bind a cytoplasm polyadenylation element (CPE) on the 3' UTR of mRNAs. The CPEB can also bind to Maskin, a protein that has a weak interaction with eIF4E. The binding of these two proteins (CPEB-Maskin) disrupts the binding of eIF4E to eIF4G and inhibits polyA growth of CPE-containing mRNA needed in oocyte meiosis (Stebbins-Boaz et al., 1999). In a similar scenario, Cup regulates germ-cell formation (oocytes) and axis specification in the fruit fly. Cup associates with Bruno (an *oskar* mRNA suppressor) only on mRNAs containing Bruno response element (BRE) to repress eIF4E-eIF4G translation of target mRNAs in nurse cells and during mRNA transport within oocytes (Richter and Sonenberg, 2005). Cup can also interact with Smaug, a protein that binds on *nanos* proteins to drive translation of posterior localized *nanos* mRNA by displacing eIF4G on the eIF4E and prevent translation of unlocalized nanos mRNAs (Nelson et al., 2004) during early embryo development. Other 4E-BPs identified include PHAS-I (4E-BP1), 4E-T (Kamenska et al., 2014), CYFIP1 (Napoli et al., 2008), 4E-BP2 (Hu et al., 1994) and 4E-BP3 (Tsukumo et al., 2016) in mammalian cells (Gingras et al., 2001; Mothe-Satney et al., 2000), as well as Caf20 (also called p20) (Altmann et al., 1997) and Eap1 (Cosentino et al., 2000) in yeast, *Saccharomyces cerevisiae.*

1.5.2 Architectural structures of eIF4E/eIF4G and eIF4E/4E-BPs complexes

The canonical eIF4E binding motif peptides found in the different translation factors in yeast include YTIDELF in Caf20, YSMNELY in Eap1 and YGPTFLL in eIF4G (Arndt et al., 2018). The mammalian eIF4E-associated proteins (eIF4E/eIF4GII complex and eIF4E/eIF4E-BP1 complex) were first reported from X-ray crystallography to bind to the convex dorsal surface of the eIF4E by undergoing a disorder-to-order transition and

forming identical L-shaped α-helical conformation with the eIF4E surface with a similar molecular mimic of each other (Marcotrigiano et al., 1999). With multidimensional NMR spectroscopy for the eIF4E in complex with the cap and eIF4G, the binding of eIF4G to the eIF4E formed a molecular bracelet in form of 5 helical rings at right angle wrapped around the N-terminus of the eIF4E and these helical rings are important in loading eIF4E to the capped mRNAs (Gross et al., 2003). It was initially believed that most 4E-BPs share no evident homology in their sequences outside their eIF4E binding motifs (Altmann et al., 1997; Cosentino et al., 2000). However, it is now clear that some metazoan 4E-BPs also have a conserved (non-canonical) structural motif of about 15-30 amino acid residues. Although the non-canonical motifs of metazoans are not similar in sequence, they all bind on the same lateral surface of eIF4E, a feature they do not share with their eIF4G (Gosselin et al., 2011; Gruner et al., 2016; Igreja et al., 2014; Kinkelin et al., 2012; Paku et al., 2012). In yeast, 4E-BPs and eIF4G both bind to the lateral and dorsal surfaces of eIF4E (Gruner et al., 2018).

Peter *et al.* (2015) described the molecular architecture of three 4E-BPs (Thor, 4E-T and 4E-BP1) binding on eIF4E (**Fig 1.7A**). They proposed three structural elements common to 4E-BPs: an N-terminal α helix formed by the conserved (canonical) motifs which binds to the dorsal surface of the eIF4E; an elbow loop in between that bends the peptide backbone downwards by 90˚ to the lateral surface of the eIF4E and the third structure is a C-terminal (non-canonical) loop formed by the non-canonical motifs. In relation to their competition with eIF4G, 4E-BPs show bipartite binding to the eIF4E. eIF4G and all 4E-BPS can bind to the dorsal surface of eIF4E, while only 4E-BPs also bind to the lateral surface of the eIF4E. As such, mutations in the metazoan canonical motifs have been found to disrupt eIF4G binding to eIF4E but not most 4E-BPs as the elbow linker and the non-canonical motifs can still anchor the 4E-BP to the eIF4E but mutations at the lateral site of the eIF4E disrupts 4E-BP binding to the eIF4E as the eIF4G has a higher chance of sitting on the dorsal surface of the eIF4E binding site (Igreja *et al.*, 2014; Peter *et al.*, 2015). Recent eIF4G/eIF4E and 4E-BP/eIF4E structures of the yeast factors suggest that their eIF4E-eIF4G and eIF4E-4E-BP complexes both showed bipartite binding of the dorsal and lateral surfaces to the eIF4E (**Fig 1.7B, C and D**). The crystal structure of Caf20 of residues 1-49 (only 1-45 visible in the structure) in complex with eIF4E is shown in **Fig 1.7 C** and **D**. Here, the first helical structure of the crystal falls between residues 6-12 of the canonical region of Caf20 (1-17) on the dorsal surface, the linker site falls at 12-24 and the second helix

is situated at 24 and 41 of the non-canonical region (18-49) on the lateral surface of eIF4E (**Fig 1.7B, C** and **D**). The lateral binding of the yeast eIF4G contribute immensely to its stability on eIF4E on which when mutated reduces its binding with the eIF4E unlike the 4E-BP (Caf20) where disruption of the lateral surface has no effect on its binding to the eIF4E (Gruner et al., 2018).

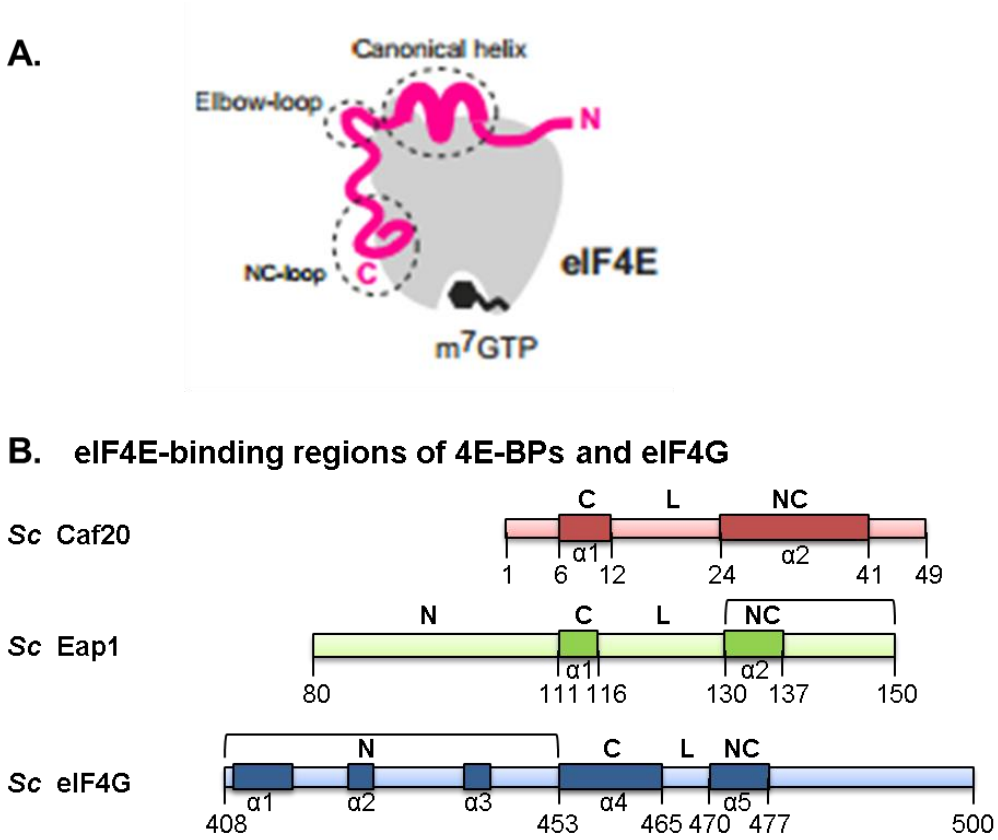

Figure 1.7. Systematic representation of the molecular structure of 4E-BP–eIF4E binding. A. The diagram shows three main structural elements for 4E-BP anchorage on the eIF4E surface; the canonical α helix produced by the canonical (conserved) motifs for binding to the dorsal surface, the elbow-loop (linker) and the non-canonical loop for binding at the lateral surface. **B.** A representation of the eIF4E-binding regions of S. cerevisiae Caf20, Eap1 and eIF4G proteins. **C.** cartoon representation of the eIF4E-binding region of S. cerevisiae Caf20 (p20) (indicated in fuchsia) in complex with eIF4E (in grey) shown as a surface in three orientations. Selected secondary structure elements are labelled in black and fuchsia for eIF4E and Caf20 respectively. **D.** close up view of the canonical and non-canonical helices of S. cerevisiae Caf20 (p20) bound to the dorsal and lateral surfaces of eIF4E. Structure from Protein Data bank, 6FC3. Selected residues are shown as sticks and coloured in black and fuchsia for eIF4E and p20 (Caf20) respectively. Sc – *Saccharomyces cerevisiae*. Note: Indicated are the N-terminal region (N), the canonical (C) and non-canonical (NC) eIF4E-binding motifs, and the connecting linker (L) are indicated. Secondary structural elements (helices) are shown below the protein sketch. Source (Gruner et al., 2018; Peter et al., 2015).

1.5.3 Phosphorylation of 4E-BPs and eIF4E Disrupt Affinity for eIF4E and mRNA Cap Respectively

The recruitment of the 40S subunit to the 5' end of the mRNA is a crucial and rate-limiting step during cap-dependent translation. A number of translation initiation factors including eIF4E and 4E-BPs have essential roles in this process (Ma and Blenis, 2009). Regulation of the 4E-BPs in mammalian cells can be achieved by phosphorylation (**Fig 1.8**). Phosphorylation of 4E-BPs typically leads to their dissociation from eIF4E and hence improves assembly of eIF4F complexes by enhancing eIF4E-eIF4G interaction. The best described protein kinase regulating the activities of the 4E-BPs are the mammalian target of rapamycin, mTOR/FRAP kinase which targets the 4E-BP1 (Gingras et al., 2001; Mothe-Satney et al., 2000) and ribosomal protein S6 kinase, S6K (Tavares et al., 2015) (**Fig 1.8**). mTORCs (mTORC1 and mTORC2 complexes) are protein kinase complexes and sensors important in cell response to nutrient (amino acids) fluctuations, enzyme growth factors (such as insulin and IGF-1) and cellular energy (ATP). mTOR/S6K signalling pathways are implicated in cellular responses to growth, survival and metabolism as well as contributing to several diseases, including cancer, obesity and diabetes (Tavares et al., 2015). The activities of the mTORCI on 4E-BPs and SK6 can be inhibited by subjecting the cells to rapamycin drug treatment, because rapamycin is an allosteric inhibitor of mTOR.

Hypophosphorylation of 4E-BP1 by mTOR inactivation favours 4E-BP/eIF4E complex formation that represses translation by displacing eIF4G from the eIF4F complex (eIF4E, eIF4G and eIF4A). mTORC1-mediated phosphorylation of 4E-BPs

releases the 4E-BP from eIF4E, resulting in the recruitment of eIF4G to the 5'cap as well as eIF4A, and thereby allow translation initiation to proceed(Gingras et al., 1999b) (**Fig 1.8A**). When 4E-BP1 is hyperphosphorylated (double phosphorylation) by the mTOR at residues Ser65 and Thr76 within the linker region, it reduces 4E-BP1 affinity for eIF4E and enables translation and cell proliferation through enhanced synthesis of eIF4F complexes by eIF4E-eIF4G interactions. The phosphorylation of the Thr70 is brought about when there is a phosphorylation of Thr37/46 upstream to the conserved motif which in turn phosphorylate the Thr70 to inhibit the binding of 4E-BP1 to eIF4E (Gingras *et al.*, 1999a; Gingras *et al.*, 2001). Induction of phosphorylation of a mammalian 4E-BP, 4E-BP2, at multisite is essential for structural change. Phosphorylation of 4E-BPs occurs first at sites T37 and T46, secondly on T70 and S65 (Bah *et al.*, 2015; Gingras *et al.*, 1999a) and also at S83 (Bah et al., 2015) (**Fig 1.8B**). Bah *et al.* (2015) reported that phosphorylation at two sites T37 and T46 resulted in the folding up of the residue P18-R62 into four-stranded β-domain where the canonical eIF4E-interacting motif (YXXXXLϕ, from Y54) becomes partly buried inside the phosphorylated β-domain. The fold state created by phosphorylation of either site T37 or T46 was weak, enhanced eIF4G affinity for the cap and decreased 4E-BP2-eIF4E interaction by 100-fold while full phosphorylation from the two sites created a more stable domain with lesser affinity for eIF4E by 4000-fold. It was concluded that stabilization of phosphorylated 4E-BP is critical for phospho-regulation of 4E-BP-eIF4E interaction and facilitated by a large-scale structural rearrangement.

Another well-studied initiation factor that is targeted by signal transduction pathways is eIF4B. Some mRNA species contain inhibitory secondary structures in the 5' UTR. Following 40S ribosomal protein S6 kinase (S6K)-mediated phosphorylation via growth factors, eIF4B is recruited to the translation pre-initiation complex and enhances the RNA helicase activity of eIF4A (**Fig 1.8C**). This is particularly important for translating mRNAs that contain long and structured 5'UTR sequences, because the unwinding of this RNA structures is required for efficient 40S ribosomal subunit scanning towards the initiation codon (Ma and Blenis, 2009).

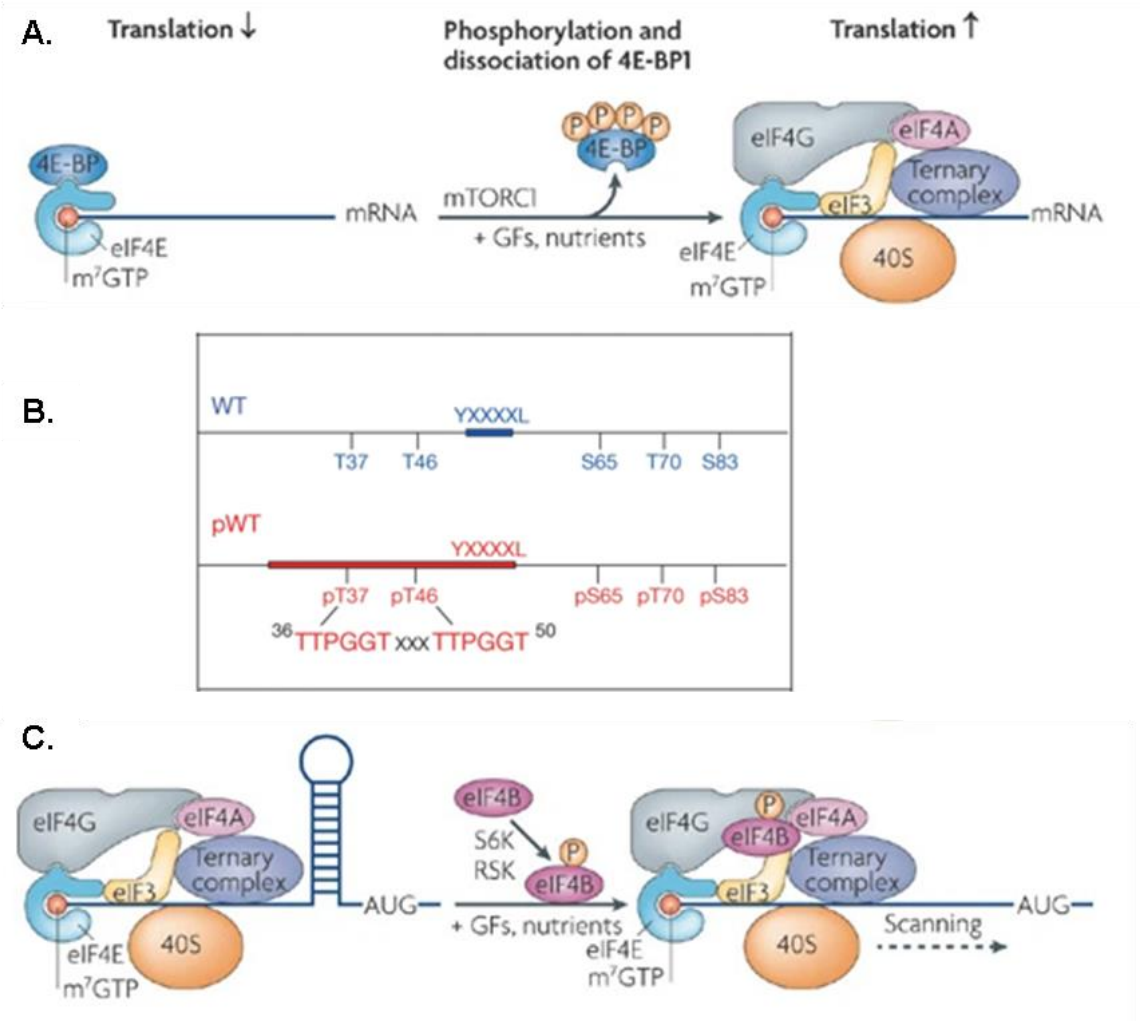

Figure 1.8. Regulation of translation initiation through phosphorylation of 4E-BP by mTOR and S6K. **A.** mammalian target of rapamycin complex1 (mTORC1)-mediated phosphorylation of 4E-BPs releases the 4E-BP from eIF4E, leading to the recruitment of eIF4G to the 5'cap, and thereby initiation protein translation (Ma and Blenis, 2009). **B.** Schematic representation of 4E-BP2 showing the relative positions of the phosphorylation sites, the canonical eIF4E-binding site (thick blue bar) and the region which undergoes phosphorylation-induced folding (thick red bar) (Bah et al., 2015). **C.** Following S6K phosphorylation, eIF4B is recruited to the translation pre-initiation complex and enhances the RNA helicase activity of eIF4A. This is particularly important for translating mRNAs that contain long and structured 5' untranslated region sequences, because the unwinding of these RNA structures is required for efficient 40S ribosomal subunit scanning towards the AUG initiation codon (Ma and Blenis, 2009). **GFs** – growth factors.

1.6 Cell signalling responses in Yeast

1.6.1 Overview of nutrient cell signalling to filamentous growth in yeast.

Pseudohyphal or filamentous growth is a common response of budding yeast to extracellular stimuli, typically nutrient starvation such as nitrogen and glucose limitations. It is an adaptive response that allow non-motile yeast to forage for scarce nutrients under stressful conditions. Pseudohyphal growth (PHG) vary from growth by

budding in the sense that budding constitute normal cell growth and activities surrounding cell division cycle in yeast. PHG occurs when there is a delay in G2/M phase progression that results in elongation of apical directed polar growth such that the budding pattern changes from axial (in haploid cells) or bipolar (in diploids) to unipolar pattern (Cullen and Sprague, 2002; Kron et al., 1994; Song and Kumar, 2012). Four different signalling pathways are implicated in promoting PHG. First, the interaction of RAS GTPase with cyclic adenosine monophosphate, cAMP to activate protein kinase A, PKA (Ras2/cAMP-PKA pathway). The second pathway is the sucrose nonfermentable, SNF pathway. The Snf1 pathway is triggered during glucose starvation and regulate the *FLO11* promoter required for filamentous growth. The third control point is the target of rapamycin, TOR, pathway. TOR is evolutionarily programmed to regulate the Gcn4 transcription factor in response to nitrogen signal which then regulate *FLO11* expression. The fourth is the mitogen activated protein kinase (MAPK) pathway which essentially controls the entire factors fundamental in the other pathways including proteins important in mating, P21-activated kinase, Ste20, Ste11, Ste7, Kss1 and transcription factors, Ste12 and Tec1 (Cullen and Sprague, 2012; Gancedo, 2001; Madhani et al., 1999; Pan and Heitman, 2002; Park et al., 2006). Each one and every of the pathways separately eliminate pseudohyphal growth such that knockout (KO) of important genes regulated in each pathway has been shown to influence PHG (Cullen and Sprague, 2012). These pathways also have the potential of regulating each other activities. A typical report is the RAS pathway which has been shown to regulate the filamentous MAPK pathway (Mosch et al., 1996). The MAPK pathway is the most widely studied signalling pathway which in turn controls three cell signal pathways - cell mating, filamentous or PHG and osmotic tolerance (Cullen and Sprague, 2012). In PHG, the MAP kinase, Kss1 is the major regulator for filamentous growth which targets the transcription factors, Ste12 and Tec1 and Dig1 and Dig2 proteins to influence PHG (Cullen and Sprague, 2012).

1.6.2 The roles of yeast 4E-BPs in cell signalling

1.6.2.1 The yeast 4E-BPs

Saccharomyces belong to the subphylum Saccharomycotina of the yeast kingdom (Ross and Altmann, 2016). Caf20 and Eap1 are the two 4E-BPs in *Saccharomyces cerevisiae*. They are non-essential genes, but where deletions can show some growth defects alone or in combination with other factors. From the information on the Saccharomyces genome database (SGD), both factors can be phosphorylated at different sites most

especially the serine and threonine residues at the middle of each protein (information retrieved in May, 2019 from https://www.yeastgenome.org/). They have a half live of approximately 8 hours (Christiano et al., 2014). The two proteins do aligned at their eIF4E-binding site, (Y109-L114 for Eap1 and Y4-L9 for Caf20) shown with a red line and at other sites with Bioedit (Hill, 2005) software v.7.0.5 ClustalW multiple alignment (**Fig 1.9A** and **B**). The percentage of identity and similarity are estimated to be 6% and 11% respectively. They show sequence homology mainly around the eIF4E-binding site (**Fig 1.9B**).

The Caf20 is an 18 KDa acidic protein (Pi = 5.85) with 161 amino-acid. The average abundance (molecule per cell) is 17776 +/- 6230 (SGD database). Caf20 is comparable in size to that of the metazoan 4E-BPs of which they maintain some sequence homology only at the eIF4E-binding site (**Fig 1.9A**). The physical and genetic interactors of Caf20 total close to 500 and 100 proteins respectively, of which CDC33 (eIF4E), DHH1, MPT5, SRO9, DED1 and TIF4631 are the major physical and genetic interactors from affinity capture and dosage lethality experiments respectively (retrieved from BioGRID database, https://thebiogrid.org/34665/summary/saccharomyces-cerevisiae/caf20.html in May, 2019)

Eap1 is a large basic protein (pI=10.16) of about 70 KDa. It has a total of 632 residues. Eap1 is implicated to accelerate mRNA degradation (Blewett and Goldstrohm, 2012). Hence one idea is that Eap1-eIF4E interaction may prevent new translation initiation on mRNAs that are to be degraded, as this would help prevent initiating ribosomes starting translation on mRNAs without full-length ORFs. Such incomplete proteins may have interfering properties that would be deleterious to cells. Eap1 was also shown to be a target of the yeast TOR signalling cascade, providing a potential parallel to mammalian 4E-BP control (see later section 1.5.3 (Cosentino et al., 2000). Eap1 is less abundant than Caf20 occurring at a ratio of about one quarter (4877+/-1412) of the amount of Caf20 molecules/cell, suggesting that Caf20 is the major yeast 4E-BP (information retrieved from SGD database of average of multiple studies). Eap1 protein and gene targets show some overlaps as well as differences to Caf20, totalling about 45 physical interactions and 353 genetic interactions which the most reported protein interactors are CDC33 (eIF4E), DHH1, SMY2, PUF3, CTF8, XRN1, RVS161 (retrieved from BioGrid 23rd May 2019; https://thebiogrid.org/33919/summary/saccharomyces-cerevisiae/eap1.html).

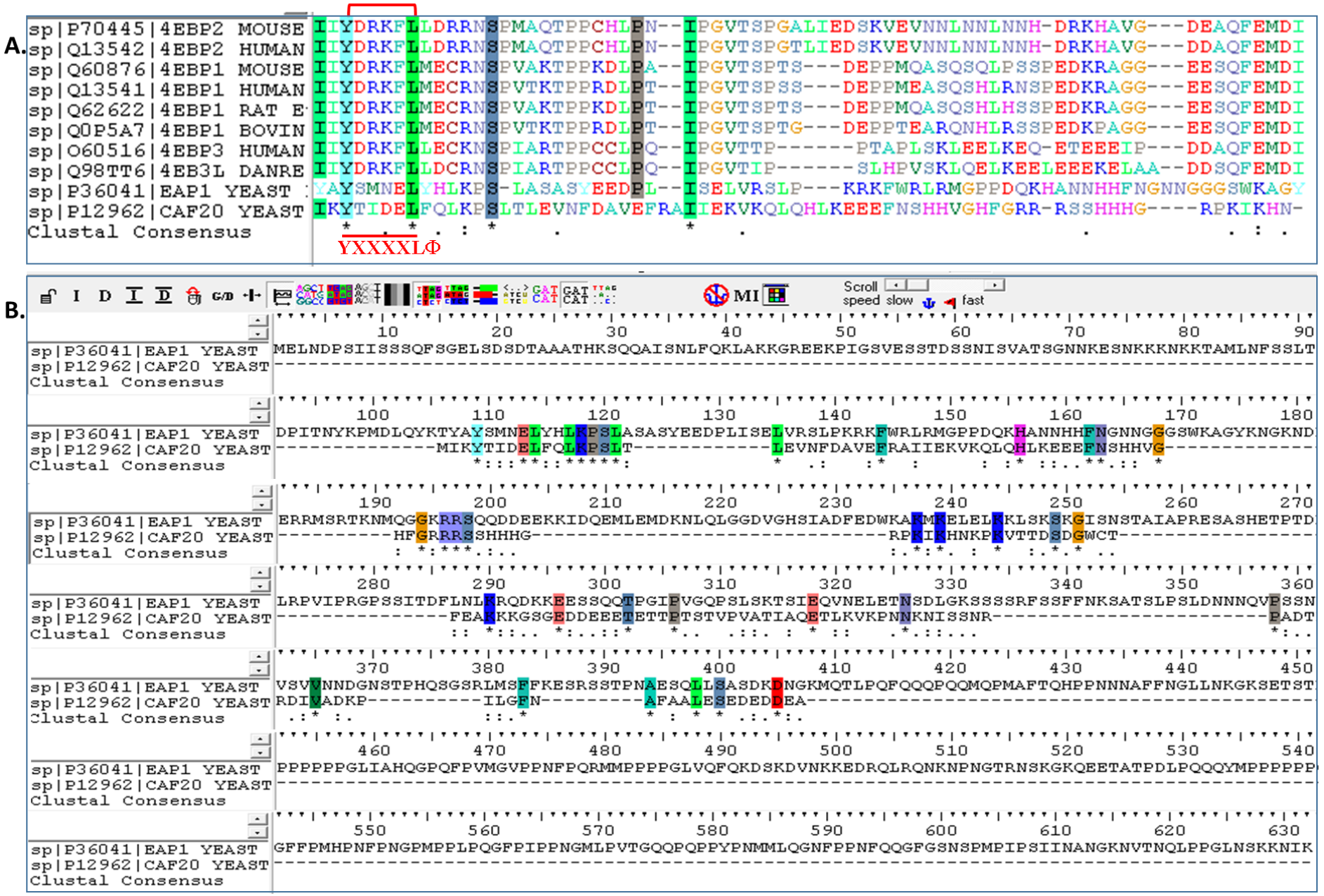
A.
sp|P70445|4EBP2_MOUSE
sp|Q13542|4EBP2_HUMAN
sp|Q60876|4EBP1_MOUSE
sp|Q13541|4EBP1_HUMAN
sp|Q62622|4EBP1_RAT
sp|Q0P5A7|4EBP1_BOVIN
sp|O60516|4EBP3_HUMAN
sp|Q98TT6|4EB3L_DANRE
sp|P36041|EAP1_YEAST
sp|P12962|CAF20_YEAST
Clustal Consensus
YXXXXLΦ
B.
MI
Scroll
speed slow fast
sp|P36041|EAP1_YEAST
sp|P12962|CAF20_YEAST
Clustal Consensus

Figure 1.9 Multiple sequence alignment of eukaryotic 4E-BPs. Protein sequences are retrieved from Uniprot protein database with unique accession numbers and aligned with ClustalW multiple alignment of BioEdit v7.0.5 software. The Clustal consensus and the shaded residues indicate identities and similarities at a given threshold. The shared conserved motif with the eIF4E underlined in red (Common motif is YXXXXLΦ [where Φ is LM or F]) A**.** Multiple alignment of Caf20 with other Metazoan 4E-BPs from Mouse, Human, Rat, Bovin (cattle) and Danre (Zebra fish). A little similarity present especially around the eIF4E-canonical binding region at a shade threshold of 90%. **B.** Pairwise sequence alignment of Eap1 and Caf20 at a shade threshold of 100%. Caf20 and Eap1 show some similarities at the eIF4E binding site and other parts of the protein. Similarities and identities were estimated with similarity matrix: BLOSUM62

In simple organisms, eIF4E is an important factor in protein synthesis. Insights on the impact of loss of binding to eIF4E site or loss of a 4E-BP have been studied through investigations of effects on growth or translation of such mutations (Altmann et al., 1989b; Altmann and Trachsel, 1989; de la Cruz et al., 1997). The roles of the yeast 4E-BPs Caf20 and Eap1 have been studied by both genetic and biochemical approaches and discussed below.

The 4E-BPs have shown to be involved in regulation of phenotypes under different stress conditions. Deletion of caf20 has shown to rescue slow growth rate and cold sensitivity in translation mutants of eIF4E, eIF4B, and F4G1 whereas the overexpression of Caf20 enhances the growth defects of these mutant strains (de la Cruz et al., 1997). The differentiation of diploid yeasts into pseudohyphal forms and the formation of processing bodies (p-bodies) in limiting nitrogen sources were found to be under the influence of Caf20 and a decapping activator, Dhh1 (Dead-box RNA helicase) by regulating *STE12* expression (Ka et al., 2008; Park et al., 2006) while lack of Caf20 alleviates the phenotypes (Ibrahimo et al., 2006). Pseudohyphal yeast forms are reported only in Sigma strain, Σ1278b and SK1 forms but not in non-filamentous BY-derivatives (Song and Kumar, 2012). Knockout of Caf20 has no effect on adhesive properties of haploid yeast cell. In contrast eIF4E mutations cause temperature sensitivity and deletions of components of the eIF4F influence adhesive properties in haploid cells and pseudohyphal growth in diploid cells of which weakening the Caf20-eIF4E interactions or Caf20 deletions do not rescue the loss of adhesion in haploid cells (Ross et al., 2012). Eap1, on the other hand, is reported to mediate translation attenuation (Deloche et al., 2004), regulate the formation of pseudohyphae under nitrogen starvation (Ibrahimo et al., 2006); control certain oxidative stress agents like diamide and cadmium (Mascarenhas et al., 2008), control stress granule formation via glucose starvation

(Buchan et al., 2008) and can associate with Puf protein, Puf5 and Dhh1 to direct mRNA decapping and hasten mRNA decay (Blewett and Goldstrohm, 2012).

The 4E-BPs are also important in cell cycle control (Castelli et al., 2015) and appear to function in an mRNA-specific manner (Arndt et al., 2018; Castelli et al., 2015; Costello et al., 2015; Cridge et al., 2010; Ibrahimo et al., 2006). Initially, identifying specific mRNAs regulated by the yeast 4E-BPs was difficult. The best described specific mRNA was *CLN3*, a G_1 cyclin controlled by altering eIF4E activity (eIF4E binding is critical for *CLN3* expression). The *CLN3* mRNA has a short ORF upstream to main ORF which represses the expression of Cln3. In a temperature sensitive eIF4E mutant strain (*cdc33-1*) a defect in G_1-S phase transition is observed. Artificial enhancement of *CLN3* expression alleviates the cell cycle defect enabling cells to enter into a new cycle, but then growth arrested randomly due to the lack of eIF4E for translation of other mRNAs (Danaie *et al.*, 1999). Caf20 is reported to repress the translation of cyclin genes and genes important for polarised growth (Cridge et al., 2010). Mad2 (mediator complex 2), an identified interactor of Caf20 and also member of the spindle assembly checkpoint important in bipolar spindle attachment of the chromosome to the microtubules during mitotic cell cycle. Mad2 is found to improve cyclin (Clb5) protein translation and enhance cell survival to stress response by associating with Caf20 to inhibit its interactions with the translation machinery (Castelli et al., 2015; Gay et al., 2018).

Caf20, like Eap1, may also have a role in RNA-decay via interactions with the helicase Dhh1. The deadenylation of the 3' poly (A) tail result in degradation of the capped mRNAs in a 5'-3' direction as a result of removal of the of the 5' m7 GpppN cap structure and is important in mRNA turnover for both stable and unstable mRNA transcripts in yeast (Decker and Parker, 1993). Dhh1 belongs to the conserved subfamily of DEAD box helicase called the RCK/p54 helicases (Akao et al, 1992) and is known to play a vital role during mRNA remodelling and decay via interactions with members the decapping complex and deadenylation enhancers. Thus Dhh1 is thought to improve the efficiency of mRNA decapping. Deletion of Dhh1 is reported to show cold-sensitivity lethality at 18°C and temperature-sensitivity at 36°C. Caf20 deletion alleviates these phenotypes (de la Cruz et al., 1997). However, this phenotype was not rescued by Caf20 on a plasmid, suggesting that *dhh1*Δ strains can accumulate other mutations that contribute to the phenotypes (Lydia Castelli and Graham Pavitt, unpublished observations). Apart from the Caf20 and other 4E-BPs, other proteins such

as Pat1 and Lsm1-7 are important in regulating mRNA metabolism and decay by either suppressing or enhancing phenotypes (Coller et al., 2001; Lobel et al., 2019).

1.7 Roles of Caf20 in Translation Regulation

1.7.1 Overview of Caf20 translation regulation

Until recently it has not been clear whether Caf20 is a general regulator of all protein synthesis or if it has any mRNA specificity. In vitro studies have suggested Caf20 has only modest affinity for eIF4E and was a non-specific binding protein (Ptushkina et al., 1998). In contrast, recent studies with eIF4E-binding fragments of Caf20 suggest the canonical binding motif interacts with eIF4E with high specificity (Gruner et al., 2018). By using micro-array techniques, Cridge et al. (2010) showed caf20Δ alters translation of only a subset of mRNAs both up and down-regulating the association of many hundreds of mRNAs with polysomes (784 mRNAs, 471 up- and 313 down-regulated) and 3'UTR-binding proteins such as Puf proteins were implicated in providing at least some mRNA target specificity (Cridge et al., 2010). This latter study therefore suggests Caf20 can act on specific mRNAs. In agreement with this RNA-immunoprecipitation and RNA-sequencing identified many mRNA targets of Caf20 (Castelli et al., 2015) that is described in more detail in section 1.7.2.

In addition to the accepted role of Caf20 as a 4E-BP, a recent study has suggested Caf20 can bind to eIF4E to promote translation (Arndt et al., 2018). In *in vitro* reactions Caf20 formed a stable ternary complex with eIF4E and capped mRNAs to promote their translation. Caf20 could also inhibit translation on uncapped mRNA. Caf20 was reported to bind directly to mRNA via repeated positive charged residues within its middle region (residues 55-57 and 60-62), because mutating these prevented this interaction and caused a growth defeat (Arndt et al., 2018). These studies suggest that Caf20 can bind to specific mRNAs and may act as either a 4E-BP to repress translation, but may also act as an activator of translation.

1.7.2 Identification of Caf20-eIF4E Dependent and Independent regulation

In prior work by the Pavitt lab, mRNA enrichment for the components of the closed loop complex (eIF4E, eIF4G1 and eIF4G2, Pab1) including the 4E-BPs (Caf20 and Eap1) and how their targets are regulated during translation was assessed. Next generation sequencing (RIP-Seq) method of TAP (Tandem affinity purification) tagged proteins and RNA-binding protein immunoprecipitation (IP) revealed that the Caf20 and

Eap1 showed overlaps with each other and with the other proteins tested as well as some specificity in their mRNA targets. The 4E-BP enriched transcripts are characterized to have low polyA and ribosome occupancy; have tightly regulated protein products that are dependent on the cap-interacting proteins, the eIF4F and the eIF4E repressors. The study confirmed the specificity of 4E-BPs to some mRNAs as the RIP-Seq pointed some group of mRNA targets enriched for the 4E-BPs alone and not in other proteins tested including eIF4E which is believed to be the sole binding partner of the 4E-BPs. (Costello et al., 2015).

To address the mechanism underlying the specificity of the 4E-BP bound mRNAs, Castelli *et al* (2015) analysed the proteins associated with Caf20 and Eap1-TAP tagged and FLAG-tagged proteins IPs and mass spectrometry of 4E-BPs. It was found that apart from their known protein-binding partner eIF4E, the two 4E-BPs interact with translating ribosomes. This was an interesting finding as ribosomes are associated with active translation and the 4E-BPs with repression. The ribosome interaction was considered as a 4E-IND association as the Caf20^{m2} mutant disrupted for binding with eIF4E, interacted well with the ribosome. A further analyses by RNA-Seq revealed a core set of over 500 distinct Caf20 interacting mRNAs of which are grouped into two (**Fig 1.10**). One group making up the larger proportion (75%) are dependent on the eIF4E interaction motif for Caf20-interaction (termed the 4E-Dependent or 4E-DEP mRNAs) while the other group of mRNAs (25%) bound to Caf20 and to Caf20m2, showing binding was independent of eIF4E interactions (4E-IND mRNAs). The functionality of the 4E-IND mRNA targets showed that they are physiologically relevant in mitochondrial and ribosome-directed regulation. Incorporation of Caf20 mutant plasmid with 4E-IND regulation into cells rescues the slow-growth rate in respiratory media (Castelli et al., 2015). Comparison of their structural features indicated that the 4E-Independent mRNAs have longer poly-A tail and half-life, shorter ORFs. There was evidence for a shared AUAUAUAU repeating motif in 3'UTRs. Screening the importance of the 3'UTR in one mRNA *ERS1* showed that it could confer 4E-independent and Caf20-dependent repression to a luciferase reporter gene *in vivo*.

These findings suggest that caf20 can act independently of its interaction with eIF4E to bind to specific sequences in some mRNA 3'UTRs (4E-IND mRNAs) to repress their translation. It is not clear if Caf20-ribosome interactions are involved in this repression, or are involved in the separately described translational activation function (Arndt et al., 2018). How Caf20 and 3'UTR sequences act together to cause

translational repression is also not understood. One hypothesis is through binding both to the ribosomes and with specific mRNA 3'UTR sequences or structures to regulate translation (**Fig 1.10B)**.

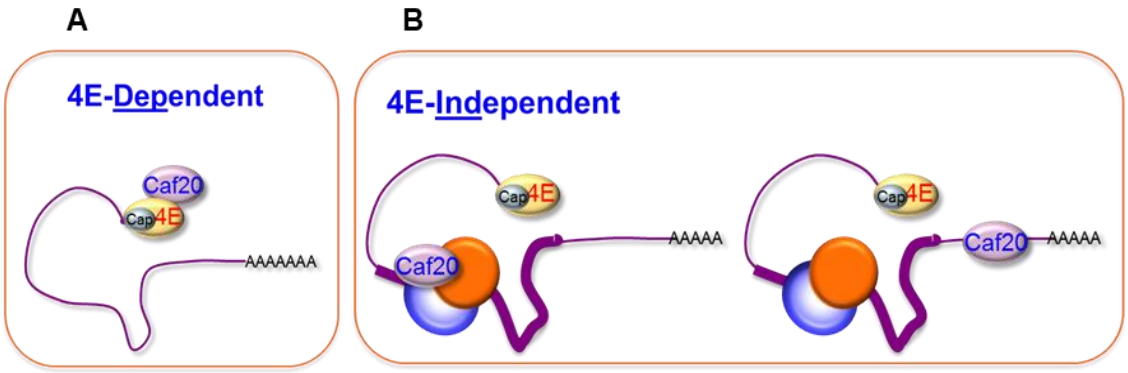

Figure 1.10 Models for 4E-DEP and 4E-IND Caf20-mediated translational repression. A. Caf20 mediated 4E – DEP translation regulation. Binding of Caf20 to many mRNAs is dependent on Caf20 - eIF4E interactions. **B.** 4E-IND repression mechanisms. Caf20 3' UTR motif binding, either alone or in addition to 80S binding facilitates translational repression.

1.8 Current study aims and objectives

This study is a follow up research of the previous Caf20 reports from the Pavitt's laboratory most especially on the report of Caf20-eIF4E dependent and independent regulation (Castelli et al., 2015). As discussed in section 1.7, Caf20 has been reported to perform other roles by interacting with some specific mRNAs. It was also reported that Caf20 carries out its function either through eIF4E-dependent or eIF4E-independent mediated controls. In eIF4E-independent control, Caf20 can interact with the ribosome and with some elements in the 3'UTR of mRNAs. However, what was not known was how Caf20 interacts with the ribosome, the elements on Caf20 required to interact with the ribosome and where Caf20 binds on the ribosome.

In view of the already set findings, this study investigated Caf20 regulation through screening its interactions with the eIF4E, mRNAs and ribosome.

The following objectives were addressed in this study

- To explore elements of Caf20 important for interacting with eIF4E, the ribosome and can dimerize.

- To determine where Caf20 binds on the ribosome
- To identify interacting partners of Caf20 through protein-protein interaction
- To assess more physiological roles of Caf20

Different molecular tools and assays employed gave an insight on how Caf20 binds with the eIF4E and the ribosomes, novel ribosome-interacting partners of Caf20 were assessed and identified and additional physiological roles of Caf20 were reported.

1.9 Thesis structure

The thesis is composed of 6 themed chapters. The theme for the remaining chapters has been structured as follows. The second Chapter will consider both the sources and the methods adopted in the course of this research. This would include the lists and sources of strains used, cell culture, different DNA recombinant manipulations used in bacterial and yeast transformations, yeast protein extractions and different tag-purifications for biochemical analysis. Chapter 2 also highlights the methods employed in screening ribosome association and a new technique adapted to carryout proteomics studies of crosslinked-Caf20 targets in whole and ribosome-rich extracts. Chapter 3 assesses Caf20 association with eIF4E, ribosome and between Caf20 molecules. It will discuss the function of Caf20 in relation to its structure. Special emphasis will be drawn to Caf20 interaction with the ribosome. Chapter 4 analyses the results of the different crosslinking experiments and addresses the Caf20 targets in crosslinked whole extracts and ribosome associated proteins. Chapter 5 is concerned with physiological validations of some ribosome-Caf20 targets and additional phenotypes of Caf20 functions. Chapter 6 gives a brief summary of the key findings of the research and discusses the findings with other reports. It discusses some results of unfinished experiments. It will present some of the researcher's ideas and personal suggestions in relation to the work and then puts together future plans for the research

Chapter 2

Materials and Methods

2.1 Bacterial and yeast strains used in this study

A number of strains were sourced or generated for this study. Copies of the strains used were saved in GP's research group -80°C with unique identification numbers.

2.1.1 List of bacteria plasmids

All bacterial plasmids used are high copy plasmids. The bacterial plasmids used in this study are enumerated in Table 2.1

Table 2.1 Bacterial Plasmid collections used for this research

Collection number	Genotype	Source
pAV1302	*LEU2/ 2µm*	High copy plasmid-LEU2 (Christianson et al., 1992).
pAV2421	*CAF20-FLAG/LEU2/2µ*	CAF20-FLAG sub cloned from PAV2229 into pRS425 using SalI and SpeI Castelli et al. (2015)
pAV2422	*CAF20^{m2}-FLAG/LEU2/2µ*	CAF20^{m2}-FLAG subcloned from PAV2230 into pRS425 using SalI and SpeI (Castelli et al., 2015)
pAV2475	*clone1 CAF20 Δ3-22-FLAG/LEU2/2µ*	Site directed mutagenesis of pAV2421
pAV2476	*clone2 CAF20 Δ3-22-FLAG/LEU2/2µ*	Site directed mutagenesis of pAV2421
pAV2477	*clone1 CAF20 Δ23-42-FLAG/LEU2/2µ*	Site directed mutagenesis of pAV2421
pAV2478	*clone2 CAF20 Δ23-42-FLAG/LEU2/2µ*	Site directed mutagenesis of pAV2421
pAV2479	*clone1 CAF20 Δ43-62-FLAG/LEU2/2µ*	Site directed mutagenesis of pAV2421
pAV2480	*clone2 CAF20 Δ43-62-FLAG/LEU2/2µ*	Site directed mutagenesis of pAV2421
pAV2481	*clone1 CAF20 Δ63-82-FLAG/LEU2/2µ*	Site directed mutagenesis of pAV2421
pAV2482	*clone2 CAF20 Δ63-82-FLAG/LEU2/2µ*	Site directed mutagenesis of pAV2421
pAV2483	*clone3 CAF20 Δ63-82-FLAG/LEU2/2µ*	Site directed mutagenesis of pAV2421
pAV2484	*clone1 CAF20 Δ83-102-FLAG/LEU2/2µ*	Site directed mutagenesis of pAV2421
pAV2485	*clone2 CAF20 Δ83-102-FLAG/LEU2/2µ*	Site directed mutagenesis of pAV2421
pAV2486	*clone3 CAF20 Δ83-102-FLAG/LEU2/2µ*	Site directed mutagenesis of pAV2421
pAV2487	*clone1 CAF20 Δ103-122-FLAG/LEU2/2µ*	Site directed mutagenesis of pAV2421
pAV2488	*clone2 CAF20 Δ103-122-FLAG/LEU2/2µ*	Site directed mutagenesis of pAV2421
pAV2489	*clone1 CAF20 Δ123-142-FLAG/LEU2/2µ*	Site directed mutagenesis of pAV2421
pAV2490	*clone2 CAF20 Δ123-142-FLAG/LEU2/2µ*	Site directed mutagenesis of pAV2421
pAV2491	*clone3 CAF20 Δ123-142-FLAG/LEU2/2µ*	Site directed mutagenesis of pAV2421
pAV2492	*clone1 CAF20 Δ143-161-FLAG/LEU2/2µ*	Site directed mutagenesis of pAV2421
pAV2493	*clone2 CAF20 Δ143-161-FLAG/LEU2/2µ*	Site directed mutagenesis of pAV2421
pAV2525	*clone1 CAF20 Δ3-48-FLAG/LEU2/2µ*	Site directed mutagenesis of pAV2421
pAV2526	*clone2 CAF20 Δ3-48-FLAG/LEU2/2µ*	Site directed mutagenesis of pAV2421
pAV2527	*clone1 CAF20 Δ49-107-FLAG/LEU2/2µ*	Site directed mutagenesis of pAV2421
pAV2528	*clone1 CAF20 Δ108-161-FLAG/LEU2/2µ*	Site directed mutagenesis of pAV2421
pAV2529	*clone1 CAF20 Δ3-107-FLAG/LEU2/2µ*	Site directed mutagenesis of pAV2421
pAV2530	*clone2 CAF20 Δ3-107-FLAG/LEU2/2µ*	Site directed mutagenesis of pAV2421
pAV2531	*clone3 CAF20 Δ3-107-FLAG/LEU2/2µ*	Site directed mutagenesis of pAV2421
pAV2532	*clone1 CAF20 Δ3-48,108-161-FLAG/LEU2/2µ*	Site directed mutagenesis of pAV2421
pAV2533	*clone1 CAF20 Δ49-161-FLAG/LEU2/2µ*	Site directed mutagenesis of pAV2421

pAV2534	*clone1 CAF20^{m2}Δ49-107-FLAG/LEU2/2μ*	Site directed mutagenesis of pAV2422
pAV2535	*clone2 CAF20^{m2}Δ49-107-FLAG/LEU2/2μ*	Site directed mutagenesis of pAV2422
pAV2536	*clone1 CAF20^{m2}Δ108-161-FLAG/LEU2/2μ*	Site directed mutagenesis of pAV2422
pAV2537	*clone2 CAF20^{m2}Δ108-161-FLAG/LEU2/2μ*	Site directed mutagenesis of pAV2422
pAV2538	*clone1 CAF20^{m2}Δ49-161-FLAG/LEU2/2μ*	Site directed mutagenesis of pAV2422

2.1.2 List of yeast strains

The yeast strains are in BY background. The *MATα* strains all derived from BY4742 and *MAT***a** strains are from BY4741. The strains sourced or generated for this research are outlined in the table below.

Table 2.2 Yeast strain lists used for this research

Collection number	Genotype	Construction
GP4158	*MATα his3Δ1 leu2Δ0 lys2Δ0 ura3Δ0*	Euroscarf BY4742 (Brachmann et al., 1998)
GP4789	*MATα his3Δ1 leu2Δ0 lys2Δ0 ura3Δ0 caf20Δ::KanMX4*	Cridge et al. (2010)
GP5094	*MATα his3-Δ1 leu2Δ0 lys2Δ0 ura3Δ0 CAF20-9MYC-HIS3MX6 [pYM19*]	Cridge et al. (2010)
GP5996	*MAT***a** *his3-Δ1 leu2Δ0 met15Δ0 ura3Δ0 Caf20::TAP::HIS3*	*Cridge et al. (2010)*
GP6323	*MAT***a** *leu2Δ0 ura3Δ0 met15Δ caf20Δ::KanMX4 cdc33-TAP*	*Castelli et al. (2015)*
GP6844	*MATα his3Δ1 leu2Δ0 ura3Δ0 caf20Δ::KanMX eap1Δ::KanMX pRS426[URA3 2μ] p[Eap1-HA LEU2]*	*caf20Δ* strain transformed with empty *[LEU2]* plasmid used in previous study (Castelli et al., 2015)
GP6846	*MATα his3Δ1 leu2Δ0 ura3Δ0 caf20Δ::KanMX eap1Δ::KanMX p[Caf20-FLAG URA3] p[Eap1-HA LEU2]*	*Δcaf20* strain transformed with wildtype *CAF20* plasmid used in previous study (Castelli et al., 2015)
GP6849	*MATα his3Δ1 leu2Δ0 ura3Δ0 caf20Δ::KanMX eap1Δ::KanMX p[Caf20^{m2} -FLAG URA3 2μm] p[Eap1-HA LEU2]*	*Δcaf20* strain transformed with *CAF20^{m2}* plasmid used in previous study (Castelli et al., 2015)
GP7164	*MATα his3Δ1 leu2Δ0 lys2Δ0 ura3Δ0 caf20Δ::KanMX4 pAV2421[CAF20-FLAG/LEU2]*	Transformation of GP4789 with pAV2421
GP7165	*MATα his3Δ1 leu2Δ0 lys2Δ0 ura3Δ0 caf20Δ::KanMX4 pAV2475[CAF20 Δ3-22-FLAG/LEU2]*	Transformation of GP4789 with pAV2475
GP7166	*MATα his3Δ1 leu2Δ0 lys2Δ0 ura3Δ0 caf20Δ::KanMX4 pAV2478[CAF20 Δ23-42-FLAG/LEU2]*	Transformation of GP4789 with pAV2478
GP7167	*MATα his3Δ1 leu2Δ0 lys2Δ0 ura3Δ0 caf20Δ::KanMX4 pAV2479[CAF20 Δ43-62-FLAG/LEU2]*	Transformation of GP4789 with pAV2479
GP7168	*MATα his3Δ1 leu2Δ0 lys2Δ0 ura3Δ0 caf20Δ::KanMX4 pAV2482[CAF20 Δ63-82-FLAG/LEU2]*	Transformation of GP4789 with pAV2482

GP7169	*MATα his3Δ1 leu2Δ0 lys2Δ0 ura3Δ0 caf20Δ::KanMX4 pAV2484[CAF20 Δ83-102-FLAG/LEU2]*	Transformation of GP4789 with pAV2484
GP7170	*MATα his3Δ1 leu2Δ0 lys2Δ0 ura3Δ0 caf20Δ::KanMX4 pAV2488[CAF20 Δ103-122-FLAG/LEU2]*	Transformation of GP4789 with pAV2488
GP7171	*MATα his3Δ1 leu2Δ0 lys2Δ0 ura3Δ0 caf20Δ::KanMX4 pAV2491[CAF20 Δ123-142-FLAG/LEU2]*	Transformation of GP4789 with pAV2491
GP7172	*MATα his3Δ1 leu2Δ0 lys2Δ0 ura3Δ0 caf20Δ::KanMX4 pAV2493[CAF20 Δ143-161-FLAG/LEU2]*	Transformation of GP4789 with pAV2493
GP7173	*MATα his3Δ1 leu2Δ0 lys2Δ0 ura3Δ0 caf20Δ::KanMX4 pAV2422[CAF20m2-FLAG/LEU2]*	Transformation of GP4789 with pAV2422
GP7174	*MATα his3Δ1 leu2Δ0 lys2Δ0 ura3Δ0 caf20Δ::KanMX4 pAV1302[LEU2]*	Transformation of GP4789 with pAV1302
GP7460	*MAT**a** his3-Δ1 leu2Δ0 met15Δ0 ura3Δ0 CAF20::TAP-HIS3+ pAV2421[CAF20-FLAG/LEU2]*	Transformation of GP5996 with pAV2421
GP7461	*MAT**a** his3-Δ1 leu2Δ0 met15Δ0 ura3Δ0 CAF20::TAP-HIS3+ pAV2525[CAF20 Δ3-48-FLAG/LEU2]*	Transformation of GP5996 with pAV2525
GP7462	*MAT**a** his3-Δ1 leu2Δ0 met15Δ0 ura3Δ0 CAF20::TAP-HIS3+ pAV2527[CAF20 Δ49-107-FLAG/LEU2]*	Transformation of GP5996 with pAV2527
GP7463	*MAT**a** his3-Δ1 leu2Δ0 met15Δ0 ura3Δ0 CAF20::TAP-HIS3+ pAV2528[CAF20 Δ108-161-FLAG/LEU2]*	Transformation of GP5996 with pAV2528
GP7464	*MAT**a** his3-Δ1 leu2Δ0 met15Δ0 ura3Δ0 CAF20::TAP-HIS3+ pAV2532[CAF20 Δ3-48, 108-161-FLAG/LEU2]*	Transformation of GP5996 with pAV2532
GP7465	*MAT**a** his3-Δ1 leu2Δ0 met15Δ0 ura3Δ0 CAF20::TAP-HIS3+ pAV2479[CAF20 Δ43-62-FLAG/LEU2]*	Transformation of GP5996 with pAV2479
GP7466	*MAT**a** his3-Δ1 leu2Δ0 met15Δ0 ura3Δ0 CAF20::TAP-HIS3+ pAV2482[CAF20 Δ63-82-FLAG/LEU2]*	Transformation of GP5996 with pAV2482
GP7467	*MAT**a** his3-Δ1 leu2Δ0 met15Δ0 ura3Δ0 CAF20::TAP-HIS3+ pAV2484[CAF20 Δ83-102-FLAG/LEU2]*	Transformation of GP5996 with pAV2484
GP7468	*MAT**a** his3-Δ1 leu2Δ0 met15Δ0 ura3Δ0 CAF20::TAP-HIS3+ pAV2488[CAF20 Δ103-122-FLAG/LEU2]*	Transformation of GP5996 with pAV2488
GP7832	*MAT**a** his3Δ1 leu2Δ0 met15Δ0 ura3Δ0 RpS24B::TAP::HIS3*	*Pavitt Lab Tap collection*
GP7833	*MAT**a** his3Δ1 leu2Δ0 met15Δ0 ura3Δ0 Rps27A::TAP::HIS3*	*Pavitt Lab Tap collection*
GP7834	*MAT**a** his3Δ1 leu2Δ0 met15Δ0 ura3Δ0 Rps27B::TAP::HIS3*	*Pavitt Lab Tap collections*
GP7835	*MAT**a** his3Δ1 leu2Δ0 met15Δ0 ura3Δ0 Rpl27A::TAP::HIS3*	*Pavitt Lab Tap collections*
GP7836	*MAT**a** his3Δ1 leu2Δ0 met15Δ0 ura3Δ0 Rpl27B::TAP::HIS3*	*Pavitt Lab Tap collections*
GP7837	*MAT**a** his3Δ1 leu2Δ0 met15Δ0 ura3Δ0 Rpl30::TAP::HIS3*	*Pavitt Lab Tap collection*
GP7838	*MAT**a** his3Δ1 leu2Δ0 met15Δ0 ura3Δ0 Rps27A::TAP::HIS3 caf20Δ::KanMX4*	Genomic knockout of Caf20 with G418
GP7839	*MAT**a** his3Δ1 leu2Δ0 met15Δ0 ura3Δ0 Rps27B::TAP::HIS3 caf20Δ::KanMX4*	Genomic knockout of Caf20 with G418

GP7840	*MAT***a** *his3Δ1 leu2Δ0 met15Δ0 ura3Δ0 Rpl27A::TAP::HIS3 caf20Δ::KanMX4*	Genomic knockout of Caf20 with G418
GP7841	*MAT***a** *his3Δ1 leu2Δ0 met15Δ0 ura3Δ0 Rps27A::TAP::HIS3 caf20Δ::KanMX4 pAV2421[CAF20-FLAG/LEU2]*	Isogenic strain- Transformation of GP7838 with pAV2421
GP7842	*MAT***a** *his3Δ1 leu2Δ0 met15Δ0 ura3Δ0 Rps27B::TAP::HIS3 caf20Δ::KanMX4 pAV2421[CAF20-FLAG/LEU2]*	Isogenic strain- Transformation of GP7839 with pAV2421
GP7843	*MAT***a** *his3Δ1 leu2Δ0 met15Δ0 ura3Δ0 Rpl27A::TAP::HIS3 caf20Δ::KanMX4 pAV2421[CAF20-FLAG/LEU2]*	isogenic strain- Transformation of GP7840 with pAV2421
GP7844	*MAT***a** *his3Δ1 leu2Δ0 met15Δ0 ura3Δ0 Rps27A::TAP::HIS3 caf20Δ::KanMX4 pAV1302[LEU2]*	Transformation of GP7838 with pAV1302
GP7845	*MAT***a** *his3Δ1 leu2Δ0 met15Δ0 ura3Δ0 Rps27B::TAP::HIS3 caf20Δ::KanMX4 pAV1302[LEU2]*	Transformation of GP7839 with pAV1302
GP7846	*MAT***a** *his3Δ1 leu2Δ0 met15Δ0 ura3Δ0 Rpl27A::TAP::HIS3 caf20Δ::KanMX4 pAV1302[LEU2]*	Transformation of GP7840 with pAV1302
GP7847	*MAT***a** *his3Δ1 leu2Δ0 met15Δ0 ura3Δ0 Rps27B::TAP::HIS3 caf20Δ::KanMX4 pAV2525[CAF20 Δ3-48-FLAG/LEU2]*	Transformation of GP7839 with pAV2525
GP7848	*MAT***a** *his3Δ1 leu2Δ0 met15Δ0 ura3Δ0 Rps27B::TAP::HIS3 caf20Δ::KanMX4 pAV2475[CAF20 Δ3-22-FLAG/LEU2]*	Transformation of GP7839 with pAV2475
GP7849	*MAT***a** *his3Δ1 leu2Δ0 met15Δ0 ura3Δ0 Rps27B::TAP::HIS3 caf20Δ::KanMX4 pAV2532[CAF20 Δ3-48, 108-161-FLAG/LEU2]*	Transformation of GP7839 with pAV2532
GP7850	*MAT***a** *his3Δ1 leu2Δ0 met15Δ0 ura3Δ0 Rpl27A::TAP::HIS3 caf20Δ::KanMX4 pAV2525[CAF20 Δ3-48-FLAG/LEU2]*	Transformation of GP7840 with pAV2525
GP7851	*MAT***a** *his3Δ1 leu2Δ0 met15Δ0 ura3Δ0 Rpl27A::TAP::HIS3 caf20Δ::KanMX4 pAV2422[CAF20m2-FLAG/LEU2]*	Transformation of GP7840 with pAV2422
GP7852	*MAT***a** *his3Δ1 leu2Δ0 met15Δ0 ura3Δ0 Rpl27A::TAP::HIS3 caf20Δ::KanMX4 pAV2532[CAF20 Δ3-48, 108-161-FLAG/LEU2]*	Transformation of GP7840 with pAV2532
GP7853	*MAT***a** *his3Δ1 leu2Δ0 met15Δ0 ura3Δ0 Rps24B::TAP::HIS3 pAV2421[CAF20-FLAG/LEU2]*	Transformation of GP7832 with pAV2421
GP7854	*MAT***a** *his3Δ1 leu2Δ0 met15Δ0 ura3Δ0 Rpl30::TAP::HIS3 pAV2421[CAF20-FLAG/LEU2]*	Transformation of GP7837 with pAV2421
GP7855	*MAT***a** *his3Δ1 leu2Δ0 met15Δ0 ura3Δ0 Rpl27B::TAP::HIS3 pAV2421[CAF20-FLAG/LEU2]*	Transformation of GP7836 with pAV2421
GP7856	*MAT***a** *his3Δ1 leu2Δ0 met15Δ0 ura3Δ0 Rps27A::TAP::HIS3 pAV2421[CAF20-FLAG/LEU2]*	Transformation of GP7833 with pAV2421
GP7857	*MAT***a** *his3Δ1 leu2Δ0 met15Δ0 ura3Δ0 Rps27B::TAP::HIS3 pAV2421[CAF20-FLAG/LEU2]*	Transformation of GP7834 with pAV2421
GP7858	*MAT***a** *his3Δ1 leu2Δ0 met15Δ0 ura3Δ0 Rpl27A::TAP::HIS3 pAV2421[CAF20-FLAG/LEU2]*	Transformation of GP7835 with pAV2421
GP7859	*MAT***a** *his3Δ1 leu2Δ0 met15Δ0 ura3Δ0 Rpl27A::TAP::HIS3 caf20Δ::KanMX4 pAV2475[CAF20 Δ3-22-FLAG/LEU2]*	Transformation of GP7840 with pAV2475
GP7860	*MAT***a** *his3Δ1 leu2Δ0 met15Δ0 ura3Δ0 Rps27B::TAP::HIS3 caf20Δ::KanMX4 pAV2422[CAF20m2-FLAG/LEU2]*	Transformation of GP7839 with pAV2422

2.2 Cell growth

2.2.1 Growth media preparations

Escherichia coli (*E. coli*) and yeast, *Saccharomyces cerevisiae* (*S. cerevisiae*) were cultured in appropriate media supplemented with the necessary nutrients required for its optimum growth. The recipes for the preparation of the different growth media and amino acids used are shown in the **Tables 2.3** and **2.4** respectively. Double distilled (ddH_2O) was used in all media, amino acid and buffer preparations.

2.2.1.1 Bacterial growth medium

2.2.1.1.1 Luria-Bertani, LB medium

LB medium is a very rich medium (containing peptone, yeast extract and NaCl) required for fast growth of bacteria and good plasmid yield. The LB medium is supplemented with antibiotics to inhibit other bacterial growth and enhance recombinant bacterial growth as the recombinant bacterial plasmid has a selective antibiotic resistance marker to maintain growth on antibiotic-containing medium. Carbenicillin is the choice antibiotic because it is more stable under lower pH and the by-product is less toxic when compared to ampicillin.

2.2.1.2 Yeast growth media

Yeast culture media are YPD/YPGE (Yeast peptone dextrose or glycerol/ethanol), SCD/SCGE (Synthetic complete dextrose or glycerol/ethanol) complete or SCD-dropout media and minimal media or SD/SGE (synthetic dextrose or glycerol/ethanol). The carbon source or many of the media could be either D-glucose or glycerol/ethanol. D-glucose was used for normal cell anaerobic growth while glycerol/ethanol was used for respiratory/fermentative growth. The components of the different media are described in **Table 2.3**.

2.2.1.2.1 Yeast peptone dextrose or glycerol/ethanol, YPD/YPGE medium

The YPD is a very nutrient rich medium to support yeast growth. It is regarded as the best medium as both auxotrophic and prototrophic yeast strains can be maintained on it. It can be used to maintain nonselective growth, culture cells for transformation and to richly sustain cells when a drug or stress is applied.

2.2.1.2.2 Synthetic complete dextrose or glycerol/ethanol, SCD/SCGE medium

The synthetic complete mix medium is a yeast extract medium containing all the twenty different amino acids and a nitrogenous base in the right proportion. However, it is not as rich as the YPD medium but adequate to sustain yeast growth.

2.2.1.2.3 Synthetic complete dextrose or glycerol/ethanol, SCD/SCGE 'drop out' medium

The SC- drop out medium is a medium lacking in one or more amino acids or nitrogen base of which a selective growth is required. The 'drop out' mix medium is used to maintain auxotrophic strains carrying plasmids and can be used to select transformed cells by dropping out the amino acid integrated in the recombinant DNA vector.

2.2.1.2.4 Minimal, SD medium

This is the yeast complete minimal nutrient requirement for the growth of yeast. It comprises dextrose, bacto-yeast extract (salt and vitamins) and a nitrogen source without any amino acid. Auxotrophic strain could be grown on a minimal medium by supplementing the lacking amino acids to the plate or liquid as selective medium (see **Table 2.4**). It can also be used as a selective medium to select transformed cells.

Table 2.3 Growth medium recipes

YPD medium[1]	**1 L**	**Source**
1% (w/v) Yeast extract	10 g	Melford Biolab
2% (w/v) Peptone	20 g	
2% (w/v) Dextrose-D-glucose	20 g	Fischer Scientific
2% (w/v) Agar (for plate), then autoclave	20 g	Melford Biolab
SCD medium[1]	**1 L**	**Source**
0.5% (w/v) Yeast nitrogen base without amino acid	6.9 g	Formedium
0.17% (w/v) Synthetic complete mixture	1.47 g	Formedium
2% (w/v) Dextrose-D-glucose	20 g	Fischer Scientific
2% (w/v) Agar (for plate), then autoclave	20 g	Melford Biolab
SCD drop out medium[2]	**1 L**	**Source**
0.5% (w/v) Yeast nitrogen base without amino acid	6.9 g	Formedium
Synthetic complete mixture 'drop out'[2]	-	Formedium
2% (w/v) Dextrose-D-glucose	20 g	Fischer Scientific
2% (w/v) Agar (for plate), then autoclave	20 g	Melford Biolab
SD medium	**1 L**	**Source**
0.5% (w/v) Yeast nitrogen base without amino acid	6.9 g	Formedium
2% (w/v) Dextrose-D-glucose	20 g	Fischer Scientific
2% (w/v) Agar (for plate), then autoclave	20 g	Melford Biolab
LB medium + Carb (adjust pH to 7.0 with NaOH)	**1 L**	**Source**
1% (w/v) Bacto-Tryptone	10 g	Melford Biolab

0.5% (w/v) Bacto-Yeast extract	5 g	Melford Biolab
1% (w/v) NaCl	10 g	Fischer Scientific
1.5% (w/v) Agar (for plate), then autoclave.	15 g	Melford Biolab
Add Carbenicillin antibiotics (100 µg/ml) prepared by dissolving 1 g of Carbenicillin powder in 10 ml ddH_2O. Aliquot into 500 µl and store at -20°C. Add stock to LB medium in ratio of 1:1000, store the LB + carb at 4°C	100 mg	Sigma
NZY⁺ Broth (adjust pH to 7.5 with NaOH)	**1 L**	
NZ amine (casein hydrolysate)	10 g	Sigma
Yeast extract	5 g	Melford Biolab
NaCl, then autoclave	5 g	Fischer Scientific
Add the following filer-sterilized supplements prior to use: 12.5 ml of 1 M $MgCl_2$, 12.5 ml of 1 M $MgSO_4$, 20 ml of 20% (w/v) glucose (or 10 ml of 2 M glucose)		

[1] *For respiratory media SCGE and YPGE, the 2%* (w/v) *D-glucose listed above was replaced with 1% (v/v) glycerol and 3% (v/v) ethanol added to the media after autoclaving.*

[2] *Formedium Synthetic complete drop-out mixture (SC-His, DSCK1003; SC-Leu-Ura, DSCK1017)*

Table 2.4 Amino acid preparation recipes

Amino acid	Stock Concentration	Molecular Weight	gm/100ml	ml/litre	ml/plate
Arginine	50 mM	210.7	1.054	10	0.2
	100 mM		2.107	5	0.1
Asparagine	300 mM	132.1	7.926	10	0.2
Histidine HCl	100 mM	209	2.09	3	0.1
Isoleucine	50 mM	131.2	0.656	10	0.2
Leucine	100 mM	131	1.31	20	0.2
Lysine	100 mM	182.7	1.827	10	0.1
Methionine	50 mM	149.2	.0746	20	0.15
Phenylalanine	30 mM	165.2	.0.5	10	0.2
Proline	100 mM	115.1	1.15	10	0.2
Serine	100 mM	105.1	1.05	10	0.2
Threonine	300 mM	119.1	3.57	5	0.1
Tryptophan*	40 mM	204.2	0.8	10	0.2
Tyrosine**	7 mM	181.2	0.127	10	0.2
Valine	50 mM	117.5	0.59	3.4	0.07
Uracil	20 mM	112.1	0.224	10	0.2

Store at room temperature (RT)

(Add few drops of NaOH to solubilize as necessary)

**Filter sterilize, do not autoclave and do not make more than 100ml as deteriorates in 2-3 months.*

***Filter sterilize, do not autoclave (keep frozen).*

2.2.2 Bacterial and yeast culturing

The *E. coli* plasmid were cultured at 37°C in Luria-Bertani (LB) liquid or plates supplemented with antibiotics (Table 2.3) in either 37°C static (Gallenkamp) or bacteria shaker incubator (Innova 4230, New Brunswick Scientific-Edison, NJ. USA) set at 180 rpm overnight. After which minipreparations of the bacterial plasmid DNA were made and stored at -20°C (**Table 2.1)**.

The yeasts were incubated at 30°C in either static (Gallenkamp) or yeast shaker incubator (Innova 44, New Brunswick Scientific, USA). For selective media, the amino acid on which the strains was selected against was used to sustain its growth and for gene marking.

2.2.3 Doubling time determination

Single colonies of yeast strains were grown to stationary phase and they were seeded into 50 ml culture at optical density, OD_{600} = 0.05. The yeast were grown at 30°C, 180 rpm in the shaker incubator for no less than 8 hours. To study the glucose (anaerobic) growth, strains were grown in growth media supplemented with 2% (w/v) glucose (YPD and SCD) as the carbon source and to study the respiratory (aerobic) growth phase, strains were grown in media with either 1% glycerol/3% ethanol (v/v) or 3% glycerol/1% ethanol (v/v) as its carbon source for YPGE and SCGE respectively. SGE media was not used to assess the strains. SGE has a limiting effect as the strains did not grow passed OD_{600} = 0.1. The OD_{600} readings were taken hourly with a spectrophotometer and the readings were used to plot the growth curve. Doubling times are calculated from the measurements in mid-log phase (OD_{600} between 0.2 and 0.6), deduced from the intercept of log exponential equation given as $y = Ae^{Bx}$. The doubling time given as: $Td = \frac{ln2}{B}$, *where* $ln2$ *is* 0.693 *and* B *is the coefficient of* x *from the exponential curve fitting equation.*

2.2.4 Storage of cell cultures

2.2.4.1 Bacterial cultures

The bacterial cultures were stored in plates for few weeks at 4°C or indefinitely at -80°C. To save at -80°C, two to five millilitres bacterial culture were grown overnight to saturation in LB + carb to maintain a plasmid. Sterile screw capped tubes were numbered and labelled sequentially with a unique pAV number (**Table 2.1**). 77 µl of DMSO plus 1 ml of the overnight culture were pipetted into the labelled sterile tube (Nunc® CryoTubes®, Thermo Fisher scientific) and frozen on dry ice. It was transferred to a storage box in the -80ºC freezer. The bacterial strains paper works were filed and saved electronically.

2.2.4.2 Yeast cultures

In the case of yeast storage, the yeast strains were numbered sequentially with a unique GP number (Table 2.2) to be used for storage in the -80^{o}C freezer. Sterile screw capped cryogenic vials were numbered with their names. 400 µl of 50% (v/v) glycerol (**Table 2.21**) was pipetted into each labelled tube and 800 µl of overnight culture was added and mixed together. The tubes were frozen on dry ice and transferred to -80°C in their appropriate box position.

2.2.5 Drug sensitivity assays and phenotypic analyses

Ability of yeast to grow in different media could be important when evaluating yeast phenotypes. Drugs were tested at different concentrations. Then the phenotypes were screened and scored. The sensitivity of the strains were ranked around 0 and 3 (>3 = normal growth, >2 = sensitive >1 = highly sensitive, 0 = no growth) or by calculating the diameter of zone of inhibition (in mm) around a filter disk.

2.2.5.1 Disc drug tests

Yeast strains were grown to stationary phase in SCD-L media and diluted to A_{600} of 0.3 in 12 ml of 0.6% (w/v) SCD-L/Agar broth (which was incubated at 37°C water bath to prevent setting before use). 3.5 ml of this broth was poured over 20 ml 2% (w/v) solid SCD-L/Agar plate of 90 mm x 16mm dimension. Sterilized filter discs made from Whatmann 3MM filter paper using a hole punch were placed round the quadrat of the 0.6% (w/v) SCD/Agar plate. 5 µl of each drug tested (**Table 2.5** below) was added to the centre of the filter disc and incubated at 30°C for 1 to 2 days. Images were captured in UVIDOC HD6 (UVITEC, Cambridge) with a ruler placed inside to serve as a guide to analyse and correct to actual size using ImageJ software. The diameter of zone of inhibition of each drug tested was determined and ranked. Controls used were water, DMSO and 100% (v/v) ethanol depending on the solvent used in the dilution of the drugs.

Table 2.5 Disc drug concentrations tested

Drug tested	Stock Concentrations (mg/ml)	Amount of stock used	Source
Cliquinol (5-Chloro-7-iodoquinolin-8-ol) in DMSO	2, 1, 0.75, 0.5, 0.15, 0.075, 0.025, 0.010	5 µl of stock	CAS: 130-26-7, Maybridge
Cycloheximide in DEPC-treated H_2O	10, 1, 0.010, 0.004, 0.002	5 µl of stock	A0879.0005, VWR
Paromomycin in 100% (w/v) ethanol	100, 50, 25, 5	5 µl of stock	CAS: 1263-89-4, Fisher BioReagent

2.2.5.2 Serial dilution growth assays 'Spot tests'

Yeast was grown overnight and diluted to A_{600} of 0.1. Yeast was serially diluted tenfold to prepare 10^{-1}, 10^{-2}, 10^{-3} and 10^{-4} cultures, and 2 µl of each spotted on the SCD-L agar plates. The spotted cultures were allowed to soak in and dry before incubation. Growths were recorded from day two of incubation. When a drug was used, the drug was added into the media, poured on plates; the plates were allowed to set and dried before spotting the yeast cells. The final concentration of different drugs added to media in SCD-L media used in growth inhibition spot tests is shown in **Table 2.6** below.

Table 2.6 Chemical concentrations used

Drug tested	Final concentrations on plate	Source
$CuSO_4$	2 mM – 5 mM	CAS Number: 7758-98-7, Sigma
Rapamycin	50 nM, 100 nM, 200 nM and 1 µM	CAS Number: 53123-88-9, Sigma
Paromomycin	18 mg/ml, 200 mg/ml	CAS:1263-89-4, Fisher BioReagent
Cycloheximide	10 µg/ml, 4 µg/ml, 2 µg/ml, 1 µg/ml, 0.5 µg/ml, 0.25 µg/ml	A0879.0005, VWR

2.2.6 Sterilization of equipment and reagents

2.2.6.1 Filtration sterilization

All the amino acid stock solutions and extraction buffers were sterilized through filtration over a membrane with 0.2 microns pore size to remove biological contaminants including bacteria, mould and yeast. The solution was passed through a 250 ml or 500 ml filtering unit connected to a vacuum pump under aseptic condition.

2.2.6.2 Autoclave sterilization

Flasks, growth media, replica cloths and some buffers were sterilized through sterilising in the autoclave (Priorclave). For growth media containing d-glucose, the autoclave was set to heat gradually to 115°C for 30 minutes to prevent degradation of the glucose. Other sterilisations were set at 126°C for 10 minutes.

2.3 Mutagenesis of DNA

The different DNA recombinations used in both bacterial plasmids and in the yeast for this research were described in this section.

2.3.1 Site-directed Mutagenesis (SDM) using plasmid DNA

2.3.1.1 Bacterial plasmid DNA extraction using 'Isolate II' plasmid minikit

SDM is a DNA manipulation to create specific changes in double stranded plasmid DNA by either deletion, insertion or substation. Bioline Isolate II plasmid minikit (Cat No: BIO-52056) was used to extract plasmid DNA following the kit manual. Briefly, the bacterial cells were first revived from -80^{o}C on LB + carb plate at 37^{o}C overnight. A colony was picked from the plate and incubated at 37^{o}C overnight in 2 ml LB + carb liquid media. The cells were pelleted for 30 seconds at 11,000 x g and supernatant discarded. The cells were lysed by mixing with 250 µl of buffer, P1 (containing RNAse) and 250 µl of buffer, P2. Lysate was incubated for 5 minutes at room temperature. Then, 300 µl of buffer, P3 added and mixed thoroughly by inverting 6-8 times. It was centrifuged for 5 minutes at 11,000 x g at room temperature to clarify lysate. The supernatant was transferred into a mini-spin column placed in a collection tube. The supernatant was spun for 1 minute at 11,000 x g and flow-through discarded. The silica membrane was washed by adding 600 µl of wash buffer PW2 (augmented with ethanol) to the column and it was centrifuged for 1 minute at 11,000 x g. Flow-through was discarded and the tube was centrifuged again for 2 minutes to remove all ethanol. The mini-spin column was transferred into a fresh 1.5 ml microcentrifuge tube. 50 µl of elution buffer, P, was added into the column to elute the DNA from the silica membrane and centrifuged for 1 minute at 11000 x g. Afterwards, the DNA concentration was quantified by Nanodrop (ThermoScientific) and it was stored at -20^{o}C freezer.

2.3.1.2 SDM, PCR and transformation of bacterial plasmids

2.3.1.2.1 SDM in Caf20 by deletions of 20 amino acids in series

The SDM through Polymerase chain reaction, PCR, was performed with QuikChange Lightning Site-Directed Mutagenesis kit (Catalog #210518, Agilent technologies) on wildtype *CAF20-FLAG* plasmid (*p*AV2421). The initial sets of Caf20 mutants were made up of small deletions of 20 amino acids. The first eight sets of primers were designed in an overlapping orientation by deleting 60 nucleotides (20 amino acids) base pairs (bp) consecutively of the *CAF20* open reading frame, ORF region starting from the 7^{th} bp (3^{rd} amino acid) designated as Δ1-Δ8. The first eight different mutant primer pairs designed for SDM and their expected products are listed in **Tables 2.7** and **2.8** respectively. The deleted nucleotides in the mutants are shown in the **Table 2.8**. The synthetic oligonucleotides were assessed for compatibility and sourced from the Sigma database (Sigma Oligos).

Table 2.7 Oligonucleotide primer pairs (Sigma Oligos) used in this study

Name	Nucleotide sequence	Length (Bases)	Tm °C	GC%
CAF20Δ1F	CACGACATGATCGATGCGGTGGAATTTAGAGCCATC	36	80	50
CAF20Δ1R	TTCCACCGCATCGATCATGTCGTGAAATTAAATAAAAG	38	75.8	37
CAF20Δ2F	GGAAGTTAATTTCGAAGAGTTTAACAGTCATCATGTTGG	39	71.7	36
CAF20Δ2R	GTTAAACTCTTCGAAATTAACTTCCAAAGTTAAACTTGG	39	68.5	31
CAF20Δ3F	CAACACTTGAAAGAGGGTAGACCAAAGATTAAGCACAAC	39	73.2	41
CAF20Δ3R	CTTTGGTCTACCCTCTTTCAAGTGTTGCAATTGCTTAAC	39	74.1	41
CAF20Δ4F	CTTCCCACCATCATACATTTGAAGCCAAGAAGAAGGG	37	76.9	46
CAF20Δ4R	GGCTTCAAATGTATGATGGTGGGAAGATCTTCTACGACC	39	76.6	46
CAF20Δ5F	CAGATGGTTGGTGCCCAACTTCTACTGTGCCAGTTGCTAC	40	80.2	53
CAF20Δ5R	CACAGTAGAAGTTGGGCACCAACCATCTGAATCGGTTGTAAC	42	79.3	48
CAF20Δ6F	GAAACAGAAACCACAAACAAAAATATTTCTTCCAACAGACC	41	73.5	34
CAF20Δ6R	GAAATATTTTTGTTTGTGGTTTCTGTTTCTTCTTCATC	38	69.3	29
CAF20Δ7F	GTCAAGCCAAATATTCTTGGTTTCAACGCATTTGCTGC	38	78.1	42
CAF20Δ7R	GAAACCAAGAATATTTGGCTTGACTTTTAAAGTTTC	36	68.1	31
CAF20Δ8F	GCGGACAAGCCATCCGGAGACTACAAGGACGACGATGAC	39	83.9	59
CAF20Δ8R	GTAGTCTCCGGATGGCTTGTCCGCAACAATATCTCTGG	38	79.3	53
Caf20A F	CACGACATGATCCATGTTGGTCATTTCGGTCGTAGAAG	38	81.4	47.3
Caf20A R	CCGAAATGACCAACATGGATCATGTCGTGAAATTAAATAAAAG	43	78.5	34.8
Caf20B F	GAGTTTAACAGTCATCCAGTTGCTACCATTGCCCAAGAAAC	41	78.8	43.9
Caf20B R	GGGCAATGGTAGCAACTGGATGACTGTTAAACTCTTCCTC	40	79.2	47.5
Caf20C F	CAACTTCTACTGTGTCCGGAGACTACAAGGACGACGATG	39	79.7	51.2
Caf20C R	GTAGTCTCCGGACACAGTAGAAGTTGGTGTGGTTTCTG	38	77.5	50
CAF20BC F	GAGTTTAACAGTCATTCCGGAGACTACAAGGACGACGATGAC	42	79.7	47.6
CAF20BC R	GTAGTCTCCGGAATGACTGTTAAACTCTTCCTCTTTCAAGTG	42	76.3	42.8
CAF20AB F	CACGACATGATCCCAGTTGCTACCATTGCCCAAGAAAC	38	82.7	50
CAF20AB R	GGGCAATGGTAGCAACTGGGATCATGTCGTGAAATTAAATAAAAG	45	80.3	40

CAF20A2 F	CATGTTGGTCATTTCGGTCGTAGAAG	26	69.9	46.1
CAF20A2 R	GATCATGTCGTGAAATTAAATAAAAGTTCTTAATCC	36	68.3	27.7
CAF20AB2 F	CCAGTTGCTACCATTGCCCAAG	22	69.4	54.5
CAF20AB2 R	GATCATGTCGTGAAATTAAATAAAAGTTCTTAATCC	36	68.3	27.7
CAF205'UTR F	CATTATTTGAGCTGTAACCTGAATATAGG	29	63.5	34.5
CAF203'UTR R	GAGTAAAAACTGTTTATTAAAAAAAATGTTATTCA	35	63.2	17.1

Table 2.8 Deleted nucleotides in the eight mutants

Primer pairs	Deleted nucleotides (amino acids)	Expected nucleotide product (Deleted nucleotides in bold letters)	Corresponding deleted amino acids
CAF20 Δ1	7-66 (residues 3-22)	ATGATC**AAGTATACTATCGATGAGCTTTTTCAACTGAAGCCAAGTTTAAC TTTGGAAGTTAATTTC**GATGCGGTGGAATTTAGAGCCATCATTGAAAAA GTTAAGCAATTGCAACACTTGAAAGAGGAAGAGTTTAACAGTCATCATGT TGGTCATTTCGGTCGTAGAAGATCTTCCCACCATCATGGTAGACCAAAGA TTAAGCACAACAAGCCTAAGGTTACAACCGATTCAGATGGTTGGTGCACA TTTGAAGCCAAGAAGAAGGGTAGTGGAGAAGATGATGAAGAAGAAACA GAAACCACACCAACTTCTACTGTGCCAGTTGCTACCATTGCCCAAGAAAC TTTAAAAGTCAAGCCAAATAACAAAAATATTTCTTCCAACAGACCTGCTG ATACCAGAGATATTGTTGCGGACAAGCCAATTCTTGGTTTCAACGCATTT GCTGCTTTGGAAAGTGAAGACGAAGACGACGAAGCATAA	KYTIDEL FQLKPS LTLEVN F
CAF20 Δ2	67-126 (residues 23-42)	ATGATCAAGTATACTATCGATGAGCTTTTTCAACTGAAGCCAAGTTTAACT TTGGAAGTTAATTTC**GATGCGGTGGAATTTAGAGCCATCATTGAAAAAG TTAAGCAATTGCAACACTTGAAAGAG**GAAGAGTTTAACAGTCATCATGT TGGTCATTTCGGTCGTAGAAGATCTTCCCACCATCATGGTAGACCAAAGA TTAAGCACAACAAGCCTAAGGTTACAACCGATTCAGATGGTTGGTGCACA TTTGAAGCCAAGAAGAAGGGTAGTGGAGAAGATGATGAAGAAGAAACA GAAACCACACCAACTTCTACTGTGCCAGTTGCTACCATTGCCCAAGAAAC TTTAAAAGTCAAGCCAAATAACAAAAATATTTCTTCCAACAGACCTGCTG ATACCAGAGATATTGTTGCGGACAAGCCAATTCTTGGTTTCAACGCATTT GCTGCTTTGGAAAGTGAAGACGAAGACGACGAAGCATAA	DAVEFR AIIEKVK QLQHLK E
CAF20 Δ3	127-186 (residues 43-62)	ATGATCAAGTATACTATCGATGAGCTTTTTCAACTGAAGCCAAGTTTAACT TTGGAAGTTAATTTCGATGCGGTGGAATTTAGAGCCATCATTGAAAAAGT TAAGCAATTGCAACACTTGAAAGAG**GAAGAGTTTAACAGTCATCATGTT GGTCATTTCGGTCGTAGAAGATCTTCCCACCATCAT**GGTAGACCAAAGA TTAAGCACAACAAGCCTAAGGTTACAACCGATTCAGATGGTTGGTGCACA TTTGAAGCCAAGAAGAAGGGTAGTGGAGAAGATGATGAAGAAGAAACA GAAACCACACCAACTTCTACTGTGCCAGTTGCTACCATTGCCCAAGAAAC TTTAAAAGTCAAGCCAAATAACAAAAATATTTCTTCCAACAGACCTGCTG ATACCAGAGATATTGTTGCGGACAAGCCAATTCTTGGTTTCAACGCATTT GCTGCTTTGGAAAGTGAAGACGAAGACGACGAAGCATAA	EEFNSH HVGHF GRRRSS HHH
CAF20 Δ4	187-246 (residues 63-82)	ATGATCAAGTATACTATCGATGAGCTTTTTCAACTGAAGCCAAGTTTAACT TTGGAAGTTAATTTCGATGCGGTGGAATTTAGAGCCATCATTGAAAAAGT TAAGCAATTGCAACACTTGAAAGAGGAAGAGTTTAACAGTCATCATGTTG GTCATTTCGGTCGTAGAAGATCTTCCCACCATCAT**GGTAGACCAAAGATT AAGCACAACAAGCCTAAGGTTACAACCGATTCAGATGGTTGGTGC**ACAT TTGAAGCCAAGAAGAAGGGTAGTGGAGAAGATGATGAAGAAGAAACAG AAACCACACCAACTTCTACTGTGCCAGTTGCTACCATTGCCCAAGAAACTT TAAAAGTCAAGCCAAATAACAAAAATATTTCTTCCAACAGACCTGCTGAT ACCAGAGATATTGTTGCGGACAAGCCAATTCTTGGTTTCAACGCATTTGC TGCTTTGGAAAGTGAAGACGAAGACGACGAAGCATAA	GRPKIK HNKPKV TTDSDG WC

CAF20 Δ5	247-306 (residues 83-102)	ATGATCAAGTATACTATCGATGAGCTTTTTCAACTGAAGCCAAGTTTAACT TTGGAAGTTAATTTCGATGCGGTGGAATTTAGAGCCATCATTGAAAAAGT TAAGCAATTGCAACACTTGAAAGAGGAAGAGTTTAACAGTCATCATGTTG GTCATTTCGGTCGTAGAAGATCTTCCCACCATCATGGTAGACCAAAGATT AAGCACAACAAGCCTAAGGTTACAACCGATTCAGATGGTTGGTGC**ACAT TTGAAGCCAAGAAGAAGGGTAGTGGAGAAGATGATGAAGAAGAAAC AGAAACCACA**CCAACTTCTACTGTGCCAGTTGCTACCATTGCCCAAGAAA CTTTAAAAGTCAAGCCAAATAACAAAAATATTTCTTCCAACAGACCTGCT GATACCAGAGATATTGTTGCGGACAAGCCAATTCTTGGTTTCAACGCATT TGCTGCTTTGGAAAGTGAAGACGAAGACGACGAAGCATAA	TFEAKK KGSGED DEEETE TT
CAF20 Δ6	307-366 (residues 103-122)	ATGATCAAGTATACTATCGATGAGCTTTTTCAACTGAAGCCAAGTTTAACT TTGGAAGTTAATTTCGATGCGGTGGAATTTAGAGCCATCATTGAAAAAGT TAAGCAATTGCAACACTTGAAAGAGGAAGAGTTTAACAGTCATCATGTTG GTCATTTCGGTCGTAGAAGATCTTCCCACCATCATGGTAGACCAAAGATT AAGCACAACAAGCCTAAGGTTACAACCGATTCAGATGGTTGGTGCACATT TGAAGCCAAGAAGAAGGGTAGTGGAGAAGATGATGAAGAAGAAACAG AAACCACA**CCAACTTCTACTGTGCCAGTTGCTACCATTGCCCAAGAAACT TTAAAAGTCAAGCCAAAT**AACAAAAATATTTCTTCCAACAGACCTGCTGA TACCAGAGATATTGTTGCGGACAAGCCAATTCTTGGTTTCAACGCATTTG CTGCTTTGGAAAGTGAAGACGAAGACGACGAAGCATAA	PTSTVP VATIAQ ETLKVK PN
CAF20 Δ7	367-426 (residue 123-142)	ATGATCAAGTATACTATCGATGAGCTTTTTCAACTGAAGCCAAGTTTAACT TTGGAAGTTAATTTCGATGCGGTGGAATTTAGAGCCATCATTGAAAAAGT TAAGCAATTGCAACACTTGAAAGAGGAAGAGTTTAACAGTCATCATGTTG GTCATTTCGGTCGTAGAAGATCTTCCCACCATCATGGTAGACCAAAGATT AAGCACAACAAGCCTAAGGTTACAACCGATTCAGATGGTTGGTGCACATT TGAAGCCAAGAAGAAGGGTAGTGGAGAAGATGATGAAGAAGAAACAG AAACCACACCAACTTCTACTGTGCCAGTTGCTACCATTGCCCAAGAAACTT TAAAAGTCAAGCCAAAT**AACAAAAATATTTCTTCCAACAGACCTGCTGAT ACCAGAGATATTGTTGCGGACAAGCCA**ATTCTTGGTTTCAACGCATTTGC TGCTTTGGAAAGTGAAGACGAAGACGACGAAGCATAA	NKNISS NRPADT RDIVAD KP
CAF20 Δ8	427-483 (residues 143-161)	ATGATCAAGTATACTATCGATGAGCTTTTTCAACTGAAGCCAAGTTTAACT TTGGAAGTTAATTTCGATGCGGTGGAATTTAGAGCCATCATTGAAAAAGT TAAGCAATTGCAACACTTGAAAGAGGAAGAGTTTAACAGTCATCATGTTG GTCATTTCGGTCGTAGAAGATCTTCCCACCATCATGGTAGACCAAAGATT AAGCACAACAAGCCTAAGGTTACAACCGATTCAGATGGTTGGTGCACATT TGAAGCCAAGAAGAAGGGTAGTGGAGAAGATGATGAAGAAGAAACAG AAACCACACCAACTTCTACTGTGCCAGTTGCTACCATTGCCCAAGAAACTT TAAAAGTCAAGCCAAATAACAAAAATATTTCTTCCAACAGACCTGCTGAT ACCAGAGATATTGTTGCGGACAAGCCA**ATTCTTGGTTTCAACGCATTTGC TGCTTTGGAAAGTGAAGACGAAGACGACGAAGCA**TAA	ILGFNA FAALES EDEDDE A

The SDM-PCR standard procedure consists of a synthesis of short oligonucleotide DNA primer pairs containing the desired deletion mutation. PCR thermal reaction using the two synthetic primers bearing desired deletion mutation and is complementary to the template DNA around the mutation site hybridizes with the DNA in the gene of interest. During the PCR, short fragments of DNA were amplified from the template DNA with the help of the mutated primers (**Fig 3.1A**). New DNA is synthesized by extending the primer by DNA polymerase. PCR reaction produced double stranded DNA molecules, consisting of an old template strand and a newly synthesized mutagenic strand with nicks in it, which are sealed by the components in the QuikChange lightning enzyme blend. Three reactions were performed ie one

positive control reaction with control primers and pWhitescripts template, a second negative control with no primers and double stranded DNA (dsDNA) vector carrying insert of interest i.e. *CAF20* and a third reaction with the mutagenic primer and *CAF20* vector DNA. The composition of Quikchange SDM-PCR reaction mixes for the eight primer pairs (**Table 2.9)** were set up and the thermal cycle program for the PCR runs is shown in **Table 2.10**. After PCR reactions, the products were resistriction digested with 2 µl of the kit's DpnI enzyme overnight at room temperature to denature the plasmid DNA. The digested PCR products were then resolved on 1% (w/v) agarose gel electrophoresis (**Table 2.21**) to ascertain successful amplification of products and cleavage by DpnI.

Table 2.9 Quikchange SDM-PCR reaction mix (Agilent technologies)

Reagent/solution	Each sample mix	Control (+ve) mix	Control (-ve) mix
Quikchange lightning enzyme	1 µl	1 µl	1 µl
Reaction buffer	5 µl	5 µl	5 µl
dNTP mix	1 µl	1 µl	1 µl
Quiksolution reagent	1.5 µl	1.5 µl	1.5 µl
Primer 1(125 ng)	1.25 µl oligonucleotide forward primer	1.2 5µl quikchange control primer 1	-
Primer 2 (125 ng)	1.25 µl oligonucleotide reverse primer	1.25 µl quikchange control primer 2	-
Plasmid DNA template	1 µl (100 ng) - pAV2421	5 µl of pWhitescript 4.5 kb control template (5 ng/µl)	1µl (100 ng/µl) - pAV2421
ddH2O	38 µl	34 µl	40.5 µl
Final Volume	50 µl	50 µl	50 µl

Table 2.10 Quikchange SDM-PCR thermal cycles

Cycles	Step	Temperature	Time
1	Denaturation	95°C	2 minutes
20	Denaturation	95°C	20 seconds
	Annealing	60°C	10 seconds
	Extension	68°C	6 minutes
1	Final extension	68°C	5 minutes
	Stop	4°C	hold

2.3.1.2.2 Transformation of bacterial plasmids

All the mutated plasmids were transformed into XL10-GOLD ultracompetent cells. The ultracompetent cells from -80°C were thawed on ice and 45 µl aliquots made in chilled 14 ml BD Falcon polypropylene round-bottom tube for each sample and controls. Then,

2 µl of β-mercaptoethanol was added to each aliquot, swirled and incubated on ice for 2 minutes. 2 µl of the Dpn1-treated DNA for each sample and control reaction was added to the aliquots and incubated on ice for 30 minutes. Each tube mixture was heat shocked in a 42°C water bath for 30 minutes, followed by incubation on ice for 2 minutes. 500 µl of preheated (42°C) NZY^+ (recipe in **Table 2.3**) was added and incubated at 37°C for 1 hour with shaking at 180-250 rpm. Each mixture was plated on LB agar plate supplemented with carbenicillin and incubated at 37°C overnight. For a successful transformation, colonies were expected to appear only on transformed samples and positive control plates but not on the negative control plates.

2.3.1.2.3 SDM by large deletions of Caf20

Along the line of analysing Caf20 association with the ribosome, further larger deletions of Caf20 residues were made following three possible domains predicted from homolog alignments of related yeast species obtained from the Jpred4 secondary structure prediction server (http://www.compbio.dundee.ac.uk/jpred/). The three regions defined for Caf20 named: regions A, B and C were based on the amount of α helices and beta sheets. SDM are performed by knocking out each of the regions or two out of the three regions. When 'A' region is deleted with regions 'B' and 'C' intact, the mutant is regarded as ΔA and when two regions, 'A' and 'B', are deleted leaving only the 'C' region, the mutant is referred as ΔAB. Also, a similar set of mutants were created in Caf20m2 plasmid, labelled as ΔBm2, ΔCm2 and ΔBCm2. With SDM in *Caf20wt-FLAG* plasmid (*pCaf20-FLAG*), the mutants generated from it have ***wt*** at the end of the name whereas ^{m2} is attached to the name if the mutant is made from *Caf20^{m2}-FLAG* plasmid (*pCaf20m2-FLAG*). T**able 2.7** showed the primer combinations used to generate the mutants. The composition of the amino acid residues of the expected mutants are listed in **Table 2.11**.

Table 2.11 Composition of the deleted residues of the large Caf20 mutants

Caf20 construct	Amino acid deleted	Deleted Amino acid sequence	PI value	SDM-PCR method & annealing temperature	Expected molecular weight (KDa)	PI value
Wt	-	-	-	-	20.902	4.97
ΔA	3-48	KYTIDELFQLKPSLTLEVNFDAVEF RAIIEKVKQLQHLKEEEFNSH	5.17	Inverse PCR and DNA ligation	15.401	4.90
ΔBwt	49-107	HVGHFGRRRSSHHHGRPKIKHN KPKVTTDSDGWCTFEAKKKGSG EDDEEETETTPTSTV	8,15	Quikchange SDM-PCR (60°C)	14.265	4.36
ΔBm2	49-107	HVGHFGRRRSSHHHGRPKIKHN KPKVTTDSDGWCTFEAKKKGSG EDDEEETETTPTSTV	8.15	Quikchange SDM-PCR (60°C)	14.130	4.36
ΔCwt	108-161	PVATIAQETLKVKPNNKNISSNRP ADTRDIVADKPILGFNAFAALESE DEDDEA	4.34	Quikchange SDM-PCR (55°C)	15.079	5.32
ΔCm2	108-161	PVATIAQETLKVKPNNKNISSNRP ADTRDIVADKPILGFNAFAALESE DEDDEA	4.34	Quikchange SDM-PCR (55°C)	14.945	5.32
ΔAB	3-107	KYTIDELFQLKPSLTLEVNFDAVEF RAIIEKVKQLQHLKEEEFNSHHVG HFGRRRSSHHHGRPKIKHNKPKV TTDSDGWCTFEAKKKGSGEDDE EETETTPTSTV	6.47	Inverse PCR and DNA ligation	8.763	4.08
ΔAC	3-48; 108-161	KYTIDELFQLKPSLTLEVNFDAVEF RAIIEKVKQLQHLKEEEFNSH PVATIAQETLKVKPNNKNISSNRP ADTRDIVADKPILGFNAFAALESE DEDDEA	6.47	Quikchange SDM-PCR (60°C)	9.578	5.40
ΔBCwt	49-161	HVGHFGRRRSSHHHGRPKIKHN KPKVTTDSDGWCTFEAKKKGSG EDDEEETETTPTSTVPVATIAQET LKVKPNNKNISSNRPADTRDIVA DKPILGFNAFAALESEDEDDEA	5.85	Quikchange SDM-PCR (60°C)	8.442	4.38
ΔBCm2	49-161	HVGHFGRRRSSHHHGRPKIKHN KPKVTTDSDGWCTFEAKKKGSG EDDEEETETTPTSTVPVATIAQET LKVKPNNKNISSNRPADTRDIVA DKPILGFNAFAALESEDEDDEA	5.85	Quikchange SDM-PCR (60°C)	8.308	4.38

2.3.1.2.4 SDM by inverse polymerase chain reaction, PCR

Some of the large deletion mutants were difficult to knock down following the method described in section 2.3.1.2.1. So, there were some adjustments to the PCR annealing temperatures or a different primer design was made, inverse PCR and DNA ligation technique were adopted to create the mutants (**Table 2.11**). Inverse PCR is a technique where a whole pRS425 plasmid instead of short fragments is amplified, by deletions of fragments, to create constructs. The primers were designed to flank the region to be

deleted so that the primers amplify the entire complementary sides of the plasmid DNA to produce linear plasmids that can be ligated together. So that during the ligation step, the deleted region would be lost from the parent plasmid. Primers CAF20A2 F, CAF20AB F and their reverse primers were made to generate ΔA and ΔAB respectively (**Table 2.7**). High Fidelity (HF) Phusion PCR kit (Phusion™ High-Fidelity PCR master mix; F-531S, Finnzymes) was used to amplify 10 ng/µl DNA templates of both plasmids (*pAV2421* and *pAV2422*). The PCR reaction mix and run were set as described in **Tables 2.12** and **2.13** below.

Table 2.12 HF Phusion SDM-PCR reaction mix (F-531S, Finnzymes)

Reagent/solution	Each sample mix	Control mix	Final concentration
Plasmid DNA template (10ng/µl)	1 µl (10 ng/µl) - pAV2421 or pAV2422	1µl (10 ng/µl) - pAV2421 or pAV2422	10 ng
HF Phusion Mix (2x)	25 µl	25 µl	1X
oligonucleotide forward primer (10 µM)	2.5 µl	-	0.5 µM
oligonucleotide reverse Primer (10 µM)	2.5 µl	-	0.5 µM
ddH_2O	19 µl	24 µl	
Final Volume	50 µl	50 µl	

Table 2.13 HF Phusion SDM-PCR thermocycling

Cycles	Step	Temperature	Time
1	Denaturation	98°C	45 seconds
35	Denaturation	98°C	10 seconds
	Annealing	60°C	25 seconds
	Extension	72°C	3 minutes
1	Final extension	72°C	10 minutes
	Stop	4°C	hold

After thermocycling, ten microliter (10 µl) of the PCR product was electrophoresed on 0.7% (w/v) agarose set at 80 Volts for 45 minutes to confirm PCR amplification. After confirmation of amplification, the remaining PCR product was purified with Isolate II PCR and gel kit (Cat No: BIO-52059, Bioline) following the manufacturer's procedure. The concentration of purified product was measured in a Nanodrop spectrophotometer. The PCR product was incubated at 70°C for 10 minutes and quickly placed on ice to prevent reannealing of the ends of the DNA in preparation for phosphorylation. The phosphorylation reaction mix was done in a 20 µl volume comprising 200 ng of DNA mixed with water, 1 µl of T4 polynucleotide kinase (New

England Biolabs), and 2 µl of 10X T4 DNA ligase buffer (New England Biolabs). 17 µl of the phosphorylation reaction mix is added to each PCR sample and the mixture was incubated at 37°C for 40 minutes. After phosphorylation, 1 µl of T4 ligase (New England Biolabs), was added and incubated for 2 hours at room temperature to ligate the plasmid DNA to form a Circular plasmid. Once the ligation step was completed, 2 µl of Dpn1 enzyme was added and left at 37°C overnight to digest the parent DNA. 4 µl of the Dpn1 digested sample was then transformed into ultra-competent cells following the procedure in section 2.3.1.2.2.

2.3.1.3 Restriction enzyme digestion

The segment of Caf20 constructs on pRS425 plasmid (Appendix 1) can be cut out and its length checked. The Caf20 gene on the plasmid is flanked by two restriction sites; SpeI (A/CTAGT) and EcoRI (G/AATTC).

After plasmid transformation, 3 – 5 colonies of the transformed plasmids were picked and their minipreps made as described in section 2.3.1.1. The miniprep samples were digested with restriction enzymes to check for proper deletions before they are sent out for sequencing. In summary, for each restriction digest reaction, a 20 µl volume reaction was set comprising 2 µl of 10X restriction buffer, 1 µl of each restriction enzyme (SpeI and EcoRI), 5 µl of each miniprep and 11 µl of ddH2O. This was incubated at 37°C for 1 hour. Then the digested sample was confirmed on 1% (w/v) agarose gel for the right deletion as against an untransformed plasmid. Three samples with the right deletions were sent for sequencing as described in the section 2.3.1.4 below.

2.3.1.4 Sequencing of bacterial plasmids

Three colonies were picked from each of my sample transformation plate (their minipreps) and deletions confirmed by Sanger Sequencing technique (GATC, Biotech). The *p*[*CAF20-FLAG*] 3'UTR forward primer or T7 vector was used for the sequencing. The sequenced chromatograms were viewed with BioEdit and FinchTV software (http://www.geospiza.com/finchtv/finchtv-client/index.htm) and pairwise comparison between two sequenced datasets performed through nucleotide BLASTN on the NCBI Database (blast.ncbi.nlm.nih.gov/bl2seq/wblast2.cgi) and Serial cloner software (Appendix I). *E. coli* containing each mutant plasmid with the correct deletions and good chromatogram were stored in -80^{o}C freezer.

2.3.2 Yeast transformation with lithium acetate

Single colonies of yeast strains to be transformed were grown overnight in liquid media in 30°C incubator with shaker set at 180 rpm. The overnight culture OD_{600} was taken and 0.1 OD_{600} is inoculated back to a 50 ml YPD media and grown for about 6 hours until the OD_{600} reaches 0.5-1. The culture is centrifuged for 5 minutes at 5000 rpm using 50 ml "Falcon" tubes. Cell pellets were washed with 1 ml of sterile water and again in 1 ml of 0.1 M lithium acetate/TE, (LiAc/TE). The preparation of the transformation buffers are shown in **Table 2.14** below. Following the second wash, pellets were resuspended in 0.1 M LiAc/TE ready to be transformed. The transformation mix was added in this order: plasmid DNA (approximately 1 μg); denatured single stranded carrier DNA (50 μg i.e. 5 μl of 10 mg/ml); 50 μl of the LiAc/TE yeast cell suspension; 250 μl of 40% (w/v) PEG 3550/0.1 M LiAc. The mixture was vortexed. At the same time, a control that included all the transformation mix except the plasmid DNA was also set up. The tubes were incubated at 30°C for 30 minutes with agitation. After that, the tubes were heat shocked in a water bath set at 42°C for 15 minutes. After heat shocking, the cells were pelleted at high speed (14,000 x g) for 30 seconds in a microtube centrifuge and the PEG removed by pipetting off the supernatant leaving the pellet. The yeast pellets were resuspended in ~ 200 μl SD media. The mixtures were plated out on SD plate supplemented with the appropriate nutrients leaving out the nutrient to be complemented by the plasmid and incubated for three days at 30°C. Formation of colonies on the transformation plates with plasmids and not on the negative controls indicate that the transformation has worked. The transformants were streaked in three replicates for correct phenotype screening. The growths of the colonies were expected to be of uniform size as the parent strains. A colony from one of the replicates was stored at -80°C as backup after the plasmid expression has been verified.

Table 2.14 Yeast transformation buffers

Buffer Solution	Protocol
10xTE Buffer (100 mM Tris-HCl, 10 mM EDTA, pH 8.0)	Weigh 3.152 g of Tris-HCl and 0.745 g of EDTA. Make up to 200 ml. Filter sterilize and store at RT.
TE buffer (10 mM Tris-HCl, 1 mM EDTA)	Take 50 ml of 10xTE and add 450 ml of ddH_2O.
1 M LiAc/TE buffer	Stir 25.5 g of Lithium acetate to 250 ml TE buffer. Filter sterilize and store at room temperature.
0.1 M LiAc/TE buffer	Mix 5 ml of sterile 1M LiAc/TE with 45 ml of sterile TE
44% (w/v) polyethylene glycol (PEG)	Dissolve 110 g of PEG3550, 155 ml of TE buffer. Bring up to 250 ml. Filter sterilize and store at room temperature.
40% (w/v) PEG/0.1M LiAc	Mix 45 ml of sterile 44% (w/v) PEG with 5 ml sterile 1 M LiAc/TE buffer

2.3.3 Mutagenesis of yeast genomic DNA

Mass spectrometry was used to identify ribosomal proteins (RPs) that crosslink with Caf20. The TAP-tagged strains for each of these RPs were taken from the strain collection and Caf20 was deleted from each to assess the effect of its loss. The TAP-tagged strains of either isoforms of the RPS27 genes (*RPSS27A*, *RPS27B*) were revived from the -80°C freezer on YPD plates. Then, Caf20 was deleted from each strain using a PCR-based gene deletion. In summary, the yeast DNA of *caf20*Δ strain (GP4789) with KanMX cassette (*Kan* gene) was extracted using Promega Wizard Genomic DNA purification kit (Cat No: A1125). Then, the Phusion® High-Fidelity DNA Polymerase (Catalog # M0530S, New England BioLabs) of was used to PCR up the region of Caf20 deleted and replaced with a KanMX cassette gene following the kit's protocol. The KanMX gene region was amplified through PCR with two primers (CAF20 5'UTR F and Caf20 3'UTR R, **Table 2.7**) designed to synthesize only the 5'UTR region of Caf20 upstream to the start codon and the 3' UTR downstream the stop codon. 100 ng of the genomic yeast DNA (strain GP4789) was used for the PCR reaction. The PCR product (15 µl) was resolved on 2% (w/v) agarose gel at 120V for 60 minutes and a single band of about 1.8 kb suggested the right product has been amplified. The concentration of the PCR DNA band was compared against the genomic DNA of GP4789 of known concentration. The dilute PCR products were concentrated with 3 M sodium acetate, pH 5.2 to a final concentration of 0.3 M sodium acetate and precipitated in ethanol. Afterwards, the DNA is resuspended in small volumes of TE buffer. The transformation was performed as above except that 50 µg of the PCR product was used for successful deletion of Caf20 from the gene locus for three of the ribosomal protein strains (i.e. approx. 15 µg for each strain). Towards the final step of the transformation after the PEG had been remove, the yeast pellet is resuspended in 1 ml of YPD and allowed to grow for at least 4 hours or overnight. All of the transformation mix (1ml) was plated on YPD plate supplemented with 200 µg/ml G418 disulfate salt (A1720, Sigma) for KanMX cassette selection. The plates were left to grow for up to 5-7 days. A replica of the G418 plate was made on a nutrient selective plate for proper selection of G418 transformants. Caf20 replacement from the gene locus was confirmed through western blotting of total extracts of G418 transformants.

2.4 Yeast protein extraction and identification

2.4.1 'Rough' protein extractions using Laemmli sample buffer

A 'rough' protein extraction with SDS sample buffer (recipe in **Table 2.15**) was used for total protein extraction to check for gene expression of yeast transformants. The yeast cultures were grown from OD_{600} of 0.1 to OD_{600} of 2 at 30°C. The cells are pelleted and resuspended in 30 µl of 2x Laemmli SDS loading dye. The tubes were boiled in 95°C heat block for 1 minute to denature proteases. A 0.2 ml PCR cap full acid washed glass beads (G8772, Sigma) was added to the tubes with the yeast pellets placed on wet ice. The yeasts were lysed 3 x 20 seconds at 4°C (40 seconds rest on ice between beats). After grinding, 70 µl of 2x Laemmli loading dye was added, boiled for 5 minutes and 10 µl was loaded on an resolving Acrylamide Electrophoresis Gel; NuPAGE 4% - 12% (w/v) Bis-Tris polyacrylamide precast protein gel (Life Technologies) or Novex 10-20% (w/v) Tricine Protein Gels (Invitrogen) for mutant proteins of very low molecular weight. Standard ladders, 250 kDa (Precision plus Protein™ All blue standard, BIO-RAD, USA) was used as protein marker. The protein samples were resolved either at 200 volts for 50 minutes on Bis-tris gels or at 120 volts for 120 minutes on tricine gels. The resolved gel was stained in Coomassie blue stain (Instant blue) and left in stain for at least 1 hour. The stained SDS-PAGE gel image was taken with UV transilluminator (GelDoc-It2 Imager, UVP; Cambridge).

2.4.2 Yeast cryogenic grinding with 6870 Freezer Miller (Spex)

Large cell cultures can be harvested, lysed in a freezer mill and stored at -80°C for long term usage. At least a litre of yeast cell culture was grown to exponential phase of OD_{600} 0.6 at 30°C. The cells were poured into 1 L Beckman bottle and pelleted at 6,000 rpm for 5 minutes in a High Speed Fixed Angle Rotor (JLA8.1000), floor standing centrifuge (Avanti J20). The cell pellet was resuspended in small volume in a growth medium with 3X glucose and 2X amino acids to prevent induction of cell stress responses. It was centrifuged at maximum speed (Sigma centrifuge) for 5 minutes 4°C in a 50 ml Falcon. The Falcon tubes were snap freeze in liquid nitrogen and stored at -80°C. The frozen cells were transported from -80°C freezer in liquid nitrogen and transferred into a cryogenic grinding tube submerged in liquid nitrogen. The cryogenic tubes were ground in liquid nitrogen inside a Freezer Mill (#6870, Spex) set at 3 cycles (2 minutes per cycle

and 2 minutes rest). The ground yeast is transferred into a 50 ml Falcon and stored at -80°C until needed.

2.4.3 Quantification of protein concentration with Bradford reagent

Braford assay (Bradford, 1976) was used to quantify the total protein concentrations. The reagent contains coomassie dye which binds proteins at OD_{595}. The Bradford reagent (Bio-Rad) was diluted to a ratio of 1:5 concentration. The BSA albumin at concentrations 0.031 – 2 mg was used with the diluted Bradford reagent to generate a protein concentration standard curve. Total extracts of the strains were diluted in ten folds (5 µl in 50 µl), then 5 µl of the dilution was mixed with 1 ml of Braford and allowed to stand for 5 minutes. The absorbance was taken at OD_{596} with a spectrophotometer and the reading was used to work out the concentration of the protein (in mg/ml) normalized with the standard curve value.

2.4.4 Immunoprecipitation of tagged proteins

2.4.4.1. FLAG-tagged protein affinity purification

Immunoprecipitation (IP) of FLAG-tagged proteins was carried out with Anti-FLAG (R) M2 magnetic beads (Sigma, M8823-5ML). A 50 - 100 ml culture was grown at 30°C to exponential phase of 0.6-0.8. The culture was then transferred into 50 ml Falcon tube and spun at 5,500 x g for 5 minutes, 4°C. The cells were washed in 1ml of chilled IP lysis buffer of a given salt concentration with protease inhibitor added just before use (**Table 2.15**) and pellet at 5,500 x g for 5 minutes, 4°C. The cells were resuspended in 600 µl of chilled lysis buffer and lysed with 500 µl of acid washed glass beads at 6 x 20 seconds with 1 minute rest on ice between beats. Centrifuged first at maximum speed (16100 x g) for 4 minutes to separate extract from beads into a fresh tube and a second time at maximum speed for 20 minutes, 4°C. Total protein was quantified with Bradford (see section 2.4.3). FLAG magnetic beads in the bottle were mixed to homogenise its content and a wide orifice tip made by cutting about 1 cm off the pipette tip was used to dispense 50 µl of FLAG magnetic resin into Eppendorf tubes placed on a magnetic bar (Invitrogen). The buffer used to preserve the resin was removed and the resin washed twice with 600 µl of IP lysis buffer per wash. 1 mg of the total extract was diluted in 500 µl IP lysis buffer. Part of the total extract was saved as input sample for western blotting and the rest transferred to the beads for affinity purification. This was incubated for 1-2 hours on a rotator set at 30 rpm, 4°C. After binding, part of the suspension was

saved in a new tube as the unbound protein fraction. The beads were washed four times; two washes in 600 µl of IP lysis buffer and two washes in 600 µl of IP_{low} buffer (**Table 2.15**). The bound proteins were eluted from the beads with 50 µl of low salt buffer and 5 µl of 4 mg/ml 3X FLAG peptide (Sigma F4799), so that the final concentration was 200 µg/ml. The elution was done for either 4 hours or overnight incubation on the rotator at 4°C (boiling the beads in sample buffer releases the light chain of the IgG which interferes with the signal of our protein of interest). The eluted fraction was transferred to a new tube and stored at -20°C, to be used for SDS-PAGE and western blotting. The beads were boiled in sample buffer to assess what was left on beads after eluting with 3X FLAG peptide. SDS-PAGE and western blotting were performed on the 15µl each of input and eluted fractions for further analysis and probed with different antibodies listed in **Table 2.16**.

Alternatively, a large culture was grown, harvested and lysed in liquid nitrogen as described in section 2.4.2 above. To carry out a largescale IP, for every 1g of cryogenic ground cell, 2 ml of IP lysis buffer was added to it and it is left to thaw on ice. The tube was centrifuged for 10 minutes at 5,500 x g, 4°C. The lysate was shared into different 5ml Eppendorf tubes without disturbing the pellet and spun at 16,100 x g for 20 minutes. The protein concentration was measured and processed accordingly. An additional preclearing step with agarose bead may be added to help reduce non-specific binding before incubating with to the FLAG magnetic beads.

2.4.4.2 TAP-tagged protein affinity purification

Here, TAP-magnetic beads, *DYNAL Dynabeads Pan Mouse IgG, Monoclonal* (Invitrogen 11041) was used for the TAP- affinity purification. The method was identical to the FLAG IP described above until the final wash. The bound protein was then eluted from the beads by boiling in 50 µl of Laemmli sample loading buffer (see **Table 2.15**).

2.4.4.3 MYC-tagged protein affinity purification

MYC-tagged protein purification was performed with MYC-agarose; *EZview Red Anti-C-MYC Affinity Gel* (Part number: E6654, Sigma). Different buffers and resins were used for this method. The buffer used was 1X LOLA (20 mM Tris-HCl, 140 mM NaCl, 1 mM MgCl, 10U/ml RNAsein (Promega RNAsin Plus), phospho inhibitors (1000X, 100X), protease inhibitor, 0.5% (v/v) NP40 (Igepal CA-420)). As it was not a

magnetic resin but an agarose resin, the agarose was spun at a low speed (2,000 x g), 0°C for 1 minute. The steps are similar as in FLAG-tag purification above but with small adjustments. The agarose beads were washed initially for five times before binding with the extract and five times after IP during the wash steps. After the washes, the protein can be eluted by boiling in 2X sample buffer or by eluting in low glycine pH (0.2 M glycine, pH 2.6)

2.4.5 Sodium dodecyl sulfate polyacrylamide gel electrophoresis (SDS PAGE) and staining

SDS PAGE is used to separate proteins based on their molecular weight. SDS removes the secondary structures in proteins and give negative charge to proteins so the distance travelled by protein is equivalent to the size of the protein and hence molecular wight. SDS-PAGE is a denaturing electrophoresis where the charged proteins are masked when bound by the SDS detergent giving those proteins negative charges, enabling them to separate on the acrylamide sieving matrix (gel) based on the size of the polypeptide chains and not by charged ions. Samples are prepared for SDS-PAGE by mixing protein extracts with 1X SDS sample buffer (**Table 2.15**) at a final protein concentration of 1-5 µg/µl. Samples were boiled at 95°C for 5 minutes to denature the proteins by breaking the disulphide bonds in the proteins and disrupt the protein structures. 10 - 15 µl of each sample was loaded onto the gel. Standard protein markers, 250 kDa (Precision plus Protein^{TM} All blue standard, BIO-RAD, USA) was used as guide to measure the sizes of the migrating proteins. The SDS-PAGE gel is made of the stacking and resolving gels.The system is set up in a discontinuous buffer system in which the buffer in the gel and the tank are different in which the stacking gel has pH 6.8 buffered by Tris-HCl, a resolving gel buffered to pH 8.8 by Tris-HCl and a running (electrode) buffer at pH 8.3 with Tris-Glycine. The stacking gel has a low concentration of acrylamide and the resolving (separation) gel has a higher concentration of acrylamide capable of retarding the movement of the proteins. All protein electrophoresis performed in this study used precast NuPAGE Bis-Tris SDS PAGE gels (10%, 12% and 4% - 12% (w/v) Bis-Tris,) at a voltage, between 180 – 200V for 50 minutes with 1X SDS running buffer (Life Technologies) or Novex 10-20% (w/v) Tricine protein gels set at 120V for 120 minutes with 1X Tricine running buffer (Invitrogen, EC66252BOX & LC1675). The cassette was dismantled from the tank and the gel carefully placed in a square petri dish tray. Coomassie stain (Expedeon Instant blue) was added to cover gel and incubated on a rocker for about 1 hour /overnight. The proteins on the gel turn blue colour after about

10 – 15 minutes of adding the stain. After staining, the Coomassie blue is removed and the gel was distained by couple of washes in water. The protein bands were viewed and image was taken with the UV transilluminator (GelDoc-It2 Imager, UVP; Cambridge). The essence of protein staining was to check the quality of the protein (protein degradation and proteolysis) and uniform loading of samples.

2.4.6 Western blotting/Immunoblotting

This method characterizes specific proteins, typically resolved on a polyacrylamide gel. The proteins extracts were first run on NuPAGE gel (Thermofisher) as described in **2.4.5** above. Without staining, the proteins in the gel are transferred to a membrane for western blotting. The buffer preparations are listed in **Table 2.15**. Prior to the membrane transfer, the sponges, filter papers and nitrocellulose membrane (western blot) were soaked in 1X transfer buffer. The blot cassette was assembled by placing 3 layers of sponges first, then a layer of filter paper, the gel, then the nitrocellulose membrane (Cat Number: 15259794, GE HealthCare Lifescience) follows; another 3 layer of filter paper was placed on top, rolled with a roller to secure the blot firmly to the gel and to remove any air bubbles trapped in between. Another three layers of sponges were added before closing and mounting the cassette into an electrophoresis tank. The blot cassette was filled with 1X transfer buffer and the proteins transferred at 30 Volts for 90 minutes at room temperature. After the transfer, the blot cassette was disassembled and the membrane was removed and placed inside a clean square petri dish with the side of the blot that touched the gel facing upwards. Some ponceau stain (**Table 2.15**) was added into the blot and incubated for a few minutes to confirm a good transfer without interference from any air bubbles. The ponceau stain was rinsed off with a wash buffer (1X TBST) and the membrane was incubated in a block buffer (5% (w/v) milk/1X TBST) for one hour to block off unbound proteins. The block buffer was discarded and the membrane was incubated in a primary antibody buffer (i.e. monoclonal antibody in 5% (w/v) milk/1X TBST, **Table 2.16**) for at least 1 hour. Three-wash steps at an interval of 5 minutes per wash were performed in 1X TBST. After the last wash, a suitable Licor secondary antibody (either polyclonal anti-mouse or anti-rabbit antibody, corresponding to the origin of the primary antibody) diluted in blocking buffer was added to the blot and incubated for up to 1 hour. Another round of 3X washes were performed with the wash buffer. After the last wash, the fluorescence of the protein bands were viewed on LI-COR Odyssey Fc Imager (700 channel for 680nm and 800 channel for 800nm

absorbance). The fluorescence of the proteins was quantified with the same Licor software and normalized accordingly.

Table 2.15 SDS-PAGE and Protein immunoprecipitation (Western Blotting) buffers

Solution
2X SDS Loading dye (Laemmli sample buffer) - 4% (w/v) SDS, 20% (w/v) glycerol, 120 mM Tris-HCl, 0.02% (w/v) bromophenol blue
20X NuPAGE MOPS SDS Running buffer. 1X buffer - 50 mM MOPS, 50 mM Tris base, 0.1% (w/v) SDS, 1 mM EDTA pH 7.7
10X TGS (Tris/glycine/SDS)
1X transfer buffer (1X TGS + methanol)
10X TBS (Tris Buffered saline)
1X Tris buffered Saline Tween, TBST (wash buffer)
Block buffer (5% (w/v) milk/1X TBST)
0.2% (w/v) Ponceau stain
1 M HEPES-KOH (pH 7.5) stock
0.05 M TCEP-HCl (pH 7.0) stock
IP Lysis Buffer (30 mM HEPES-KOH pH 7.5, 10% (w/v) glycerol, 1 mM TCEP-HCl pH 7.0) plus either 100 mM or 1 M KCl
Low salt buffer for wash steps, IP_{low} (10 mM HEPES-KOH pH 7.5, 100 mM KCl, 10% (w/v) glycerol, 1 mM TCEP-HCl pH 7.0)
10X LOLA buffer (200 mM Tris-HCl, 1.4 M NaCl, 10 mM $MgCl_2$)
0.2 M glycine (pH 2.6)

Table 2.16 Antibodies for Western Blotting

Antibody	Specification	**Source**
Anti-FLAG	1: 1000 of 5% milk 1X TBST	Sigma
Chicken anti-ECS (DDDDK)	1:2000 of 5% milk TBST.	Part: A190-100A, Universal Biologicals (Cambridge)
Anti-eIF4E	1: 5000 of 5% milk 1X TBST	Mark Ashe Lab
Anti-Rpl35	1: 5000 of 5% milk 1X TBST	Martin Pool's Lab
Anti-Rps3	1: 50000 of 5% milk 1X TBST	Martin Pool's Lab
Polyclonal anti-rabbit/ anti-mouse/ anti-chicken	1:10,000 dilutions of 5% milk 1X TBST	Lot# C60321-05; Lot# C60107-03; Lot# C41029-14; Li-Cor
Polyclonal anti-chicken	1:10,000 dilutions of 5% milk 1X TBST	Goat anti-Chicken IgY; Invitrogen Fisher scientific

2.4.6.1 Labelling of primary antibody

Labelling of the primary antibody was done to prevent cross reactivity with other secondary antibody. Licor, IRDye® 800CW Protein Labelling Kit (Part number: 928-38044) was used. First, the sodium azide preservative was removed from the antibody by dialysing 100 µg of antibody solution over 1 litre of 1X PBS for at least 1 hour. This procedure was repeated for up to three times. Afterwards, the antibody was transferred to a microfuge tube. The pH of the antibody was raised to 8.5 by adding a 1 M phosphate buffer included in the kit which has a pH of 9. One of the Licor labelling dye tube was removed from - 20°C and warmed to room temperature alongside with the antibody. 25 µl of ultra-pure water was added to the dye, vortexed to mix properly and an estimated amount of 1.71 µl of dye (worked out from the dye/protein ratio) was used to conjugate the antibody. The dye was quickly added to the antibody and mixed by inversion. The tube was then incubated for 2 hours at 20 - 25°C in absence of light. The conjugated protein was purified by passing it through a pre-washed Zeba spin desalting column to remove unconjugated dye. It was then stored at -20°C in aliquots to minimize freeze-thaw antibody damage.

2.5 Ribosome fractionation

2.5.1 Sucrose Cushion for Ribosome Pelleting

About 50 ml of each yeast culture was grown at 30°C to an OD_{600} of 0.6 - 0.8. Cycloheximide was added to the culture to a final concentration of 100 µg/ml, to freeze the ribosomes on to the mRNA. The culture was incubated for another 15 minutes at 30°C and it was spun at maximum speed of 5,500 x g, 0°C for 5 minutes. Then, the cells were washed in 1 ml of chilled CSB buffer (300 mM Sorbitol, 20 mM HEPES pH 7.5, 1 mM EGTA, 5 mM $MgCl_2$, 10 mM KCl, 10% (w/v) Glycerol, 100 µg/ml Cycloheximide, 10 u/ml SUPERaseIn RNAse inhibitor (AM2694, Life Technologies) and 1 Pierce protease inhibitor cocktail) and pelleted at maximum speed of 5,500 x g, 0°C for 5 minutes. Again, the cells were resuspended in 250 µl of chilled CSB and lysed with 500 µl acid washed beads at 5 x 20 seconds beat (with 1 minute rest on ice between beats). Another 300 µl of CSB buffer was added to the lysate and vortexed to homogenize it. The lysate was cleared twice by initial centrifugation at 16,100 x g, 4C for 4mins, transferred to a fresh microtube and then centrifuge for the second time at 10,000 x g, 4°C for 15 minutes. The total protein was quantified using the Bradford

assay (section 2.4.3) and 500 µg of the protein extract (500 µl) was gently lowered over a 400 µl of 50% (w/v) sucrose plus CSB buffer without sorbitol and protease inhibitor to form two distinct layers in Beckman thickwall polycarbonate tubes (part no. 343778). The tubes were centrifuged in an ultracentrifuge (rotor-TLA 120.2, S/N: 11E1035 used in Beckman Optima Max-XP centrifuge) for 2.5 hours at 4°C, 70,000 rpm. The position on the tube where the pellet was deposited was noted and the supernatant transferred into a new microfuge tube. The pellet was thoroughly resuspended in 100 µl Novex tricine SDS sample buffer (LC1676, Invitrogen). This constituted the pellet fraction. To the supernatant, an equal volume of 20% (w/v) TCA (trichloroacetic acid) was added and incubated overnight at -20°C to precipitate the protein. Two step acetone washes of the pellet at 10,000 x g, 4°C for 15 minutes was perform to get rid of the acid. The pellet was dried and resuspended in 100 µl Novex tricine SDS sample buffer (supernatant fraction). 10 µl of both the pellet and supernatant fractions were analysed on western blotting. The western blot results of the samples were normalized to the wild type sample and standard error for three replicates were determined.

2.5.2 Polysome profiling in sucrose density gradients

100 ml yeast cultures were grown at 30°C from OD_{600} 0.1 to 0.6–0.8. The yeasts were then harvested in cycloheximide to freeze the ribosome unto the mRNA. Cycloheximide treatment (at a final concentration of 100 µg/ml) was performed in some Caf20 mutants that had reduced interactions with the ribosome. After the cycloheximide treatment, the cells were harvested at 5,500 x g, 0°C for 5 minutes. This was followed by a wash in 20 ml chilled 1X polysome lysis buffer (20 mM Hepes pH 7.4, 2 mM Magnesium Acetate, 100 mM Potassium Acetate, 0.5 mM DTT and 100 µg/ml Cycloheximide, see **Table 2.17**) and centrifuge at 5,500 x g, 0°C for 5 minutes. The pellet was washed again in 800 µl polysome lysis buffer, transferred to a microfuge and spin at 1,000 x g for 30 seconds. The cell was suspended in 200 µl polysome lysis buffer and transferred to a fresh microtube containing 200 µl acid-washed glass beads. The cells were lysed by hand vortexing for 20 seconds, 6 - 7 times with about 1 minute rest on wet ice between beats. The lysate was cleared of debris by centrifuging at 1,000 x g, 4°C for 10 minutes. The supernatant was transferred into a new microtube and stored at -80°C.

The samples were analysed on sucrose gradients (15% - 50%) prepared in 12 ml polysome gradient thin-walled open polyallomer tubes (Beckman). The preparation of 12 sucrose gradients is shown in **Table 2.18**. To each tube, 2.25 ml of each concentration starting from the highest sucrose concentration was added and snap frozen in liquid nitrogen one at a time. This was repeated for successive sucrose solutions (high to low concentration) until all the sucrose concentrations have been loaded. The gradients were thawed in the cold room overnight or at room temp for at least 1 hour before loading the extracts on to them. After the gradients have thawed, 2.5 OD units of the protein extract measured on Nanodrop spectrometry ($2.5/A_{260}\ x\ 1000 = XX\ \mu l$),_where A_{260} is the Nanodrop spectrometry reading of protein concentration, were loaded drop-by-drop by gently tapping the pipette tip on top of gradient placed in the rotor buckets. After loading the extracts, the buckets were balanced and spun with SW41 rotor set at 40,000 rpm, 2°C for 2.5 hours. After spinning, the samples were taken to the UA-6 UV/VIS detector (ISCO) for polysome profiling. Adequate amount of 60% (w/v) sucrose needed to run all the samples was attached through the inlet pipe. The sensitivity was set at 0.5 for unstressed sample analysis and the noise filter set at 5 mark. The peak separator was pushed to the on button and other settings left at default. The tubing was washed through with sucrose to prepare sucrose in the inlet tube. Then the samples were attached slowly unto the UV/VIS detector one at time without shaking the gradient. It was fastened securely and 60% (w/v) sucrose was let in into the bottom of the tube. This pushes the gradients upwards into the UV/VIS detector and the profile traces was recorded at absorbance of 254 nm. When all the samples have been analysed in the UV/VIS detector, the machine was washed by passing in changes of water and ethanol. At the end, the profile traces were detached from the machine, scanned and the images analysed and manipulated on GIMP (GIMP, 2019) and ImageJ software (Schneider et al., 2012) as described in section 2.8.

Table 2.17 Polysome profiling buffers

Solution
10x polysome lysis buffer (200 mM Hepes pH 7.4, 20 mM Magnesium Acetate, 1 M Potassium Acetate)
1X polysome Lysis Buffer (20 mM Hepes pH 7.4, 2 mM Magnesium Acetate, 100 mM Potassium Acetate, 0.5 mM DTT and probably 100 µg/ml Cycloheximide)
2 M Glycine pH
10X polysome gradient buffer (100 mM Tris Acetate pH 7.4, 700 mM Ammonium Acetate, 40 mM Magnesium Acetate.
60% (w/v) sucrose

Table 2.18 Polysome gradient preparation

	Sucrose concentration				
	50%	**42%**	**33.3%**	**24%**	**15%**
10X polysome gradient buffer	5.5 ml	5.5 ml	5.5 ml	5.5 ml	5.5 ml
60% (w/v) **Sucrose**	45.9 ml	38.6 ml	30.6 ml	22.0 ml	13.8 ml
DEPC-treated H_2O	3.68 ml	11.0 ml	19.0 ml	27.6 ml	35.8 ml

2.6 Protein-protein Crosslinking

Three different crosslinkers were tested initially in small volume cultures (50 ml) namely bismaleidohexane (BMH), m-maleimidobenzoyl-N-hydroxysuccinimide ester (MBS) and disuccinimidyl suberate (DSS). BMH binds cysteine to cysteine (sulfhydryl molecules), MBS conjugates cysteine residues to lysine whereas DSS crosslinks lysine to lysine between two different proteins. Our crosslinking methods followed two approaches, one method was used for total extract culture and other approach was performed on ribosome-bound protein extracts. BMH was used for the large scale total extract crosslinking because it worked best in the trials. As for the ribosome-rich crosslinking, MBS proved to give the strongest crosslinks. The procedure for each approach is discussed in the two sub-sections below.

2.6.1 Yeast total extract crosslinking

Trials were performed in small volumes of 50 ml cultures. 50 ml cell cultures were grown in a shaking incubator set at 30°C to an OD_{600} of 0.6-0.8 in SCD – L media. The cells were harvested and washed with 1 ml IP lysis buffer pH 7.3 (30 mM HEPES-KOH pH 7.5, 10% (w/v) glycerol, 1 mM TCEP-HCl pH 7.0, 100 mM KCl and 1 Pierce protease inhibitor tablet). The cells were resuspended in 600 µl ice cold IP lysis buffer and lysed with 500 µl acid washed glass beads for 5 x 20s with 1 minute reset on ice between beats. The lysate was cleared at max speed for 20 minutes, 4°C. The cleared lysate was transferred to a fresh tube ready for crosslinking. Meanwhile, 10 mM stocks of the different crosslinkers in 1 ml DMSO and stop solutions were prepared as shown in **Table 2.19**. A corresponding dilution factor was calculated if the weight of the crosslinker or stop solution was bigger or smaller. These stocks were prepared fresh just before use in each experiment. After the stocks have been made, the amount of the crosslinker (stocks) to be used for each reaction mix and concentrations is indicated in **Table 2.20** below. The reaction mixes were incubated for 20 minutes at 30°C. The stop solution was then added to the samples at a volume of 1:10 and incubated on ice for at

least 20 minutes to stop crosslink reaction. The crosslinks produced were then assessed on western blotting. When an IP step was incorporation to the small scale crosslinking, all the lysate (~ 500 ml) was crosslinked and a low salt IP purification was carried out as described in section 2.4.4 above.

Table 2.19 Stock solution preparation

Solution	Source
10 mM BMH stock	22330, ThermoFisher Scientific
10 mM DSS stock	21655, ThermoFisher Scientific
10 mM MBS stock	22311, ThermoFisher Scientific
Stop solution (0.2 M DTT and 0.2 M ethanolamine)	

Table 2.20 Preparation of reaction volumes and concentrations

Treatment	Control	0.5mM crosslink	1mM crosslink	2mM crosslink
Volume of crosslinker	10 µl of DMSO	2.5 µl of crosslinker stock	5 µl of crosslinker stock	10 µl of crosslinker stock
Volume of extract	40 µl	40 µl	40 µl	40 µl
lysis buffer	-	7.5 µl each	5 µl	-
Total volume	50 µl	50 µl each	50 µl each	50 µl each
Volume of stop solution	5 µl	5 µl each	5 µl each	5 µl each

2.6.1.1 Proteomics of Largescale yeast total extract crosslinking

When largescale samples were to be prepared for mass spectrometry, three replicates per sample of which three litre culture (3 L) per each replicate was grown to an OD_{600} of 0.6-0.8. The cell pellets and frozen IP lysis buffer pH 7.3 are lysed with liquid nitrogen in a 6870 Freezer mill. See section 2.4.2 for largescale culture and grinding**.** The ground yeast was thawed on wet ice for 30 minutes and cleared in two steps, first at 5,500 x g for 10 minutes. It was then transferred in aliquots in 5 ml and spun for the second time at 10,000 x g for 20 minutes, 4°C. The crosslinker, BMH was used for largescale crosslinking at a final concentration of 1 mM BMH. After crosslinking, a preclearing step with Sepharose 4B agarose (Sigma) was incorporated before FLAG IP with magnetic beads. 100 µl of anti-FLAG magnetic beads was used in IP binding for each replicate (3L culture). Binding of the samples to the beads was performed for 1.5 hours (see section 2.4.4.1). A magnetic bar was used to capture the beads at the bottom of the tube and the unbound protein was removed. The beads were transferred from a

falcon tube into a 2 ml Eppendorf tube with a wide orifice pipette tip. After which the resin was given a quick wash with 1 ml of IP lysis buffer (100 mM KCl) to rinse off the unbound protein. The beads were treated with RNAses by incubating in 600 µl lysis buffer containing RNAses I, III and K (30 mM HEPES-KOH pH 7.5, 10% (w/v) glycerol, 1 mM TCEP-HCl pH 7.0, 100 mM KCl, 40U RNAse I (Ambion), 1U RNAse III (Ambion), 2 µg RNAse A) and Pierce protease inhibitor) at 30°C for 1 hour. Two times high salt plus detergent washes (30 mM HEPES-KOH pH 7.5, 10% (w/v) glycerol, 1 mM TCEP-HCl pH 7.0, 1 M KCl, 0.5% (w/v) NP40 (Igepal CA-420) and Pierce protease inhibitor cocktail) is performed followed by 2X low salt washes (100 mM KCl) without detergent. The bound proteins on the bead were eluted twice with 3X FLAG peptide (Sigma). First elution was in 500 µl of IP lysis buffer (100 mM KCl) plus 50 µl of 3X FLAG peptide (8 mg/ml stock) for 1 hour at 4°C. The second elution was done overnight at 4°C. All the elutions were combined and the proteins precipitated in TCA, followed by Acetone washes (described in section 2.5.1) and re-suspended 30 µl of 1X reducing Laemmli sample loading buffer (1 mM TCEP).

To prepare samples for mass spectrometry, 25 µl of the 30 µl of the concentrated elutant was loaded on a 12-well 10% (w/v) Bis-tris SDS gel with one well space between the samples The gel was run at 200 volts for 5 minutes, stained with Coomassie and washed twice in distilled water. The thick band was cut out and sent for mass spectrometry analysis.

2.6.2 Crosslinking of the yeast ribosome

In small scale experiments, 100 ml of culture was grown to an OD_{600} of 0.6-0.8 at 30°C. Cultures were treated with cycloheximide at a final concentration of 100 µg/ml for 15 minutes at 30°C. The cells were processed for sucrose cushion as described in section 2.5.1. After the centrifugation for 2.5 hours, the pellet fraction was resuspended in CSB (300 mM Sorbitol, 20 mM HEPES pH 7.5, 1 mM EGTA, 5 mM $MgCl_2$, 10 mM KCl, 10% (w/v) Glycerol, 100 µg/ml Cycloheximide, 10 u/ml SUPERase In RNAse inhibitor (AM2694, Life Technologies) and Pierce protease inhibitor) instead of 2X SDS buffer. This was then crosslinked (as described in section 2.6.1) with any of the three crosslinkers (**Table 2.19**) and processed on western blotting. In situations where salt washes were included, the crosslinked samples were incubated in 500 mM or 750 mM KAc (Potassium acetate) added to the CBS buffer at 4°C for 20 minutes. The high salt treated extracts were centrifuged with the 50% (w/v) sucrose + CSB at 70, 000 rpm, 4°C for 2.5 hours (rotor 120.2) before processing on western blotting.

2.6.2.1 Largescale Crosslinking of the ribosome-associated proteins

Three-litre cultures per each yeast replicate were grown to an OD_{600} of 0.6-0.8 in SCD-L media. They were harvested in cycloheximide at a final concentration of 100 µg/ml. The cells were pelleted and ground with about 25 ml of frozen CSB buffer (300 mM Sorbitol, 20 mM HEPES pH 7.5, 1 mM EGTA, 5 mM $MgCl_2$, 10 mM KCl, 10% (w/v) Glycerol, 100 µg/ml Cycloheximide, 40 U/ml RNAse in (Promega) and 1 Pierce protease inhibitor cocktail). The ground yeast was thawed on wet ice for 30 minutes and cleared in two steps, first at 5,500 x g for 10 minutes. It was then transferred in aliquots in 5 ml and for the second time at 10,000 x g for 20 minutes, 4°C. The supernatants were carefully transferred to a fresh falcon tube. The protein concentration was measure and diluted to 12 µg/µl before sucrose cushion. For the sucrose cushion, 4.9 ml of the protein extract was layered over 6.1 ml of 50% (w/v) sucrose + CSB in a 12 ml dummy tube. The sucrose cushion was performed twice in SW41 rotor set at 40,000 rpm, 2°C for 3 hours. After the first spin, the supernatant was transferred into another 12 ml dummy tube and centrifuge again. The two pellet fractions in the two dummy tubes were resuspended overnight in 150 µl CSB. All the pellets for each replicate were pooled together, then crosslinked with MBS to a final concentration of 2 mM MBS for 20 minutes as described before and quenched with stop solution. The crosslinked samples were then treated with potassium acetate to a final concentration of 750 mM at 4°C for 20 minutes. The high salt treated extract was centrifuged with the 50% (w/v) sucrose + CSB at 40, 000 rpm, 0°C for 12 hours. The pellet was resuspended in SDS overnight at 0°C in 500 µl of TE + 2% (w/v) SDS (20 mM Tris pH 7.6, 2 mM EDTA pH 8.0, protease inhibitor and phosphatase inhibitor). Ten millilitres (10 ml) of LOLA buffer without detergent (20 mM Tris-HCl, 140 mM NaCl, 1 mM MgCl, phospho inhibitors (1000X, 100X) and protease inhibitor) is added to the SDS treated sample to bring the concentration of the SDS to 0.1% (w/v) for IP. This was centrifuged at 40,000 rpm for 2.5 hours. The supernatant was then precleared with 100 µl washed sepharose 4B agarose for 1 hour at 4°C. Meanwhile, the MYC agarose beads were washed 5 times in LOLA buffer plus 0.5% (w/v) NP40 to be used for IP as described in section 2.4.4.3. The precleared extract was incubated with the MYC agarose for 2 hours. After the IP, the beads were transferred to 2 ml Eppendorf tube with a wide pipette tip. The MYC agarose was washed five times in LOLA buffer without detergent at beads with spinning at 2,000 x g for 1 minute, 0°C. The bound proteins were eluted twice from the beads by incubating in 500 µl of 0.2 M glycine pH 2.6 for 1 hour. After each elution step, 500 µl

of 1 M Tris (pH 8.0) was added to neutralize the HCl and the beads were washed 3X with 150 µl of LOLA buffer minus detergent. The elutions and the washes were joined together and precipitated with TCA to a final concentration of 20% (w/v). This was followed by 3X acetone washes in 500 µl acetone and the pH pellet was normalized with 1 M Tris (pH 8.0). The pellet was dissolved in 25 µl LDS (Laemilli sample buffer) per tube and two tubes joined together (50 µl). About 30 µl to 40 µl of the elution (load 20 µl first, run for 4 minutes and load another 10-20 µl) was loaded on a 12% (w/v) Bis-tris, 12 wells gel and ran at 200 volts for 50 minutes. The gel was transferred to a clean square petri dish, stained with Coomassie Instant Blue for 1 hour and distained by washing twice in distilled water. Area of the band of interest was cut out from the gel and submerged in water inside labelled tubes. The tubes were then sent for Mass spectrometry protein identification at the University of Manchester, Faculty of Biology, Medicine and Health, PPMS for the Biological Mass Spectrometry Core Facility.

Table 2.21 Other solutions used

Solution
50% (w/v) glycerol
Nuclease free or DEPC-Treated water.
3M Sodium Acetate (NaAc) pH 5.2
50 X TAE (Tris/Acetate/EDTA) buffer, pH 8
1% (w/v) agarose gel

2.7 Mass spectrometry identification by Label-free LC-MS/MS and analysis

The cut out gel bands as described in 2.6.2.1 were taken to the Mass spectrometry Core Facilities (University of Manchester), there the samples were dehydrated with acetonitrile and then centrifuged under vacuum. The dehydrated gels were reduced with 10 mM DTT and then alkylated with 55 mM iodoacetamide (IAM) by uniform modification of cysteine residues. The gel flakes were one after the other washed in 25 mM ammonium bicarbonate and then dried in acetonitrile. They were again washed and dried in ammonium bicarbonate and acetonitrile. After this, the gel flakes are vacuum centrifuged and then digested overnight with trypsin at 37°C.

UltiMate 3000 Rapid Separation LC (RSLC, Dionex Corporation, Sunnyvale, CA) coupled to an Orbitrap Elite (Thermo Fisher Scientific) Mass Spectrometer was

used to carry out label-free analysis of the trypsin-digested samples by LC-MS/MS. The peptides were concentrated on a pre-column (20 mm x 180 µm i.d., waters). The peptides were separated on a gradient, from 99% (w/v) A (0.1% (w/v) FA in water) and 1% (w/v) B (0.1% (w/v) FA in acetonitrile) to 25% (w/v) B, in 45 min at 200 nl min-1, using 250 mm x 75 µm i.d. 1.7 mM BEH C18, analytical column (waters). Peptides were selected from fragmentation automatically by data dependant analysis.

The MS data from the replicates were analysed on Scaffold 4.8.9 Software (www.proteomesoftware.com/products/scaffold/download) with 5 ppm peptide mass tolerance for the main search and 0.5 Da for the MS/MS fragment ions. The peak list was searched against the Uniprot *Saccharomyces cerevisiae* database from the built-in Andromeda search engine. The identified proteins were trimmed off when the peptides appear in less than two replicates out of the entire replicates for each sample. The presentations of the trimmed MS results were presented on Venn diagram (http://bioinformatics.psb.ugent.be/webtools/Venn/). The identified proteins were also confirmed on Saccharomyces Genome Database, SGD (versions 2017-2018) and the properties of the proteins identified on SGD YeastMine Gene List Identifiers https://yeastmine.yeastgenome.org/yeastmine/bag.do?subtab=upload. Statistical differences in the enrichment or depletion of peptides in each sample were calculated in log 2 algorithm and the result presented in a graph chart. An R-package integrated online software, ClustVis (Metsalu and Vilo, 2015) was used to generate the heatmaps.

2.8 Image Manipulations using ImageJ and GIMP softwares

ImageJ software (Schneider et al., 2012) was used to measure diameter and analyse images captured from the UVIDOC and the UV/VIS detector. To estimate the diameter of zone of inhibition of drug treatments, a known standard measurement is set on analyse icon. Lines are drawn across the diagonals of the image's zone of inhibition, measured on ImageJ and the mean diameter of inhibition is estimated and recorded. In manipulating images and estimating thresholds in GIMP (GIMP, 2019), the image contrast as adjusted to black on a white background, lines are drawn to demarcate the monosomes from the polysome peaks. The monosome and polysome areas are filled with the flood fill tool and the histogram pixels of each of them recorded. The ratio of monosome to polysome is estimated by dividing the histogram pixels of the monosome to that of the polysome.

2.9 Statistics and other computational data analysis.

Assays were performed in replicates and represented as means +/- the standard errors. The significant difference between samples were determined with either 2-tailed student T-test or one-way analysis of variance (ANOVA). Protein sequences were aligned with ClustalW multiple alignment of BioEdit v7.0.5 software (Hill, 2005). The presence of deletions by SDM were determined by pairwise alignment of nucleotides of wild type sequence to the mutant sequence on NCBI database and on Serial cloner 2.6.1 software (Perez, 2013). Protein identified through Mass spectrometry were characterised and their properties were confirmed from SGD database, YeastMine Gene Identifier (https://yeastmine.yeastgenome.org/yeastmine/bag.do?subtab=upload). All the group categories of the Mass spectrometry identified proteins were subjected to gene ontology (GO) categorisation for the enriched protein. The GO analysis was performed using the R package clusterProfiler (Yu et al., 2012). A heatmap dendrogram to show hierarchical clustering was drawn using an R-package integrated online software, ClustVis (Metsalu and Vilo, 2015).

Chapter 3

Assessing Caf20 association with eIF4E, ribosome and itself

3.1 Introduction

The 4E-BPs are able to regulate the activities of eIF4E through the conserved canonical motifs (YXXXXLΦ) they share with eIF4G (Mader et al., 1995). As mRNAs need to be bound to both eIF4E and eIF4G in order to recruit the 40S ribosome and initiate translation (Richter and Sonenberg, 2005). When 4E-BPs bind to eIF4E, they displace eIF4G at the eIF4E-binding site and prevent the formation of initiation complex structure (**Fig 1.4**). In this way, translation is repressed in capped mRNAs. In yeast, Caf20 (Altmann et al., 1997) and Eap1 (Cosentino et al., 2000) are the two known 4E-BPs. However it was previously demonstrated that Caf20 binds to its mRNA partners via 4E-dependent and 4E-independent interactions (Castelli et al., 2015) of which the majority of Caf20 mRNA targets are 4E-dependent (75%) whereas 25% (~131 core mRNAs) bind to both 'wt' and 'm2' mutated Caf20 when cells are grown in standard conditions (Castelli et al., 2015). Castelli et al. (2015) discovered that Caf20 can bind to translating ribosomes, even when Caf20 is mutated so that it cannot bind to eIF4E. Hence ribosome interaction is via an eIF4E-independent mechanism. What is not clear is the role of Caf20-ribosome interactions are and whether this interaction is important for functions or if binding the translating ribosomes also drive repression? The other yeast 4E-BP, Eap1 was also found to interact with the ribosome (Castelli et al., 2015), suggesting ribosome interaction was non-unique to Caf20, but a shared function among 4E-BPs. This key finding is of interest to us as it suggests that the generally accepted model of 4E-BP regulation illustrated in **Figure 1.4** is over simplified and there are additional interactions that Caf20 makes that are of unknown significance.

Before the commencement of this study, the structure of Caf20 was unknown except for a recent publication on the crystal structure of Caf20 (residues 1-49 only) in complex with eIF4E published later towards the end of this project (Gruner et al., 2018). Their 4E-BP/eIF4E structures of the yeast factors suggest that eIF4E-4E-BP complexes showed both bipartite binding of the dorsal and lateral surfaces to the eIF4E. The first helical structure falls between residues 6-12 of the canonical region of Caf20 (1-17) on the dorsal surface, the linker site falls at 12-24 and the second helix is situated at 24 and 41 of the non-canonical region (18-49) on the lateral surface of eIF4E. Also, the lateral binding of the yeast 4E-BP (Caf20) may not contribute to its stability on eIF4E on which disruption of the lateral surface has no effect on its binding to the eIF4E (Gruner et al., 2018).

This chapter sets out the findings of studies that used classical molecular and biochemical approaches to identify parts of Caf20 important for its interaction with eIF4E and the ribosome. Some key questions asked were if there were multiple parts of Caf20 important for interacting with eIF4E and the ribosome and if there were overlaps of these motifs? To assess this a series of Caf20 mutations was constructed, each missing a different region of Caf20, and introduced into *caf20*Δ cells. Experiments were then done to determine how the mutations alter Caf20 association with eIF4E and ribosome. In addition, it has been proposed previously that Caf20 can multimerize (Pavitt lab's unpublished observation). To address this possibility double transformation of yeast bearing two different Caf20 tags was performed to assess dimer/multimer formation in yeast cells.

3.2 Creation of a series of Caf20 deletion mutant plasmid constructs

Previous work in the Pavitt lab has identified novel translational-control role for Caf20 that appears to function independently of its ability to interact with eIF4E (Castelli et al., 2015; Cridge et al., 2010). It was therefore desirable to identify features within Caf20 necessary for its regulatory roles. Before we commenced our project, the structure of Caf20 in complex with eIF4E was unknown till the publication of the Caf20 structure paper in 2018 (Gruner et al., 2018) which was towards the end of this work. Fortunately, our design is in agreement with the published structure. However, initial studies show that mammalian and other 4E-BP1 homologues possess a largely unfolded structure in the absence of eIF4E and binds eIF4E in an extended conformation (Bah et al., 2015; Elantak et al., 2010; Fletcher et al., 1998; Igreja et al., 2014). Likewise, structure prediction software also suggested that Caf20 is an unfolded protein (see section **3.4.2.1**). With this in mind, we created the first 8 deletion mutants of Caf20 starting from the third amino acid by deleting 20 amino acids (60 bp) consecutively in series from the beginning of the protein to the end of the protein. Caf20 has 161 amino acids, so the first deletion was residues 3-22 and was named Δ1, the second residues 23-42 (Δ2) etc. and the final deletion, Δ8, was 19 residues (143-161). A standard commercial site directed mutagenesis kit was used to create deletion mutations (Quikchange lightening kit, Agilent Technologies, UK) in an overlapping manner to prevent non-specific targeting of DNA sequences by the primers, see methods (**2.3.1.2.1**).

3.2.1 Generation of 8 mutants of small deletions by Site Directed Mutagenesis (SDM) and transformation into yeast.

Figures 3.1 depict how the mutants were generated. As Caf20 is a small protein with a gene sequence of 483 nucleotides (161 amino acids), thus a plasmid pAV2421 bearing the *CAF20* wild type sequence and C-terminally tagged with two copies of the FLAG epitope, pCaf20-FLAG (pAV2421, **Table 2.1.** The C-terminal Flag tags were important because although a Caf20 antibody is available it cannot be used to compare relative expression levels of all mutant forms, while the FLAG epitope does allow this comparison. Site directed mutagenesis by PCR (**Fig 3.1A**, methods **2.3.1.2.1**) in Caf20-FLAG plasmid (pAV2421) was used to create 8 different Caf20 mutant plasmid DNAs with the help of the designed synthetic oligonucleotide pairs, Caf20Δ1- Caf20Δ8 (**Table 2.7**) was used to create eight mutant forms of Caf20 by deleting 60bps (twenty amino acids) consecutively in sequence from one end of the gene.

For the first mutant (Caf20Δ1), deletion started from the 7^{th} to the 66^{th} nucleotide base nucleotide (which corresponds to the 3^{rd} – 22^{nd} amino acid) (**Fig 3.1B, Table 2.8**). The second mutant mutagenesis (Caf20Δ2) starts from the 67^{th} to the 126^{th} nucleotide base to create a loss 60 bps. This was carried on for the rest of the mutants (see **Table 2.8**). Mutant Caf20Δ8 is deleted for 57 bps (19 amino acids) instead of 60 bps which is 3 bps less than the rest of the mutants. Based on the mutations made and the recent published structure of Caf20 (Gruner et al., 2018), the first mutant deletion, Caf20Δ1 (7^{th} -66^{th} nucleotide bases or residues 3-22) map within the functional domain for the first canonical helix for eIF4E-binding and the linker region (residues 1-24). The second mutation deleted the region for non-canonical interaction with eIF4E (67^{th}-126^{th} bps or residues 23-42). The non-canonical helix of the Caf20 crystal structure map between residues 24 and 41 of which was deleted in the Δ2 (**Fig 3.1C**). As the structure of Caf20 was only performed with the N-terminal domain (1-49 nucleotides), the rest of the mutants could not show additional functional domain for Caf20 interactions.

The template DNA (pAV2421) was digested overnight with Dpn1 enzyme and SDM amplification of DpnI resistant DNA was confirmed by agarose gel electrophoresis (**Fig 3.1D**). The Dpn1 enzyme cleaves methylated DNA (template DNA) and ensured that no parent DNA remains before SDM products were transformed into XL-Gold Ultracompetent cells (Agilent Technologies, UK). The result revealed that the SDM and amplification worked as the 3 mutant plasmids, Δ1, Δ2 and Δ3 resolved

on electrophoretic gel to confirm SDM amplification shown in **Fig 3.1D** were visible on gel of about 8 kb suggesting successful mutant gene amplification. Three different plasmid DNA clone candidates for each mutant were sequenced by Sanger-sequencing to confirm that deletions were as desired and also the absence of any unwanted changes (described in **section 2.3.1.4**). The pairwise alignment results from NCBI database for the mutant sequences (Δ1- Δ8) versus the Caf20 wildtype sequence are shown in the **Appendix** (**I**).The query sequence means mutant sequence while the subject sequence is the Caf20-FLAG 3'UTR sequence. Deletions created gaps in the sequence alignment which generated 2 sequence matches for each mutant with the exception of the first mutant with only one sequence alignment as the deletion was at the beginning of the protein (**Appendix I**). This suggests correct deletion of 60 nucleotide bases.

Mutants with the best looking DNA chromatogram (correct sequence with least noise) were saved and used to transform a *caf20*Δ yeast strain (GP4789) following our standard laboratory methods in **2.3.2**. Three controls, wildtype *Caf20-FLAG* (labelled as Caf20wt in **Fig 3.2**), *Caf20m2-FLAG* (pAV2422) bearing (Caf20 Y4-A4; L9-A9) mutations known to disrupt Caf20-eIF4E binding (Ibrahimo et al., 2006) and a *LEU2* plasmid (pAV1302/pRS425), designated as empty vector plasmid, EP, without any Caf20 sequence (*caf20Δ*) were included to assess the effects of mutations on Caf20 expressions. The strains were stored with

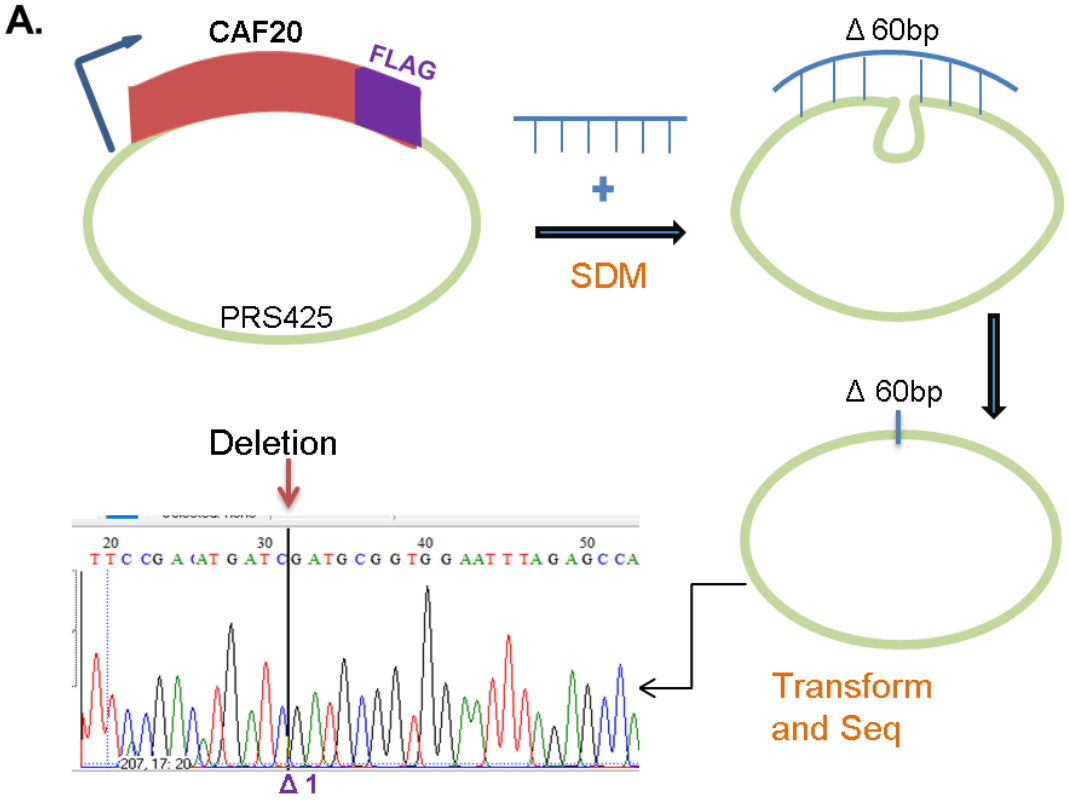
A.
CAF20
FLAG
PRS425
SDM
Δ 60bp
Δ 60bp
Deletion
Transform
and Seq
Δ 1

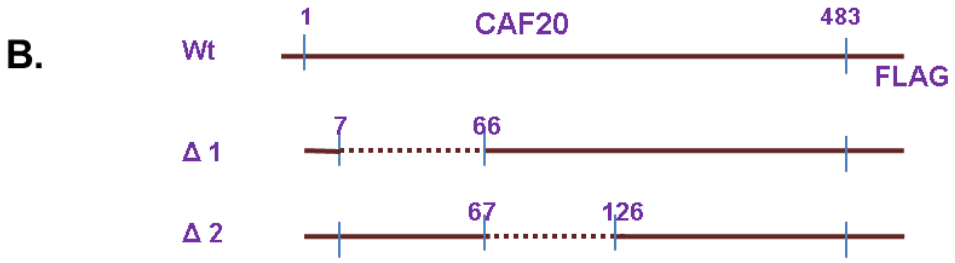
B.
Wt
1
CAF20
483
FLAG
Δ 1
7
66
Δ 2
67
126

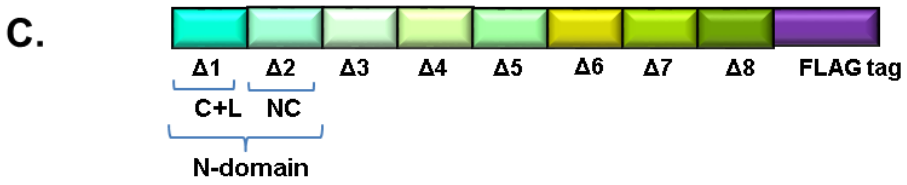
C.
Δ1
Δ2
Δ3
Δ4
Δ5
Δ6
Δ7
Δ8
FLAG tag
C+L
NC
N-domain

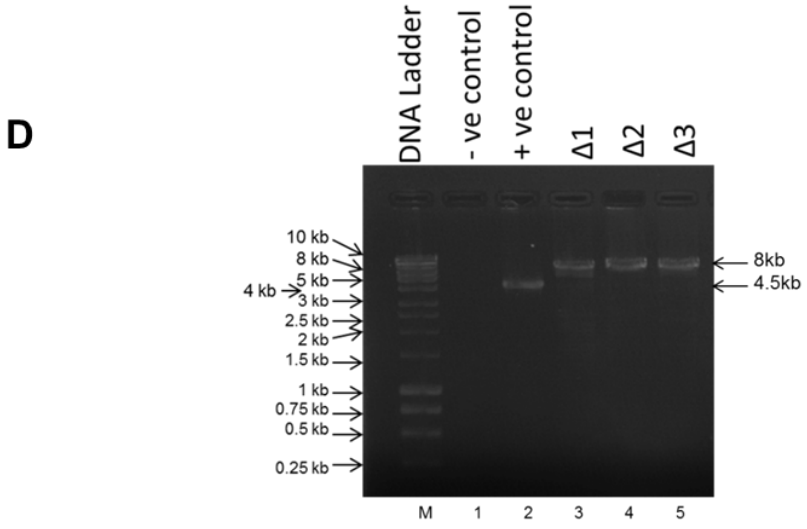
D
DNA Ladder
- ve control
+ ve control
Δ1
Δ2
Δ3
10 kb
8 kb
5 kb
4 kb
3 kb
2.5 kb
2 kb
1.5 kb
1 kb
0.75 kb
0.5 kb
0.25 kb
8kb
4.5kb
M
1
2
3
4
5

Figure 3.1. Creation of first eight mutants of Caf20. A. Site directed mutagenesis of PRS425 plasmid bearing FLAG tagged Caf20 and *Leu2* marker (pAV2421) in which 60 nucleotide bases, Δ60 bp (20 amino acids) are deleted in a series starting from the 7th nucleotide base to the end of the *CAF20* with the aid of some sets of designed primer. Transformed plasmids are sequenced and analysed. The sequence chromatogram of the first mutant (Δ1) in the figure shows successful deletion with reduction in a total of 60 bp due to deletion of 60 nucleotide bases from the 7th to the 66th nucleotide bases in the *CAF20*. The transformed mutant Caf20 plasmids are assigned accession numbers pAV2475-2493 used to later transform Caf20 delete yeast strain (GP4789). **B.** schematic representation of deletions made in each mutant plasmid. For the first mutant (Caf20Δ1), deletion started from the 7th to the 66th nucleotide base nucleotide (which corresponds to the 3rd – 22nd amino acid). The second mutant mutagenesis (Caf20Δ2) starts from the 67th to the 126th nucleotide and so on (**Table 2.8**). **C**. Relationship of mutations generated to Caf20 functional domains based on published Caf20 structure. **D**. 1% (w/v) Agarose gel electrophoresis of overnight DpnI digested PCR product of SDM. Lane M: 1 kb DNA marker, Lane 1: -ve control (Caf20wt plasmid without any primer for amplification). Lane 2 - +ve control (4.5kb whitescript control template from the quikchange kit amplified with the kit's control primers). Lane 3-5 represents digested Δ1 – DNA of Caf20 mutant 1, digested Δ2-DNA of Caf20 mutant 2 and digested Δ3 - DNA of Caf20 mutant 3 respectively. The other 5 mutants (Δ4- Δ8) were also confirmed on agarose gel electrophoresis but figure not shown.

To assess whether the mutated Caf20 proteins were stably expressed in the transformed yeast cells, whole cell protein extracts were made from the mutants (as described in **section 2.4.1**) and resolved on a precast NuPAGE SDS-PAGE gel (**section 2.4.5**) and western blotting was done (**section 2..4.6**) probing for the FLAG epitope tag (**Figs 3.2C and D**). The yeast Caf20 mutants (**Fig 3.2D,** lanes 2 - 9) all revealed a specific band migrating further down the gel than their wildtype counterpart in lane 1 and Caf20^{m2} in lane 10. No Caf20 was expressed for the empty plasmid (Caf20 delete) strain, as expected. The numbering order of Caf20 mutants 1-8 on the Figures changed because of a switch between mutant 2 and 6 at the beginning of study which was rectified later towards the end of study when all the figures have been made. The eight transformed yeast mutants (Δ1- Δ8) are stored as GP7165-GP7172 in the Pavitt's laboratory collections. The wildtype Caf20-FLAG (wt), Caf20m2 mutant and Leu2 empty plasmid are stored as GP7164, GP7173 and GP7174 respectively

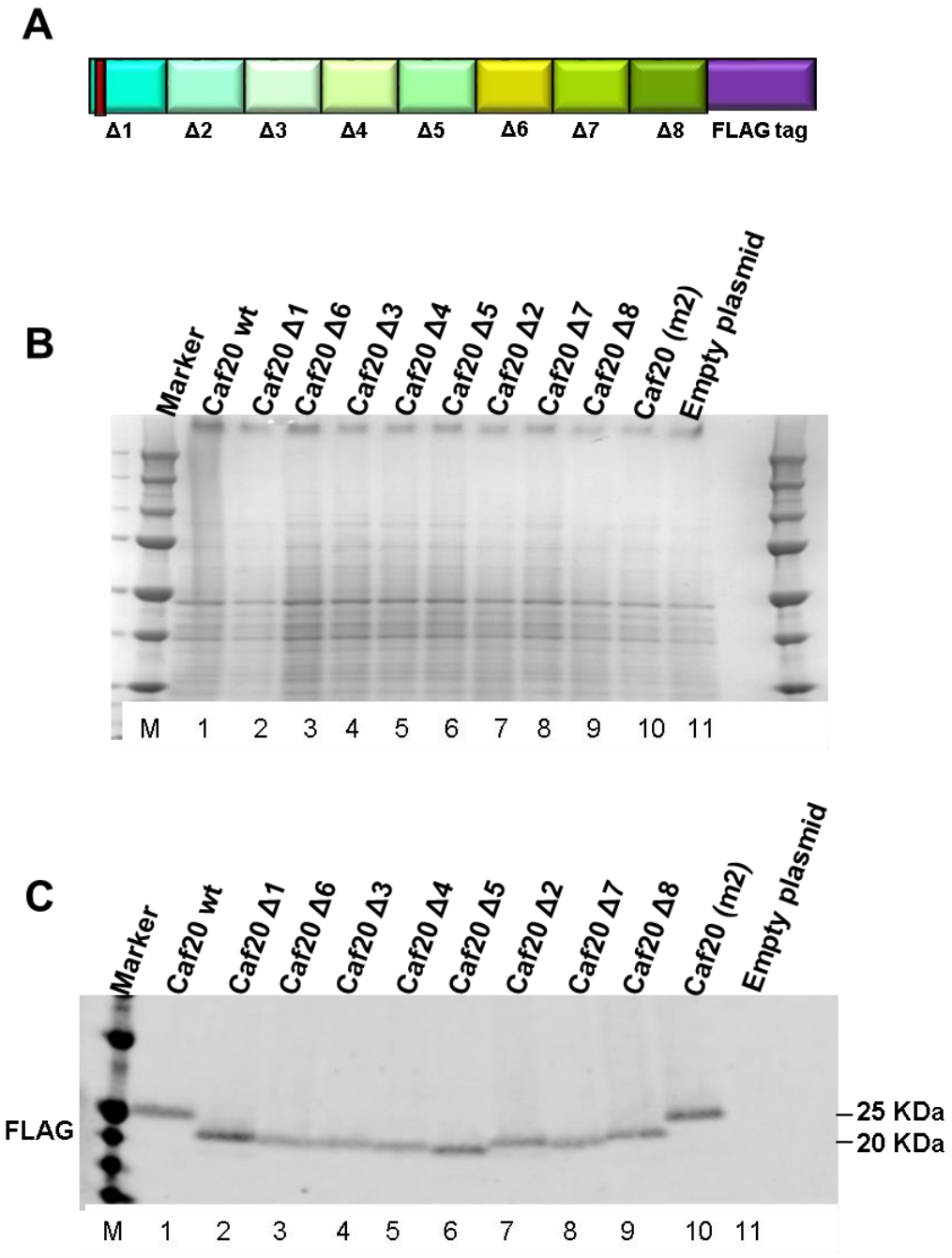

Figure 3.2 Expressed Caf20 mutants of 20 amino acid knockouts in yeast cell. **A**. protein structure of Caf20 and the eight mutant organisational structures illustrated. Filled shapes shows the different sequences deleted for each mutant. The red rectangle in Δ1 shows the eIF4E-binding motif. **B**. SDS-PAGE- Coomassie stained gel of rough protein extract of yeast transformants. **C.** Western blot of rough protein extract of yeast transformants. Protein marker in lane M, CAF20wt in lane 1, Mutant Δ1-8 in lanes 2 - 9, CAF20^{m2} in lane10 and Empty plasmid, *caf20*Δ in lane 11. 30 µg of protein extracts loaded on each lane. The yeast strains were assigned GP strain collection numbers GP7164-74 (**Table 2.2**). The numbering order of Caf20 mutants 1-8 on the Figures changed because of a switch between mutant 2 and 6 at the beginning of study which was retified later towards the end of study when all the figures have been made. N=1 rep

The calculated MWs are all between 18-19 KDa (Table 3.1) whereas **wt** Caf20-Flag is 20.9 KDa. The expected molecular weights and isoelectric points (pI) for each mutant was estimated with ExPASy-Compute pI/Mw tool (web.expasy.org/compute_pi/). For the **wt** Caf20-FLAG, the pI is 4.97. The relative migration pattern on the blot did not precisely match the predicted MW. The variability might be that local regions of charges that are causing it to migrate faster. Caf20Δ5 migrated fastest, while Caf20Δ3 was predicted to be the smallest. **Table 3.1** also outlined the prospective importance of the deleted segments. In some of the deleted segments, prior literature had suggested that some residues are sites where post-translational modifications by enzymes involved in protein folding occur (Albuquerque et al., 2008; Holt et al., 2009; Soulard et al., 2010; Swaney et al., 2013). Some of the deleted sequences are highly acidic or basic as in the case of Δ3, Δ4, Δ5, Δ8. In some, they have a close stretch of basic (Δ3) or acidic residues as in the case of Δ5 and Δ8. Mutant Δ3 and Δ7 had combinations of basic and acidic residues.

In conclusion, **Figure 3.2** confirms that each mutant Caf20 construct bearing a twenty amino acid deletion is stably expressed in these *caf20*Δ cells.

Table 3.1 Molecular weight, protein isoelectric point (pI) characteristics of deleted amino acids

Caf20 mutants	Deleted Amino acids [1]	Del. pI	Characteristics	MW (KDa)	Mut. pI
Δ1 (3-22)	K**YTIDE**L**F**QLKPSLTLEVNF	4.68	Conserved residues for interaction with eIF4E (bold). Residues mutated in Caf20^{m2} (underlined). Acidic residues at the conserved motifs	18.52	5.00
Δ2 (23-42)	DAVEFRAIIEKVKQLQHLKE	6.77	Contains acidic and basic residues	18.53	4.84
Δ3 (43-62)	EEFNSHHVGHFGRRRSSHHH	9.63	Serine residues and potential sites for phosphorylation. Very high basic residues. Frameshift and point mutations possible here.	18.47	4.53
Δ4 (63-82)	GRPKIKHNKPKVTTDSDGWC	9.63	More basic residues. Have a deletion of the only cysteine residue (sulfhydryl) in Caf20. Sites with post translational modification.	18.65	4.70
Δ5 (83-102)	TFEAKKKGSGEDDEEETETT	4.17	High acidic residues and some basic residues. Repetition of amino acids with potential sites for modification.	18.69	5.33
Δ6 (103-122)	PTSTVPVATIAQETLKVKPN	9.01	Contains residues that can be phosphorylated	18.83	4.88
Δ7 (123-142)	NKNISSNRPADTRDIVADKP	8.59	Combination of acidic and basic residues.	18.71	4.87
Δ8 (143-161)	ILGFNAFAALE**S**EDEDDEA	3.26	High acidic residues.	18.86	5.61

[1] Green amino acids indicate sites reported to be post-translationally modified (SGD). Acidic and basic amino acids are represented with red and blue letters respectively.

3.3 Optimization and monitoring of Caf20Δ mutants interactions with eIF4E by FLAG immunoprecipitation

3.3.1 Optimization of FLAG Co-immunoprecipitation

Mutations in a 4E-BP motif in the N-terminal domain (NTD) of Caf20 are known to disrupt interaction with eIF4E (Ibrahimo et al., 2006). However structural analyses have shown that other elements are also involved in stabilizing eIF4E-4E-BP interactions (Bah et al., 2015; Gruner et al., 2018; Igreja et al., 2014; Peter et al., 2015). To examine the effect of Caf20 deletions on the interaction of Caf20 with eIF4E, we performed a *Caf20-FLAG* IP pull down. The FLAG immunoprecipitation assay illustrated in **Fig 3.3A** made use of anti-FLAG (R) M2 magnetic beads (Sigma) to capture Caf20-FLAG from a whole cell extracts onto the beads. 1 mg of protein quantified from the Bradford standard curve (**Fig 3.3B**) were incubated with 50 µl of FLAG magnetic resin to purify Caf20. The unbound proteins were washed off and FLAG-bound material recovery was

optimized by eluting with 3X FLAG peptide as described in the methods (**section 2.4.4.1**). Caf20 elution was done rather than just monitoring the bound fraction directly, as it was observed that FLAG antibody light chain is the same molecular weight as Caf20. Hence, the magnetic resin FLAG antibody light chain was seen to cross-migrate with Caf20 mutant proteins and made it difficult to view for the presence of Caf20 as shown in **Fig 3.3C** and **D**. *caf20*Δ strain (GP7174) with only *pLEU2* in which Caf20 is absent (see **Fig 3.2D** lane 11) retains a strong band in the pellet lane at 20-25 KDa on SDS-PAGE (**Fig 3.3C**, lane 13) and on western blot (**Fig 3.3D**) because of the FLAG antibody light chain elution from the boiled sample. This prevented identification of Caf20-FLAG proteins in initial IP experiments. As regards to the amount of protein present in the pellet (P) fraction to the unbound (S), only a very small amount of total cell protein was captured by the FLAG affinity resin as expected (**Fig 3.3C**).

Including a 3X FLAG peptide elution step was necessary to assess the FLAG IP by western blotting (**Fig 3.4**). **Fig 3.4** (**B** and **C**) revealed that FLAG IP each of the mutants (Δ2-Δ8) pulled down eIF4E in tight association with Caf20. The one exception is Caf20Δ1. This confirms previous findings that Caf20 interacts with eIF4E via the canonical motifs (Arndt et al., 2018; Castelli et al., 2015; Cridge et al., 2010; Gruner et al., 2018; Ibrahimo et al., 2006). This association was apparently tight as it is maintained following binding and washing pellets with IP buffer containing 1 M KCl (**Fig 3.4C**). High salt is expected to dissociate ionic interactions, and as noted above Caf20 has many charged side-chains. Caf20Δ1 could not co-immunoprecipitate with eIF4E and behaved similar to Caf20^{m2} (Castelli et al., 2015; Ibrahimo et al., 2006). This is most likely because the conserved residues for the core-eIF4E canonical motif reside in the part deleted in Δ1 and mutated in Caf20^{m2}. Caf20Δ3 showed more binding to eIF4E both at low and high salt concentrations (**Fig 3.4B** and **C**, lanes 4). There is no clear reason for the tight association but based on the structure of Caf20, it could be argued that the deletion of the Δ3 region of Caf20 may help in stabilizing both helices in the dorsal and lateral surfaces present in regions Δ1 and Δ2 required for maintaining association with eIF4E. The co-immunoprecipitation association stringency could not be examined above 1 M KCl as that is the salt limit specified by the manufacturer for the FLAG resin.

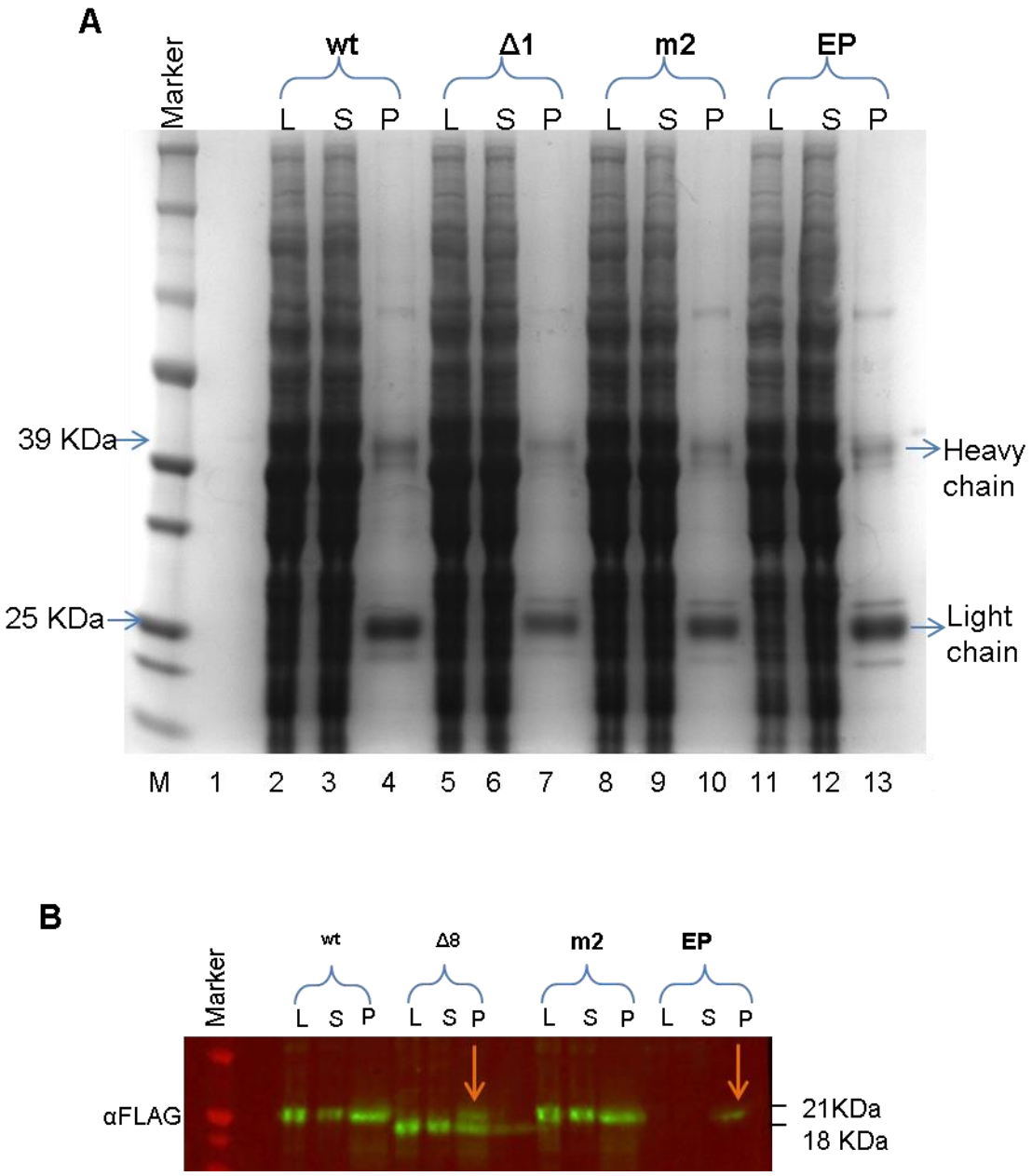

Figure 3.3 FLAG IgG light chain cross reacts with Caf20 band in FLAG IP. A. illustration of FLAG IP procedure eluted with 2X SDS sample buffer. **B.** Protein quantification using Bradford standard curve assay (constant value = 0.1207). **C.** Coomassie blue stained SDS-PAGE of FLAG IP**.** Uniform FLAG IP protein for Caf20wt, Caf20Δ1, Caf20^{m2} and EP (empty vector plasmid) respectively. Less proportion of the protein were bound to the FLAG M2 magnetic beads. More of the protein remained in the unbound or supernatant. Lane M- protein marker sizes; lane 1- empty; lanes 2 – 4 for Caf20wt input, unbound and pellet proteins; lanes 5 – 7 for Caf20Δ1 input, unbound and pellet proteins; lanes 8-10 for Caf20^{m2} input, unbound and pellet proteins and lanes 11 – 13 for *caf20*Δ input, unbound and pellet proteins **D.** Western blotting of FLAG IP for Caf20wt, Caf20Δ8, Caf20^{m2} and EP respectively. The magnetic FLAG (M2) beads light chain antibody obstructing visualization of Caf20 band in the pellet eluted with 2X SDS sample buffer. The orange arrows shows the cross-reactivity of FLAG light-chain IgG. Note: input (**L**), unbound (**S**) and pellet (**P**), wild type (**wt**), mutant (**Δ**). N=1 rep

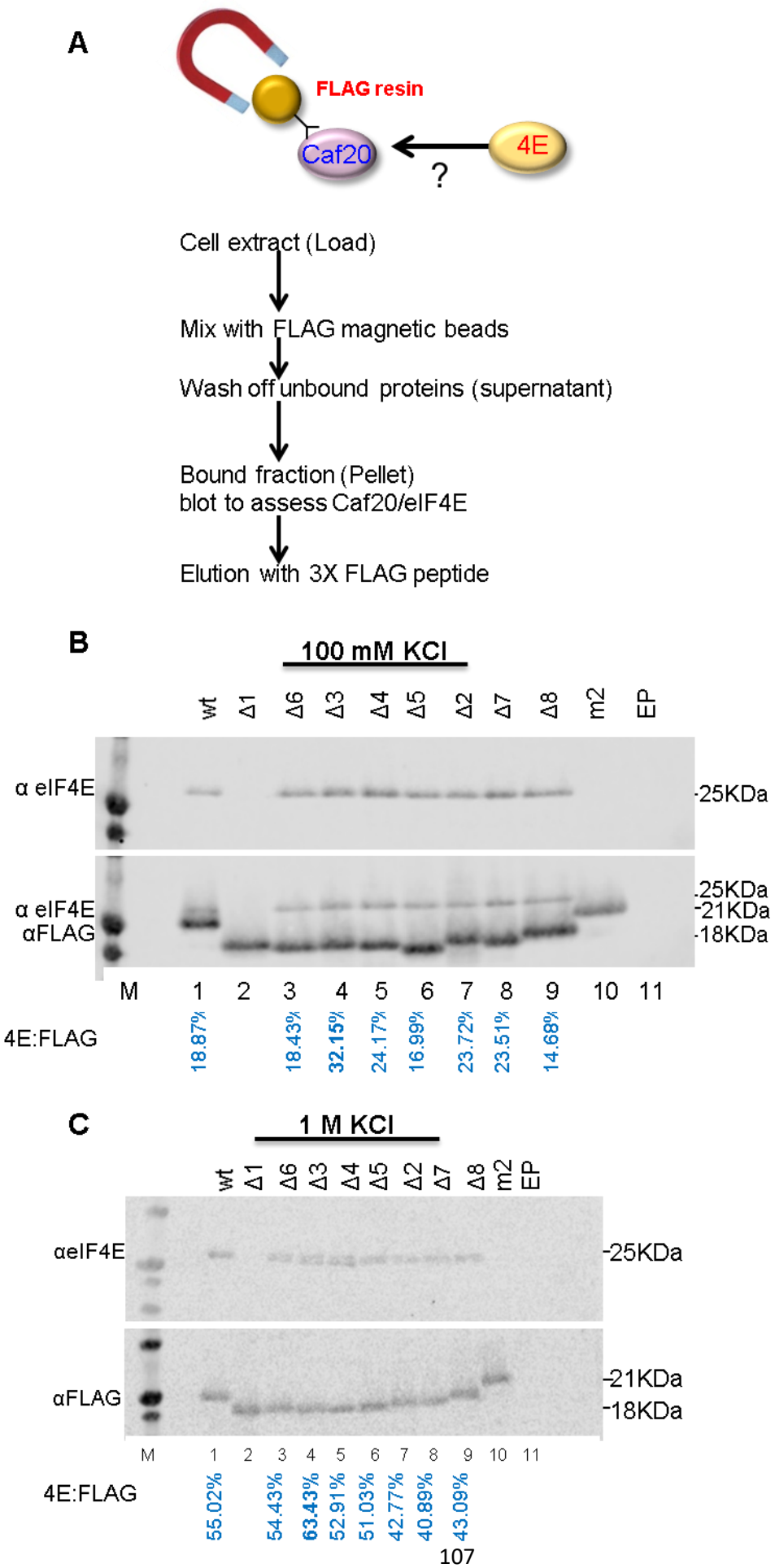
A
FLAG resin
Caf20
4E
?
Cell extract (Load)
Mix with FLAG magnetic beads
Wash off unbound proteins (supernatant)
Bound fraction (Pellet)
blot to assess Caf20/eIF4E
Elution with 3X FLAG peptide
B
100 mM KCl
wt Δ1 Δ6 Δ3 Δ4 Δ5 Δ2 Δ7 Δ8 m2 EP
α eIF4E
-25KDa
α eIF4E
αFLAG
-25KDa
-21KDa
-18KDa
M 1 2 3 4 5 6 7 8 9 10 11
4E:FLAG
18.87% 18.43% 32.15% 24.17% 16.99% 23.72% 23.51% 14.68%
C
1 M KCl
wt Δ1 Δ6 Δ3 Δ4 Δ5 Δ2 Δ7 Δ8 m2 EP
αeIF4E
-25KDa
αFLAG
-21KDa
-18KDa
M 1 2 3 4 5 6 7 8 9 10 11
4E:FLAG
55.02% 54.43% 63.43% 52.91% 51.03% 42.77% 40.89% 43.09%

Figure 3.4 Caf20 mutant co-immunoprecipitation with eIF4E. A. Optimized FLAG IP protocol using 3X FLAG peptide elution. **B.** Western blots of FLAG peptide eluted eIF4E (top panel) and FLAG-tagged Caf20 FLAG constructs (lower panel, a reprobe blot) from co-IPs of total cell extracts washed in low salt buffer (100 mM KCl). **C.** Western blots of Caf20 FLAG co-IPs performed as in panel A except that pellets were washed with high salt buffer (1 M KCl) and blots were performed independently rather than reprobing the eIF4E blot with anti-FLAG antibodies. The ratio of eIF4E to FLAG (4E: FLAG) for one replicate shown in percentage. Lane M is for protein marker, lane 1 - Caf20 wildtype, Lanes 2 – 9 for the mutants (Δ1 - Δ8), lane 10 – mutant Caf20m2 and Lane 11 – Empty vector plasmid. N=1 rep

According to a recent Caf20 structure (Gruner et al., 2018), Caf20 shows bipartite binding to both the dorsal and lateral surfaces of eIF4E. It binds to the dorsal surface through the canonical domain and laterally through the 'non-canonical' motif similar to that of the metazoan 4E-BPs. The eIF4E-binding sites on the Caf20 form two alpha helical structures, the first helix in the canonical motif falls within residues 6 and 12 and a connecting linker between residues 12 and 24. This particular area constitutes the missing region of Caf20Δ1. The second helix containing the non-canonical binding residues is situated in between residues 24 and 41. This helix region is contained within the region removed from the second mutant, Caf20Δ2. It was expected that Caf20Δ mutant would show a weakened association with eIF4E but it interacts strongly even at high salt (1 M KCl) washes. Caf20Δ3 (GP7167) showed the strongest interaction with eIF4E both in low and high salt concentration based on the ratio of eIF4E to FLAG of the bound pellet (**Fig 3.4, B** and **C**). In conclusion Caf20 mutant Δ1 disrupts interactions with eIF4E, but none of the other deletions appear to impact significantly on eIF4E binding.

3.4 Elements of Caf20 needed to bind with the ribosome

3.4.1 Caf20 mutants Δ1-Δ8 associate with the polysomes

As described in Castelli et al. (2015), it was shown that Caf20 can interact with translating ribosomes (polysomes) in an eIF4E-independent manner. We therefore used a ribosome sedimentation assay employing sucrose cushions to separate cell extracts into heavy and light fractions as a way to screen ribosome association of my mutants. A similar assay was used previously (Castelli et al., 2015). After series of assay optimizations, **Figure 3.5A** summarizes how the extracts were finally prepared and assessed. We harvested actively growing yeast following treatment with cycloheximide

to freeze the ribosomes onto translating mRNAs. The cell extracts were layered onto a 50% (w/v) sucrose cushion and then separated by centrifugation at 70, 000 rpm (TLA-120.2, Beckman). The supernatant (S) and pellet (P) fractions were dissolved in equal volumes of 2X SDS sample buffer and processed by western blotting (outlined in the methods **2.5.1)**.

Antibodies to two ribosomal proteins, Rpl35 for the large ribosomal subunit and Rps3 for the small ribosome subunit (**Fig 3.5B,** 3rd and 4th columns) were used to probe for the presence of 40S and 60S ribosomes in supernatant and pellet fractions. The results showed that majority of the ribosomal proteins were present in the pellets (polysomes). The loading control (Pgk1), a glycolytic enzyme, was only present in the supernatant as expected (**Fig 3.5B**, 1st row on Top). The eIF4E is detected in more or less equal proportions in the supernatant and pellets (**Fig 3.5B**, 2nd row). Nevertheless Caf20 is shown to be distributed in both the supernatant and pellet fractions (**Fig 3.5B**, 5th row, anti-FLAG) as can be seen in the lanes 1 and 5 for the wildtype and also for all mutants, Δ1-Δ8 and m2. One interesting observation is that Caf20Δ1, which does not co-IP with eIF4E (**Fig 3.4B** and **C**, lanes 2) was found to associate with the translating ribosomes as it was found to be present in the pellet fraction (**Fig 3.5B**, see lanes 3 and 7, 5th row). It is even enriched in the pellet more than the wildtype (lane 5). This finding is consistent with that of the Caf20^{m2} mutant, which behaves identically (lanes 2 and 6). These findings confirm the previous report that Caf20 binds to ribosomes independent of eIF4E (Castelli et al., 2015). Combining the amount of Caf20 to eIF4E showed that about 40% of Caf20 to eIF4E associated with the polysome (**Fig 3.5C**). There were some minor variability in some mutants (Δ2, Δ4, Δ6 and Δ8) which were not statistically different (**Table 3.2**) showing they could be important in the stability of ribosome interactions. Caf20 Δ2 deleted part was later reported to contain the eIF4E non-canonical motif (Gruner et al., 2018). Regions of Δ6- Δ8 constitutes the 3' region of Caf20. Castelli et al. (2015) reported that Caf20 can bind to 3' UTRs of its target mRNA in an eIF4E-independent manner of which they demonstrated on *ERS1* mRNA 3'UTRs. Also Caf20 can regulate itself (Castelli et al., 2015; Costello et al., 2015). This could be reasoned that 3'UTR binding elements of Caf20 resides between Δ6- Δ8. In essence, the eIF4E non-canonical motifs and the 3'UTRs maybe important for Caf20 interaction with the ribosome in an eIF4E-independent manner. It is known from previous report that Caf20 is binding to the ribosomes as Caf20 still maintain interaction with some ribosomal proteins after been treated RNAseI and high salt but loose interaction with

some RNA-binding proteins suggesting that Caf20 is binding to the ribosome and not just to the mRNA (Castelli et al., 2015).

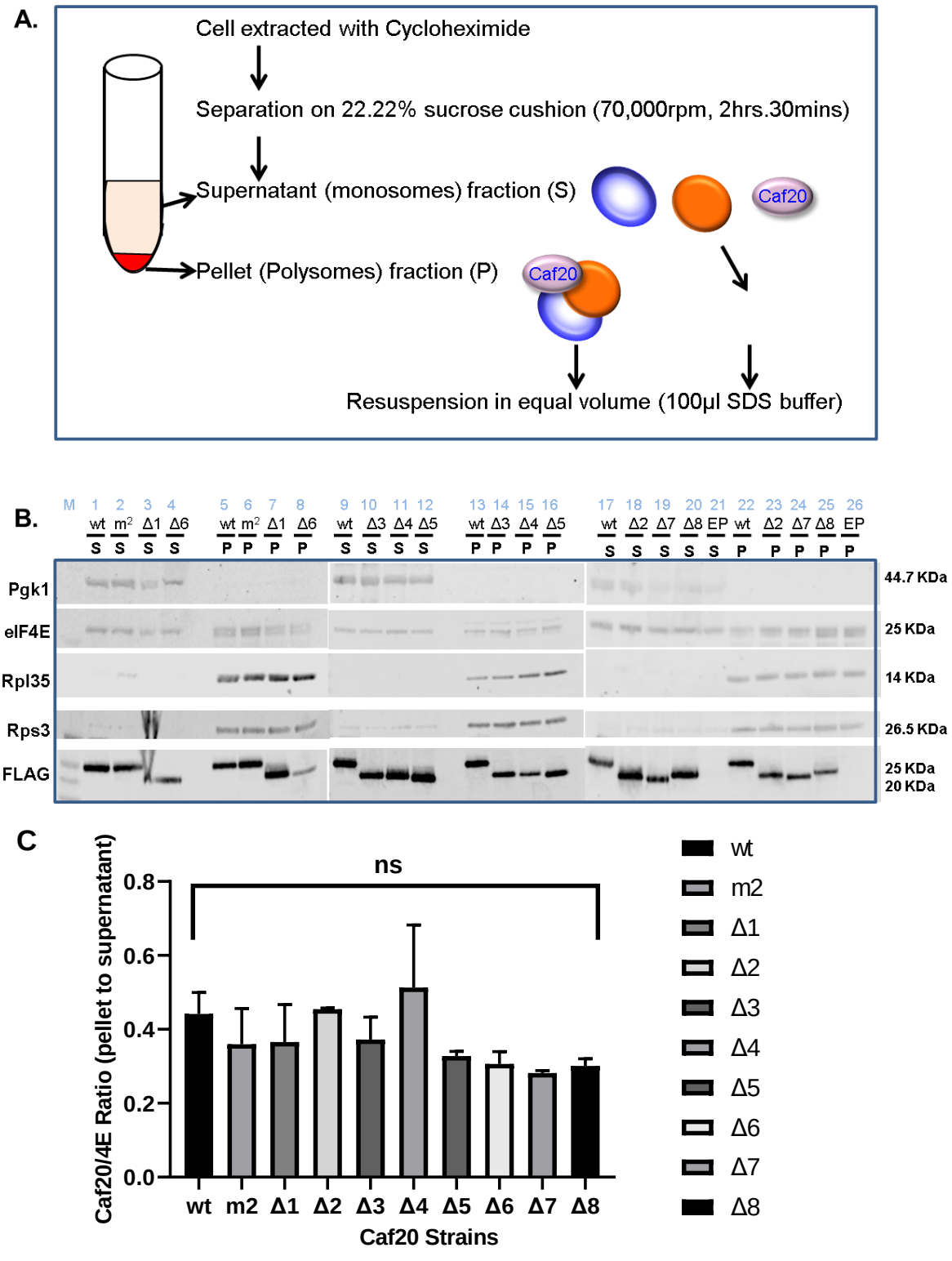

Figure 3.5. Sucrose cushion extract analysis of Caf20 binding to polyribosomes is eIF4E-Independent. A. Sucrose cushion and ultracentrifugation technique used to separate extract into supernatant and pellet fractions. **B.** Supernatant and pellet fractions were collected and proteins distributed between cushions were viewed on western blot. Western blot of Sucrose cushion probed for Pgk1, a loading control (1st column), eIF4E (2nd column), Rpl35 (3rd column), Rps3 (4th column) and Caf20-FLAG (5th column). **S** = Supernatant fraction, **P** = Pellet fraction, **EP** = Empty Plasmid. Lane M is for protein marker, lanes 1 – 26 for all the strains tested (Caf20 wildtype, mutant $Caf20^{m2}$, mutants (Δ1 - Δ8), and empty vector plasmid). **C.** Histogram chart of relative ratio of Caf20 to eIF4E (mean ratio with error bars) in the pellet fraction to the supernatant for the Caf20 strains. N=2 reps

Table 3.2. One-way ANOVA multiple comparison of Caf20wt, Caf20m2 and Caf20 Δ1- Δ8 at p value = 0.4984 (analysis not significant)

Newman-Keuls multiple comparisons test	Mean Diff.	Significant?	Summary
wt vs. m2	0.08232	No	ns
wt vs. Δ1	0.07612	No	ns
wt vs. Δ2	-0.0123	No	ns
wt vs. Δ3	0.06959	No	ns
wt vs. Δ4	-0.07093	No	ns
wt vs. Δ5	0.114	No	ns
wt vs. Δ6	0.1359	No	ns
wt vs. Δ7	0.1606	No	ns
wt vs. Δ8	0.1411	No	ns
m2 vs. Δ1	-0.0062	No	ns
m2 vs. Δ2	-0.09462	No	ns
m2 vs. Δ3	-0.01273	No	ns
m2 vs. Δ4	-0.1532	No	ns
m2 vs. Δ5	0.03166	No	ns
m2 vs. Δ6	0.05355	No	ns
m2 vs. Δ7	0.07825	No	ns
m2 vs. Δ8	0.05882	No	ns
Δ1 vs. Δ2	-0.08842	No	ns
Δ1 vs. Δ3	-0.00653	No	ns
Δ1 vs. Δ4	-0.147	No	ns
Δ1 vs. Δ5	0.03786	No	ns
Δ1 vs. Δ6	0.05975	No	ns
Δ1 vs. Δ7	0.08445	No	ns
Δ1 vs. Δ8	0.06502	No	ns
Δ2 vs. Δ3	0.08189	No	ns
Δ2 vs. Δ4	-0.05863	No	ns
Δ2 vs. Δ5	0.1263	No	ns
Δ2 vs. Δ6	0.1482	No	ns
Δ2 vs. Δ7	0.1729	No	ns
Δ2 vs. Δ8	0.1534	No	ns

Δ3 vs. Δ4	-0.1405	No	ns
Δ3 vs. Δ5	0.04439	No	ns
Δ3 vs. Δ6	0.06628	No	ns
Δ3 vs. Δ7	0.09098	No	ns
Δ3 vs. Δ8	0.07155	No	ns
Δ4 vs. Δ5	0.1849	No	ns
Δ4 vs. Δ6	0.2068	No	ns
Δ4 vs. Δ7	0.2315	No	ns
Δ4 vs. Δ8	0.2121	No	ns
Δ5 vs. Δ6	0.02189	No	ns
Δ5 vs. Δ7	0.04659	No	ns
Δ5 vs. Δ8	0.02716	No	ns
Δ6 vs. Δ7	0.0247	No	ns
Δ6 vs. Δ8	0.005267	No	ns
Δ7 vs. Δ8	-0.01943	No	ns

ns = not significant at p<0.05
*** Significant at p<0.05**

3.4.2 Can larger deletions disrupt Caf20 interaction with the ribosome?

3.4.2.1 Large deletions affect levels of expression of Caf20 and interactions with eIF4E.

As all the 20 residue deletions were able to maintain interaction with the ribosome, it was decided to create further mutations in Caf20. This time, larger deletions were proposed and constructed. An online tool (Jpred4), a secondary structure prediction server was used to predict the structure of Caf20. This tool uses multiple sequence alignments from related yeast species. The Sequence alignment indicated that Caf20 is most likely composed of three regions, each with homology with Caf20 from other yeast species. The three regions were named A, B and C and the region junctions were used as a basis for further deletion mutant construction **(Fig 3.6)**. With the *Caf20-FLAG* plasmid, a series of mutation were created by SDM, by knocking out one or two regions out of the three regions as shown in **Fig 3.7B** (see methods **2.3.1.2.3** and **2.3.1.2.4**). A similar sets of mutation was created in *Caf20^{m2} –FLAG* plasmid (ΔBm^2, ΔCm^2 and ΔBCm^2) to ensure that associations of the Caf20 mutants with the ribosome were assess properly without the interaction with the ribosome through the eIF4E (**Fig 3.7**). It was possible that in the first mutant series that eIF4E interactions of Δ2-Δ8 may have contributed to the observed ribosome interactions. As previously, some the mutations in the pRS425 plasmid were made following the normal SDM by PCR and others by inverse PCR mutagenesis (**Fig 3.7C**) (method described in section **2.3.1.2**, **Table 2.12**).

The correct deletions were assessed by digesting the mutant plasmids with two restriction enzymes, SpeI and EcoRI as Caf20 is flanked by their restriction sites on the pRS425 plasmid as described in section **2.3.1.3.** The digested plasmid DNA were resolved on 1% agarose gel electrophoresis. The expected size fragments from digestion was determined by Serial cloner's restriction analysis software for pAV2421-Caf20-FLAG in pRS425 circular plasmid incubated with SpeI and EcoRI (Perez, 2013). The three fragment sizes determined for Caf20wt-FLAG are 4766 bp from a cut between SpeI (4311) to EcoRI (1116); 2,059 bp from EcoRI (1116) to EcoRI (3175) and 1135 bp from EcoRI (3175) to Spe1 (4310) (**Fig 3.7A**). The expected molecular weights of the mutants are shown in **Table 2.11**. This is subtracted from the fragment size of 1135bp to give the actual size of the third migrating digested plasmid. **Fig 3.8A** below shows a batch of the resolved gel of some of the mutants (not all mutants included) and the sizes of the digested products. Mutants highlighted in yellow rectangle were selected for sequencing as they showed the right deletion. Some of the mutation transformations which didn't work such as ΔCwt (**Fig 3.8A**, lanes 5-7) or number of transformed replicates not adequate like ΔBm2 (**Fig 3.8A**, lanes 13, 14) and many others not shown in the figure were repeated by trying different mutagenesis techniques explained initially. Two to three plasmids containing each mutation with the correct deletion were then sent for sequencing (section **2.3.1.4**). After sequencing, the plasmids with the right deletions and clean chromatograms were transformed into yeast (GP4789) for expression analysis. From the figure, Caf20 plasmids ΔBwt (lane 4), ΔBCwt (lane 8), ΔBm2 lane (12) and ΔCm2 (lane 12) were among the plasmids selected and continued with for yeast transformation in Parts B and C (**Figure 3.8B** and **C**). Transformations with all the mutant plasmids was performed in a *caf20*Δ yeast strain (GP4789, **Table 2.2**) and the strains had untagged wildtype eIF4E (**Figure 3.8B**). Another set of transformation were performed into *caf20*Δ yeast strain (GP6323, **Table 2.2**) that had eIF4E-TAP tags. The Caf20 large deletion expression levels were monitored by western blotting (**Fig 3.8B** and **C**) and this analysis revealed that several of these large deletion mutants do not stably express Caf20. In comparison with the wild type as shown in the histogram (Fig 3.8B, right panel) mutants ΔBC*wt* and ΔBC^{m2} were the least expressed. ΔBC retains residues 1-48 which represents the combined canonical and non-canonical eIF4E-binding domain (Gruner et al., 2018). The reasons for reduced expression are not clear, but could be as a result of protein misfolding or transcript instability. It was also observed that mutants in the ^{m2} background were typically more highly expressed than

the mutants where the 4E-interacting motif remained intact (highlighted in red). To ensure the expression level is not strain specific and to analyse, and to enable reciprocal IPs of Caf20 and eIF4E. The plasmids were transformed into eIF4E-TAP *caf20*Δ tagged strain (GP6323). The Caf20 expression levels in this strain showed that Caf20 expression is dependent on eIF4E interactions to an even greater extent. All constructs with an intact region 'A' were relatively poorly expressed while equivalent constructs bearing m2 mutations were more highly expressed. In addition the ΔBC*wt* and ΔBC^{m2} which has only the NTD (48 amino acids) could not be detected in eIF4E-TAP tagged strain (**Fig 3.8C,** lanes 10 and 11) and was poorly expressed at 4% and 6% respectively in eIF4E untagged strain (**Fig 3.8B,** lanes 10 and 11). High expression levels in the m2 strains appears to be in agreement with prior studies that suggest that Caf20 can regulate its own expression when the NTD is intact (Castelli et al., 2015). The expression of eIF4E remains fairly constant across the mutants of Caf20-FLAG showing that Caf20 regulates its mRNA targets in a more specific manner and not as a general regulator (Arndt et al., 2018; Cridge et al., 2010).

Furthermore, screening the large deletions for association with eIF4E through FLAG IP was carried out as explained in methods (**2.4.4.1)** and as described for the 8 initial mutants. The results revealed that the mutants in the Caf20-FLAG (mutants ending with subscript ($_{wt}$)) with eIF4E-binding domain (intact NTD) immune-precipitated with eIF4E at 100 mM KCl in the bound fraction (pellet) (**Fig 3.9A**). They include wt, ΔB_{wt}, ΔC_{wt}, ΔBC_{wt} (**Fig 3.9A**, lanes 3, 9, 15, 18, 24, 33 and 36, upper panel blot) while mutants in the $Caf20^{m2}$-FLAG did not co-immunoprecipitate with eIF4E as expected because the motif for interacting with eIF4E is disrupted. The same blot was again probed for Caf20 without stripping (**Fig 3.9A**, lower panel). Caf20wt and Caf20m2 both co-migrate at the same level as eIF4E of which could not be distinguished from the eIF4E band. The large deletion mutants migrated faster at a lower size that could be distinguished from eIF4E band. At high salt concentrations (1 M KCl), Caf20 mutants with eIF4E-interacting motifs still maintain interaction with eIF4E (**Fig 3.9B).** However, it is observed that there was an increased pulldown of eIF4E in the mutant, ΔBC*wt* (with the NTD present) even though Caf20 signal was not detected on the 20% tricine gel used because it is not well expressed (**Fig 3.9B**, lane 10). This supports the claim that the eIF4E canonical binding motifs are important for interacting with eIF4E (Altmann et al., 1997; Bah et al., 2015; Gruner et al., 2018; Mader et al., 1995; Peter et al., 2015)

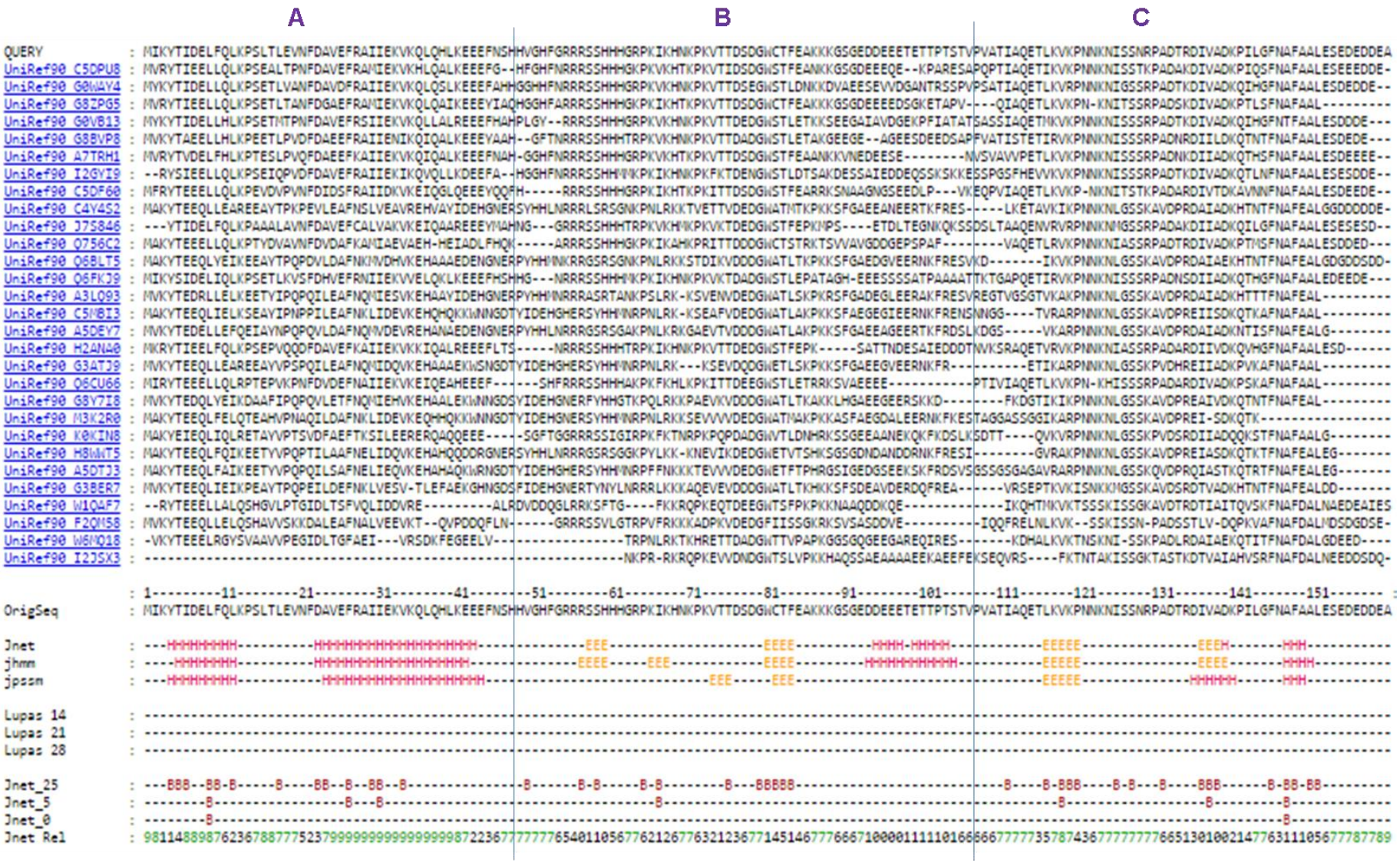
A
B
C
QUERY
UniRef90_C5DPU8
UniRef90_G0WAY4
UniRef90_G8ZPG5
UniRef90_G0VB13
UniRef90_G8BVP8
UniRef90_A7TRH1
UniRef90_I2GYI9
UniRef90_C5DF60
UniRef90_C4Y4S2
UniRef90_J7S846
UniRef90_Q756C2
UniRef90_Q6BLT5
UniRef90_Q6FKJ9
UniRef90_A3LQ93
UniRef90_C5MBI3
UniRef90_A5DEY7
UniRef90_H2AN40
UniRef90_G3ATJ9
UniRef90_Q6CU66
UniRef90_G8Y7I8
UniRef90_M3K2R0
UniRef90_K0KIN8
UniRef90_H8WWT5
UniRef90_A5DTJ3
UniRef90_G3BER7
UniRef90_W1Q4F7
UniRef90_F2QM58
UniRef90_W6MQ18
UniRef90_I2JSX3
OrigSeq
Jnet
jhmm
jpssm
Lupas 14
Lupas 21
Lupas 28
Jnet_25
Jnet_5
Jnet_0
Jnet Rel

Figure 3.6. A. Multiple sequence alignment of Caf20 in related yeast species. Single sequence of Caf20 was queried on Jpred 4 secondary structure prediction server (http://www.compbio.dundee.ac.uk/jpred4/) to obtain a likely secondary structure. The prediction showed no clear structure or domain except alpha helices (in red) predicted to be at the N-terminal end and. The beta sheet prediction confidence is low. Homolog alignments among related yeasts suggest three possible domains/regions for Caf20 (separated by blue vertical lines).

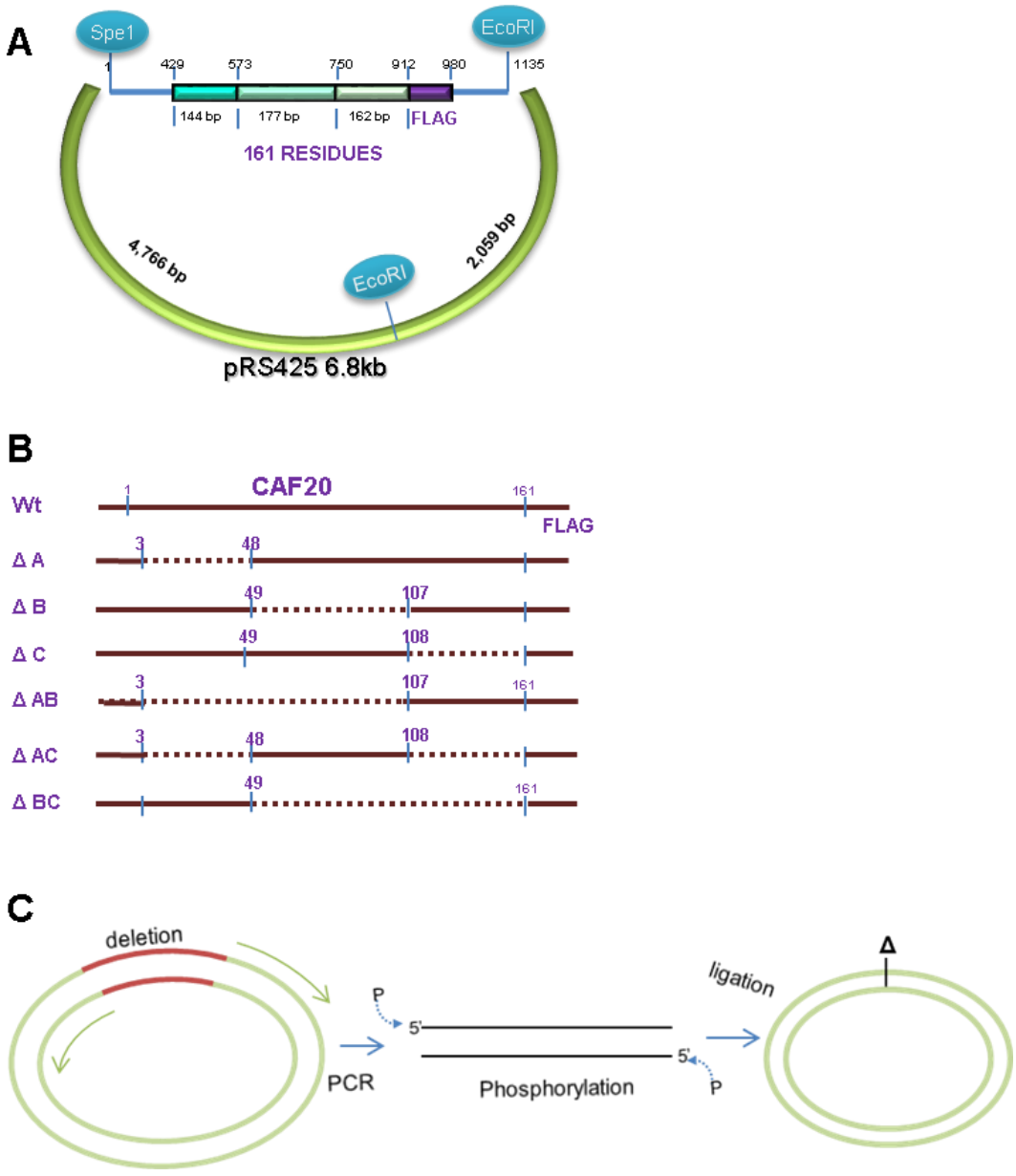

Figure 3.7. Constructs by multiple Caf20 DNA deletions. A. Site directed mutagenesis of pRS425 plasmid bearing FLAG tagged Caf20 flanked between two restriction sites of SpeI and EcoRI. Multiple deletions SDM based on the secondary structure homology prediction was used to generate sets of mutants in both pAV2421 (*pCaf20-FLAG*) and pAV2422 (*pCaf20m2-FLAG*) plasmids. The mutant Caf20 plasmids are assigned accession numbers pAV2525-2538 and are transformed into caf20Δ yeast strain (GP4789). **B.** Nine transformed yeast mutants (ΔA- ΔBC) stored as GP7305-GP7313. **C.** DNA fragment deletion by inverse PCR mutagenesis. PCR primers flank the region to be deleted (marked in red). The linear PCR plasmid is then phosphorylated and ligated to form a circular plasmid construct.

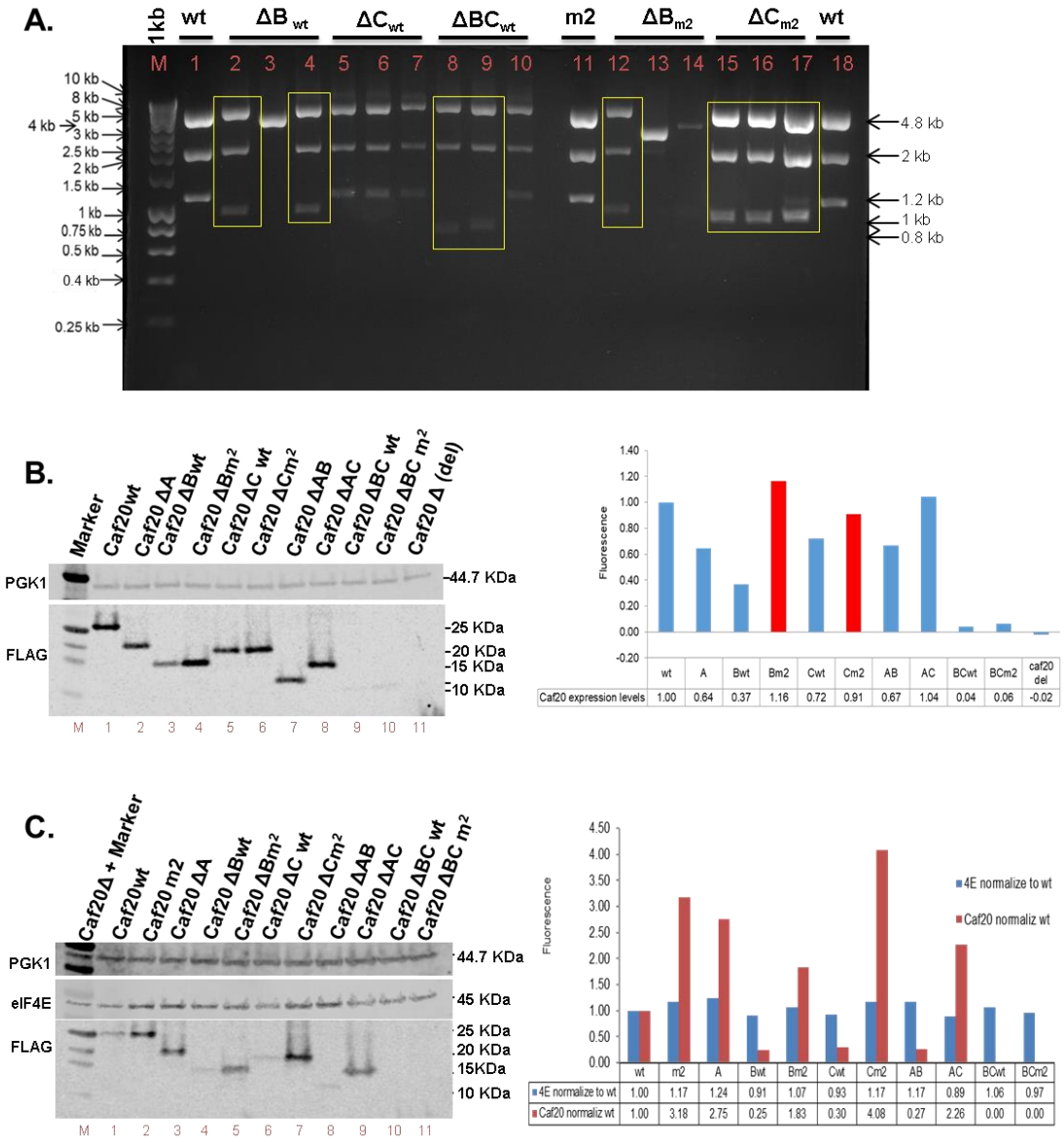

Figure 3.8. Caf20 large deletions stability in transformed strains. A. 1% Agarose Gel Electrophoresis of some Caf20 large deletion plasmid DNA digested with 1X restriction enzymes SpeI and EcoRI to check for correct deletions before sequencing. Two minipreps of each deletions were confirmed from sequencing (GATC sequencing, Eurofins). Lane M: 1 kb DNA marker, lane 1 and 18: -Caf20wt control (wildtype Caf20-FLAG digested with SpeI and EcoRI). Lane 2 - 4 is for digested ΔBwt, Lanes 5-7 for digested ΔCwt, Lanes 8-10 is for digested ΔBCwt, Lane 11– digested ^{m2}, Lanes 12-14 shows digested B^{m2} and Lanes 15-17 is for digested C^{m2} DNA. N = 3 reps. Digested Plasmids containing each mutation (hightlighted in yellow rectangle) were sent for sequencing. **B-C.** Western blots on total protein of transformed yeast strains bearing Caf20 mutants with large deletions **B.** immunoblotting of total protein of large deletions mutants expressed in *MATα* (GP4789) strain probed for Caf20FLAG and PGK1 (loading control). Lane M is for protein marker, lanes 1 for Caf20 wildtype, Lanes 2 – 10 for the Caf20 mutants (ΔA – ΔBC^{m2}) and Lane 11 – Empty vector plasmid. Histogram Panels on the right hand side depicts the same data quantified from fluorescence of the LI-COR Odyssey Fc Imager and normalized to the wildtype expression. N=1 rep. **C.** Immunoblotting of total protein of large deletions expressed in *MAT***a** (GP6323) eIF4E-TAP tagged strain. Caf20-FLAG, eIF4E (4E) and PGK1 were tested in Caf20 wt, and the deletions. Lane M is for protein marker and Caf20Δ, lane 1 is for Caf20 wildtype, Lane 2 – Caf20^{m2}, Lanes 3 – 11 for the Caf20 mutants (ΔA – ΔBC^{m2}). N=1 rep

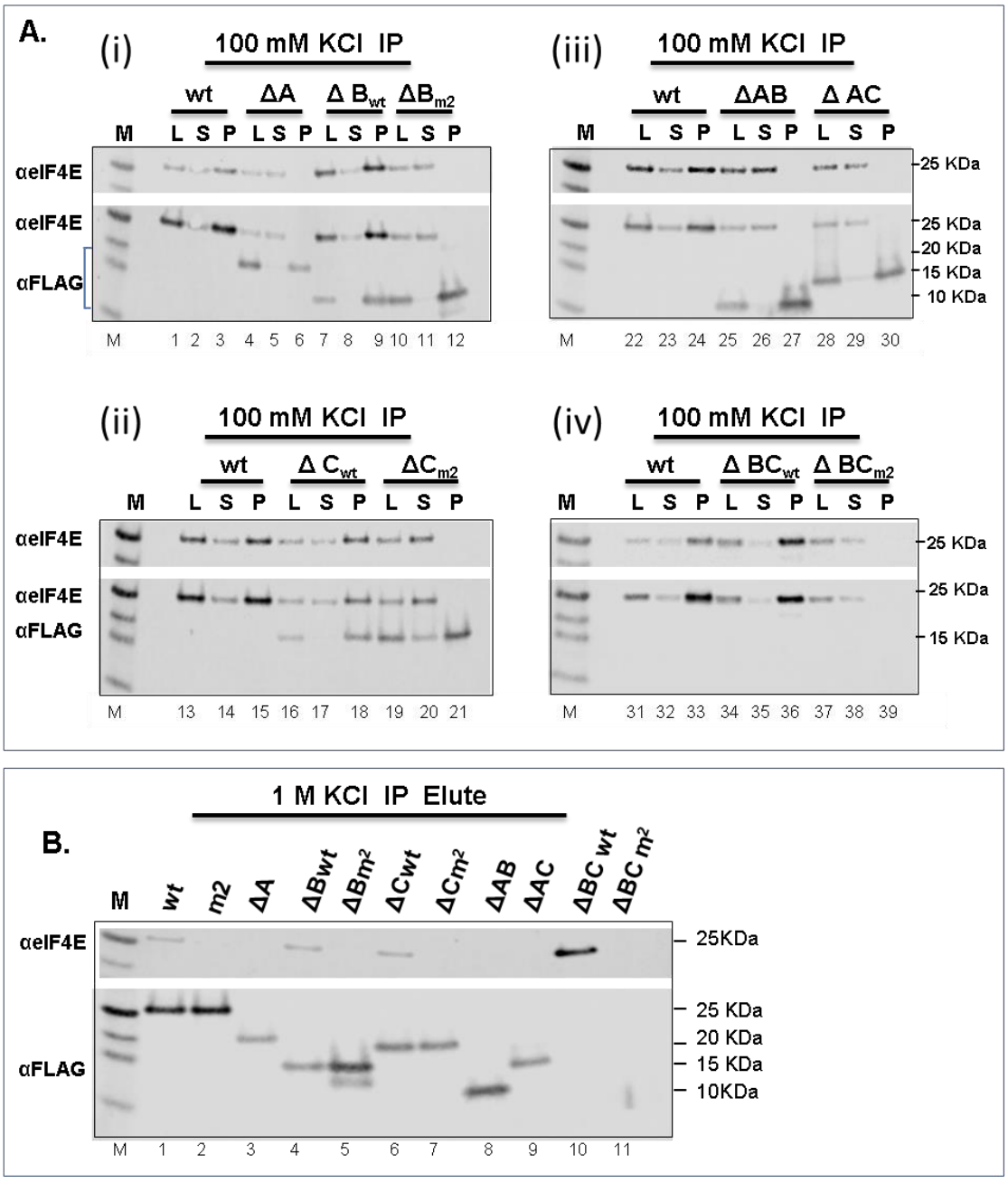

Figure 3.9. Caf20-eIF4E association in FLAG immunoprecipitation of Caf20 large deletions. A (i-iv). Western blots of FLAG IP of total extracts of Caf20 mutants washed in low salt buffer (100 mM KCl) and eluted in 3X FLAG peptide. The input load, unbound and elute were probed first with eIF4E antibody (top panel) and the same blot reprobed with Caf20-FLAG antibody (lower panel blot). Caf20 co-immunoprecipitate with eIF4E only in mutants with eIF4E-binding motif (intact NTD). Lane M is for protein marker, lane 1 – 39 for Input load (**L**), unbound supernatant (**S**) and bound pellet (**P**) of Caf20 wildtype and the mutants (ΔA – ΔBCm2). **B.** Western blots of FLAG IP Caf20 large deletes eluted samples. IP washed in high salt buffer (1 M KCl) and eluted in 3X FLAG peptides. Caf20 mutants probed with eIF4E antibody (top panel) and Caf20-FLAG antibody (lower panel). Lane M is for protein marker, lane 1 - Caf20 wildtype, Lane 2 – mutant Caf20m2, Lanes 3 – 11 for the mutants (ΔA – ΔBCm2). N = 3 reps

3.4.2.2 Extended N-terminal region of Caf20 is required for interaction with the ribosome

The large deletion constructs were next assessed for interactions with polysomes. In **Fig 3.6** it was shown that all the 8 smaller deletions (Δ1- Δ8) associated with the ribosome in sucrose cushion experiments which prompted the creation of larger deletions. It was reasoned that creating an extended deletion could disrupt Caf20-ribosome binding. Sucrose cushion experiments were performed as described for the initial eight mutants in section **3.4.1** and methods **2.5.1,** fractionating cell lysates into supernatant (ribosome free components) and pellet (polysome bound). The experiments showed that both Caf20-FLAG and Caf20^{m2}-FLAG large mutants each associate with translating ribosomes (**Fig 3.10**) reinforcing that Caf20-ribosome binding is eIF4E-independent (Castelli et al., 2015). When the relative ratio of caf20 in the ribosome to free/unbound fraction were compared, approximately 60% of Caf20-FLAGwt and Caf20m2-FLAG was typically associated with the polysomes. (**Fig 3.10**, top right histogram panel). Although none of the mutants had a complete loss of interaction with the ribosome, mutants' ΔA, ΔAB and ΔAC showed much reduced association with the ribosome with ΔAC and ΔAB have less than or equal to 10% of the total protein present in the ribosome fraction (**Fig 3.10,** top-right histogram panel). These results imply that one or more element required for binding to the ribosome might be located within the 'A' region of Caf20 (**Fig 3.10,** top panel). **Table 3.3** showed the statistical analysis using one-way ANOVA analysis ($p<0.05$) of variation in the associations of the mutants with the ribosome. Mutants with deletions in the 'A' region varied significantly in interaction with the ribosome ($p<0.05$) to the wt and m2 (**Table 3.3**). As deletions of the middle (Δ*B*^{wt} and ΔB^{m2}) or C-terminal (Δ*C*^{wt} and ΔC^{m2}) regions of Caf20 (**Fig 3.8B**) resulted in little reduction in ribosome binding compared to the Caf20-FLAG (wt) and Caf20m2-FLAG (m2) it suggests that these regions alone are not critical for ribosome interaction as they were not significantly different (**Table 3.3**). The other ribosomal proteins (Rps3 and Rpl35) and eIF4E antibodies tested (controls) behaved similar across all the mutants as expected (**Fig 3.10**, lower gel and histogram panels). Hence, it can be concluded that the extended region of NTD of Caf20 is the major determinant of Caf20 interaction with the ribosome and in agreement with previous work, that the core eIF4E interaction residues are not important for ribosome interaction.

Table 3.3. One-way ANOVA multiple comparison of Caf20wt, Caf20m large deletions of Caf20 at Pvalue = 0.0002 (***)

Newman-Keuls multiple comparisons test	Mean Diff.	Significant?	Summary
wt vs. m2	0.08639	No	Ns
wt vs. ΔA	0.2474	Yes	**
wt vs. ΔAB	0.3475	Yes	***
wt vs. ΔAC	0.3613	Yes	***
wt vs. ΔBwt	0.009366	No	Ns
wt vs. ΔBm2	0.08499	No	Ns
wt vs. ΔCwt	0.0777	No	Ns
wt vs. ΔCm2	0.1569	No	Ns
m2 vs. ΔA	0.161	Yes	*
m2 vs. ΔAB	0.2611	Yes	**
m2 vs. ΔAC	0.2749	Yes	**
m2 vs. ΔBwt	-0.07703	No	Ns
m2 vs. ΔBm2	-0.0014	No	Ns
m2 vs. ΔCwt	-0.00869	No	Ns
m2 vs. ΔCm2	0.07046	No	Ns
ΔA vs. ΔAB	0.1001	No	Ns
ΔA vs. ΔAC	0.1139	No	Ns
ΔA vs. ΔBwt	-0.238	Yes	**
ΔA vs. ΔBm2	-0.1624	Yes	*
ΔA vs. ΔCwt	-0.1697	Yes	*
ΔA vs. ΔCm2	-0.09055	No	Ns
ΔAB vs. ΔAC	0.01385	No	Ns
ΔAB vs. ΔBwt	-0.3381	Yes	***
ΔAB vs. ΔBm2	-0.2625	Yes	**
ΔAB vs. ΔCwt	-0.2698	Yes	**
ΔAB vs. ΔCm2	-0.1906	Yes	**
ΔAC vs. ΔBwt	-0.3519	Yes	***
ΔAC vs. ΔBm2	-0.2763	Yes	**
ΔAC vs. ΔCwt	-0.2836	Yes	**
ΔAC vs. ΔCm2	-0.2045	Yes	**
ΔBwt vs. ΔBm2	0.07563	No	Ns
ΔBwt vs. ΔCwt	0.06834	No	Ns
ΔBwt vs. ΔCm2	0.1475	No	Ns
ΔBm2 vs. ΔCwt	-0.00729	No	Ns
ΔBm2 vs. ΔCm2	0.07186	No	Ns
ΔCwt vs. ΔCm2	0.07915	No	Ns

Ns = not significant at p<0.05
*** Significant at p<0.05**

In order to examine if the Caf20 mutants had global impact on the overall translation profile, polysome profiling of cells of each of the Caf20 mutants strains where Caf20 showed reduced ribosome interactions (ΔA, ΔAB and ΔAC) were performed as described in section **2.5.2**. The profile traces were recorded (**Fig 3.11**). The result showed that that Caf20 mutants with modified NTD (as in m2, A, AB and AC) had a slightly higher 80S peak compared to wildtype Caf20 (wt) and Caf20ΔCwt, suggesting a modest reduction in translation initiation (**Fig. 3.11B**). However, the ratio of the polysomes to the monosomes were only slightly effected and it was decided not to examine this effect further.

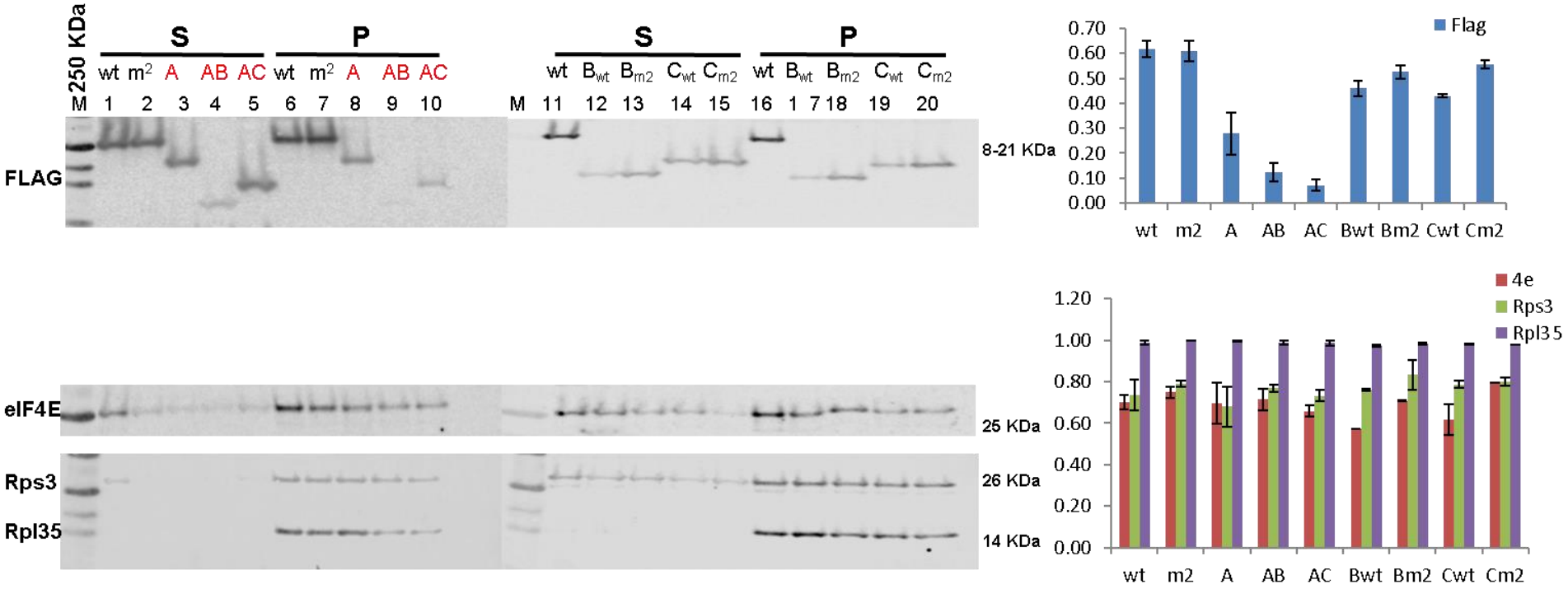

Figure 3.10. Caf20 ribosome binding elements are located at the N-terminal domain. Top panel is the western blotting of sucrose cushion for free-unbound and polysome components of different large deletion mutants probed for Caf20-FLAG. The free ribosome components are present in supernatant fractions (S) and the polysomes are in the pellet fractions (P). Lane M - marker lane, Lanes 1-5 and 11-15 represents the ribosome free components (S). Lanes 6-10 and 16-20 represent the bound pellet fractions (P). The histogram panel on the right-right corresponds to the Relative ratio of caf20 in the ribosome to free/unbound fraction. Mutants with deletions in the 'A' region varied significantly in interaction with the ribosome ($p<0.05$) using one-way ANOVA analysis to the wt and m2. Lower panel is the western blotting of sucrose cushion for free-unbound and polysome components of different large deletion mutants probed for eIF4E, Rps3 and Rpl35. Their corresponding histogram chart is shown on the bottom-right panel. The expression was fairly similar with no significant difference among the mutants. N=3 reps

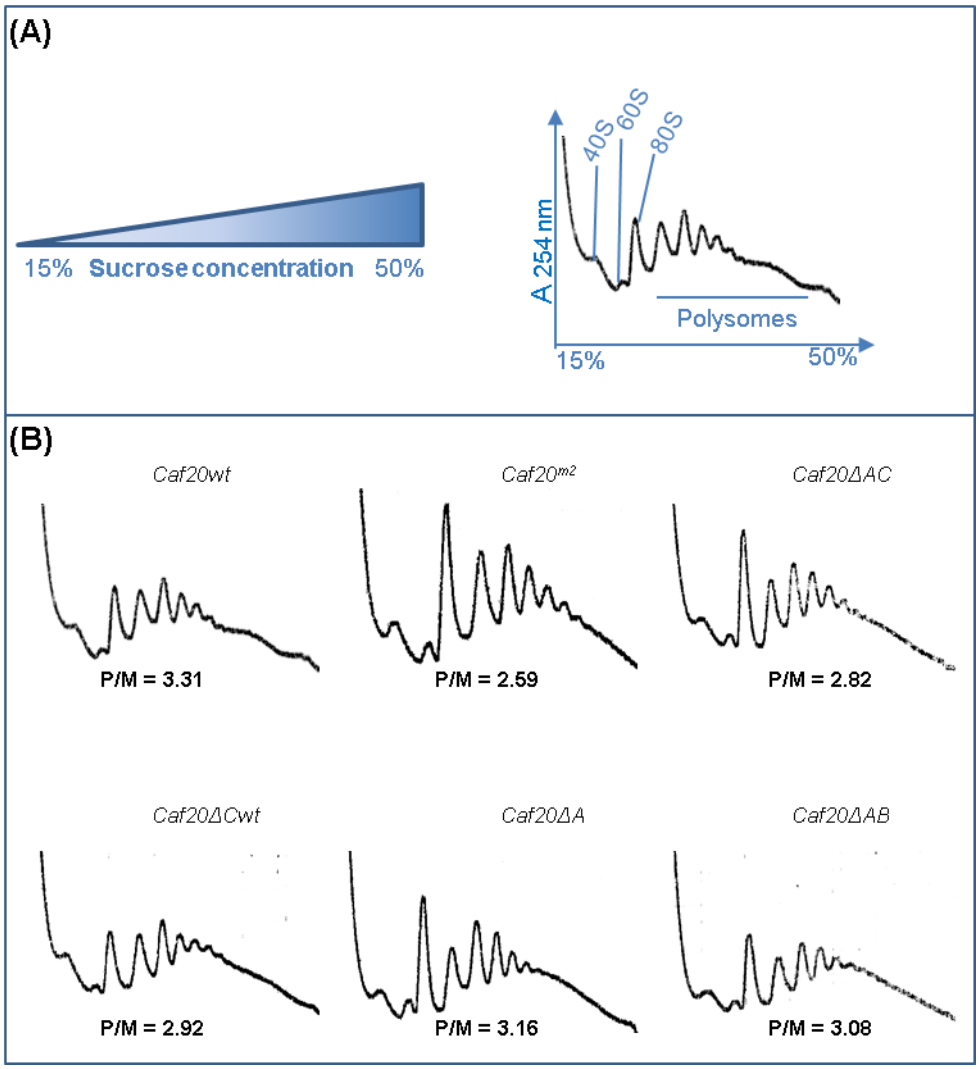

Figure 3.11. Polysome profiling of mutation in the NTD results in raised 80S polysome peaks. A. Schematic illustration of the sucrose gradient (15%-50%) used to separate ribosome-free and bound components and a poly some profile analysed at absorbance 254 nm with a UV/VIS detector. The 40S, 60S and 80S peaks and polysomes in the trace are indicated. A_{254} is the absorbance unit at 254 nm. **B.** polysome profiles of Caf20wt, Caf20m2, Caf20ΔAC Caf20ΔCwt, Caf20ΔA and Caf20ΔAB. The corresponding polysome to monosome ratio (P/M) estimated from GIMP image manipulation program is shown. The 80S peaks in Caf20m2, Caf20ΔAC, Caf20ΔA and Caf20ΔAB were slightly higher than the Caf20wt and Caf20ΔCwt but does not affect the P/M ratio. N=3 reps

3.5 Features of Caf20 needed to bind itself

3.5.1 Can Caf20 multimerize?

The mechanism of interacting with the ribosome is not fully understood. It was reasoned that if more than one Caf20 could associate together, this may enable Caf20 to bind mRNA targets to both eIF4E and to the ribosome. Previous preliminary work in our lab

had indicated that purified Caf20 protein (expressed in *E. coli*) may form a dimer with itself (unpublished). Dimerization has been reported to be involved in regulation and in forming catalytic helical structures in the protein detectable in crystal structures (Papadopoulos et al., 2014; Sun et al., 2011; Tertoolen et al., 2001). We reasoned that the range of deletion constructs generated to express Caf20 in yeast, may allow the identification of regions needed for Caf20 to interact with itself. So we decided to explore features of Caf20 important to multimerize and if such attribute is necessary to assist the eIF4E-independent function of Caf20. The strategy adopted was to use a Caf20-TAP tagged strain, where the TAP tag is integrated at the C-terminus of the genomic copy of Caf20 (GP5996, **Table 2.2**). Into this strain various *pCaf20-FLAG* plasmids were transformed, each of the three regions of Caf20 (ΔA, ΔB and ΔC). Western blotting of the total extract of the transformants (GP7460-7468) showed expression of the two different tagged Caf20 in all the mutants comparable to the expression levels of the CAf20-FLAG only mutants generated previously. This indicates that our double mutants were expressed (**Fig 3.12A**).

To assess dimer formation, Caf20-Caf20 co-immunoprecipitation was performed in two ways. First with FLAG IP (as detailed in methods **2.4.4.1, Fig 3.12B**) and a reciprocal TAP IP (as in **section 2.4.4.2, Fig 3.12C**). On performing either of the two epitope tagged IPs, Caf20 pulled down itself but in contrast, the control, [TAP] (Caf20-TAP only, GP5996) untransformed with any FLAG tag was pulled down in FLAG IP and vis-versa. This signals that there was non-specific cross reactivity with the TAP protein A tag and the FLAG antibody resin.

To overcome non-specific binding, we decided to switch to another tag instead. We transformed a Caf20-9MYC tagged strain, where the genomic copy was tagged with nine tandem copies of the MYC epitope at its C-terminus with our Caf20-FLAG plasmids (GP5094, **Table 2.2**). Both MYC and FLAG tags were expressed in the strains tested (**Fig 3.13A**). Performing a FLAG immunoprecipitation pulled down only Caf20-FLAG confirming that there was no cross-reactivity between FLAG and MYC tags (**Fig3.13B**). However, the experiment was unable to detect any co-precipitation between Caf20-9Myc and Caf20-FLAG. This result indicates that these Caf20 constructs do not stably multimerize under these conditions. It was concluded that the prior evidence of multimerization may be an artefact of *E. coli* over-expression rather than a real result and so no more experiments were done to assess Caf20 multimerization.

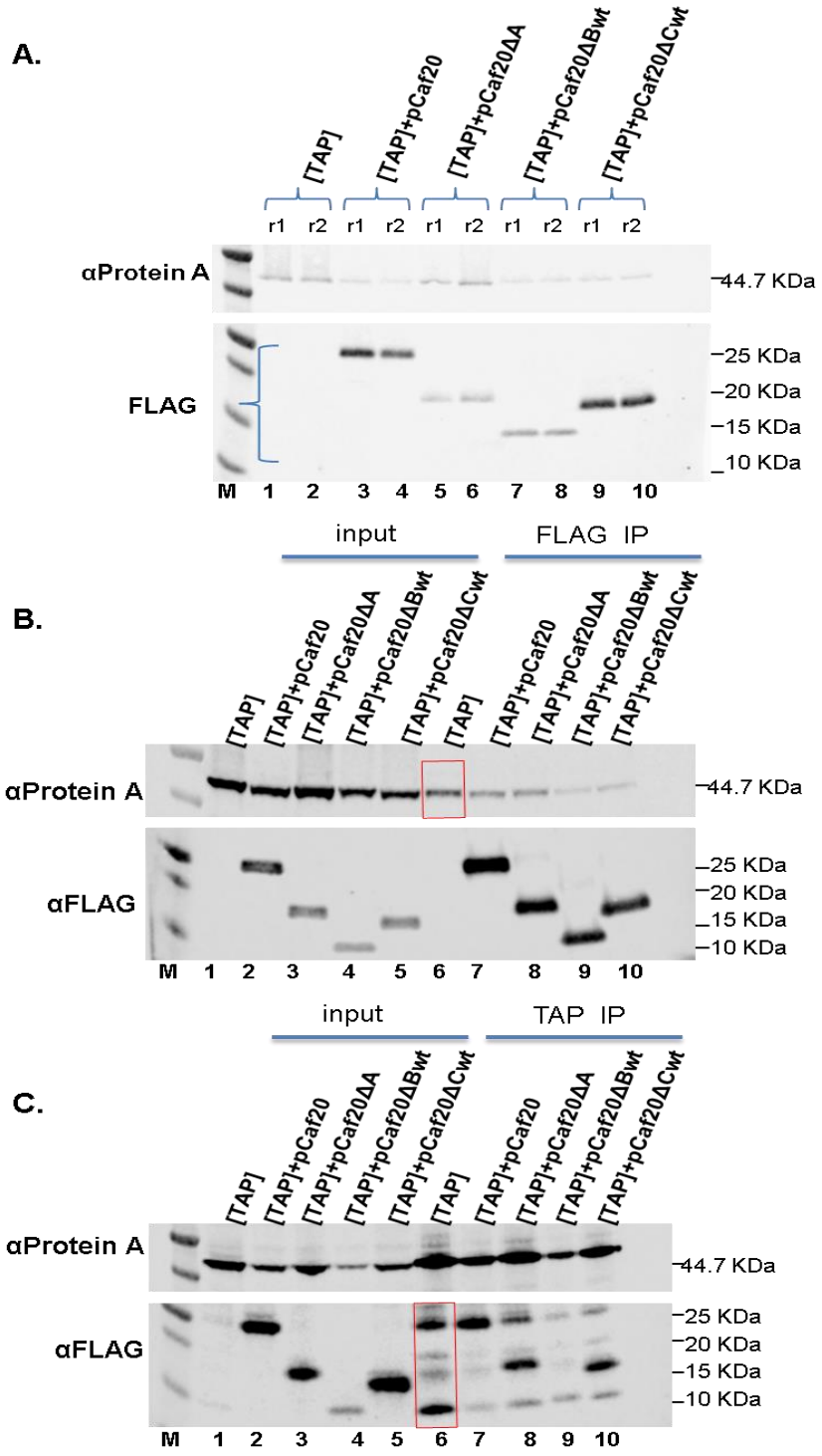

Figure 3.12. TAP tag interferes with anti-FLAG. **A.** western blotting of total extract Caf20 expression of transformation of Caf20-FLAG large deletions into genomic Caf20-TAP tag strain (GP5996) probed for Protein A and Caf20-FLAG. r1 and r2 represent transformation replicates 1 and 2 **B.** Western blotting of FLAG IP on total extract of double-tagged Caf20 (MYC and FLAG) probed for Protein A and Caf20-FLAG. . Lane M is the marker lane, Lanes 1-5 is the input lane and lanes 6-10 are the TAP IP elutes. Non-specific pulldown of TAP and FLAG in TAP control strain (indicated in red box), N=1 rep. **C.** Western blotting of TAP-IP of the double transformed strain probed for Protein A and Caf20-FLAG. **Note:** [TAP] represents chromosome integrated Caf20-TAP tag and pCaf20 represents plasmid Caf20-FLAG. Non-specific pulldown of TAP and FLAG in TAP control strain (indicated in red box). N = 1 rep

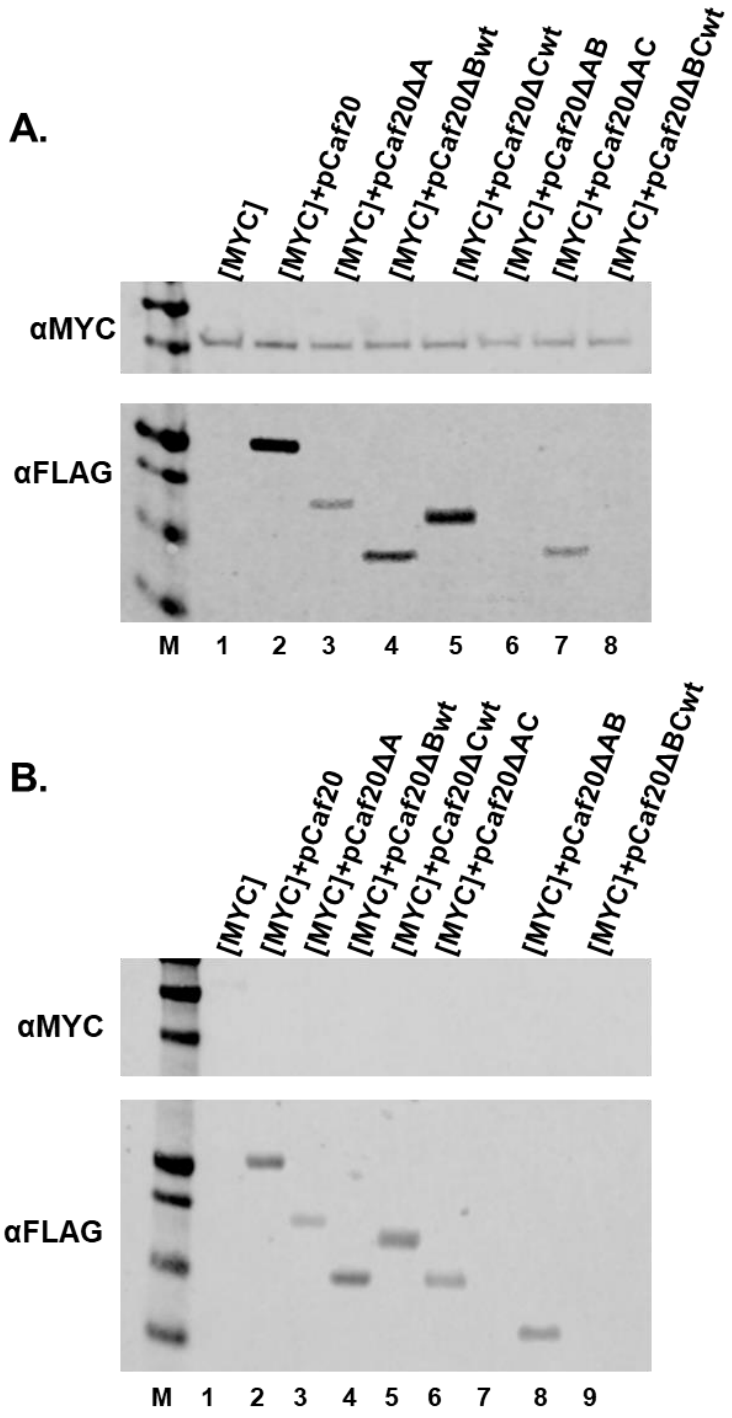

Figure 3.13 Dimerization is not important for Caf20 interactions. **A.** western blotting of total extract Caf20 expression of transformation of Caf20-FLAG large deletions into genomic Caf20-9MYC-tag strain (GP5094) probed for Caf20-MYC and Caf20-FLAG. **B.** Western blotting of eluted FLAG IP of total extract of double-tagged Caf20 (MYC and FLAG) probed for CAf20-MYC and Caf20-FLAG. [MYC] represents chromosome integrated Caf20-9MYC tag and pCaf20 represents plasmid Caf20-FLAG. N =1 rep

3.6 Discussion

All 4E-BPs in yeasts and in mammals exhibit a structural similarity within the canonical eIF4E-interaction motif (Bah et al., 2015; Peter et al., 2015; Richter and Sonenberg, 2005). However it was previously demonstrated that Caf20 binds to its mRNA partners via 4E-dependent and 4E-independent interactions (Castelli et al., 2015) of which the majority of Caf20 mRNA targets are 4E-dependent (75%) whereas 25% (~131 core mRNAs) bind to both 'wt' and 'm2' mutated Caf20 when cells are grown in standard conditions (Castelli et al., 2015). One of the key findings was Caf20 association with the ribosome was independent of its interaction with eIF4E. It remained unclear what the role of Caf20-ribosome interactions are and whether this interaction was important for Caf20 functions. The other yeast 4E-BP Eap1 was also found to interact with the ribosome (Castelli et al., 2015), suggesting ribosome interaction was non-unique to Caf20, but a shared function among 4E-BPs.

The research question addressed in this chapter was to identify features of caf20 critical for interacting with either eIF4E or the ribosome. Before the commencement of this project, the crystal structure of Caf20 (residues 1-49 only) in complex with eIF4E was not known (Gruner et al., 2018). Instead all that was known was that the canonical motif (YXXXXLΦ), shared among Caf20 (as Y_4TIDELF$_{10}$) and other 4E-BPs was critically important for interacting with eIF4E (Mader et al., 1995). Other non-canonical motifs were reported for 4E-BPs in metazoans (Igreja et al., 2014; Peter et al., 2015). So to understand more fully if there were additional elements important to bind to eIF4E, a series of deletion constructs were made using a Caf20-FLAG plasmid and then tested for elements needed to interact with eIF4E and/or translating ribosomes. The study also intended to ascertain structures in Caf20 required to bind itself through dimer formation.

As the structure of Caf20 was not known, but was believed to be at least partly unstructured with no clear identifiable domains (SGD database and **Fig 3.7A**), a series of eight different mutants (Caf20Δ1-Caf20Δ8) were generated, each missing 20 consecutive amino acids from the beginning to the end of the protein (Caf20 has 161 residues; **Fig 3.1**). When the Caf20-eIF4E structure paper was published, Caf20 constructs Δ1 and Δ2 made in this study aligned well with the published structure's canonical and non-canonical interaction regions respectively. The Caf20 crystal structure studied 45 residues in the N-terminal region of Caf20 bound to eIF4E revealed residues Y4 is the first important residue that forms the eIF4E-canonical motif and a linker region falling

between residues 12 and 24. The two regions (canonical and linker) form the missing region of our Caf20Δ1. The non-canonical α-helix for eIF4E-lateral binding (residues 24-41) of Caf20 map directly onto the deleted region of Caf20Δ2 (residues 23-42) made in this study. When the mutants were introduced into a *caf20*Δ strain, plasmids expressing each mutation demonstrated that all eight mutants (Caf20Δ1-Caf20Δ8) were stably expressed (**Fig 3.3**).

FLAG immunoprecipitation with FLAG magnetic resin was optimized to include eluting with 3X FLAG peptide to get rid of co-migration of FLAG resin antibody light chain with the Caf20 band. It was found that Caf20 co-immunoprecipitates with eIF4E (Figure 3.5) which is consistent with past findings (Arndt et al., 2018; Castelli et al., 2015). Previously it was shown that eIF4E-Caf20 interaction is maintained even when treated with RNAse I. (Castelli et al., 2015). This indicates that Caf20-eIF4E complex is maintained primarily by protein-protein interactions, in agreement with prior findings for other 4E-BPs (Napoli et al., 2008). One of our mutants (Caf20Δ1) that deleted eIF4E-binding domain and one of the controls ($Caf20^{m2}$) with two mutations in the binding domain failed to interact with eIF4E (**Fig 3.5II** and **III**, lanes 2 and 10).

The crystal structure report on yeast 4E-BPs shows that non-canonical binding motif binds eIF4E, but Caf20Δ2 binds eIF4E just fine in the IP assays (**Fig 3.4**) with very minor or no contribution of non-canonical interactions to eIF4E binding. The structure paper observed the same in their Caf20 study and concluded that non-canonical binding elements may contribute differently towards the affinity of interaction with eIF4E (Gruner et al., 2018).

The tight association of Caf20 with eIF4E, which has a negative charged surface (Cawley and Warwicker, 2012; Scheper et al., 2002) even at a high salt (1 M KCl) concentration (Figure 3.5B) affirm some previous reports that interactions of 4E-BPs and eIF4E is of high affinity (K_d = 3.20 ± 0.6 nM) (Bah et al., 2015). Arndt et al. (2018) demonstrated with MicroScale Thermophoresis and Electrophoretic Mobility Shift Assays that eIF4E in complex with Caf20 had a higher affinity for capped RNAs than eIF4E to capped RNAs only. In contrast, one earlier report used purified proteins and surface plasmon resonance to examine interactions. The study suggested Caf20-eIF4E binding was weak (Ptushkina et al., 1998). The findings here agree with most prior work and indicate very tight binding to eIF4E.

A sucrose cushion technique was used to screen for ribosome association. This was optimized to give a better separation of the ribosome –free and ribosome-bound fractions by increasing the ultracentrifugation to 213,100 xg and lowering the final sucrose concentration used in the cushion to 22.22%. Experiments with the 8 mutants (Caf20Δ1- Caf20Δ8) showed Caf20Δ1 and Caf20^{m2} are enriched in the polysomes confirming the previous report that Caf20 binds to ribosome independent of eIF4E (Fig 3.6) (Castelli et al., 2015). Caf20Δ2 deleted region was later reported to contain the eIF4E non-canonical motif (Gruner et al., 2018).

It was clear that unlike eIF4E interaction that relied on a short motif, Caf20 ribosome interaction was not significantly disrupted by any of the mutants tested. Thus either it required a longer region or perhaps multiple isolated/redundant elements combined to make the interaction surface. It was therefore decided to create further deletion alleles. Larger deletions were made following related yeast sequence homology which indicated 3 regions of the protein, termed A, B and C (**Fig 3.7A**). Region A (residues 3-48) is equivalent to the eIF4E interaction region identified in the co-crystal structure (residues 1-49).

Results from the sucrose cushion experiments points that Caf20 interaction with the ribosome require multiple elements driven more by an extended region of the N-terminal domain. Deletion of region B or C alone had no impact on ribosome interactions of Caf20, however ΔA was significantly ($p<0.05$) depleted from the ribosome pellet fractions. This interaction was further weakened by combining deletions of either B or C with A. This result suggests that the N-terminus is dual functional being important for both eIF4E and for ribosome interactions. It shows that an extended interface is able to bind Caf20 to the ribosome. As deletion of either B or C alone has little effect, it suggests region A is the dominant region of interaction, which is enhanced by both regions B and C. This demonstrates that Caf20 has important elements other than the eIF4E-binding domain at the N-terminal domain.

It remains unclear if a single caf20 monomer can bind to both eIF4E and to ribosomes simultaneously, or if binding is mutually exclusive. It has also been suggested that Caf20 can multimerise with itself. As this may contribute to our understanding of Caf20 mechanisms an assay was developed to assess Caf20 protein multimerization in vivo. The results from immunoprecipitation suggested that Caf20 dimers did not form under our experimental conditions. Instead apparent interactions were caused by tag non-

specific interactions with affinity resins. This was seen when Caf20 was tagged with TAP and separately with the FLAG epitopes (Fig.3.12). When one of the tags was switched to MYC-tag, no evidence for Caf20 multimerization was seen. In the light of this, models for Caf20 function should assume that Caf20 interacts with its binding partners as a monomer rather than a homodimer or other higher order complex.

Taking all the results together, a model was proposed which suggests that Caf20 requires a short motif, called the canonical interaction motif and found at the extreme N-terminus to bind with eIF4E (**Fig 3.14**). In contrast, an extended region of the N-terminus, including at least the eIF4E-canonical motifs, linker region and the non-canonical regions binds with the ribosome. As well, some elements within regions B and C of Caf20 likely also stabilize ribosome interactions.

In the next chapter experiments examining where on the ribosome Caf20 binds are described.

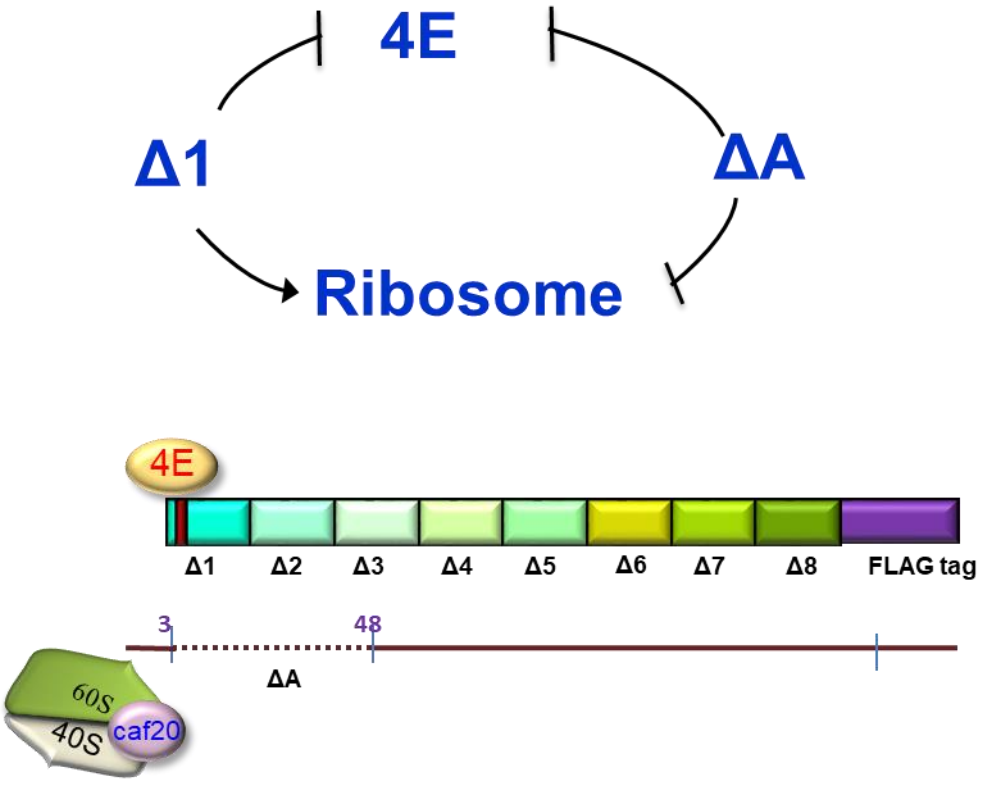

Figure 3.14. N-terminal domain of Caf20 is important to interact with eIF4E and ribosome. Caf20 requires very small region to bind to eIF4E and a larger region to bind to the ribosome

Chapter 4

Identifying Caf20-protein interaction on the ribosome through crosslinking

4.1 Introduction

In Chapter 3, it was established that Caf20 interacts with eIF4E and the ribosome through its N-terminal region. However what was not clear and has not been documented is where on the ribosome Caf20 binds. As discussed in the first chapter, ribosomes are ribonucleoprotein complexes that function in translating mRNAs into proteins. They are made up two subunits comprising 79-80 ribosomal proteins and 4 rRNAs in yeasts and other eukaryotes. Within ribosomes are sites for the entry and exit of tRNAs as well for that of mRNA and a tunnel through which the growing peptide chain emerges (Schmeing and Ramakrishnan, 2009). Many proteins and RNAs are interacting together to ensure fidelity in translating mRNAs into functional proteins. The position of these proteins on the ribosome can indicate what role they perform on the ribosome. Heterogeneity in ribosome composition resulting from differential expression and post-translational modifications of ribosomal proteins, rRNA diversity and the activity of ribosome-associated factors may generate 'specialized ribosomes' that have a substantial impact on how the genomic template is translated into functional proteins (Xue and Barna, 2012).

Many of the yeast ribosomal proteins are encoded by two paralogous genes (isoforms) (Planta and Mager, 1998), as a result of genome duplications enabling ribosomes to differ in their core subunit composition as well as in association of peripheral RNA-binding proteins. Differences in the expression, localisation and function of these paralogous ribosomal proteins is been documented for the past 25 years and recent evidence of structural differences between ribosomes has only begun to emerge due to improved mass spectrometry analysis (review in (Crawford and Pavitt, 2019)).. More evidence of stoichiometric differences between eukaryotic ribosomal proteins has been reported (Shi et al., 2017) which faults previous works that portrayed ribosomes as having a uniform or homogeneous conformation (Ben-Shem et al., 2011; Ben-Shem et al., 2010). Paralogues of many core ribosomal proteins and rRNAs may show differences in stoichiometry when modified by addition of methyl or phosphoryl groups. Though there are no much of specialized ribosomes in the cells as majority are undistinguishable, those that become specialised are important in responses to environmental stress. 59 out of the 80 ribosomal proteins exists in paralogue pair and are expressed as 'a' and 'b' forms of paralogous genes (Planta and Mager, 1998). A study of Rps27a and Rps27b found that cell lacking Rps27a exhibit ribosomal assembly defects and deficiencies in rRNA processing despite growing at the wildtype rate, demonstrating that growth rate does not

really reflect functionality (Baudin-Baillieu et al., 1997). High-throughput screens have suggested more subtle differences between duplicated ribosomal protein genes, including specific defects in sporulation, actin organisation and bud-site selection (Komili et al., 2007). A well-researched functional specificity of duplicated ribosome paralogs is the yeast protein Ash1. The Ash1 localizes specifically to the daughter cell where it acts to suppress matting-type switching during cell division. Protein localization is obtained by *ASH1* mRNA localization through a well-characterized translation and translation regulation. Studies have shown that mutation in *ASH1* mRNA that disrupt its translation hinder bud-tip anchoring, as does inhibition of translation resulting in a mislocalization of mRNA throughout the emerging daughter cell (Irie et al., 2002). Another similar study revealed specialisation in paralogous ribosomal proteins Rpl8a and Rpl8b to stress hen the carbon source was changed from glucose to glycerol. Genetic analysis to support the evidence revealed divergent function for the paralogous pair as the pair can complement each other during growth on glucose but not glycerol (Sun et al., 2018). In addition to specialisation of paralogous pair, some ribosomal proteins are non-essential for normal ribosome function but their deletion can specialize ribosome to translate certain mRNA substrates. Mutations or deletions of some ribosomal proteins in concert with the tumour suppressor gene mutations *TP53*, have been linked to some disease pathways as well as suppression of malignant tumours (cancers) and non-cancerous tumours (Ajore et al., 2017; Dolezal et al., 2018; Goudarzi and Lindstrom, 2016; Shenoy et al., 2012). Heterogeneous ribosomes can also be generated through removal of subunits which differs in application to addition of RNA-binding proteins to achieve a similar goal, but seems to be important for translational control in changing conditions (Briggs and Dinman, 2017; Crawford and Pavitt, 2019). Constitutive components of the ribosome may also exert more specialized activities by virtue of their interactions with specific mRNA regulatory elements such as ribosome entry sites (IRESs) or upstream open reading (uORFs) (Xue and Barna, 2012).

It has been reported that Caf20 interacts with the ribosome through a mechanism independent of its association with eIF4E (Castelli et al., 2015). The aim of this chapter is to discuss the experiments performed to identify proteins that directly associate with Caf20 on the ribosome. This being a first step towards discovering a site on the ribosome where Caf20 binds, which in turn may throw more light of its role on the ribosome. To fully understand where on the ribosome Caf20 interacts with and its interacting partners, a protein-protein interaction approach through chemical-crosslinking and

immunoprecipitation was employed. The method crosslinks proteins that are closest to each other based on the spacer arm length of the crosslinker and the type of residues it conjugates which can then be identified through biochemical approach of western blotting and mass spectrometry. In this Chapter, two crosslinking techniques adopted to crosslink Caf20 in total extracts and in purified ribosomes bound to Caf20 are described.

4.2 Chemical crosslinking reactions and stabilization of proteins

Crosslinking is applied for many purposes including to (i) stabilize protein tertiary and quaternary structures for analysis; (ii) capture and characterize unknown protein interaction domains and interactors, (iii) immobilize antibodies or other proteins for assays or affinity-purifications, and (iv) attach peptides to larger 'carrier' proteins to facilitate handling/storage. Some advantages of crosslinking obtained from different researches have shown that crosslinking has proven to be important in obtaining information about the structure and function of proteins. It also help reveal important information about protein interactions in receptors, signalling cascades and multiprotein complexes (Fancy et al., 1996; Interactions/Cross-linking, 2011; Lynch and Koshland, 1991). Information from crosslinking experiments allows site-directed coupling of proteins with distinct properties and are powerful in providing a higher resolution of the structural data to the point of mapping protein-protein interactions to specific amino acids or domains (Heck et al., 2013; Interactions/Cross-linking, 2011). The most important advantage of crosslinking is that it allows for noncovalent protein-protein interactions, those that are transient or dependent on specific physiological conditions, to be captured in long term covalent complexes that maintain the information even through further processing, including purification, enrichment and analysis (Interactions/Cross-linking, 2011; Trakselis et al., 2005).

On the contrary, there is the potentiality of the crosslinking reagent crosslinking to multiple proteins which could be difficult to resolve and identify. There is also the problem of crosslinking of residues in antibodies-binding domains which interfere in the isolation of protein of interest if the residues crossed could not bind to immunoprecipitation resins. The spacer arm length of the crosslinker could be an impeding factor when it is too short to target protein of interest or too long which could crosslink to many proteins farther from the protein of interest. Majority of chemical crosslinkers cannot be applied to live cells. Another important limitation is that the use of chemical crosslinking reagents can be unfavourable when applied in the areas of food

processing and tissue engineering because many of these compounds are rated as toxic or may form harmful by-products leading from the crosslinked matrix (Heck et al., 2013).

To achieve the right crosslinking, crosslinkers to be used are supposed to be very specific and with minimum noise. The 3 protein crosslinkers (**Fig 4.1**) tested are:

(a) BMH (Bismaleimidhexane) is a maleimide crosslinker with spacer arm of 13.0 Å (ThermoFisher Scientific, 22330) which conjugates sulfhydryls (cysteine to cysteine) between two specific proteins at pH of 6.5-7.5 to form stable products that are non-reducible (**Fig 4.1B**).

(b) MBS (m-maleimidobenzoyl-N-hydroxysuccinimide ester) is a crosslinker with spacer arm of 7.3 Å (ThermoFisher Scientific, 22311), containing N-hydroxysuccinimide (NHS) esters and maleimide groups and allows covalent non-reducible bonds between corresponding amines and sulfhydryl molecules. It conjugates lysine and cysteine molecules of proteins. The amine and sulfhydryl groups of the crosslinker work together at pH of 7.0-7.5.

(c) DSS (disuccinimidyl suberate) on the other hand is a crosslinker with two N-hydroxysuccinimide esters (NHS-esters) groups which creates a stable covalent bond between two primary amino-groups at pH of 7-9. The amines of the lysine side chain are the targets of the NHS-esters thereby conjugating lysine-lysine. DSS has a spacer arm of 11.4 Å (ThermoFisher Scientific, 21655).

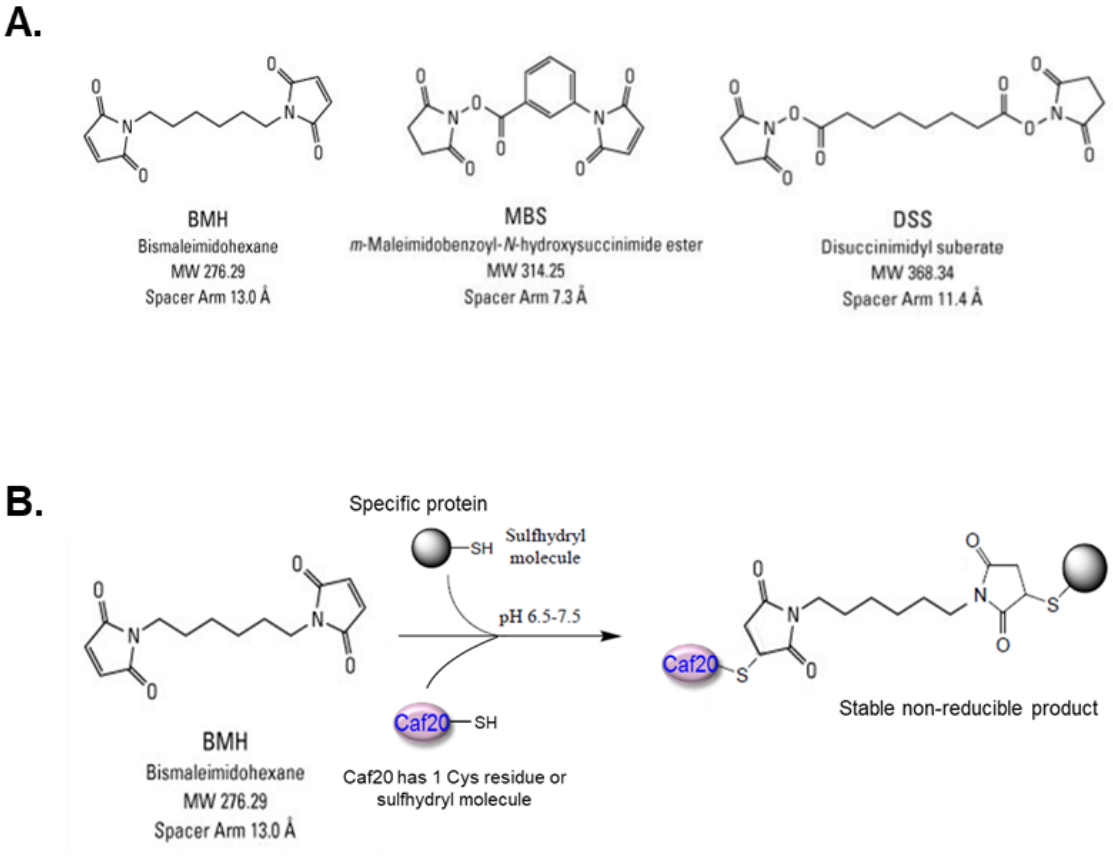

Figure 4.1. Caf20 – Protein crosslink. **A.** Three different croslinkers is tested – BMH (bismaleidohexane) crosslinks a cysteine (sulfhydryl molecule) to another cysteine; MBS (m-maleimidobenzoyl-N-hydroxysuccinimide ester) conjugates cysteine to lysine and DSS (disuccinimidyl suberate) crosslinks lysine to lysine. **B.** Reaction of maleimide-activated compounds to sulfhydryl. At pH 6.5 to 7.5, meleimides, BMH permanently binds sulfhydryl molecules between Caf20 to another molecule.

The crosslinkers used here were selected because they had been assessed by a Postdoc in our lab (Dr Martin Jennings) and have also been used by a former PhD student in Dr Martin Pool's lab. In each case the individuals were also studying the interactions of proteins known to associate with ribosomes. Because Caf20 has only one cysteine residue at position 82 outside the main ribosome binding region, the BMH crosslinker which reacts with two sulfhydryl (cysteine) molecules together appeared to be a suitable crosslinker to be used for Caf20. As cysteines are less common than lysines in proteins BMH was expected to have the least 'noise' that could arise from compound crossing of more than one residue in a protein to several proteins that could not be detected in Mass spectrometry. However a cross-linking partner may not contain an accessible cysteine residue within range so other crossliners were selected with different broader specificities.

4.3 Caf20 associates with specific binding proteins in total cell extracts.

As mentioned in the introduction of this chapter, to identify Caf20 targets on the ribosome, two crosslinking techniques were performed; crosslinking in total protein and ribosome-bound crosslinking. For ease, this section will discuss Caf20 crosslinking in total cell extracts. Total extracts and crosslinkers were prepared and crosslinked as described in methods (section 2.6.1).

4.3.1 Caf20 crosslinks to specific proteins

The initial small-scale crosslinking tests were carried out at final concentrations of 0.5-2 mM to select the optimal working concentrations for the crosslinkers and the best crosslinker to adopt in total extract crosslinking. Each 50 ml culture cell extract from Caf20-FLAG strain (GP7164, Table 2.2) was crosslinked with 0.5, 1, 2 mM of the three crosslinkers for 20 minutes. A control was included in the tests to exclude non-specific crosslinking by incubating cell extract with DMSO solvent used to dissolve the crosslinkers.

The result of the western blotting of the initial small scale total cell extracts crosslinking on Caf20-FLAG probed with FLAG antibody revealed that Caf20 crosslink to unique proteins (**Fig 4.2**). Each concentration of the crosslinker tested crosslinked proteins, with the optimal level of crosslinks achieved at final concentration of 1 mM concentration after 20 minutes incubation. Proteins crosslinked to Caf20 move higher up on the gel. BMH that crosslinks cys-cys residues gave the highest number of crosslinks indicated in small red circles (**Fig 4.2**, lanes 2, 3 and 4 at the upper panel), followed by MBS crosslinker. The DSS gave the least crosslinks for Caf20 (lanes 8, 9 and 10 at the top panel), revealing a unique protein at band size 50 KDa.

The most prominent crosslinked proteins across all the crosslinkers are the two bands at size of 35 KDa and 50 KDa. This indicates crosslinks from the cys of Caf20 (~25 KDa) to proteins of approximate sizes of 10 KDa and 25 KDa respectively, with the 50KDa band appearing at the lowest concentration used and the crosslinked protein intensities saturating at 1 mM. A significant proportion of Caf20 remained uncross-linked and migrated as in the DMSO control lane. Probing with eIF4E antibody showed that eIF4E crosslink with other proteins in MBS and DSS crosslinker at band size 50 KDa and 200KDa but does not crosslink in the presence of BMH (**Fig 4.2**, lower panel). A non-specific band of 160 KDa appeared also in the DMSO control lane making it unlikely to

be a true crosslink of eIF4E. This experiment proves BMH to be very specific and a good crosslinker to use. As a result of these initial analyses the BMH crosslinker was selected and used in subsequent total extract crosslinking.

In conclusion, the result from **Fig 4.2** suggests that Caf20 stably crosslinks with specific factors in total cell extracts

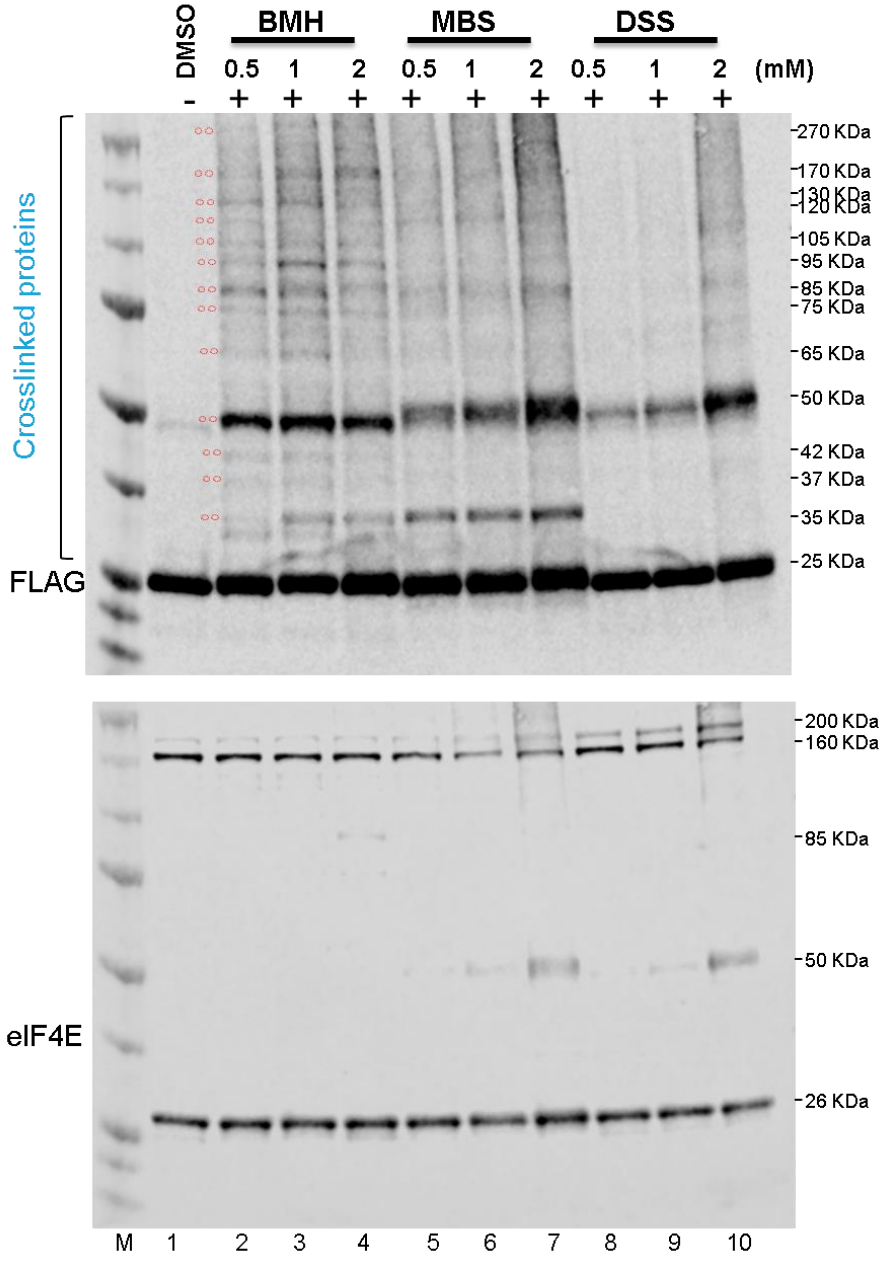

Figure 4.2. Caf20 interact with unique proteins. Western blot of small scale total cell extracts crosslinked with BMH, MBS and DSS in wildtype Caf20-FLAG, each tested at final concentrations of 0.5, 1, 2mM and probed with FLAG antibody (upper panel) and eIF4E (lower panel). Lane M is for the protein marker; lane 1 – extract crosslinked with DMSO; lanes 2-4 for extracts crosslinked with BMH at 0.5, 1 and 2 mM respectively; lanes 5-7 for extracts crosslinked with MBS at 0.5, 1 and 2 mM respectively; lanes 8-10 for extracts crosslinked with DSS at 0.5, 1 and 2 mM respectively. N = 3 reps for each crosslinker experiment

4.3.1.1. Caf20 interact with new specific proteins other than eIF4E

In order to identify potential crosslinked-partners of Caf20 in total cell extracts, the presence of some known Caf20-interacting proteins were screened in the BMH-crosslinked samples. FLAG IP was performed on crosslinked total protein and analysed on western blotting. The results in **Fig 4.3** showed some of the antibodies tested on western blot of FLAG immunoprecipitation of crosslinked total extracts. The migration of crosslinked FLAG IP input and unbound samples (in Lane 2 and 3), 3X FLAG peptide eluted crosslinks (lane 4) and second elution with SDS of what is still left on the beads after the FLAG peptide elution cleared or with some of the resin (in lanes 5 and 6) where compared relative to the control (DMSO-treated) total extracts (in Lane 1) as can be seen in (**Fig 4.3**). When FLAG antibody was switched to Caf20 antibody (**Fig 4.3A**), the blot showed more distinct crosslinks than was identified with FLAG antibody alone (**Fig 4.2**) which included the bands at the 35 KDa and 50 KDa mark, as identified previously. Some of the crosslinked proteins were eluted with the FLAG peptide but a lot were still stuck on the beads (lanes 5 and 6). However when the blot was stripped and probed with either Pab1 (**Fig 4.3B**) or eIF4E (**Fig 4.3C**), the results from the blots revealed that the FLAG IP pull down Pab1 and eIF4E of sizes 70 KDa and 26 KDa respectively on the gel of which did not crosslink with any protein (**Fig 4.3B** and **4.3C**, lane 4). Pab1 cross reacted with the resin antibody when boiled in SDS buffer (Fig 4.3B, lanes 5 and 6). In contrast, Rps3 could not be co-IP with Caf20 neither did it crosslink with any protein (**Fig 4.3D**).

Conclusion: The data from **Fig 4.3** suggests that Caf20 interacts with new specific proteins other than eIF4E and other known interacting partners of Caf20

4.3.1.2. The crosslinks are cysteine specific

In order to assess if the crosslinks are cysteine dependent, one of the initial 8 Caf20 constructs (Caf20Δ4, GP7168) with deletion of the cysteine residue was included in the crosslinking experiment. The western blotting of SDS eluted FLAG IP of BMH-crosslinked Caf20Δ4 FLAG, caf20Δ and resin only revealed that the crosslinks are dependent on cysteine molecules (**Fig 4.4**). The Caf20wt yielded about 7 different specific crosslinks minus the two Caf20 uncrosslinked bands (indicated with red small circles) whereas crosslinked extracts of Caf20Δ4 (cysteine deleted strain) did not bind with any protein (lane 3) behaving similar to *caf20Δ* (lane 4) and resin eluted in SDS buffer (lane 5) (**Fig 4.4**). There were some non-specific bands at 20 KDa, 75 KDa and 85 KDa (shown in green small circle) due to cross reactivity of the FLAG antibody light and

heavy chains. In summary, **Fig 4.4** confirms that most of the BMH-crosslinks are dependent on the cysteine residue within Caf20, as expected for a cysteine-specific crosslinking reagent.

4.3.1.3. Some of the Caf20 crosslinks in total extracts are eIF4E independent

As shown earlier in **Fig 4.3,** Caf20 binds with unique factors other than eIF4E. To confirm if the crosslinks are truly eIF4E independent, a comparison were made between crosslinks of Caf20 wt to that of mutant Caf20m2 (GP7173, a mutant with double alanine (a/a) point mutations disrupted for binding to eIF4E). The western blotting of FLAG IP for the crosslinked total extracts of Caf20wt and Caf20m2 presented that the crosslink bands are similar (**Fig 4.5**). In conclusion, the data from **Fig 4.5** suggests that Caf20 interact with new specific factors not eIF4E and independent of eIF4E.

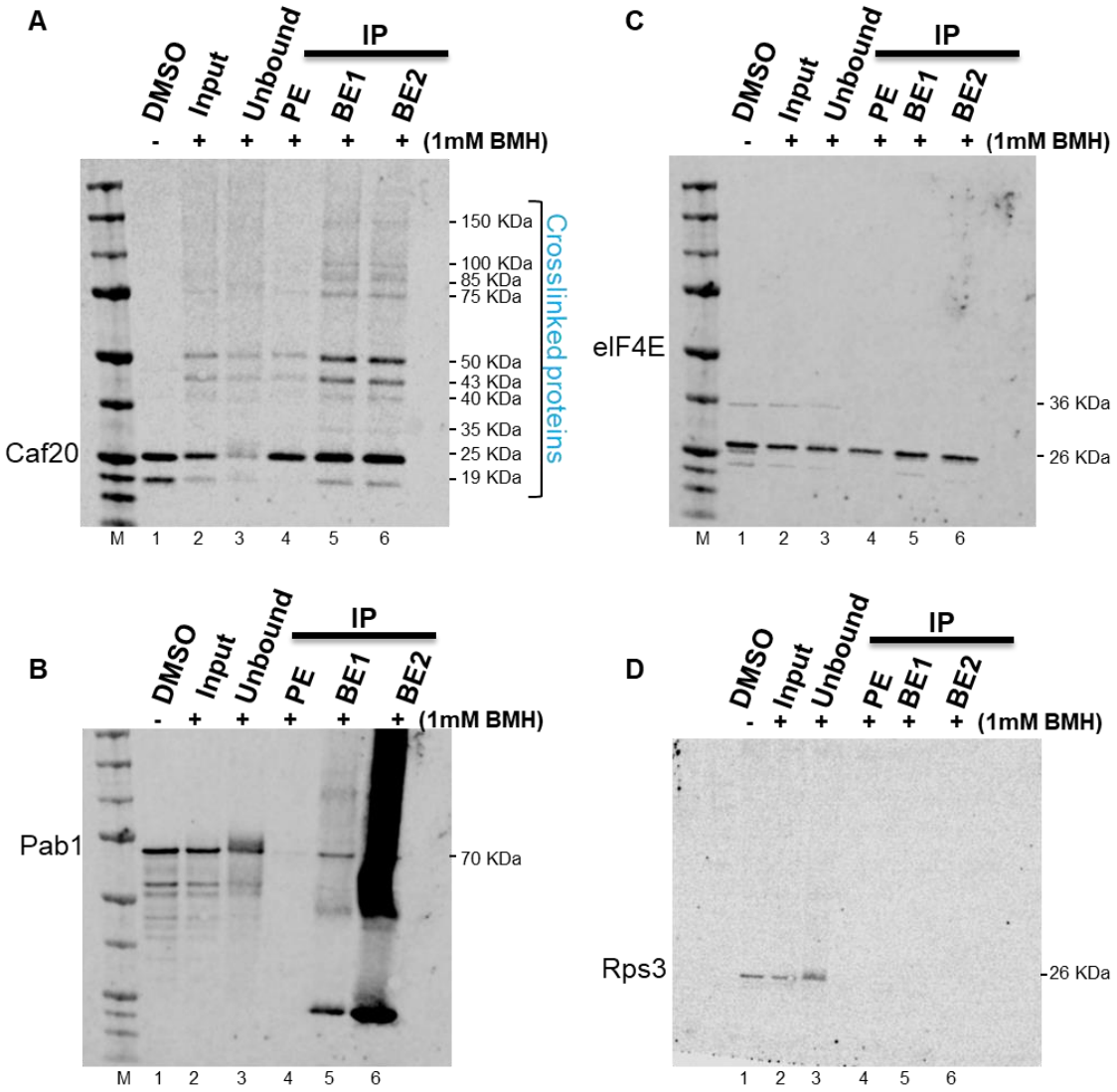

Figure 4.3. Caf20 crosslink with specific proteins. A-D. Immunoblotting of crosslinked total protein and IP of crosslinked wildtype Caf20-FLAG. Lane M - Protein marker lane, Lane 1: control total extract of willdtype Caf20-FLAG crosslinked with DMSO, lanes 2-6: wildtype Caf20-FLAG crosslinked with 1mM BMH-crosslinker. Lane 2- input, Lane 3 – IP unbound fraction, Lanes 4-6: IP elutions; **PE**- 3x FLAG peptide elute, BE1- 2nd elution with SDS loaded without beads, **BE2**- 2nd elutant with SDS loaded on the gel with some of the magnetic beads. **A.** Western blot of Crosslinked total and IP protein of Caf20-FLAG probed with Caf20 antibody showed specific crosslinked proteins of various sizes **B.** Western blot of Crosslinked total and IP protein of Caf20-FLAG probed with Pab1 pulled down Pab1 but did not crosslink. Non-specific bands present in untreated sample (lane 1). Cross reactivity between Pab1 and FLAG magnetic beads when boiled in SDS buffer (lanes 5 and 6) **C.** Western blot of Crosslinked total and IP proteins of Caf20-FLAG probed with eIF4E co-immunoprecipitated eIF4E without crosslinking to it. Non-specific band at 36 KDa **D.** Western blot of Crosslinked total and IP protein of Caf20-FLAG probed with Rps3 antibody didn't pull down Rps3 and showed no crosslinks. N = 1 rep

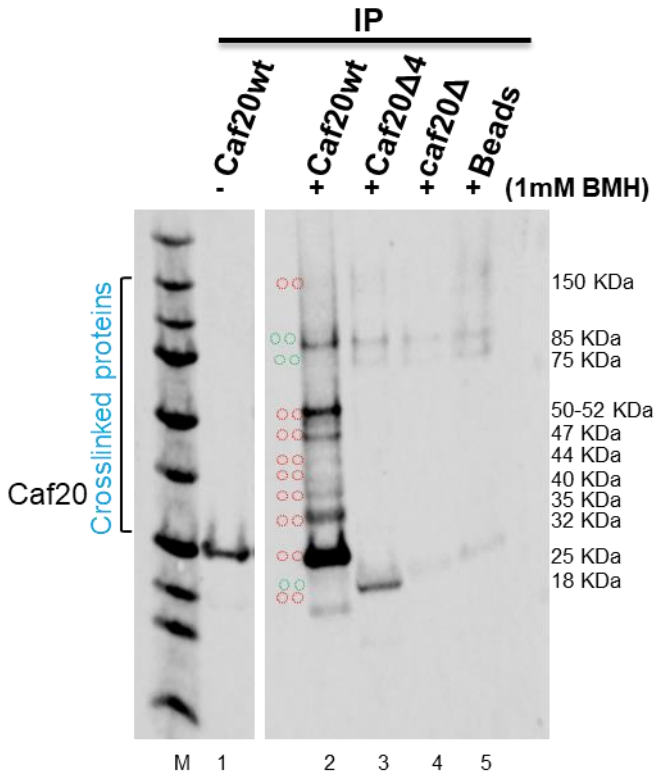

Figure 4.4. Crosslinked proteins require Caf20's cysteine. Western blotting of SDS-eluted IPs of crosslinked total samples of Caf20wt, Caf20Δ, caf20Δ and FLAG beads showing crosslinks in Caf20wt only. 9 crosslinks were observed of which 7 are specific and 2 are Caf20 uncrosslinked bands. Cross-reactivity of the FLAG antibody light chain below at 18 KDa and the heavy chains above at 75 and 85 KDA (non-specific crosslinks indicated with green circles). wt – wildtype; Ctrl- DMSO treated control; Caf20Δ4 – Caf20 mutant without cys residue, caf20Δ – Caf20 delete. N= 1 rep

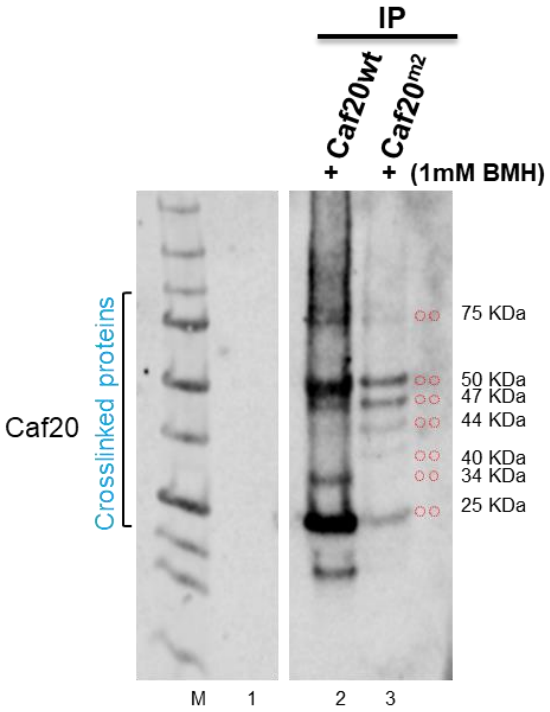

Figure 4.5. Some of the Caf20 crosslinks are eIF4E independent. A. Western blotting of SDS-eluted IPs of crosslinked totals probed for Caf20. Caf20wt and Caf20m2 crosslinks are similar. **wt –** wildtype; **Caf20 Δm² –** Caf20 mutant double a/a mutation disrupted for Caf20-eIF4E association. Lane M=marker lane, Lane 1=blank, Lane 2= eluted crosslinked Caf20wt, Lane 3=eluted crosslinked Caf20m2. N = 1 rep

4.3.2. Caf20 crosslinks in stressed and unstressed conditions.

Previous reports had shown the impacts of Caf20 on translational control in response stress conditions (Castelli et al., 2015; Cridge et al., 2010; de la Cruz et al., 1997; Ibrahimo et al., 2006; Park et al., 2006). Typical effects are the formation of pseudohyphae, recruitment of Caf20 into p-bodies and mRNA decapping (Ibrahimo et al., 2006). It was decided to explore the effects an introduction of stress could have on Caf20 crosslinking. This is to ensure that the crosslinks are stable under stress and not adversely affected by prolonged exposure to experiment techniques including immunoprecipitation. Ashe et al. (2000) demonstrated that glucose has a limiting effect on translation initiation where he showed from polysome profiling that when yeast are harvested and washed in lysis buffer resulted in ribosome runoff such that they appeared stressed with only the free ribosome subunits intact (40S and 60S) and the 80S. They reported that the polysomes were depleted in lysis buffer only washed cells but when the cell are harvested and washed in 3% glucose and 2x amino acids before lysing kept the polysomes intact. With this in mind, two different cell cultures were grown to OD = 0.6,

one portion was harvested and washed in lysis buffer to create ribosome runoff and the 2nd portion was washed in 3x glucose and 2x amino acids to maintain the ribosome before lysing as described in section 2.6.1. These were crosslinked with BMH-crosslinking reagent, immunoprecipitated with FLAG magnetic resin and analysed on western blotting.

The result of the western blotting (**Figure 4.6**) showed that there were some differences in the level of enrichments between the stressed and unstressed cells in the FLAG IPs eluted with 3X FLAG peptides (PE) and SDS beads elution (BE), though the major crosslinks remained identical. The blue arrows in the figure indicated where there were differences between the stressed and unstressed cells.

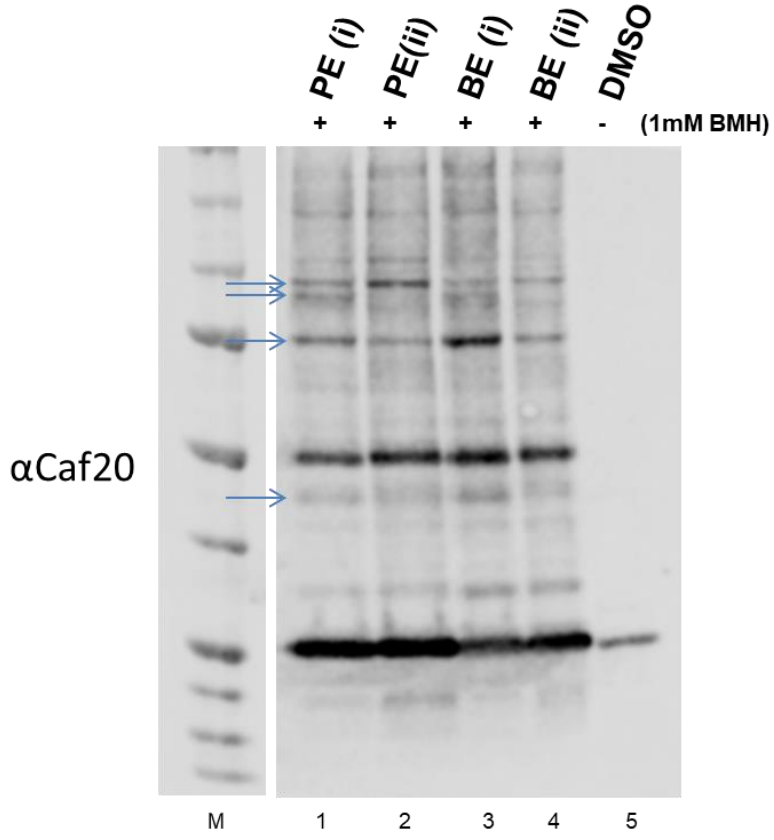

Figure 4.6.Caf20 associate with proteins in stressed and unstressed cells. Immunoblotting of eluted FLAG IPs of crosslinked total extracts of Caf20wt in stressed and unstressed yeast cells. See the blue arrows pointing where there differences. Note: **(i) –** yeast washed with lysis buffer only before grinding. **(ii) –** yeast washed with 3% glucose and 2X amino acids before grinding. **PE –** 3x FLAG peptide elute **BE –** 2nd elute from Bead with SDS. N = 2 reps

4.3.3. Proteomics analysis of Largescale Crosslinked Caf20 complexes in total extract

4.3.3.1 One rep Mass spectrometry trial.

To identify proteins that associate with Caf20, a large scale crosslinking and immunoprecipitation was performed from 3L cell cultures grown to exponential phase. For the initial large scale trial and Mass spectrometry identification, three strains-wildtype Caf20-FLAG (GP7164) and two controls, Caf20Δ4-FLAG (GP7168, a mutant with a 20 amino acid deletion including cysteine residue) and *caf20*Δ (GP7174) were used. The Caf20Δ4 was used to exclude peptides which were not cysteine dependent and the caf20Δ was included to identify non-specific targets. The three strains where crosslinked with 1 mM BMH crosslinking reagent and processed as described in methods **2.6.1.1** (**Fig 4.7A**).

The free-label LC-MS/MS results of the samples of the crosslinked total extract yielded identification of 120 proteins (which had a cut off of 2 or more peptides per protein from the scaffold output file) (**Fig 4.7**). The identified proteins were of varying molecular weights (**Fig 4.7B**). There were overlaps of proteins seen among the samples (**Fig 4.7C**). 24% of the proteins identified (which included eIF4E, a cysteine independent factor) were present in all three samples. 3 proteins, Caf20 itself, Sse1 and Ubi4 (Caf20 dependent factors) were unique to Caf20wt and the Caf20Δ4 (**Fig 4.7C**). 17 proteins (14% of all) were exclusive to Caf20wt (**Fig 4.7C**, **Table 4.1**). The majority are proteins important in cell signalling and mRNA decay pathway, however 3 of them (Rpl3, Rpl18, Rpl23) were large subunit ribosomal proteins (**Table 4.1**). In terms of the location on the ribosome of some of the identified proteins, the structural architecture of the 80S ribosome (Jenner et al., 2012) revealed that the three ribosomal proteins are situated at the junction between the 40S and 60S subunits (**Fig 4.8**).

In summary, the Mass spectrometry data suggest that Caf20 associated with cysteine dependent proteins and ribosomal proteins location at the bridge between the 40S and 60S ribosomes.

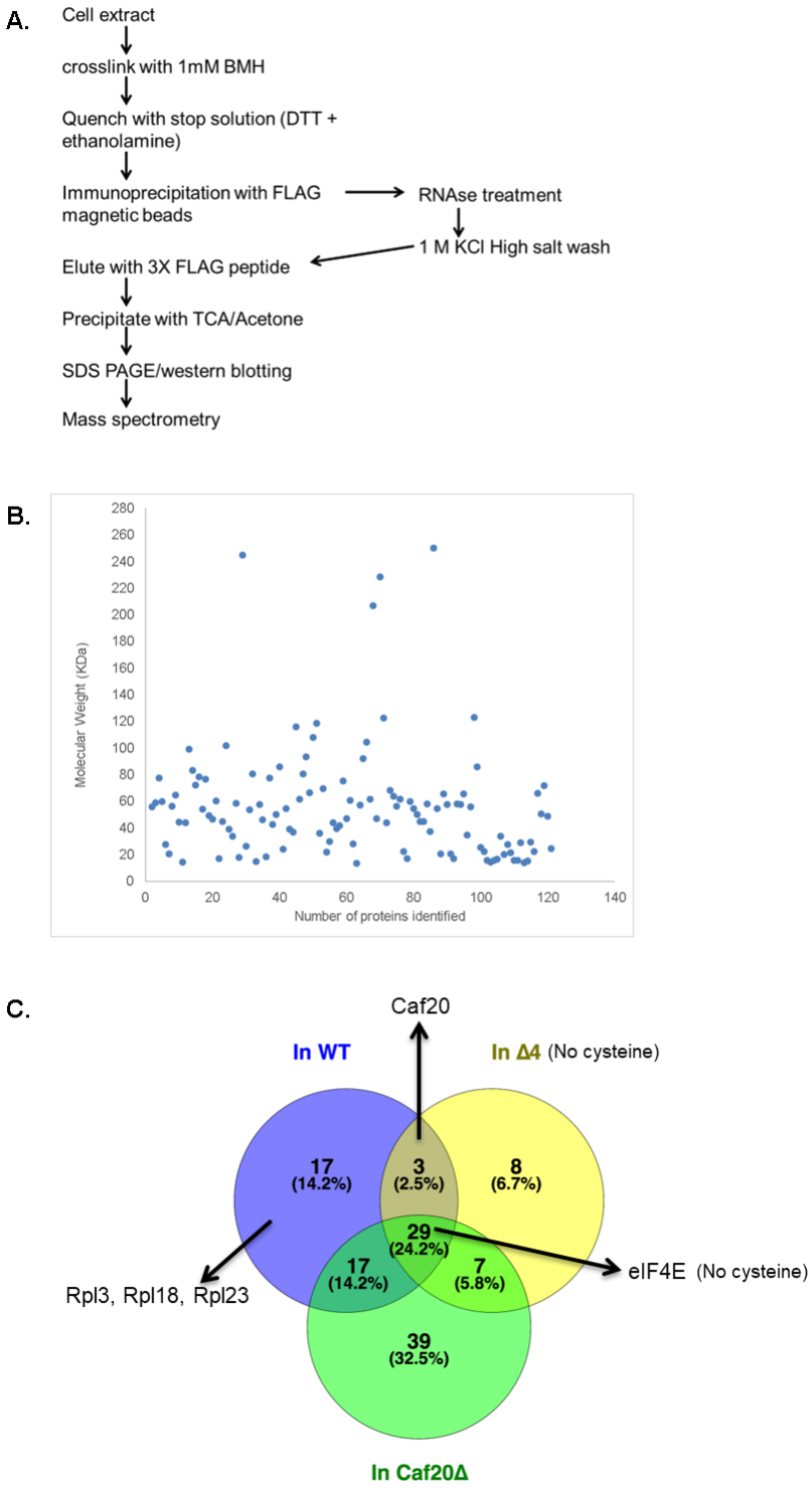

Figure 4.7 Caf20-associated proteins in trial Experiment. A. Experimental technique. Total extract was crosslinked with 1mM BMH and quenched with DTT and ethanolamine, then IP with FLAG magnetic beads which include RNAse treatment and 1 M KCL salt wash was carried out. Caf20-crosslinked proteins were eluted with 3X FLAG peptide and precipitated in TCA/acetone washes. The SDS PAGE of the crosslinked were either analysed on western blotting or identified through mass spectrometry. **B.** scatter plot showing the molecular weights of the 120 identified proteins. **C.** Venn diagram of recovery of BMH-crosslinked transcripts of one biological repeat. N = 1 rep

Table 4.1. Seventeen proteins present only in Caf20wt

S/N	Cross-linked proteins	Brief Description	No of peptides	Closest XL size (KDa)[1]	Expected size (KDa)[2]	no of cys	Possible cross-link[3]
1	Rpl23A (L14)	Ribosomal 60S subunit protein L23A (New name L14)	2	42	39.5	2	likely
2	Rpl18B (L18e)	Ribosomal 60S subunit protein L18B (New name L18e)	3	42	45.6	1	likely
3	Gpm1	Tetrameric phosphoglycerate mutase	3	50	52.6	0	unlikely
4	Rpl3 (L3)	Ribosomal 60S subunit protein L3 (New name L3)	2	65	68.8	2	likely
5	Nsr1p	Nucleolar protein that binds nuclear localization sequences;	2	65	69.5	1	likely
6	Svf1	Protein with a potential role in cell survival pathways	2	75	79.3	3	likely
7	Ugp1	UDP-glucose pyrophosphorylase (UGPase)	7	85	81	4	likely
8	Aro8	Aromatic aminotransferase I	2	85	81.2	4	likely
9	Cct3p	Subunit of the cytosolic chaperonin Cct ring complex	5	85	83.8	11	likely
10	Cct6	Subunit of the cytosolic chaperonin Cct ring complex	4	85	84.9	5	likely
11	Cps1	Vacuolar carboxypeptidase S	2	95	89.6	4	likely
12	Snf1	AMP-activated S/T protein kinase	2	95	97	4	likely
13	Trp5	Tryptophan synthase	2	105	101.6	7	likely
14	YHR020W	Prolyl-tRNA synthetase	5	105	102.4	9	likely
15	Srb4p	Subunit of the RNA polymerase II mediator complex	2	105	103.5	2	likely
16	Sky1p	SR protein kinase (SRPK)	2	105	108.2	10	likely
17	Sec27	Essential beta'-coat protein of the COPI coatomer	2	130	124.4	6	likely

[1] migration size of XL band closest to expected size in SDS-PAGE gel

[2] Expected size is Identified protein MW + Caf20-flag (25 KDa)

[3] Possible crosslink is likely when the migration size is comparable to expected size plus presence of cysteine residue in the protein otherwise it is unlikely

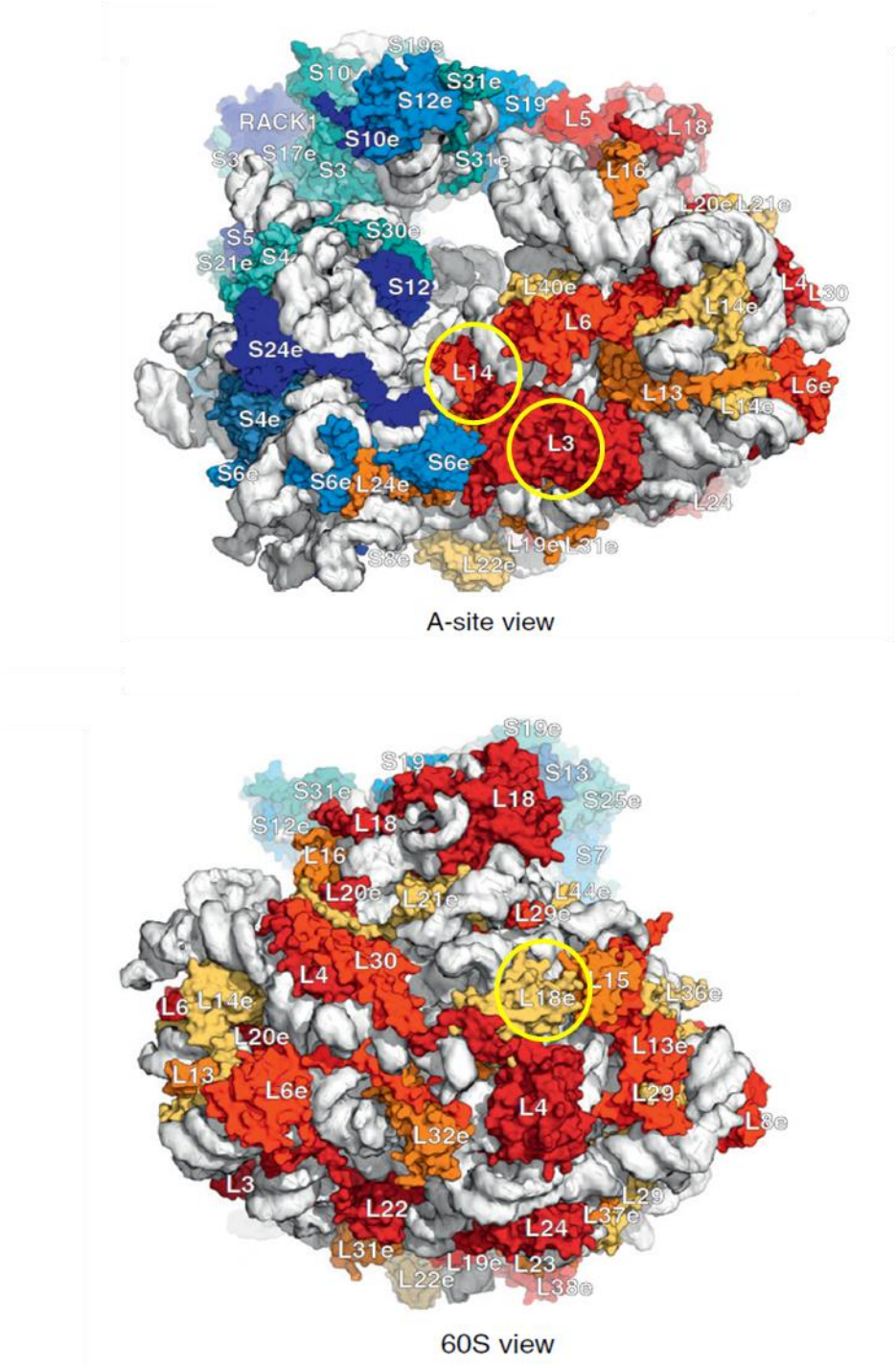

Figure 4.8 Location of identified ribosomal proteins on the 80S yeast ribosome. The structural architecture of the 80S ribosome (Jenner et al., 2012) showed the views of some ribosomal proteins named according to new standard nomenclature. Ribosomal proteins of interest are highlighted in yellow ring. Ribosomal RNAs are represented in white, the blue proteins belong to the 40S subunit and the proteins in red, orange and yellow are for the 60S subunit.

4.3.3.2 Three Biological repeats Largescale Crosslinking and Mass spectrometry.

4.3.3.2.1 Experimental strategy

Because the initial one biological repeat crosslinking and Mass spectrometry results looked promising, a second experiment on a larger scale with three biological replicates each for Caf20wt (GP7164), Caf20^{m2} (GP7173), Caf20Δ4 (GP7168) and Caf20ΔAC (GP7311) were performed and another three uncrosslinked replicates of Caf20wt were used as controls. Caf20m2 (two point mutation to disrupted for eIF4E) and Caf20ΔAC (mutant with reduced interaction with the ribosome) were included to understand how the crosslinked data vary in those strains. The initial one rep largescale experiment and the three biological repeat experiments follow the same methodological procedure. Though more strains (Caf20m2 and Caf20ΔAC) were included in the three biological replicates. The total extracts of all the samples and controls were crosslinked with 1 mM BMH and DMSO respectively. Proper crosslinking of the total extracts was confirmed on western blotting before proceeding with the FLAG immunoprecipitation and other steps as enumerated in **Fig 4.7A**. The western blot result of one rep of each strain and control in **Fig 4.9** confirmed that the samples were stably crosslinked. The molecular weights of the crosslinked bands for each strain showed the predicted sizes of crosslinked proteins of sizes ~10 KDa, 18KDa, 21 KDa, 25 KDa, 50KDa, 75KDA, 85 KDa, etc.

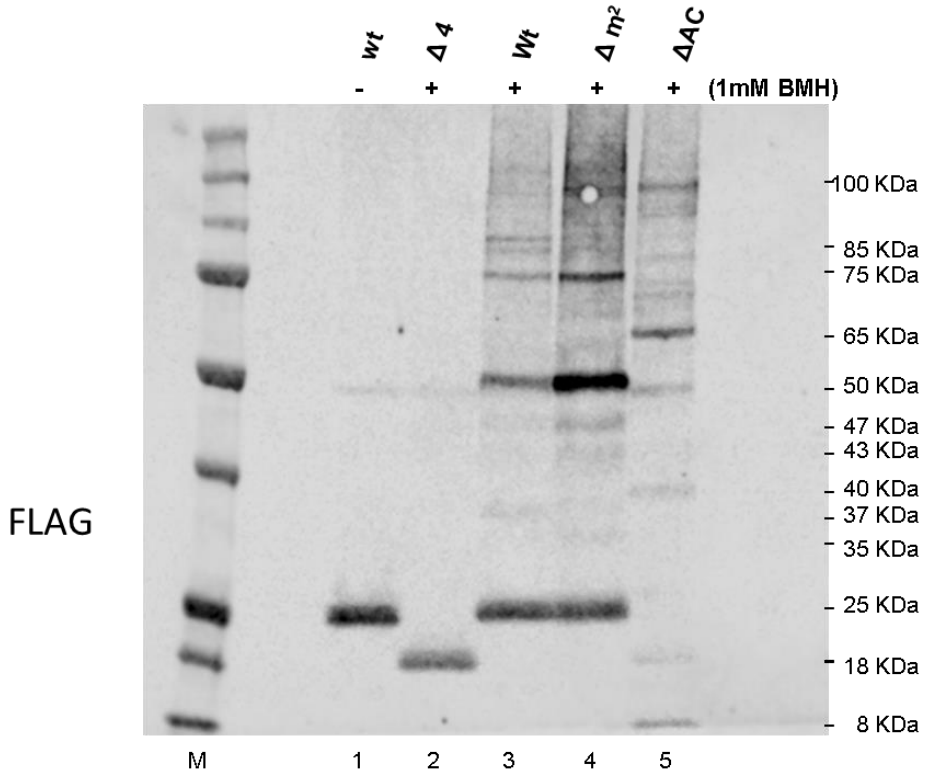

Figure 4.9. Western blot of crosslinked total extracts of tested Caf20 strains showed correct pattern of crosslinks. Note: **wt –** wildtype; **Δ4-** Caf20 mutant with deletion of 20 amino acids including cysteine (Δ63-Δ82 residues); **Caf20 Δm^2 –** Caf20 mutant double a/a mutation disrupted for Caf20-eIF4E association, **ΔAC-** Caf20 mutant with deletion of the N- and C-terminal regions and have reduced association with the ribosome (Δ3-Δ48 and Δ108-Δ161 residues). N = 1 rep

Again, the free-label LC-MS/MS for the three biological repeats produced a large data of 630 identified proteins (FDR<0.05, 2 or more peptides used for the quantification). The data were trimmed down to exclude proteins that did not appear in at least 2 out of 3 repeats. 262 proteins were identified in the crosslinked Caf20wt. When the recovered proteins of Crosslinked Caf20 were compared to the non-crosslinked control, about 60% of the proteins were common in the crosslinked and non-crosslinked and 86 proteins were specific to crosslinked Caf20 (**Fig 4.10A**). When the specific proteins were compared in the other strains, 15 proteins were common to Caf20wt and Caf20m2, 10 proteins were common to Caf20wt and Caf20ΔAC while 6 proteins were present in Caf20wt only (**Fig 4.10B**). This suggested that about 30 percent of the crosslinked proteins were specific proteins.

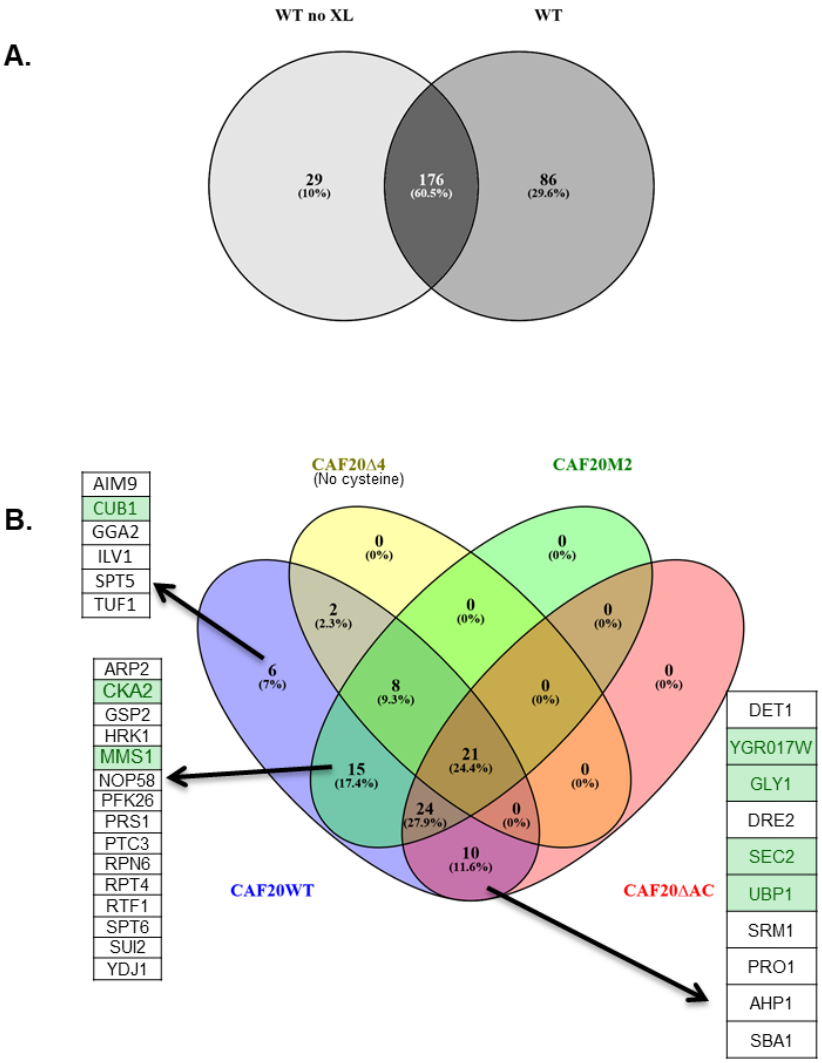

Figure 4.10. Identification of Caf20-associated proteins in total extracts. Venn-style diagrams of identified proteins showing overlaps between crosslinked and non-crosslinked Caf20wt. Venn diagrams of crosslinked proteins associating with Caf20wt, Caf20m2, Caf20Δ4 and Caf20ΔAC, highlighting proteins specific to wt only, to both wt and m2 and to both wt and ΔAC. Proteins highlighted in green have peptides detected in all the three replicates. Venn diagrams prepared with Venny 2.1 (Oliveros, 2007-2015). N = 3 reps

4.3.3.2.2 Classification of the crosslinked proteins and Functional significance of the group categories

The 262 crosslinked proteins of Caf20wt was subjected to analysis to determine levels of enrichment or depletions over the non-crosslinked caf20. The proteins were grouped into four based on their log value and whether they were identified in the non-crosslinked sample (**Fig 4.11**). Group I comprises those that are upregulated in Caf20wt and absent

in the non-crosslinked control samples. They are made up of 42 proteins with $\log_2$ values of 8.1- 5.6. The list of Group 1 proteins are listed on Table 4.2. Group II are made up of proteins which are present in the non-crosslinked samples but are enriched in the crosslinked samples. They are 41 in number and falls between $\log_2$ values of 3.8 and 1.3. Group III include proteins that are stably unaltered and didn't vary between the crosslinked and non-crosslinked ones. Their $\log_2$ values ranged from 1.2 to 0.6. The Group IV are made up proteins that are underrepresented in the crosslinked wildtype samples. They have $\log_2$ values below 0.6 to -1. Among the proteins in this group include Caf20, Cdc33, Ola1, Tef4, Sro9, Ssa2, Fas2, Eno2, Ded1, Ilv2, Ilv5, Hsc82, Tif2, Ade5,7, etc. Most of the ribosomal proteins identified were depleted in the crosslinked Caf20wt. The 262 crosslinked proteins of Caf20 and their log values are shown in **Appendix II**.

All the groups were subjected to gene ontology categorisation for the enriched protein. The GO analysis was performed using the R package clusterProfiler (Yu et al., 2012). **Figure 4.12** showed the functional classification of the proteins enriched for each group. Group I and II (information retrieved from 81 proteins) are enriched for translation factors, RNA binding, transferase activity and kinase activity. Group III are known to have Ligase activity and Group IV have more functions that are important structural constituent of ribosome, structural molecules, mRNA binding, rRNA binding ATPase activities etc. Group III and IV proteins are both are enriched pyrophosphatase and hydrolase activities. All the 262 crosslinked proteins of Caf20 shown in Appendix II. The proteins found in each functional class, their p-values and GO terms are also summarized in **Appendix II.**

Comparing the likely crosslinked proteins based on the expected size, migration size closest to crosslinked size and number of cysteine residues showed that many of the Group1 proteins are likely to be true crosslinks (**Table 4.2**). The prominent 50 KDa cross-linked band should mean that the most enriched proteins is ~25 KDa of which Sba1 and to some extent Ygr017w, Sui2 and Ess1 are likely candidates (**Table 4.2**). In summary, the results grouped crosslinked proteins into enriched and depleted proteins that are significantly represented in gene functional classes, however the significance of this is not clear. Unfortunately, the numbers of proteins enriched exceed expectations from the cross-linking western blots, suggesting that the majority of proteins found here are not specific proteins BMH cross-linked to Caf20.

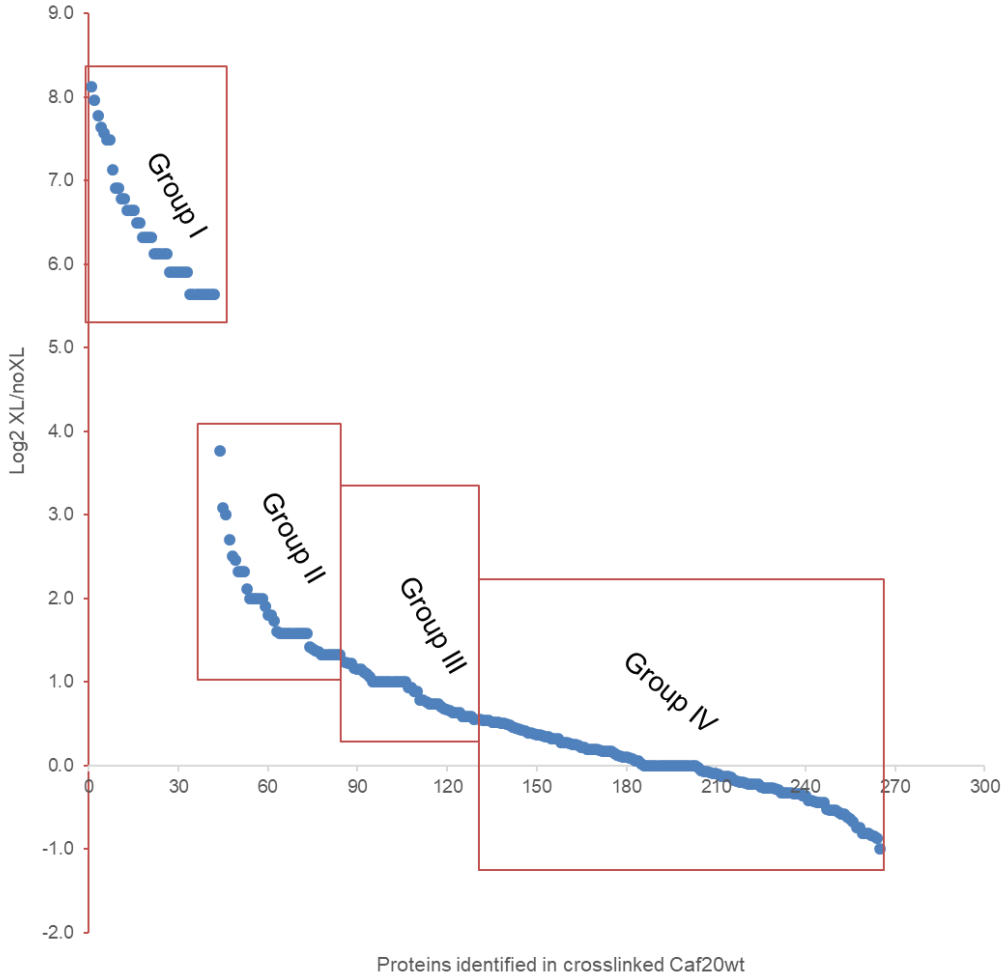

Figure 4.11. Scatter chart of Log2 levels of enrichments classified the 262 crosslinked wildtype Caf20-FLAG transcripts into four groups. Group I are upregulated and absent in the non-crosslinked, group II are upregulated and present in the non-crosslinked. Group III proteins are unaltered while Group IV are depleted in the crosslinked. The red box highlights the proteins in each group (2 or more peptides used for the quantification of each protein, FDR<0.05). N = 3 reps

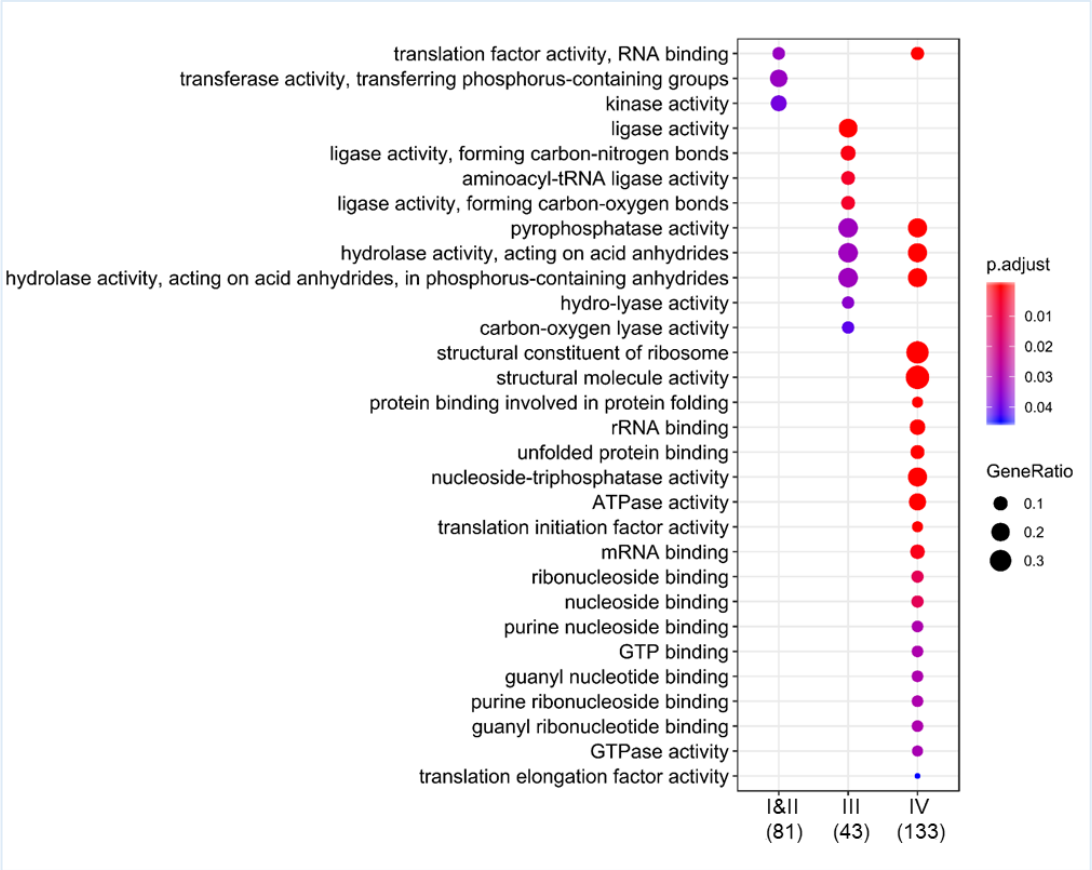

Figure 4.12. Functional significance of Gene ontology classification for the proteins represented among the groups in the crosslinked Caf20wt. p-adjust value shown colour variation and the gene ratio of each category represented by size. N = 3 reps

Table 4.2. Group I specific BMH cross-linked proteins in total extract

S/N	Cross-linked protein	Brief Description	No of peptides	Closest XL size (KDa)[1]	Expected size (Da)[2]	Cys	Possible cross-link[3]
1	Rps10b	Protein component of the small (40S) ribosomal subunit	6	37	37.7	0	unlikely
2	Hyp2	Translation elongation factor eIF-5A	7	42	42.1	2	likely
3	Ess1	Peptidylprolyl-cis/trans-isomerase (PPIase)	8	42	44.4	2	likely
4	Sba1	Co-chaperone that binds and regulates Hsp90 family chaperones	5	50	49.1	1	likely
5	Ygr017W	Putative protein of unknown function	12	65	59.7	8	likely
6	Sui2	Alpha subunit of the translation initiation factor eIF2	5	65	59.7	5	likely
7	Prs3	5-phospho-ribosyl-1(alpha)-pyrophosphate synthetase	6	65	60.1	5	likely
8	Glc7	Type 1 S/T protein phosphatase (PP1) catalytic subunit	10	65	60.9	12	likely
9	Snf4	Activating gamma subunit of the AMP-activated Snf1p kinase complex	5	65	61.4	4	likely
10	Gvp36	BAR domain protein that localizes to early and late Golgi vesicles	5	65	61.7	3	likely
11	Dre2	Component of the cytosolic Fe-S protein assembly (CIA) machinery	7	65	63.5	9	likely
12	Det1	Acid phosphatase	5	65	64.2	5	likely
13	Cka2	Alpha' catalytic subunit of casein kinase 2 (CK2)	18	65	64.4	5	likely
14	Asp1	Cytosolic L-asparaginase, involved in asparagine catabolism	10	65	66.4	10	likely
15	Sam2	S-adenosylmethionine synthetase	5	65	67.2	5	likely
16	Ydj1	Type I HSP40 co-chaperone	7	65	69.7	11	likely
17	Cka1	Alpha catalytic subunit of casein kinase 2 (CK2)	25	65	69.7	2	likely
18	Prs1	5-phospho-ribosyl-1(alpha)-pyrophosphate synthetase	5	75	72.0	8	likely
19	Pro1	Gamma-glutamyl kinase	8	75	72.2	3	likely
20	Tuf1	Mitochondrial translation elongation factor Tu (EF-Tu)	9	75	73	3	likely
21	Idp1	Mitochondrial NADP-specific isocitrate dehydrogenase	19	75	73.2	3	likely
22	Wrs1	Cytoplasmic tryptophanyl-tRNA synthetase	6	75	74.3	6	likely
23	Pro2	Gamma-glutamyl phosphate reductase	8	75	74.7	3	likely
24	Rpn5	Subunit of the CSN and 26S proteasome lid complexes	6	75	76.8	2	likely
25	Srm1	Nucleotide exchange factor for Gsp1p	8	75	78.0	9	likely
26	Svf1	Protein with a potential role in cell survival pathways	28	75	79.3	3	likely
27	Zpr1	Essential protein with two zinc fingers	6	85	80.0	15	likely
28	Tps1	Synthase subunit of trehalose-6-P synthase/phosphatase complex	10	85	81.2	4	likely

29	Trp2	Anthranilate synthase	5	85	81.8	6	likely
30	Dhh1	Cytoplasmic DEAD-box helicase, stimulates mRNA decapping	11	85	82.5	7	likely
31	Pdi1	Protein disulfide isomerase	19	85	83.2	6	likely
32	Cub1	Conserved fungal gene linked to DNA repair and proteasome function	12	85	87.7	6	likely
33	Ilv1	Threonine deaminase, catalyzes first step in isoleucine biosynthesis	6	85	88.8	5	likely
34	Cps1	Vacuolar carboxypeptidase S	18	95	89.6	4	likely
35	Ncl1	S-adenosyl-L-methionine-dependent tRNA: m5C-methyltransferase	7	105	102.9	14	likely
36	Sky1	SR protein kinase (SRPK)	22	105	105.2	10	likely
37	Sec2	Guanyl-nucleotide exchange factor for the small G-protein Sec4p	11	105	109.6	9	likely
38	Hrk1	Protein kinase	9	120	110.7	19	likely
39	Ubp1	Ubiquitin-specific protease	10	120	117.7	9	likely
40	Vas1	Mitochondrial and cytoplasmic valyl-tRNA synthetase	6	170	150.8	13	likely
41	Spt6	Nucleosome remodeling protein	7	170	193.2	7	likely
42	Tom1	E3 ubiquitin ligase of the hect-domain class	14	270	399	36	unlikely

[1] migration size of XL band closest to expected size in SDS-PAGE gel
[2] Expected size is Identified protein MW + Caf20-flag MW on gel (25 KDa)
[3] Possible crosslink is likely when the migration size is comparable to expected size plus presence of cysteine residue in the protein otherwise it is unlikely

4.3.3.2.3 Hierarchical clustering of cross-linked proteins revealed correlation for the Cross-linked Caf20 proteins

The 262 crosslinked proteins identified in the wildtype strain were screened across all the other crosslinked Caf20 mutant strains (Caf20m2, Caf20ΔAC and Caf20Δ4) to create a hierarchical relationship among the strains based on their level of protein enrichments and depletions. A dendrogram in form of a heatmap was created to show the relative amount of the core 262 cross-linked proteins identified in crosslinked Caf20wt to the other Caf20 strains (Caf20m2, Caf20ΔAC and Caf20Δ4). The $\log_2$ values of total peptides for three biological reps of crosslinked Caf20wt over the non cross-linked sample were inputted and compared to the $\log_2$ values of the other cross-linked Caf20 mutants obtained by dividing their total peptides for three biological reps to the total peptides of the Caf20wt. A hierarchical clustering was obtained using an R-package integrated online software, ClustVis (Metsalu and Vilo, 2015). The ClustVis generated a heatmap showing the relationships of the proteins, the group types and correlation among the strains. A heatmap of nine distinct clusters (1 to 9) and a further 9 sub-clusters (a – i) generated is shown in **Fig 4.13**. On a general outlook, Caf20ΔAC and Caf20Δ4 in **Fig 4.13** were more

underrepresented for the crosslinked proteins. Clusters 1 and 2 are predominantly over-represented for proteins in Group I. Cluster 1 class comprised proteins that are over expressed in the Caf20 wt only. This is further divided into three sub-clusters (a to c), sub-cluster (a) are more depleted in Caf20Δ4 and Caf20ΔAC,while sub-cluster (b) are depleted for Caf20Δ4 and sub-cluster (c) are depleted in Caf20Δ4 and Caf20Δ^{m2}. Cluster 1 consists mostly of kinases and some important translation factors such as Dhh1, Gcd11, Gcd6, Sui2, Tef2, Eft2, Cluster 2 are still enriched in cross-linked Caf20wt, though with fewer group I proteins and some Group II, III and IV proteins. The Caf20ΔAC is well under represented in this group. Cluster 3 are cross-linked proteins that are moderately enriched in the Caf20 wt and Caf20Δm2 only. They are made up of binding proteins-Sro9, Rpg1, Sub2, Cct6, Cct7,Ded1, Gga2, Arp2, Sup35, Pgi1, Eno2, Pfk26, They are mostly Group IV proteins and few of Group II and III class.

Cluster 4 are underrepresented in the Caf20wt and Caf20Δ4 but are moderately enriched in Caf20ΔAC and over expressed in Caf20Δm2. They contain fatty acid processing proteins Fas1 and Fas2. Clusters 4 and 5 are enriched for Caf20ΔAC and underrepresented for Caf20Δ4. These two clusters (4 and 5) contain stress regulator proteins that are important of the protein folding, transportation and survival pathway. They include Ugp1, Kap123, Hsp60, YHR020W, Cop1, Aro8, Nsr1, Adh1, Ssa2 etc. Cluster 6 are predominantly enriched in Caf20Δ4 and depleted in the Caf20 ΔAC. They are sub-divided into two clusters, sub-cluster (f) and (g). Sub-cluster (f) are moderately enriched in the Caf20wt and Caf20 Δm2 whereas sub-cluster (g) is underrepresented in Caf20 Δm2. The three proteins that fall in this sub-cluster (g) are RPP0, Cdc33 (eIF4E) and Tpd3. Clusters 7 and 8 are depleted for the Caf20wt and comprise proteins in the Group IV category. They are overrepresented in Caf20Δm2 and they are mostly ribosomal proteins. Cluster 9 are proteins underrepresented in both Caf20wt and Caf20Δm2.

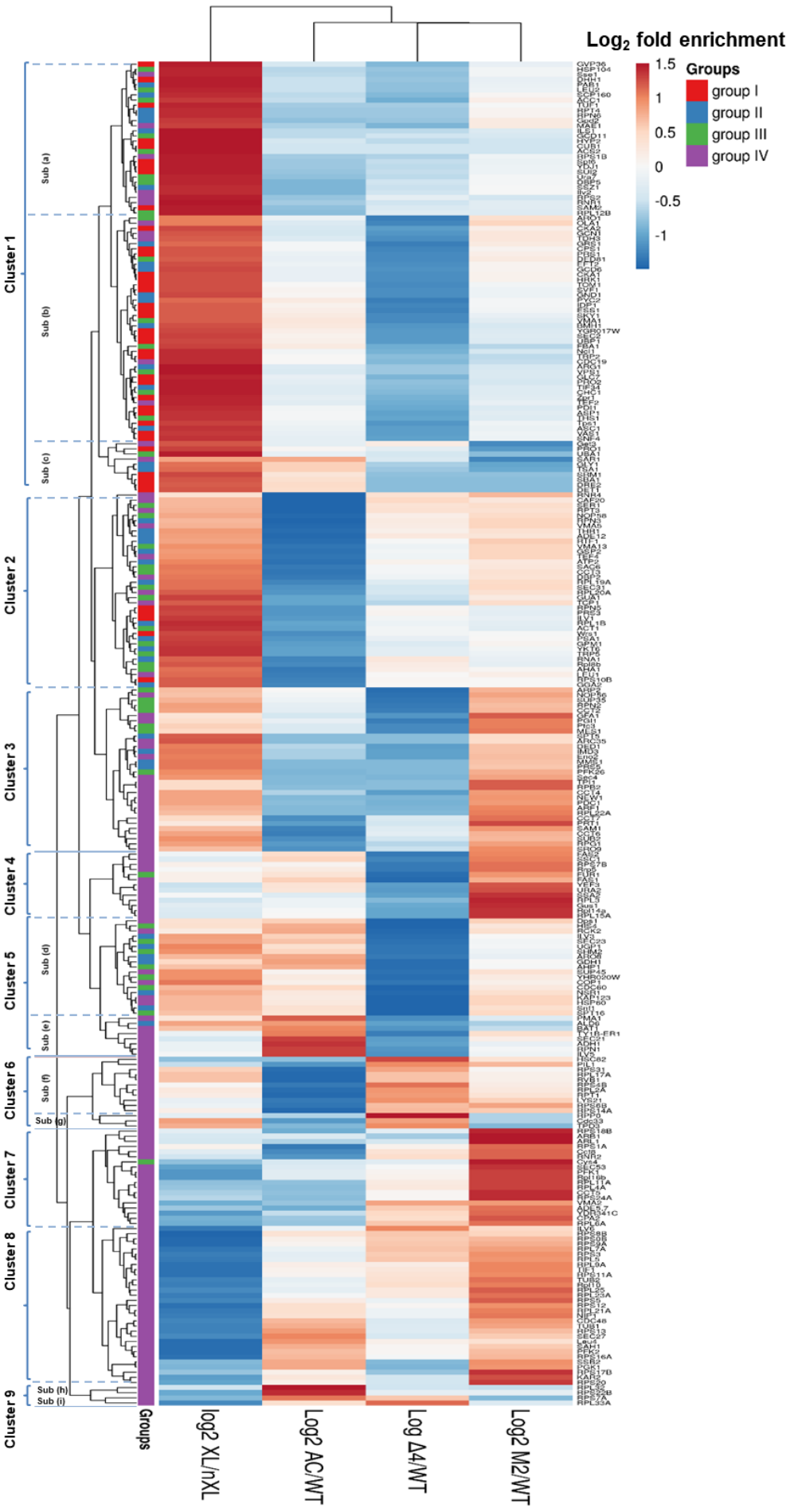
Log2 fold enrichment
1.5
1
0.5
0
-0.5
-1
Groups
group I
group II
group III
group IV
Cluster 1
Cluster 2
Cluster 3
Cluster 4
Cluster 5
Cluster 6
Cluster 7
Cluster 8
Cluster 9
Sub (a)
Sub (b)
Sub (c)
Sub (d)
Sub (e)
Sub (f)
Sub (g)
Sub (h)
Sub (i)
Groups
log2 XL/nXL
Log2 AC/WT
Log Δ4/WT
Log2 M2/WT

Figure 4.13. Nine distinct clusters are visible among the crosslinked Caf20 strains in total extracts. A heatmap revealing the levels of enrichments among the Caf20 strains for the 262 selected proteins in the Caf20wt. The log2 values for the crosslinked wt/no.XL to the crosslinked m2/wt, ΔAC/wt, and Δ4/wt were used plot the dendrogram. The red and blue colours represent proteins that are enriched and depleted in the samples respectively. N = 3 reps

These results were more complicated than expected and were variable, as data from the trial and 3 reps Mass spectrometry gave different 'hits'. The results did not provide a strong steer to where on the ribosome Caf20 binds. Most of the top hits as shown in **Table 4.2** and **Fig 4.12** were proteins kinases and proteins involved in cell signalling. They also do not all conform to what was anticipated (expected sizes and the number of cysteine in the protein) at the outset from the series of western blots of the experiments conducted. It was concluded that the MS experiment lacked specificity and that further purification of ribosome-interacting Caf20 was needed.

4.4 Caf20 crosslinking to purified ribosomes

The experimental strategy was modified to perform crosslinking to ribosome-bound Caf20. Intact ribosomes bound by Caf20 were first purified, after which recovered material was crosslinked and processed according. There was also a change in the choice of crosslinker to use. It was reasoned that the crosslinker (BMH) might not target most ribosomal proteins as these have few surface exposed cysteines, but contain more lysine residues exposed at the surface of the protein which could be readily be crosslinked to Caf20.

4.4.1 Caf20 specific interacting proteins are enriched with ribosomes

The first experiment conducted was to compare the crosslinking of the total extracts with ribosome-enriched crosslinking. For the ribosome crosslinking, a sucrose cushion of the cell extract (see section 2.6.2) was first performed to pellet ribosomes and remove cytoplasmic proteins that are in the supernatant. As shown in Chapter 3, Caf20 partitions into both cytoplasmic and ribosome pellet fractions. Three crosslinkers (BMH, MBS and DSS) were tested on the total extract and the ribosome enriched extracts at final concentrations of 0.5, 1 and 2mM for each of the crosslinkers (**Fig 4.14**). On the total extract crosslink, BMH crosslinker gave the highest Caf20-FLAG crosslinks as expected

(**Fig 4.14A**, top panel). However with ribosome crosslinking, MBS crosslinker showed more crosslinks that are unique and distinct than BMH and DSS, as the ~10 KDa protein enrichment (indicated with blue arrow) was enhanced in the ribosome extracts than in the total extract (**Fig 4.14A** and **B,** top panel). The eIF4E crosslinked with other proteins only when MBS or DSS crosslinker was used (**Fig 4.14A** and **B**, bottom panels). The eIF4G form crosslink with a protein in DSS crosslinker (**Fig 4.14B**, middle panel). Since MBS crosslinks between lysine and cysteine residues, it has the potential to crosslink ribosomal proteins which have lysine residues exposed at the ribosome surface.

Conclusion: Caf20 form crosslinks with the ribosome enriched proteins

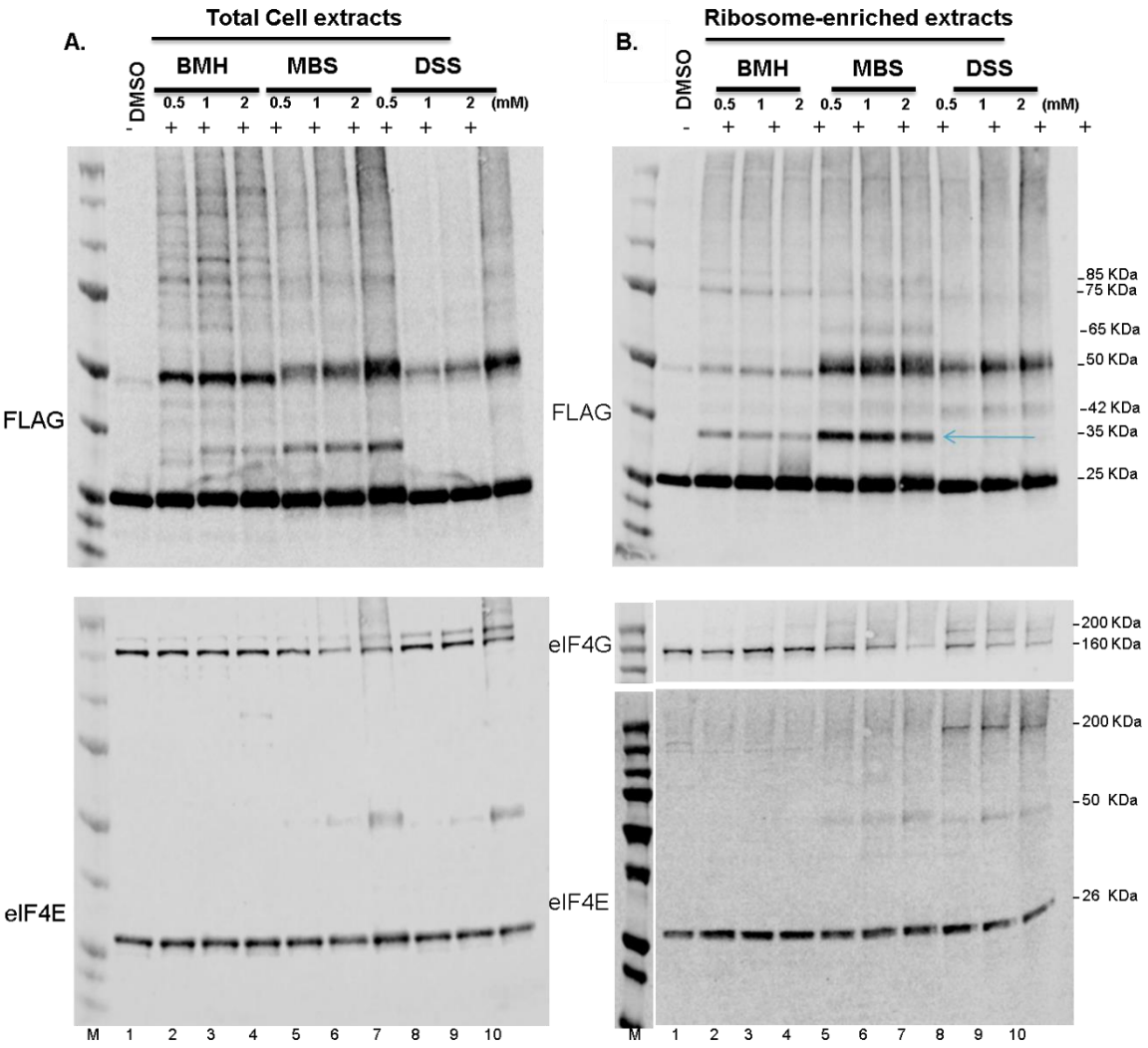

Figure 4.14. Caf20 crosslinks are enriched in the ribosomes. A. Western blotting of small scale total cell extracts crosslinked with BMH, MBS and DSS in wildtype Caf20-FLAG, each tested at final concentrations of 0.5, 1, 2mM and probed with FLAG and eIF4E antibodies. B. Western blots of small-scale ribosome-enriched extracts prepared by sucrose cushion and then crosslinked with BMH, MBS and DSS in wildtype Caf20-FLAG, each tested at final concentrations of 0.5, 1, 2mM. The western blots were probed with FLAG (upper panel), eIF4G (middle panel) and eIF4E antibodies (lower panel). Lane M is for the protein mw marker; lane 1 – extract crosslinked with DMSO solvent; lanes 2-4 for extracts crosslinked with BMH at 0.5, 1 and 2 mM respectively; lanes 5-7 for extracts crosslinked with MBS at 0.5, 1 and 2 mM respectively; lanes 8-10 for extracts crosslinked with DSS at 0.5, 1 and 2 mM respectively. The blue arrow shows the enriched ~10 KDa protein. N = 3 reps for each crosslinker

To confirm if the specific proteins enriched in the ribosome are eIF4E independent, we included Caf20m2 (strain disrupted for eIF4E interaction). The immunoblotting of the ribosome-rich extracts purified through sucrose cushion and crosslinked with MBS crosslinker showed that Caf20m2 also crosslinked with similar sized proteins to the 'wt' as expected because Caf20 ribosome interaction in not eIF4E-dependent, as well as additional crosslinked products at ~75 KDa (**Fig 4.15**). This suggests that Caf20 crosslinks with ribosome-enriched specific proteins that are independent of eIF4E interactions.

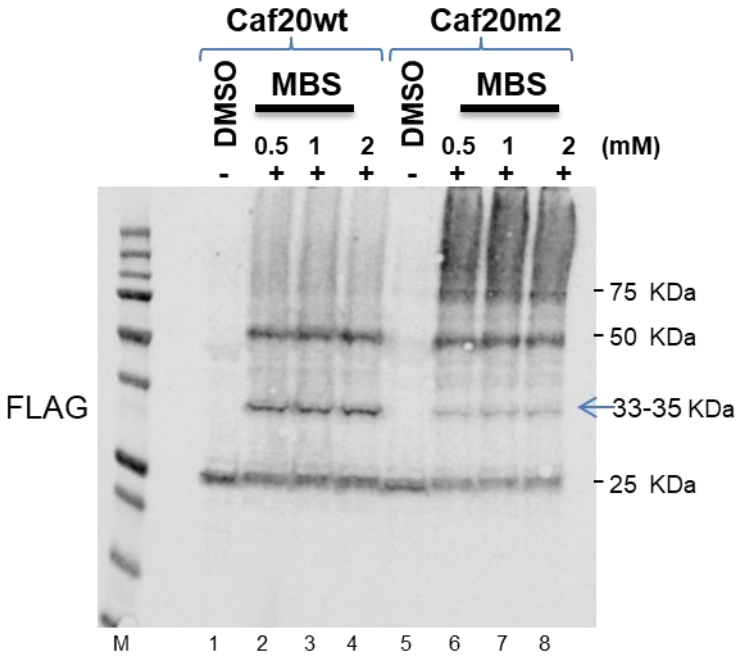

Fig 4.15. Caf20 crosslinks are enriched in the ribosomes. Western blotting of small scale ribosome-enriched extracts of Caf20wt and Caf20m2 crosslinked with BMH and MBS, each tested at final concentrations of 0.5, 1, 2mM and probed with FLAG and eIF4E antibodies. The western blots were probed with FLAG. Lane M is for the protein marker; lane 1 and 5 – extracts crosslinked with DMSO solvent; lanes 2-4 for extracts crosslinked with BMH at 0.5, 1 and 2 mM respectively; lanes 6-8 for extracts crosslinked with MBS at 0.5, 1 and 2 mM respectively. The blue arrow shows the enriched ~10 KDa protein, N= 3 reps for each crosslinker

4.4.2. High salt wash affects ionic Caf20wt interactions more than Caf20m2

To determine if the ribosome crosslinks obtained in the Caf20wt-FLAG and Caf20m2-FLAG are truly specific crosslinks or due to ionic interactions between the proteins and Caf20 which could be lost at high salt concentrations, the MBS-crosslinked samples were treated with high salt. The ribosome-crosslinked products were resuspended in potassium acetate (KAc) salt buffer to final concentrations of 500 mM and 750 mM KAc as described in method section 2.6.2. The result of the western blotting indicated that when Caf20wt was treated with high salt, some FLAG reactive signal shifted into ribosome free components present in the supernatant samples (**Fig 4.16A**, lanes 3 and 7). However the major crosslinks were still retained in the polysome pellets (**Fig 4.16A**, lanes 4 and 8). For Caf20m2 (eIF4E independent Caf20 mutant), there was a little effect by the salt even at 750 mM concentrations (**Fig 4.16B**). Most crosslinked proteins were retained in the polysome pellet (**Fig 4.16B**, lanes 4 and 8). This confirms that Caf20 crosslinks are truly covalent interaction and not due to ionic interactions.

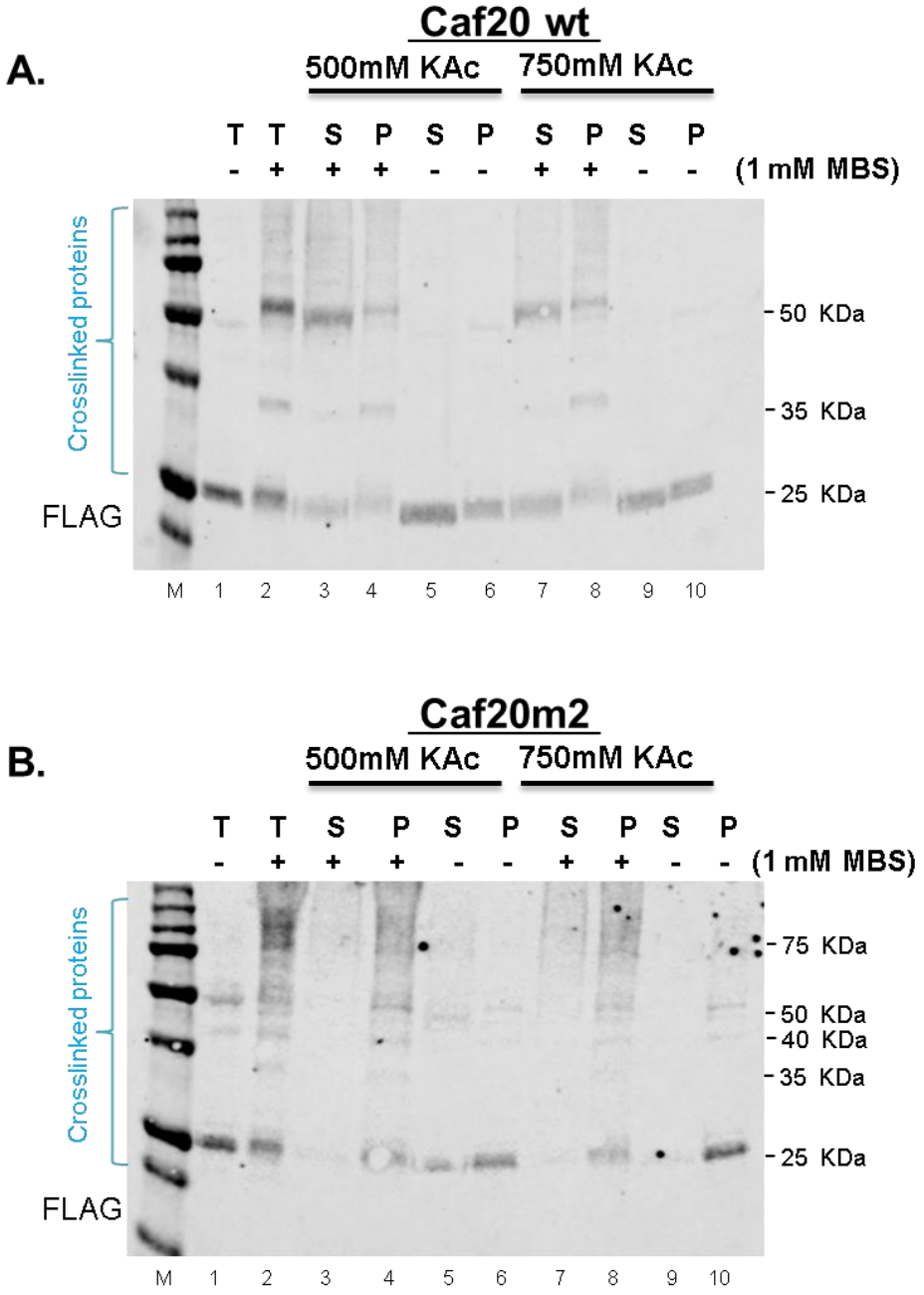

Figure 4.16. High salt treatment helps release non-ribosomal Caf20 cross-linked proteins from the ribosome pellet. A. High salt washes of Caf20wt ribosome extracts of crosslinked and uncrosslinked samples at 500mM and 750mM KAc. **B.** High salt washes of Caf20m2 ribosome extracts of crosslinked and uncrosslinked samples at 500mM and 750mM KAc. N = 1 rep for each salt wash

4.4.3 Purification of Caf20 specific proteins enriched in the ribosome is tag dependent.

After ascertaining that Caf20 crosslinks with specific ribosome-associated factors, the next action was to carryout largescale ribosome crosslinking experiment to generate sufficient material for MS identification. The ribosome enriched extracts were prepared as explained before, crosslinked, FLAG-purified using FLAG magnetic beads, washed and prepared as was done for the largescale total extracts crosslinking studies. When the immunoprecipitated Caf20wt and Caf20m2 were checked by western blotting (**Fig 4.17A**), it was seen that some of the crosslinked proteins of interest disappeared from the eluted samples (**Fig 4.17A**, lanes 9 to 12). This effect was seen for multiple purifications. It was reasoned that the purification of caf20 crosslinked proteins may be impeded as the FLAG tag has a number of lysine residues in it which could potentially be crosslinked by the MBS crosslinker (which binds cys-lys). If lysine residues of the FLAG tag have been crosslinked to other proteins then the crosslinks would be difficult to be retrieved as the crosslinked FLAG tag can no longer bind to the FLAG resin of which might be what happened to our purified samples in **Fig 4.17A**. Alternatively, the large size of the ribosome may cause steric interference with Caf20-FLAG resin interactions limiting the ability of the FLAG antibody resin to bind to the crosslinked caf20. This is because the FLAG epitope is only a short peptide sequence. This would also impair our ability to capture and elute cross-linked products using FLAG-affinity resin.

To test if purification of MBS-crosslinked Caf20 is tag dependent, we compared the results of similar experiments where three different strains each bearing Caf20 tagged to a different tags- Caf20-FLAG (GP7164), Caf20-9MYC (GP5094) and Caf20-TAP (GP5996). Ribosome extracts from the three Caf20 tagged strains and an untagged strain (GP4158) were crosslinked with MBS and immunoprecipitated accordingly as described for each tag in section 2.4.4. The immunoprecipitation at a low salt buffer revealed that MYC tagged Caf20 present the highest recovery of crosslinked products (**Fig 4.17B**). This could be partly be attributed to multiple copies of the MYC tag (9MYC) in the strain. The results showed that the mass-shifts for the cross-linked protein partners are similar across the three strains. This suggests that the major ribosome-associated cross-linked proteins are binding to Caf20 and not to the tag. The Caf20-FLAG and TAP crosslinks had a faint band for the 10 KDa protein which could disappear on high salt washes and RNAse treatments as could be seen in the **Fig 4.17A,** lanes 9-12. In conclusion, the results from Figure 4.17 suggested that the ribosome-pellet associated cross-linked proteins are

not dependent on the tag, but that their purification efficiency may be dependent on the tag used to capture Caf20 and its associated proteins.

In follow-up experiment, when crosslinked Caf20-MYC on the ribosome was treated with high salt (750mM KAc), the western blotting result showed that the free caf20 and some Caf20 cross-linked proteins moved to the supernatant (**Fig 4.18**, lane 2) but that other crosslinked factors were still retained in the ribosome pellet (Fig 4.18, lane 3). This suggested that the ribosome-associated proteins (~10 KDA and ~25 KDa) crosslinked to Caf20-MYC are identical in size to those crosslinked to Caf20-FLAG and are likely the same proteins.

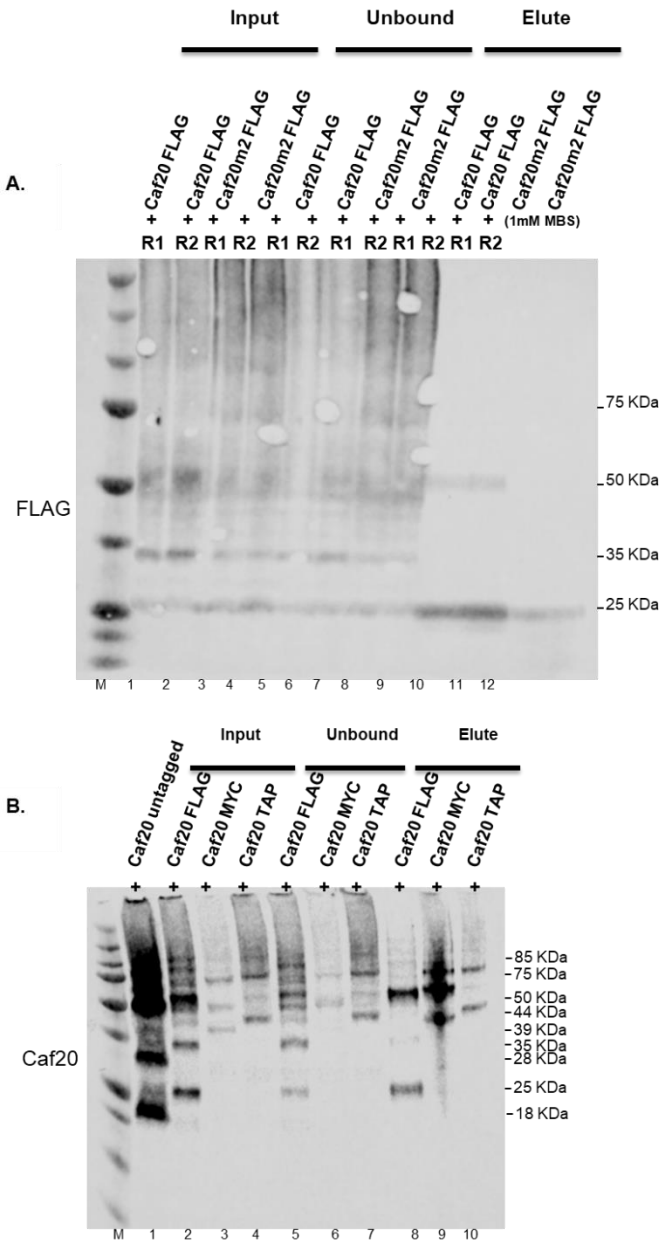

Figure 4.17. Immunoprecipitation recovery of crosslinked-Caf20 specific proteins is tag dependent. A. Western blotting of FLAG-IP of MBS-crosslinked ribosome extracts in Caf20wt and Caf20m2 showing input, unbound and eluates for two reps treated with high salt and RNAses. The blot was probed for FLAG. **B.** Immunoblotting of MBS-crosslinked purified ribosome from extracts of different tagged and untagged Caf20 strains showing input, unbound and elutes that was probed with anti Caf20 antibody. N = 2 reps

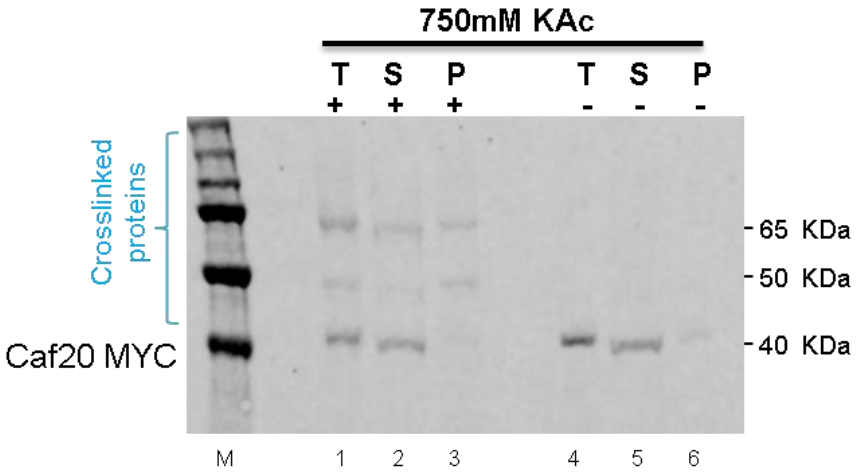

Figure 4.18. Caf20 MYC-ribosome MBS crosslinks are specific proteins. Western blot of Caf20-MYC crosslinked to ribosome enriched factors and ribosome-enriched uncrosslinked Caf20-MYC extracts were treated with 750mM KAc. Unique crosslinked proteins of about 10 KDa and 25 KDa are identified in total crosslinked ribosome-enriched Caf20-MYC extract. T= total extract, S=supernatant, P= pellet N = 2 reps

4.4.4 Largescale crosslinking of Ribosome-rich Caf20-MYC

4.4.4.1 Experimental strategy for largescale ribosome crosslinking

The strategy adopted was to crosslink the ribosome at low salt and repeat series of sucrose cushion to maintain the ribosome after each successive high salt and high detergent washes. The detergent concentration was finally diluted to 0.1% before the MYC IP and the bound proteins were eluted with glycine as described in section **2.6.2.1** (Fig 4.19). Slices of gel from the area of interested were digested with trypsin and processed for Mass spectrometry as discussed in section 2.7.

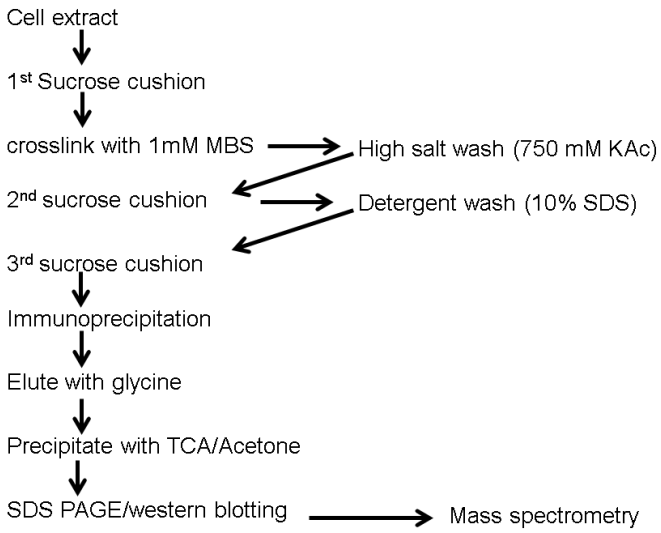

Figure 4.19. Experimental strategy for largescale crosslinking of ribosome-rich extracts.

4.4.4.2 Four Biological repeats Largescale Crosslinking and Mass spectrometry.

MS was performed across multiple biological replicates. Four reps were used for crosslinking and two replicates were used as control. They were processed as described in Fig 4.19A. A gel area of interest was sliced out, digested with trypsin and processed on a free-label LC-MS/MS. The free-label LC-MS/MS identified a number of proteins which was trimmed to proteins with peptides that appear in at least 2 out of the 4 reps for each protein. Each rep had a cut off of a minimum of 2 peptide, FDR 0.05 on the scaffold generated file. 44 proteins were common to the crosslinked and the non-crosslinked samples and 7 proteins were specific to the crosslinked Caf20-MYC only. The 7 specific true cross-linked proteins are enumerated on **Table 4.3,** with the number of cysteine

residues present and their other characteristics. All the seven crosslinked present in only the Caf20wt appeared to have the right characteristics of the most likely cross-linked protein (Table 4.3).

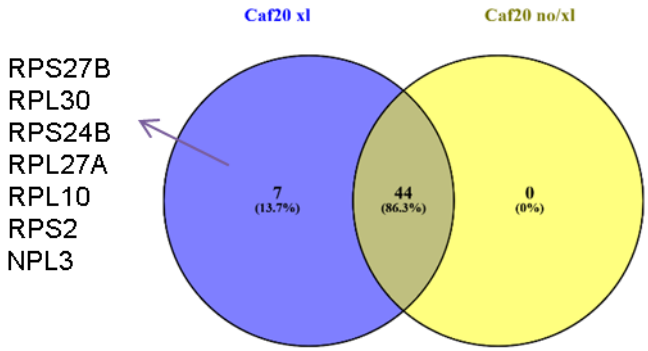

Figure 4.20. Identification of Caf20-associated proteins in ribosome-enriched extracts. Venn-style diagram showing MBS crosslinked proteins associating with Caf20-MYC in 3 three biological repeats identified through Mass spectrometry, highlighting proteins specific to crosslinked Caf20-MYC only. Venn diagrams prepared with Venny 2.1 (Oliveros, 2007-2015). N = 4 reps for crosslinked Caf20-MYC (Caf20 xl) and 2 reps for control uncrosslinked Caf20 (Caf20 no/xl)

4.4.4.3 Grouping and Gene ontology Classification of the crosslinked proteins

Just like what was obtained for the total extract crosslinks, the 51 crosslinked specific proteins of Caf20-MYC ribosome extracts were grouped based on their levels of enrichments or depletions over the non-crosslinked caf20. The transcripts were grouped into four based on their $\log_2$ values and whether they were true positive crosslinks or identified in the non-crosslinked sample. **Figure 4.21** showed a scatter plot of the $\log_2$ values of the identified crosslinked ribosome-rich proteins. Group I are true positive crosslinks that are absent in the non-crosslinked samples and they are upregulated. They are made up of 7 proteins with $\log_2$ values of 5.6 to 4.3. The list of Group 1 proteins are enumerated on **Table 4.3**. Group II are made up of peptides which are present in the non-crosslinked samples and are enriched in the crosslinked samples. Their log values ranged between 1.7 and 0.74 and comprised four proteins (Rps13, Rpl1A, Rpl17B and Rps17B). Group III are made up of 17 proteins that remain unchanged and didn't vary between the crosslinked and non-crosslinked ones. Their $\log_2$ values ranged from 0.6 to 0.0. The

Group IV are made up of proteins that are downregulated in the crosslinked samples. They have $\log_2$ values below zero. In summary, the result suggested that the ribosome-crosslinked proteins are upregulated and downregulated in some groups.

The gene ontology (GO) classification for the enriched transcripts of each group revealed that the crosslinked groups of I, II and III showed a very significant preference for structural constituent of the ribosome and structural molecular activity. The ribosome MS-identified ribosome enriched crosslinked proteins found in each functional class, their p-values and GO terms are summarized in **Appendix III.** In conclusion, the ribosome enriched crosslinks are significantly enriched for molecular functions regulation in forming structural components of the ribosome.

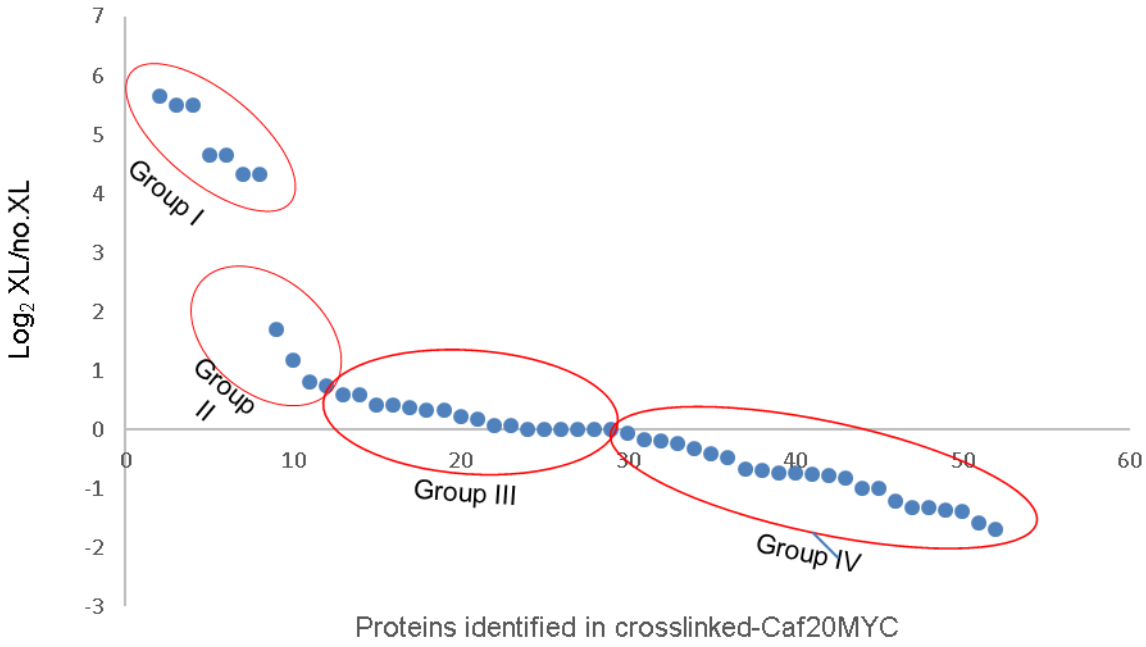

Figure 4.21. Scatter Graph of Log2 levels of enrichments classified the 51 ribosome-crosslinked Caf20-MYC transcripts into four groups. Group I are true positive crosslinks, upregulated and absent in the non-crosslinked, group II are upregulated and present in the non-crosslinked. Group III proteins are unaltered while Group IV are depleted in the crosslinked. The red sphere highlights the proteins in each group (2 or more peptides used for the quantification of each protein, FDR<0.05). N = 4 reps for crosslinked Caf20-MYC (Caf20 xl) and 2 reps for control uncrosslinked Caf20 (Caf20 no/xl)

Table 4.3. Seven proteins present only in Caf20wt

Cross-linked protein	systematic Name	Brief Description	No of peptide	Closest XL size (KDa)[1]	Expected size (KDa)[2]	Cys	Lys	Possible cross-link[3]
Rps2	S5	Protein component of the small (40S) ribosomal subunit	9	65	67.5	1	20	likely
Rps24B	S24e	Protein component of the small (40S) ribosomal subunit	5	50	55.3	0	19	likely
Rps27B	S27e	Protein component of the small (40S) ribosomal subunit	10	50	48.9	5	7	likely
Rpl10	L16	Ribosomal 60S subunit protein L10	4	65	65.4	4	22	likely
Rpl27A	L27e	Ribosomal 60S subunit protein L27A	4	50	55.6	0	23	likely
Rpl30	L30e	Ribosomal 60S subunit protein L30	9	50	51.4	0	12	likely
Npl3	Npl3	RNA-binding protein	5	85	85.4	1	8	likely

[1] migration size of XL band closest to expected size in SDS-PAGE gel
[2] Expected size is Identified protein MW + Caf20-MYC MW on gel (40 KDa)
[3] Possible crosslink is likely when the migration size is comparable to expected size plus presence of cysteine or lysine residue in the protein otherwise it is unlikely

4.5 Caf20 associates with ribosomal proteins located at the interface between 40S and 60S ribosomes

Among the Caf20 true positives crosslinked (Group I of the ribosome cross-linked proteins), the 6 ribosomal proteins (Rps27B, Rpl30, Rps24B, Rpl27A, Rpl10 and Rps5) identified by LC-MS/MS results are components of the 40S and 60S ribosome. Recent findings of ribosomes and its proteins have significant relevance in oncogenesis. This can be seen in recent discovery of somatic mutations in ribosomal proteins in several cancers, ribosome defects and cancer progression (Sulima et al., 2017). Of the six ribosomal proteins identified, Rpl30, Rps24, Rpl27 and Rps27 has implication on congenital diseases such as Diamond-Blackfan anaemia, a congenital bone marrow failure syndrome (Hao et al., 2020; Wang et al., 2015). Apart from the Diamond-Blackfan anaemia, mutation in Rps27 is also implicated in melanoma cancers and for ribosomopathies, a syndrome as a result of defective ribosome function and biogenesis and cancer. Rpl10 is linked to T-cell acute lymphoblastic leukemia and Rps24 is also reported in ribosomopatthies (Sulima et al., 2017). Cells lacking Rps27 exhibit ribosomal assembly

defects and deficiencies in rRNA processing (Baudin-Baillieu et al., 1997). Rps2 is a pre-40S export competence protein that is very essential in cell viability of fission yeast. Mutations that leads to depletion of Rps2 leads to inhibition of 40S ribosomal subunit productuction (Perreault et al., 2008).

Mapping of the crosslinked ribosome proteins on the ribosome structure (Ben-Shem et al., 2011) showed that the ribosomal proteins (Rps27B, Rpl30 and Rpl27A) which are closest to each other are situated at the interface between the 40S and 60S ribosomal subunits (**Fig 4.22**). These proteins are found on the solvent exposed surface, away from the mRNA/tRNA Exit site. Each subunit has several surface-exposed lysine residues, but no surface exposed cysteine (except for Rps27A, where the cysteines all co-ordinate a zinc ion and so would be expected to be unavailable for crosslinking). This suggests that Caf20 associates with intact translating ribosomes and that the MBS crosslinking is likely to have occurred between the single cys in Caf20 (cys 82) and a surface exposed lysine on one or more of these ribosome proteins.

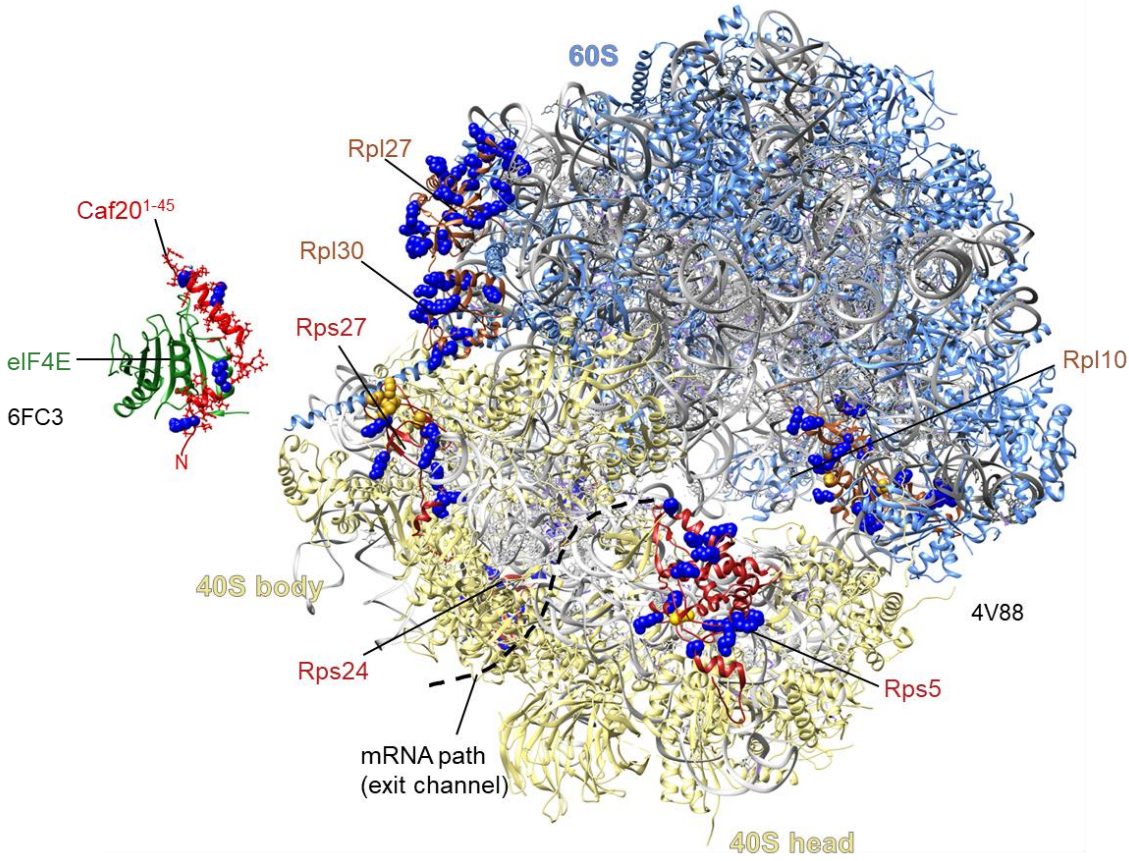

Figure 4.22. Location of identified ribosomal proteins on the 80S yeast ribosome. The structural architecture of the 80S ribosome (4V88) showed the views of some

ribosomal proteins, their exposed charged residues and functional part of the ribosome. The mRNA path (exit channel) is indicated in broken lines (Ben-Shem et al., 2011). Also represented is the 3D structure of Caf20 (6FC3) of the N-region (1-45 residues) interacting with eIF4E deduced from recent Caf20 structure paper (Gruner et al., 2018). The 60S subunit is represented in blue and the 40S subunit in light yellow.

4.6 Independent validation of interacting ribosomal proteins reveals that Caf20 associates with rps27B

4.6.1 Transformations in ribosomal TAP tagged protein strains are expressed.

In order to provide an independent cross validation of the cross-linked ribosomal proteins identified through MS, crosslinking with tagged versions of the identified ribosomal proteins (RPs) was performed. The rationale was that if Caf20 crosslinks with protein X, then changing the molecular weight of protein X should cause a shift in the combined mass of the Caf20-protein X crosslinked band on a western blot. The TAP-tag adds ~26 KDa to the mass of the tagged protein, so should shift one of the Caf20-crosslinked proteins by this amount, providing that our MS candidates are true binding partners. One complication to this analysis approach is that several yeast RPs exist in two isoforms A and B and each strain available has only one ORF tagged. Of the six identified ribosomal proteins (**Table 4.3**), it was only possible to source strains bearing a genomically-integrated C-terminal TAP tag for four RPs from the Open Biosystems collection of over 4200 TAP-tagged strains. For two RPs both A and B isoform ORF tags were available, making 6 strains in total to analyse. The collection was generated by integrating a TAP tag cassette comprising calmodulin binding peptide and a protein A IgG-binding domain along with a generic 3'UTR and HIS3 selectable marker within a separate transcription unit just upstream of the natural stop codon of each ORF. ORFs missing from the collection are likely not amenable to C-terminal tagging. The strains available for analysis are all in the BY4741 *MAT***a** background and had TAP tags integrated at either Rps27B, Rps27A, Rpl27A, Rpl27B, Rps24B or Rpl30.

Western blotting of whole cell extract (WCE) with an anti-protein A antibody revealed that only 4 strains expressed a significant level of the TAP-tagged protein of the expected size (**Fig 4.23**). The Rpl30-TAP was either very poorly expressed or had lost its tag (**Fig 4.23**, lane 6), Rps24B-TAP was not well expressed (lane 1) and was difficult to detect on western blots. It was noted that the Rpl27B-TAP strain had a very poor rate of

growth indicative that the tag likely at least partially disrupts its function. In summary, the Rpl27 and Rps27 candidate ribosomal TAP-tagged proteins are each stably expressed.

To validate the MS results, the ribosomal TAP tagged strains which all possessed untagged wild type Caf20 were transformed with plasmid version of Caf20-FLAG in order to assess the impact of crosslinking of FLAG tagged Caf20 on the TAP tagged ribosomal proteins. Western blotting whole cell protein extracts of the transformed strains showed that the FLAG antibodies used to detect CAf20 cross react with the protein A domain of the TAP-tagged RP (**Fig 4.24)**. This result shows that the Caf20-FLAG were stably expressed in the RP TAP-tagged strains, but that antibody cross-reactivity is an additional issue to resolve.

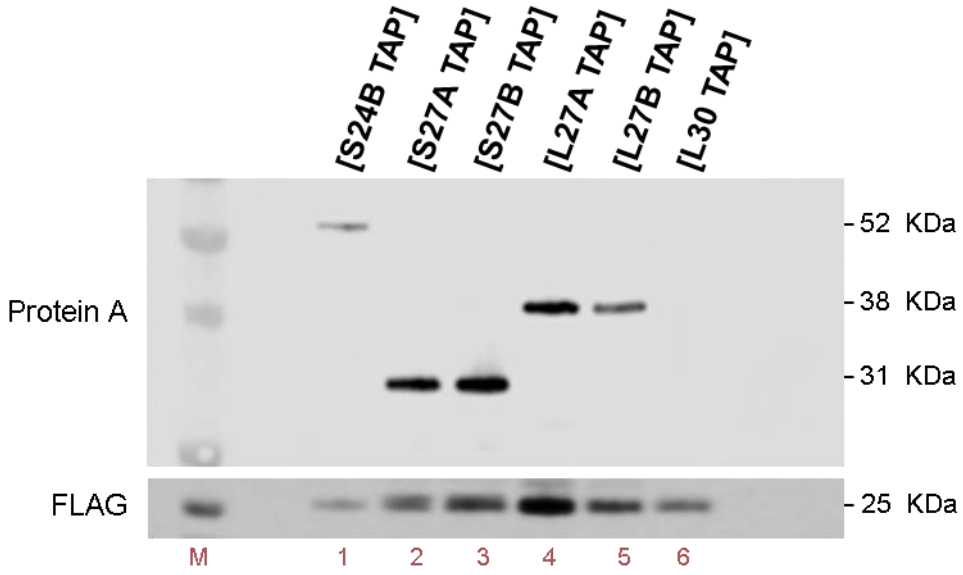

Figure 4.23. TAP tagged Ribosomal proteins are expressed. Western blotting of total extracts of genomic TAP tagged ribosomal proteins probed for Protein A (TAP) and FLAG. Rpl30 TAP is not expressed. Note: [S24B TAP] represents chromosome/genomic integrated Rps24B-TAP tag. M is the marker lane, Lanes 1-6 are the input lanes. N = 1 rep

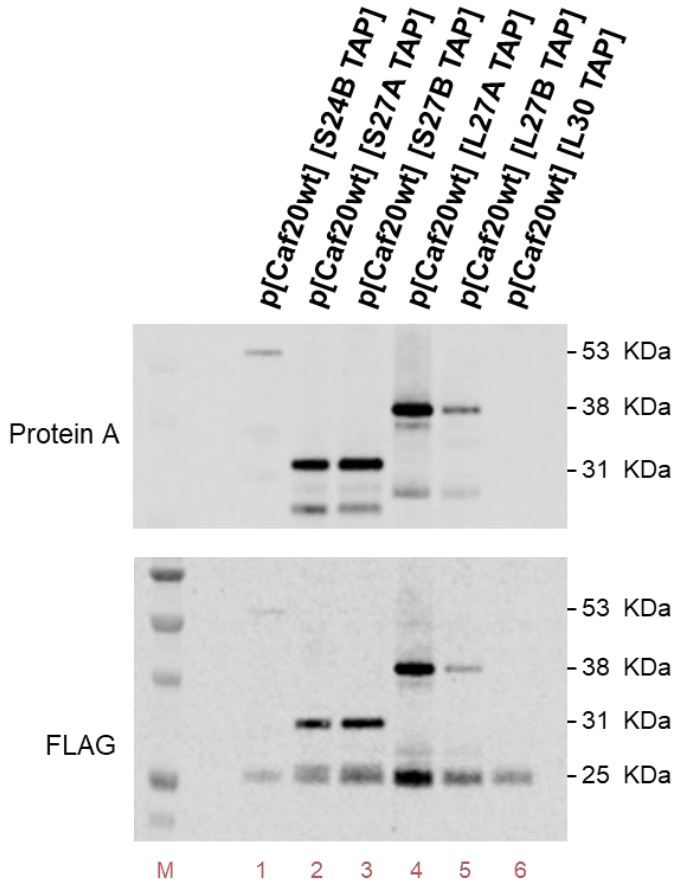

Figure 4.24. Caf20-FLAG are stably expressed in the TAP-tagged ribosomal proteins yeast strains. Western blotting of total proteins of transformed TAP tag strains probed for Caf20FLAG expression. . Note: **p[Caf20]** indicates double expressed Caf20 of chromosomal and FLAG plasmid forms of Caf20; **[S27A TAP]** is genomic TAP tagged RPS27A. M is the marker lane, Lanes 1-6 are the input lanes. The yeast strains were assigned GP strain collection numbers GP7853-58 (**Table 2.2**). N = 1 rep

4.6.2 Solution to FLAG-TAP antibodies cross-reactivity.

To study the interactions of Caf20-FLAG to the six selected TAP-tagged RPs, MBS cross-linking was performed on the ribosome pellet fractions from sucrose cushion experiments (prepared as described in sections 2.5.1 and 2.6.2). Although no Rpl30-TAP was detected, this strain served as a negative control for this experiment. The results from the immunoblotting of the double tagged strains revealed that specific cross-linked products could be detected for the three-most highly expressed TAP-tagged strains. Both Rps27A- and B-TAP tagged strains identified crosslinked products with a combined migrating masses of 40, 45, 53, 75 and 100 KDa. Rpl27A crosslinked products were different, as expected, with combined masses of 46, 53 and 65 KDa (**Fig 4.25**). Rps24B and Rpl27A TAP signals were difficult to detect on the blot in both the non-crosslinked

(**Fig 4.25**, lanes 1 and 5) and crosslinked samples (**Fig 4.25**, lanes 7 and 11) respectively. The results suggested that the TAP tagged ribosomal proteins crosslink to specific proteins. As Caf20-FLAG is ~25 KDa, a Caf20-Rps27 product would be ~57 KDa, while a Caf20-Rpl27 product would be ~63KDa. However, the crosslinking process may not result in proteins that run true to their combined mass, or the crosslinked product may not run the same as an un-crosslinked protein of the same combined mass. To resolve this it was necessary to identify where Caf20-FLAG was in these experiments.

However, when the blot was probed with anti-FLAG antibody, it was challenging to analyse the crosslink pattern on the blot because of the cross reactivity with TAP and FLAG tag antibodies or the secondary antibodies used (**Fig 4.26A**). It was not clear what could be contributing to the cross-reactivity. Potential reasons could be that the animal in which the primary or secondary antibodies were raised may be causing non-specific interactions between the FLAG and the TAP since the blot in **Fig 4.26A** was tested with Rabbit polyclonal anti-FLAG (**Table 2.16**). Also Caf20-FLAG signal for RPL27B was not clearly detected (**Fig 4.26A**, lanes 5 and 11). Protein A (TAP-tag) is known to react strongly with Rabbit IgG, but not chicken IgY. An anti-FLAG chicken IgY (**Table 2.16**) was assessed for cross-reactivity with the TAP. This approach was also not successful as a range of non-specific signals were again observed with either the goat-anti Chicken secondary antibody or when the chicken antiFLAG antibody was labelled (Method section 2.4.6.1) so that no secondary antibody was required (**Fig 4.26B** and **C**).

With the results obtained from **Fig 4.26** and **Fig 3.11** of Chapter 3, it was important to look at the effects different secondary antibodies has on monoclonal antibodies raised in different animals and possible obtain a solution to stop the cross-reactivity between the tags so as to effectively analyse the migration of cross-linked products on western blotting. Different secondary (polyclonal) antibodies to detect monoclonal anti-FLAG of mouse, rabbit and chicken were incubated first with the blot, washed and viewed on fluorescence Imager (LI-COR Odyssey Fc Imager) before it was incubated in a primary (monoclonal) antibody and process the second time. Also a labelled primary anti-FLAG was also tested to see if it could solve the cross reactivity obtained from the secondary antibodies.

Figure 4.27 presented the results from different combinations of antibodies screened for cross reactivities among strains that are untagged, bear single tags or double tags and/or crosslinked. When the blots were first tested with secondary antibodies (**Fig**

4.27A-D on the left panel), the blots cross reacted with the secondary antibodies at varying degree. Goat Secondary antibodies for anti-mouse and anti-rabbit had minimal cross reactivity than either of the polyclonal antibodies for anti-chicken which cross reacted with a lot of non-specific proteins on the blot. Goat anti-rabbit and Donkey anti-chicken detected the TAP tag signals (**Fig 4.27B** and **D**). However, when the blots were then incubated in corresponding monoclonal antibodies, there were still some cross reactivity of the monoclonal antibodies (**Fig 4.27 F-J**). Monoclonal anti-mouse showed the least cross reactivity to TAP signal (**Fig 4.27F**). The anti-FLAG rabbit (**Fig 4.27G**) and anti-Caf20 rabbit (**Fig 4.27J**) detected the TAP tag signal the most while the monoclonal anti-FLAG chicken cross reacted to every non-specific proteins even in its Labelled form (**Fig 4.27E**).

In conclusion, all of the anti-FLAG and secondary antibody combinations tested failed to specifically recognise only FLAG tagged Caf20 in the TAP-tagged strains. This means it was not possible to use this double-tagging approach to independently evaluate the RP crosslinks to Caf20 by this approach. Instead, a genetic approach was adopted that is described in the next chapter.

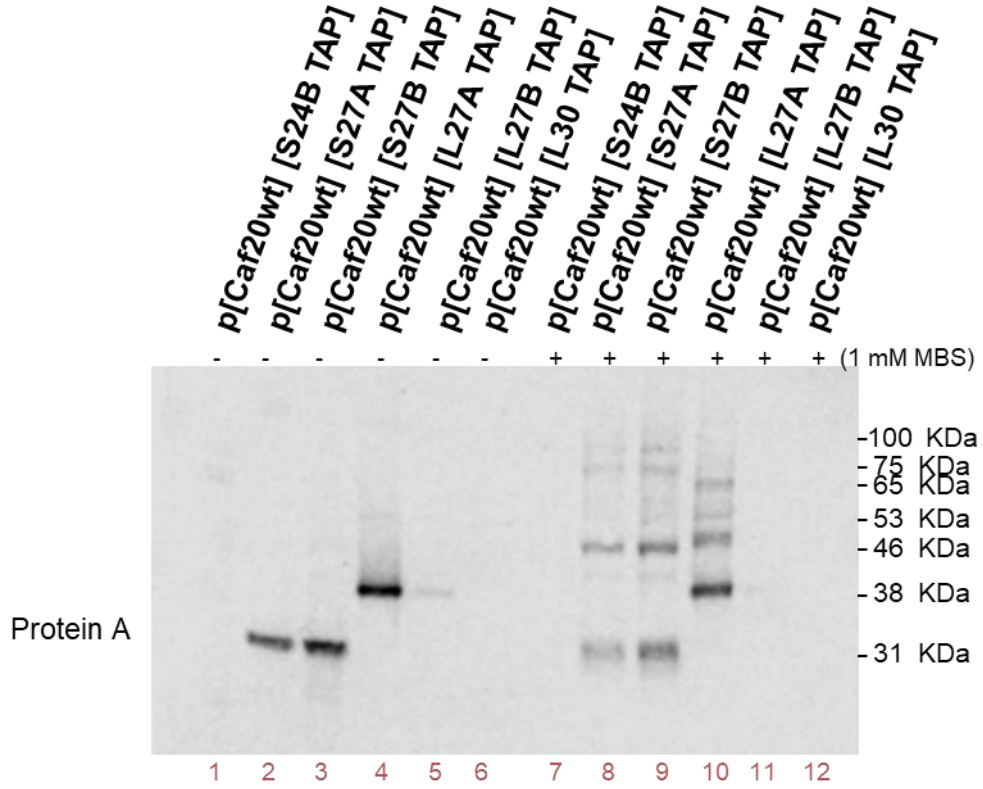

Figure 4.25. Ribosomal proteins crosslink to specific proteins. Western blotting of crosslinked ribosome-bound extracts of transformed TAP tag strains probed for Protein A (TAP) expression. Note: **p[Caf20]** indicates double expressed Caf20 of chromosomal and FLAG plasmid forms of Caf20; **[S27A TAP]** is genomic TAP tagged RPS27A. M is the marker lane, Lanes 1-12 are the extracts lanes. N = 2 rep

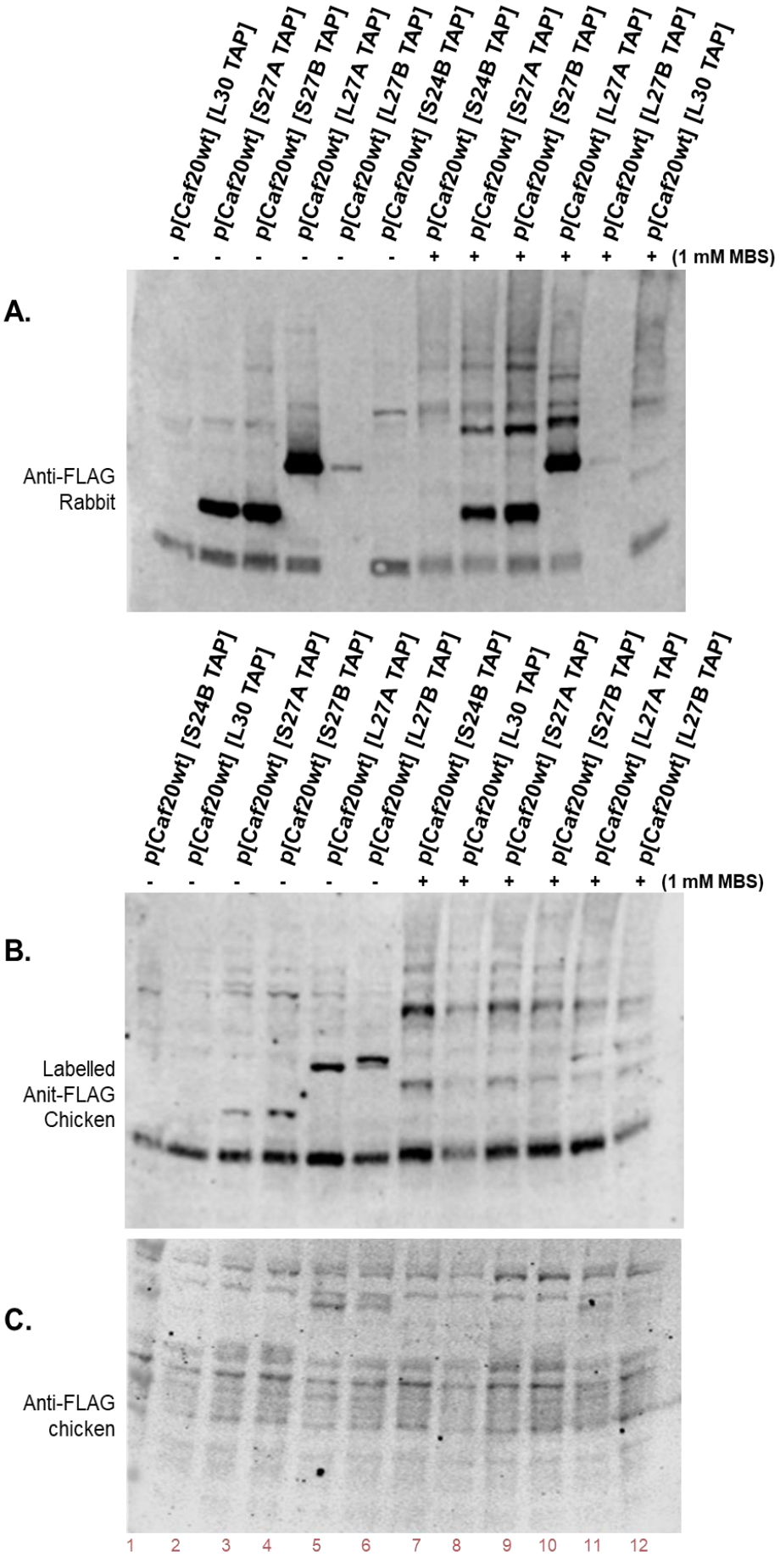
p[Caf20wt] [L30 TAP]
p[Caf20wt] [S27A TAP]
p[Caf20wt] [S27B TAP]
p[Caf20wt] [L27A TAP]
p[Caf20wt] [L27B TAP]
p[Caf20wt] [S24B TAP]
- - - - - - + + + + + + (1 mM MBS)
A.
Anti-FLAG
Rabbit
p[Caf20wt] [S24B TAP]
p[Caf20wt] [L30 TAP]
p[Caf20wt] [S27A TAP]
p[Caf20wt] [S27B TAP]
p[Caf20wt] [L27A TAP]
p[Caf20wt] [L27B TAP]
- - - - - - + + + + + + (1 mM MBS)
B.
Labelled
Anit-FLAG
Chicken
C.
Anti-FLAG
chicken
1 2 3 4 5 6 7 8 9 10 11 12

Figure 4.26. FLAG-TAP tags signals cross react in double tagged strains. Western blotting of crosslinked ribosome-bound extracts of transformed TAP tag strains probed for Protein A (TAP) expression. **A.** Blot probed with monoclonal anti-FLAG rabbit and secondary antibody (Goat anti-rabbit) showed cross-reactivity between the FLAG and TAP signals. **B.** western blot probed with labelled monoclonal anti-FLAG chicken showed cross reactivity with TAP and to non-specific proteins**. C.** Western blot probe with monoclonal anti-FLAG chicken and secondary antibody (Goat anti-chicken) showed non-specific cross-reactivity of the antibodies. Note: all strains contain Caf20-FLAG. **[S27A TAP]** is genomic TAP tagged RPS27A. M is the marker lane, Lanes 1-12 are the extracts lanes crosslinked with/without MBS reagent. N = 2 reps

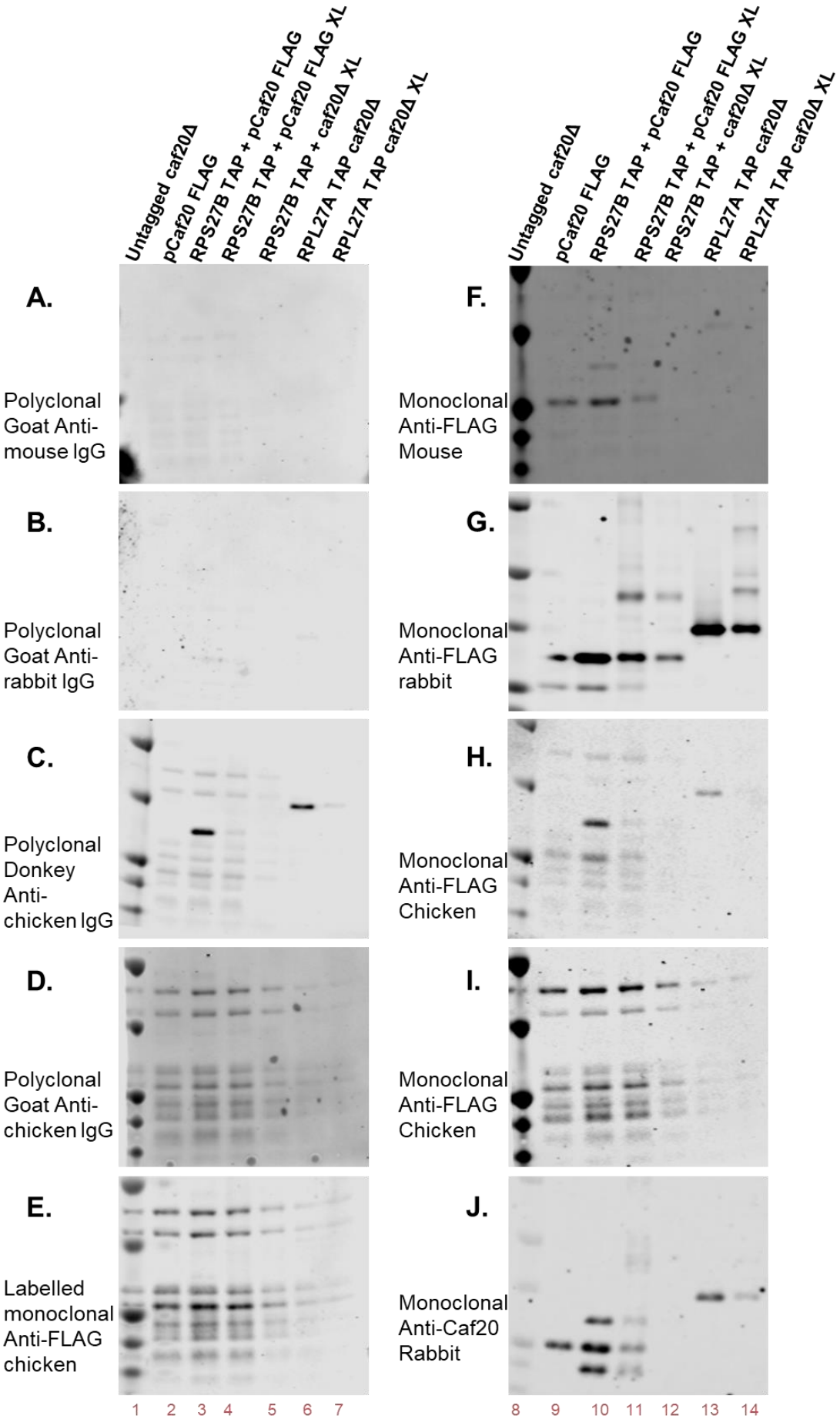
Untagged caf20Δ
pCaf20 FLAG
RPS27B TAP + pCaf20 FLAG
RPS27B TAP + pCaf20 FLAG XL
RPS27B TAP + caf20Δ XL
RPL27A TAP caf20Δ
RPL27A TAP caf20Δ XL
A.
Polyclonal Goat Anti-mouse IgG
B.
Polyclonal Goat Anti-rabbit IgG
C.
Polyclonal Donkey Anti-chicken IgG
D.
Polyclonal Goat Anti-chicken IgG
E.
Labelled monoclonal Anti-FLAG chicken
1 2 3 4 5 6 7
F.
Monoclonal Anti-FLAG Mouse
G.
Monoclonal Anti-FLAG rabbit
H.
Monoclonal Anti-FLAG Chicken
I.
Monoclonal Anti-FLAG Chicken
J.
Monoclonal Anti-Caf20 Rabbit
8 9 10 11 12 13 14

Figure 4.27. Cross reactivity with different primary and secondary antibodies on different tagged strains. Western blotting of strains untagged or tagged with single or double tags tested with different combinations of secondary and primary antibodies. **A-D.** Western blots incubated first with secondary antibodies only. **E-J.** Western blots incubated with different monoclonal FLAG antibodies. **F-I.** Western blots tested second with monoclonal (primary) antibodies and a corresponding secondary antibody used on the left panel **(A-D)** after the blot was initially tested with secondary antibody. **E.** Western blot probed first with labelled monoclonal anti-FLAG chicken. **J.** Western blot probed with anti-Caf20 rabbit to support the effects of anti-rabbit on FLAG-TAP double tags. Anti-FLAG mouse showed the least cross reactivity while anti-FLAG chicken showed the highest cross reactivity on the blots. Lanes 1-7 shows strains extracts on western blot incubated in secondary or labelled antibodies. Lane 1 represents the untagged caf20Δ (GP4789) + marker, lane 2 is Caf20-FLAG (GP7164), lane 3 – Caf20-FLAG, RPS27B-TAP double tag strain (GP7857), lane 4 – MBS crosslinked double tagged strain (GP7857), lane 5 – MBS crosslinked caf20Δ, RPS27B-TAP (GP7839), lane 6 - caf20Δ, RPL27A-TAP (GP7840), lane 7 – MBS crosslinked caf20Δ, RPL27A-TAP (GP7840. Lanes 8-14 corresponds to strains as in lanes 1-7 but are incubated in primary antibodies. Note: XL represents MBS cross-linked. N = 1 rep

4.7 Discussion

Ribosomes are specialized machines in living cells critically important in translating mRNA to polypeptides which folds up to form proteins through a regulated integrated circuit system. Many proteins and RNAs are interacting together to ensure fidelity in translating mRNAs into functional proteins. The position of these proteins on the ribosome can indicate what role they perform on the ribosome. It has been reported previously (Castelli et al., 2015) and from our third chapter that Caf20 could bind to the ribosome independent of eIF4E of which they do though the N-terminal region. In this chapter, we described an approach to determine where on the ribosome Caf20 binds to by identifying Caf20-interacting partners on the ribosome through protein-protein interaction. We employed a crosslinking technique to conjugate proteins closest to Caf20 as a way of identifying Caf20 key targets.

From the large scale crosslinking of total extract, the results were more complicated than expected because of the large data that was obtained from the identified peptides. There were inconsistency in the mass spectrometry results as the initial one rep trial and the 3 rep results showed little correspondence in the identified peptides. The first one replicate identified 3 ribosomal proteins, Rpl23A, Rpl18B and Rpl3 (**Table 4.1**) whereas in the 3 replicates data, the only ribosomal protein (Rps10b) identified is not a true crosslink as the protein has no cysteine residue (**Table 4.2**). Out of the 17 true crosslink in one rep MS (**Fig 4.7**) and 42 true crosslinked proteins in the 3 reps experiments, only 3 proteins (Svf1, Sky1 and Cps1) were common between the two MS

data. The top targets of the 3 reps total extract crosslinking were proteins functioning in cell signalling pathways and kinases. Because of above reasons, no clear inference could be drawn from the results. Moreover, ribosomal proteins were not among the top hits. This could be because ribosomal proteins are small and contain few cysteine residues available at the ribosome surface, reducing our ability to detect interactions with the BMH crosslinker. Because of these reasons, no proper inference could be drawn from the result. In view of this, the crosslinker was switched from BMH crosslinker (cys-cys) to MBS (cys-lys) and it was also decided to perform ribosome pelleting to enrich for ribosomal proteins in the cross-linking experiments. With further refinements, including using Caf20-Myc in place of Caf20-FLAG the approach successfully identified a small number of ribosomal proteins of both 40S and 60S ribosome supporting the findings of Castelli et al. (2015) from Mass Spectrometry analysis of TAP-IP purification in which both ribosomal proteins of 40S and 60S subunits were identified. The identified proteins were grouped into four groups where Group I and II are enriched crosslinks and Group IV are downregulated crosslinks. The Gene ontology classification showed that the groups are significantly enriched structural components of the ribosome.

Caf20 associated with translating ribosome as the top ribosomal proteins identified in Mass spectrometry of one rep total extract crosslinking (Rpl23A, Rpl18B, Rpl3)and multiple rep ribosomal crosslinking (Rps5, Rps24, Rps27, Rpl10, Rpl27 and Rpl30) were proteins found to be adjacent to each other across the 40S and 60S subunits. This is consistent with the results of the ribosome interactions which showed that Caf20 associating with polysomes and the 80S subunits (**Figs 3.6, 3.9** and **3.10**) which has been confirmed on Mass spectrometry with Caf20 associating with ribosomal proteins of 40S and 60S subunits. A similar observation was also reported by Dr Lydia Castelli, a former researcher in Professor Graham Pavitt's Lab group where she showed that Caf20 can bind stably to only 80S ribosomes and not free 40S or 60S subunits. Taken together, it could be suggested that Caf20 preferentially select intact ribosome. Also from **Table 4.3**, the most likely crosslinked protein was shown to be Rps27, which seemed promising by having multiple surface accessible lysine residues (**Fig 4.22**) and a molecular weight of 8.9 KDa, closest to the molecular weight of ~10 KDa predicted by western blot mobility shifts in the initial cross-linking studies.

The Caf20 structure study showing N-terminal part (region A of this study) show bipartite binding with eIF4E on the dorsal and lateral surfaces of eIF4E through its canonical and non-canonical motifs respectively connected by a flexible extended linker

(Gruner et al., 2018). Since they used The N-terminal part (1-45) in their crystal structure, it wasn't clear if all of Caf20 may be unfolded or folded. It is also feasible that the cysteine in Caf0 could mediate some of the crosslinking obtained as some of the crosslinks went away when Caf20 was used with no cysteine (**Fig 4.10**). Rps27 and Rpl27 which are true ribosome-crosslinks were also detected in one rep out of three replicates of the total extract crosslinked wildtype Caf20 but were not included a specific-crosslinked protein.

Attempts to cross validate using tap-tagged subunits were thwarted by non-specific interactions (**Figs 4.26-4.27**) between the tag-'specific' antibodies and the lack of availability specific antibodies to the identified yeast ribosomal proteins from literature searches. If time had permitted, MYC or HA tagged ribosomal protein (RP) constructs could have been made. The KanMX interaction cassettes are available in the lab collection for future work which was not possible due to time constraint.

Chapter 5
Functional characterization of Caf20

5.1 Introduction

Some functional assays were conducted to understand more physiological relevance of Caf20 in yeast. Previously reports had ascertained Caf20 effects in relation to limiting nitrogen, slow growth rate, translation repression, cold sensitivity, cell cycle regulation and other stress conditions (Castelli et al., 2015; Cridge et al., 2010; de la Cruz et al., 1997; Ibrahimo et al., 2006). Some phenotypic effects already reported showed that deletion of caf20 rescue slow growth rate and cold sensitivity in translation mutants of eIF4E, eIF4B, eI F4G1 whereas the overexpression of Caf20 enhances the growth defects of these mutant strains (de la Cruz et al., 1997). Under limiting nitrogen sources, Caf20 deletion impact on the ability of diploid yeast (Σ1278b) to differentiate into pseudohyphal forms and form p-bodies (Ibrahimo et al., 2006). Deletion of Caf20 in auxotrophic yeast strains showed some mild growth defeacts on amoniumium sulphate and serine deficient growth media (Cridge et al., 2010). According to Castelli et al. (2015), yeast growth in respiratory medium (mitochondrial function) can be independent of eIF4E-binding motifs and eIF4E-interactions. They showed that deletion of Caf20 reduces the growth of cells in glucerol/ethanol medium (respiratory medium) which is rescued with the incorporation of plasmids bearing either Caf20wt or Caf20m2 mutation (Castelli et al., 2015).

This chapter sets to discuss different phenotypic characterisation studies performed for Caf20 in yeast as a way to either affirm/dispute previous findings and/or to report novel observations discovered. The phenotypic characterisation were obtained by conducting growth studies in different growth media, drugs and/or at different temperatures. Drugs were tested for Caf20 either by incorporating it in the growth media and studying the inhibitory effect or by measuring the zone of inhibition around a drug disc. Also, Caf20 synergetic effects were studied in relationship with different ribosomal proteins identified from the Mass spectrometry in order to validate the Caf20 relationship with the MS identified ribosomal proteins.

5.2 Physiological studies of parent and control strains.

5.2.1 Measuring Doubling Times of parental and control Strains in different growth media.

The first physiology study performed was to determine the doubling times of the parent strains i.e. Untagged mating pairs of Caf20wt (GP4158 or GP6991) and *caf20*Δ (GP4789 or GP6992). This was a preliminary assay aimed towards determining regions of Caf20

important for function. A difference in the doubling times experiment would create a basis to screen the different Caf20 mutants generated in order to identify elements of importance. Both the growth doubling times in aerobic and fermentative media were determined. The growth media used were complete media YPD and SCD (both 2% glucose), as well as YGE and SCGE media containing both glycerol and ethanol (3% glycerol and 1% ethanol). The strains were first grown to stationery phase in the same medium to be able to adapt to the medium before being transferred to fresh medium for the doubling time monitoring.

Figure 5.1 revealed the growth curve of the mating types in SCGE complete medium for one biological repeat. The growth in SCD (2% glucose) and SCGE (3% glycerol and 1% ethanol) complete media showed no significant difference in growth rate at the exponential phase for both *MAT***a** and *MAT*α wildtype and *caf20*Δ strains (**Table 5.1**). Likewise, the growth on YPD (2% glucose) and YPGE (1% glycerol and 3% ethanol) media showed no statistical difference in growth rate of *MAT*α pair (**Table 5.2**). In glucose containing media, the parent strains grew the fastest in YPD medium (**Table 5.2**) because it is a very rich media with all the nutrients required for a robust growth. The doubling time was approximately one and half hours. In SCD medium, the growth rates were slightly slower with means of 1.78 – 1.88 hrs (**Table 5.1**). Whereas in the glycerol/ethanol media, both 'wt' and *caf20*Δ strains grew more slowly, as expected. This suggested that there were no differences in the doubling times during the exponential phases of the Caf20wt and *caf20*Δ in different growth media.

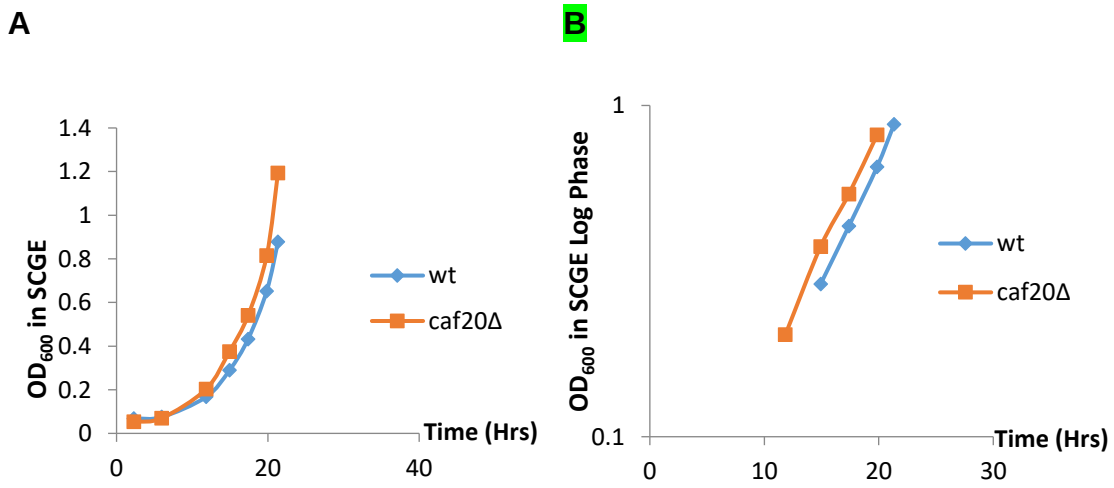

Figure 5.1 Growth curve for *MAT*α pair in SCGE medium. This figure shows the growth curve in SCGE for one of the replicates for *MAT*α wt (GP4158) and *caf20*Δ (GP4789). **A.** Growth curve of two parental strains from lag to the exponential phase measured over a time frame at OD600. **B.** The log scale growth plot of the exponential phase of Fig 5.1A only. N= 1 rep

Table 5.1 Doubling times in SCD and SCGE for both *MAT*a and *MATα* strains (in hrs)

Strain	SCD [1]	2-tailed T-test Value (SCD)	SCGE [1]	2-tailed T- test Value (SCGE)
*MAT*α Caf20wt[a]	1.79 ± 0.014	[2]0.293[NS]	4.44 ± 0.22	[2]0.389[NS]
*MAT*α *caf20*Δ[b]	1.82 ± 0.014		4.20 ± 0.11	
*MAT***a** Caf20wt[c]	1.78 ± 0.028	[3]0.590[NS]	4.66 ± 0.28	[3]0.298[NS]
*MAT***a** *caf20*Δ[d]	1.88 ± 0.151		4.23 ± 0.21	

[1] Doubling times (in hrs) for three biological replicates (mean ± Standard error), n = 3 reps
[2]T-test value for *MAT*α pair
[3]T-test value for *MAT***a** pair
[a]*MAT*α wt (GP4158)
[b]*MAT*α *caf20*Δ (GP4789)
[c]*MAT***a** wt (GP6991)
[d]*MAT***a** *caf20*Δ (GP6992)
[NS] T-Test value not significant at p value<0.05

Table 5.2 Doubling times (in hrs) on YPD and YPGE Media for *MATα* pair: wt and *caf20*Δ

Strain	YPD [1]	2-tailed T-test Value (YPD)	YPGE [1]	2-tailed T-test Value (YPGE)
*MAT*α Caf20wt[a]	1.48 ± 0.024	[2]0.606[NS]	3.78 ± 0.251	[2]0.220[NS]
*MAT*α *caf20*Δ[b]	1.50 ± 0.027		3.33 ± 0.173	

[1] Doubling times (in hrs) (mean ± Standard error) for three biological replicates
[2]T-test value for *MAT*α pair
[a]*MAT*α wt (GP4158)
[b]*MAT*α *caf20*Δ (GP4789)
[NS]T-Test value not significant at p value<0.05

Growth rates were also calculated for the control strains, Caf20 wt, Caf20^{m2} and *caf20*Δ (GP7164, GP7173 and GP7174 respectively). This was performed because these strains each contained a *LEU2* plasmid (leucine plasmid selection was required) and were grown in dropout medium that may influence the growth rate. In this scenario, the strains were grown to exponential phase in SCD medium (OD_{600} = 0.6), re-suspended in SCGE 1% glycerol/3% ethanol medium and then back-diluted to OD_{600} = 0.1 before sampling the cultures to determine doubling times. The results showed that there were no significant differences in the exponential phases among the control strains (Table 5.3). The growth rates observed for three biological repeats of their strains was between 6.8-7 hrs. The *caf20*Δ strain doubles fastest, followed by the Caf20 wildtype and then the

Caf20^{m2}. However, the doubling times were higher compared to the parent strains (Table 5.1). Although not entirely clear why, it is likely a result of differences in the media/back dilution method used and/or the need to accurately segregate the LEU2 plasmid. Leucine was added in the complete SCD medium which reduced the time for the auxotrophic strains (Table 5.1) to double in the SCD medium, while prototrophic strains with LEU2 plasmid marker (Table 5.3) depend on the plasmids to biosynthesis of enzymes for leucine snythesis in SCD-L 'dropout' media which may have impacted on the differences in the doubling times obtained for similar strains in Tables 5.1 and 5.3. Taken together, the results suggested that there are no differences in the doubling times of the exponential growth phases of the parent strains and the control strains both in aerobic and anaerobic (respiratory) media. As there were no differences in the doublings times of the parent and control strains, the doubling times of other Caf20 mutants were not assessed.

Table 5.3 Doubling times in SCGE medium

Control strains (used in this study)	Doubling times in SCGE (in hrs) [1]	2-tailed T-test Value (YPGE)
Caf20wt[a]	6.81 ± 0.117	
Caf20^{m2}[b]	6.97 ± 0.172	0.494^{NS} wt VS m2
*caf20*Δ[c]	6.77 ± 0.065	0.766^{NS} wt VS Δ

[1] Doubling times (in hrs) (mean ± Standard error) for three biological replicates
[a]Caf20wt (GP7164)
[b]Caf20^{m2} (GP7173)
[c]*caf20*Δ (GP7174)
^{NS}T-Test value not significant at p value<0.05

5.2.2 High temperatures are lethal for yeast cells in respiratory media

In previous Caf20 functionality studies, Caf20 was reported to alter the levels of proteins important in nitrogen metabolic process and mitochondrial functions (Castelli et al., 2015. This Caf20 regulation was shown to be under eIF4E-independent control as both Caf20wt and Caf20m2 behaved similarly {Castelli, 2015 #2015. This Caf20 regulation was shown to be under eIF4E-independent control as both Caf20wt and Caf20m2 behaved similarly {Castelli, 2015 #2015; Cridge et al., 2010). Caf20 had previously been reported to have a negative role on the translation initiation factors, eIF4B and Ded1 (de la Cruz et al., 1997). In that phenotypic study, it was reported that the deletion of Caf20 was found to partially alleviate the slow-growth and cold-temperature sensitivity caused by deletion of

the initiation factor eIF4B (*tif3*Δ). Conversely Caf20 overexpression of Caf20 was found to enhance severity of the *tif*3Δ slow-growth phenotype as well as modestly impair the slow-growth of other translation initiation factor mutants. Similarly, the effects of the presence of Caf20 overexpression, deletion and mutation in low and high temperatures but under respiratory media (mitochondrial function) were assessed in this study to ascertain if temperature-sensitivity in respiratory media holds for Caf20. Temperature could impact on yeast respiratory growth as aerobic respiration could be limited the amount of oxygen available for respiration at high temperatures and the amount of energy and CO_2 released (Graduateway, 2017).

To test if there are any phenotypic effects of Caf20 mutants in respiratory media at different temperatures, yeast strains bearing Caf20wt, Caf20m2 and caf20Δ were grown in respiratory media spot plates incubated in different temperatures (16°C, 25°C, 30°C, 33°C and 37°C). In the control plates (SCD plates), all the strains grew normal in all temperatures tested between 2 and 4 days (**Fig 5.2 a-e**). but in the SCGE media, all the strains grew slower, but Caf20wt cells appeared more sensitive to growth at 16°C (**Fig 5.2 f-g**, left images), but does catch up after a day or two (Fig **5.2 f-g**, right images). However, at higher temperatures of 33°C and 37°C, there were no growth as the media became lethal for the strain growth. In conclusion, Caf20wt is shown to be more cold-sensitive in respiratory media than the *caf20Δ* and Caf20m^2 mutants. This is possibly caused by a longer lag-phase for wt cells at this temperature compared with the mutant cells, as after time it does grow. As both the *caf20*Δ and Caf20m^2 strains behave identically this suggests the difference is caused by an eIF4E-dependent effect, rather than specifically eIF4E-independent effect.

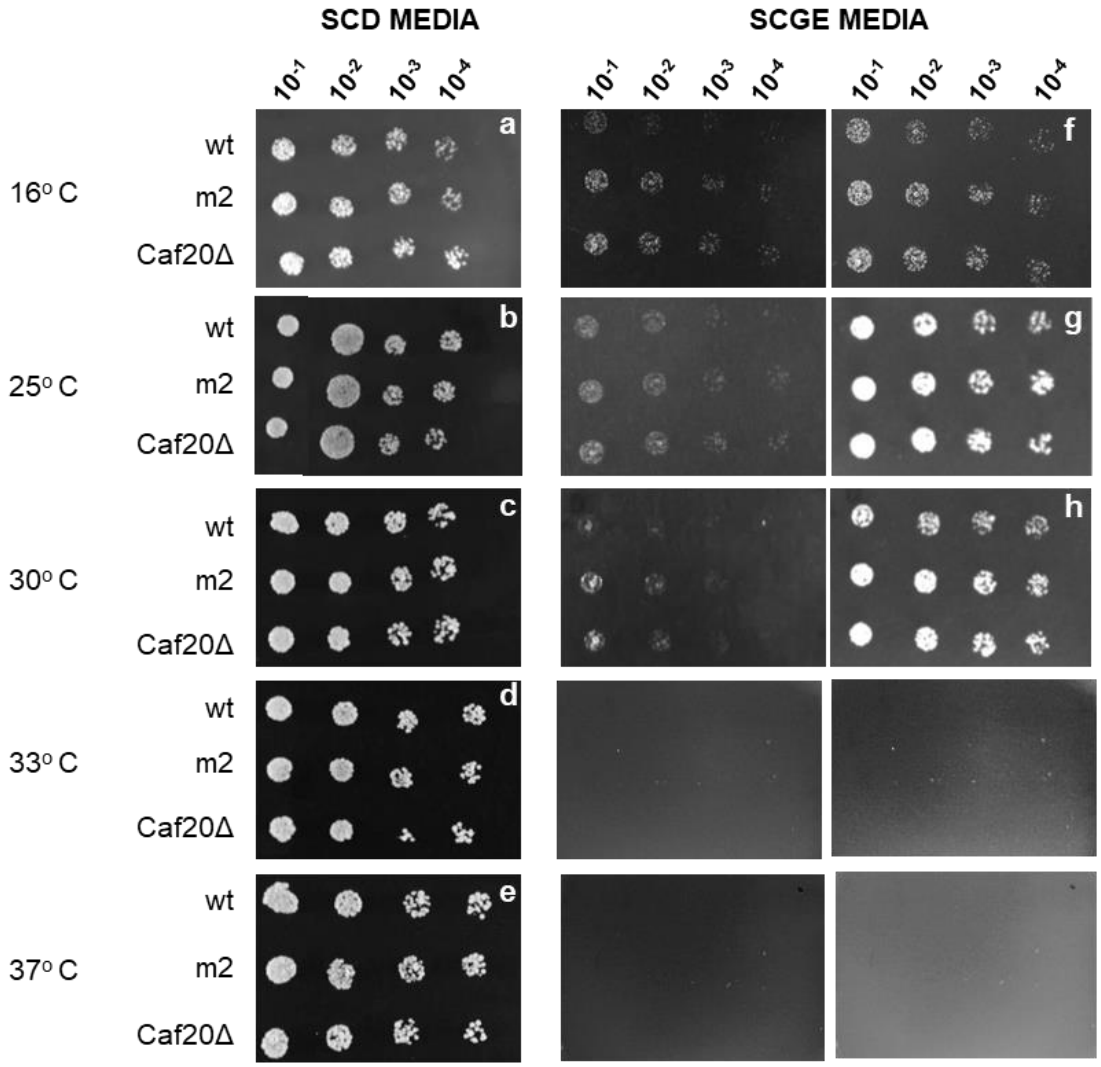

Figure 5.2. The phenotypic effect of respiratory media at different temperatures. **(a-f)** Growth of the control strains (wild type Caf20FLAG WT, Caf20m2 and Caf20Δ) in SCD media at different temperature. **(a)** Growth at 16° C after 4days. **(b-e)** Growth of controls at 25° C, 30° C, 33° C and 37° C respectively after 2 days. **(f-h**) Growth of strains at onset (left image) and after few days (right image) on SCGE media. **(f)** Growth on SCGE at 16° C after 9 days (left) and 10 days (right). **(g-h)** Growth on SCGE after 4 days (left) and 6 days (right). No growth of the strains at higher temperatures of 33°C and 37°C. Note: **wt** is wildtype Caf20 strain, **m2** is Caf20m2 mutant strain and *caf20Δ* is Caf20 delete strain. N = 1 rep

5.3 Phenotypic response of Caf20 to protein synthesis inhibitory drugs.

As Caf20 can interact with the ribosome, it was necessary to study the phenotypic response of Caf20 to some group of drugs which had been shown to affect translation at some stages of translation inhibition either at the translation initiation, elongation, degradation and other post translation stages. Among the protein synthesis inhibitory drugs used include rapamycin (an allosteric inhibitor of the TOR kinases that regulate

translation and transcription and ribosome biogenesis to control cell growth); paromomycin (which targets the A-site of the small ribosome subunit by preventing sensing of mismatches between tRNA- mRNA codon interaction and thereby causing ribosome decoding errors); clioquinol (inhibits protein synthesis indirectly by interfering with the metal uptake of yeast for metabolism); cycloheximide (inhibits translation elongation by binding to the ribosomal E-site, freezing the ribosome onto the mRNA) and $CuSO_4$ (which among many defects can result in protein misfolding and degradation.

5.3.1 Caf20 is not sensitive to rapamycin drug

Rapamycin is a drug used in inhibiting the activities of the target of rapamycin (TOR) signalling pathways and the ribosomal protein S6 kinases, S6Ks (Choo et al., 2008). It is also used in the activation of the GCN4 (a gene which is expressed in limiting nutrient conditions) important in amino acid biosynthesis (Ashe et al., 2001; Cherkasova and Hinnebusch, 2003). In mammalian cells, the phosphorylation of the 4E-BP1 and the S6Ks are partly controlled by the mammalian target of rapamycin (mTOR)/FK506-binding protein (FKBP)-rapamycin-associated protein (mTOR/FKBP) (Beretta et al., 1996; Brunn et al., 1997; Choo et al., 2008; Gingras et al., 1999a). The TOR pathways in both yeast and mammalian cells share some similarities in function in that they arrest cell growth in early G1 phase and causes great reduction in protein synthesis (Heitman et al., 1991). In yeast, TOR pathway is responsible for the inhibition of cap-dependent translation initiation machinery by more than 90%. Rapamycin inhibition of TOR function has been reported to cause translation defects due to abrupt inhibition of translation initiation by lack of G1 progression (Barbet et al., 1996). Eap1 has been implicated to be regulated thorough the TOR signalling cascade (Cosentino et al., 2000).

To work out the concentration of rapamycin to use, a previous report had showed that at lower concentrations (≤ 50 nM), rapamycin was found to show a linear variable level of inhibition of selected eIF2B mutant yeast strains, which were more sensitive than the wildtype and when used at higher concentrations (> 50 nM), the variability diminished (Kousar, 2013). To test the effects of rapamycin on Caf20 yeast strain, spot tests were performed in SCD media supplemented with different concentrations of rapamycin and incubated at 30°C as described in section 2.2.5.2. The results showed that the rapamycin greatly inhibited the growth of the cells (**Fig 5.3**). At day 2, growth was visible on only the control and 5 nM rapamycin-treated plates. At day 7, the growth of the strains were still greatly reduced. However, there was not much difference between the wildtype

Caf20 and the *caf20Δ* strains (**Fig 5.3**) for all the concentrations of rapamycin tested. It could be concluded from this result that *CAF20* is not a target of the TOR signalling pathway in yeast.

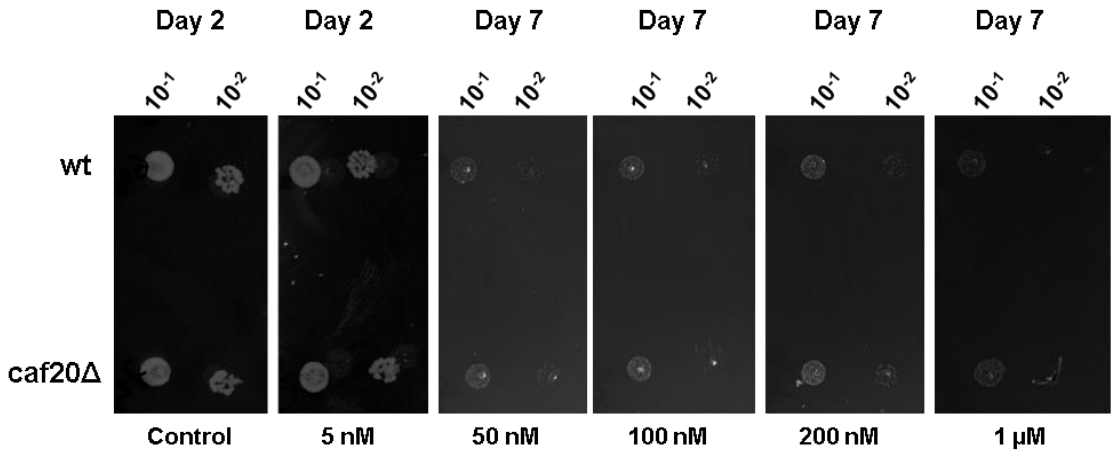

Figure 5.3. Caf20 regulation does not require the TOR pathway. Wildtype Caf20 and caf20Δ strains were serially diluted tenfold to prepare 10^{-1} and 10^{-2} cultures. 2 µl of each strain-culture was spotted on the SCD-L agar plates complemented with different concentrations of rapamycin. The spotted cultures were incubated at 30°C for 2-7 days. Growth was recorded at day 2 and 7 of incubation. N= 1 rep each

5.3.2 Caf20 is resistant to paromomycin treatment.

Paromomycin belongs to a group of antibiotics called the aminoglycosides which act against gram negative bacilli and mycobacteria. They inhibit the protein synthesis of the bacteria by binding to the receptor of the 30S ribosome to interfere with the reading of the microbial genetic code (Kumar, 2017). Paromomycin target the A-site of the small ribosome subunit by preventing the ribosome sensing a mismatch between tRNA anticodon and the mRNA codon interaction. Such interactions are normally resolved by rejection of the tRNA, instead the non-cognate interactions are tolerated causing subsequent production of incorrect proteins (Ogle et al., 2001). Its mode of action is conserved in eukaryotes.

Paromomycin was tested for inhibition of isogenic Caf20, m^2 and *caf20Δ* strains to determine the interference of the drug on the strain growths. Paromomycin was tested in two ways, as applied to a filter-paper disc in a plate assay and also by incorporation into the growth medium for spot tests as described in Section 2.2.5. For the filter disc assay, 5µl of each concentration of paromomycin was added on a filter paper disc placed on a plate lawn of culture and incubated for a day. After which, the diameter of a zone of

inhibition was determined by analysis of a photograph in ImageJ software (Schneider et al., 2012). The results of both tests showed that all the strains tested showed high level of resistance to paromomycin treatment (**Fig 5.4**). The resistance could be seen even at very high concentrations of 200mg/ml on filter disc (**Fig 5.4A**). The figures for other lower concentrations tested on filter disc are not shown. On the spot test plate, there weren't any difference among the strains at 18 mg/ml (**Fig 5.4B**, lower panel). However, Caf20 proved to show more resistance to paromomycin on the onset (at day 2) when the concentration of the drug was increased to 50 mg/ml (**Fig 5.4B**, upper panel). In conclusion, as the strains are isogenic and contain a KanMX resistant cassette. KanMX resistance provides cross-resistance to paromomycin, invalidating this assay.

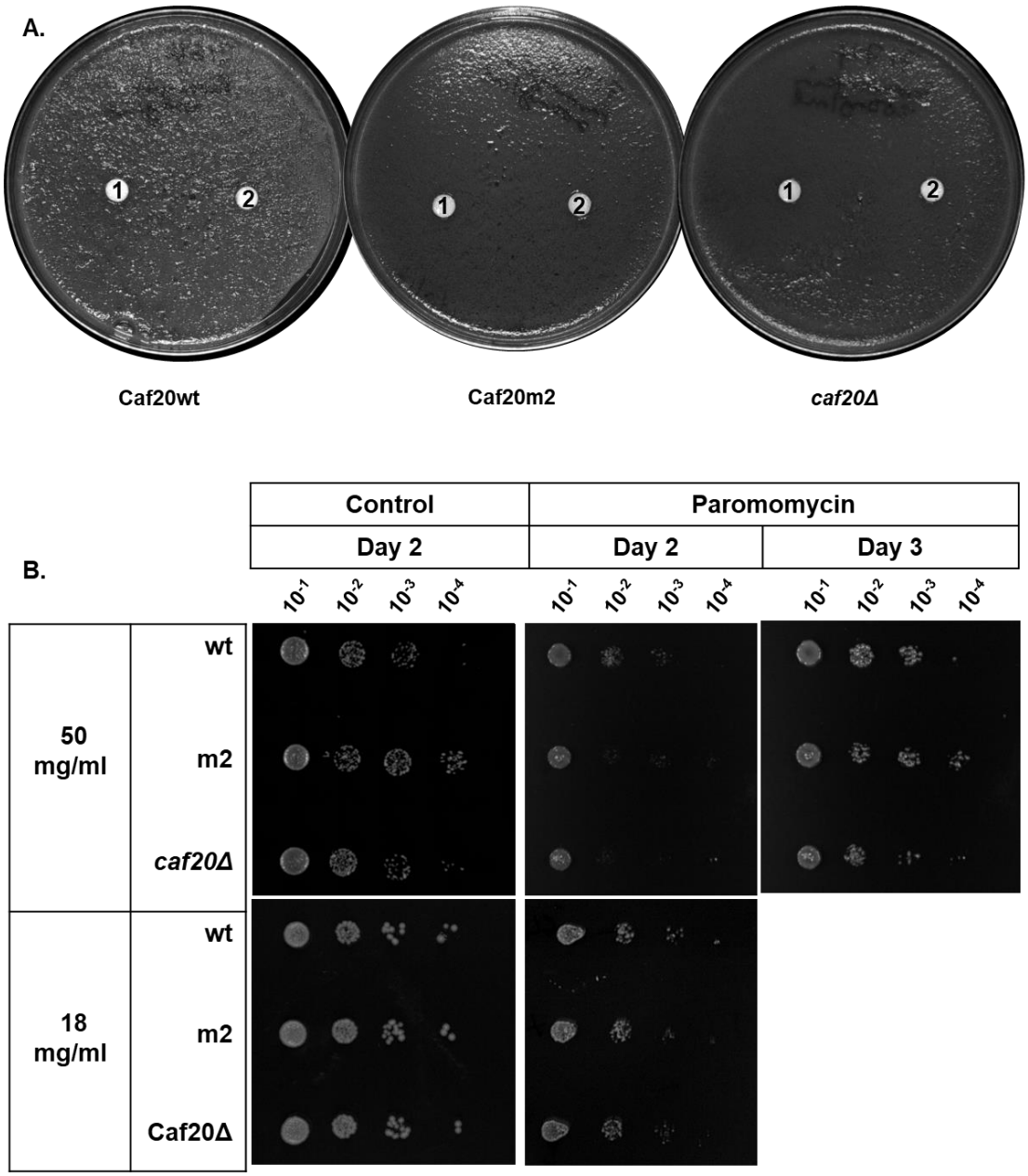

Figure 5.4. Caf20wt is more resistant to Paromomycin antibiotics activities. A. Filter disc tests of Paromomycin were performed by adding 5 µl of paromomycin at 200 mg/ml concentration on approx. 0.65 cm diameter filter discs in two reps (1 and 2) on each strain as described in section 2.2.5.1. All strains bear *LEU2* plasmid and have KanMX cassette which conferred resistance to Paromomycin drug. **B.** Spot test of Caf20 yeast strain in SCD-L plus paromomycin media plates tested at 18mg/ml and 50mg/ml concentrations for 2-3 days. N = 3 reps

5.3.3 Caf20 is sensitive to clioquinol treatment

Clioquinol (5-Chloro-7-iodoquinolin-8-hydroxyquinoline) is an antibiotic drug prominent for its use in the treatment of diarrhoea and skin infections in the mid 1900's. It is also a metal chelator of copper, zinc and iron (Ding et al., 2005). It was clinically

banned because of possible association with subacute myelo-optic neuropathy in Japan (Tsubaki et al., 1971). Of recent, interests in the drug was resuscitated after the report of its potency to kill cancer cells (Ding et al., 2005) and in the treatment of neurodegenerative diseases such as Huntington's disease (Nguyen et al., 2005), Parkinson's disease (Kaur et al., 2003) and to slow down memory loss in Alzheimer's disease by drastic reduction in the amyloid-β levels (Cherny et al., 2001). The amyloid-β levels reduction by clioquinol was found to be coordinated in a metal-dependent mechanism (Tardiff et al., 2017). Clioquinol drug treatment (at 160 µM) in yeast causes inhibition of yeast growth of which could be partially relieved by supplementation of copper or iron (Li et al., 2010). This inhibition by clioquinol treatment was later reported to be caused by upregulation of TDH3 expression that arrest the cell cycle at G2/M phase. Since Caf20 could also influence cell cycle (Castelli et al., 2015), it was speculated that clioquinol could potentially have effect on cells with altered Caf20 activity.

To test the sensitivity of cells to clioquinol treatment, clioquinol treated drug discs of varying concentrations were placed on agar plates containing lawns of Caf20wt, Caf20m^2 mutant and the *caf20Δ* strains and the zone of inhibition around the drug was determined on ImageJ software as described in the methods section 2.2.5.1. The results revealed that clioquinol inhibited yeast growth (**Fig 5.5A**). The zone of growth inhibition caused by the drug increases progressively with concentrations from 100 µg/ml up to 1 mg/ml where it saturates (**Fig 5.5A** and **B**). Caf20wt is more susceptible to the drug treatment than both the Caf20m2 and the *caf20Δ* strains (**Fig 5.5**). There was a significant difference ($p<0.05$) between Caf20wt and the other strains in terms of the area of the toxic zone (**Fig 5.5B**). The minimum inhibitory concentrations (MIC) for clioquinol in yeast falls below 0.05 mg/ml (<50 µg/ml) (**Fig 5.5A**).

In conclusion, Caf20wt is more sensitive to clioquinol treatment more than either Caf20m2 or caf20Δ, at 1 mg/ml concentration suggesting that an eIF4E-dependent mechanism is responsible.

A.

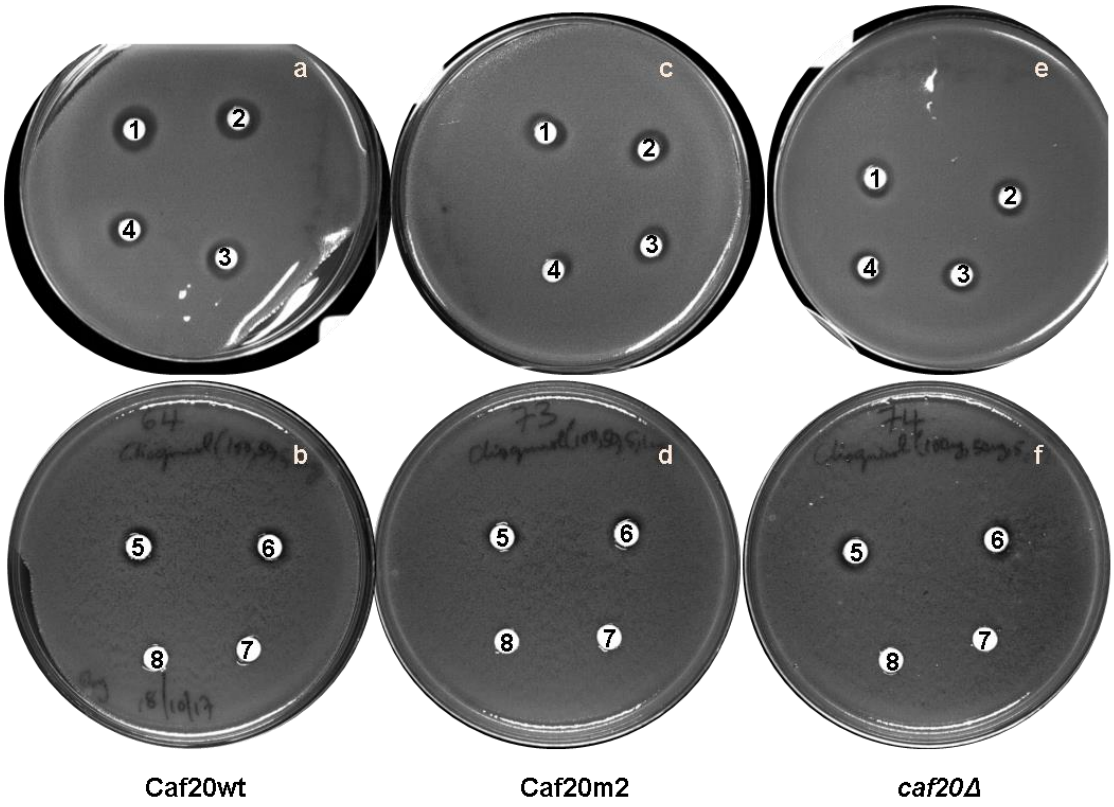

B.

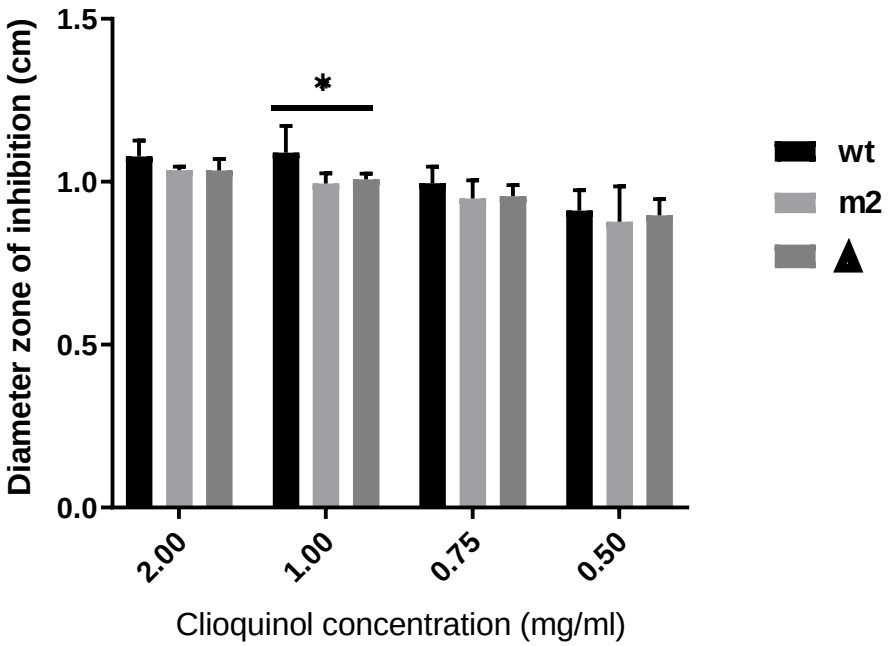

Figure 5.5. Caf20 mutants are less sensitive to Clioquinol treatment. A. Filter disc tests of Clioquinol were performed by adding 5 µl of clioquinol at different concentration as numbered **1**=2.0 mg/ml, **2**=1.0 mg/ml, **3**=0.75 mg/ml, **4**=0.5 mg/ml, **5**=0.1 mg/ml, **6**=0.05 mg/ml, **7**=0.005 mg/ml and **8**=0.001 mg/ml concentrations on approx. 0.65 cm filter discs on lawn of each strain as described in section 2.2.5.1. **B.** Quantification of zone of inhibition in the three strains (Caf20wt, Caf20m2 and caf20Δ) from clioquinol treatment. Diameter of inhibition was calculated with ImageJ software and it was plotted against the drug concentration. There was a statistical difference at 2-tailed T-test

between wt vs m2 and wt vs Δ and no statistical difference between m2 and Δ at $p<0.05$ at 1 mg/ml clioquinol concentrations. N=3 reps

5.3.4 $CuSO_4$ toxicity is coordinated in Caf20-eIF4E dependent manner

As described in section 5.3.3, it was discovered that Caf20 mutants are less sensitive to a metal chelator, clioquinol that Caf20wt cells. It was reasoned that it is important to explore further the relationship of Caf20 status to metal toxicity. Heavy metals are known to cause protein misfolding and protein aggregation in living cell which affects structural integrity and protein degradation (Tamas et al., 2014). Copper is one of the transition metals that is required in minute amounts and essential for cell growth. It is also a component of enzymes such as the superoxide dismutase, catalase, dopamine hydroxylase and an important component of the mitochondrial electron transport chain (Liang and Zhou, 2007). However, at high concentrations, it causes toxicity. In humans, high concentrations of copper has been linked to some neurodegenerative diseases such as Wilson's disease (Bandmann et al., 2015). In yeast, exposure to copper at 2-10 mM has been reported to cause toxicity and apoptosis (Liang and Zhou, 2007). Of which one of the possible ways copper causes apoptosis is by generating reactive oxygen species (ROS). ROS impair protein, lipids and nucleic acid synthesis which in turn inhibits growth and cause cell death (Vallieres and Avery, 2017). Copper affects protein synthesis in many ways; it is a primary target of an essential yeast protein, Rli1 (an iron-sulphur protein) important in many steps of mRNA translation. Rli1 is involved in ribosome recycling in release of 60S after termination, controls translation reinitiation at 3'UTRs and also for resolving stalled ribosomes during elongation as part of no-go decay and ribosome quality control (RQC) pathways (Alhebshi et al., 2012; Vallieres and Avery, 2017; Young et al., 2015).

To test the sensitivity of cells to copper treatment, a spot test was performed with Ca20wt, Caf20m2 mutant and *caf20Δ* strains in increasing concentrations of copper sulphate ($CuSO_4$). $CuSO_4$ concentrations of 2, 3, and 4 mM were mixed with growth media and poured on plates. 2 µl of each serial dilution of the strain were plated in spots and assessed as described in methods, section 2.2.5.2. The result of the spot test showed that Caf20wt cells were more inhibited by $CuSO_4$ compared to either Caf20m^2 mutant or *caf20Δ* at day 2 for 2 mM $CuSO_4$, day 3 at 3 mM $CuSO_4$ and day 4 at 4 mM $CuSO_4$ (**Fig 5.6**). As the concentration of $CuSO_4$ increases from 2-4 mM, the more toxic it is to cells and survival rates of the cells decreases.

In conclusion, the presence of Caf20 results in increased sensitivity to copper of which is coordinated in Caf20 – eIF4E dependent manner, which is consistent with the observed effects of clioquinol.

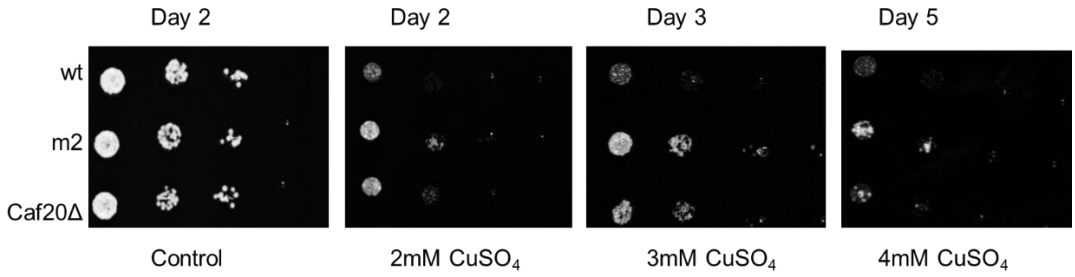

Figure 5.6. Caf20 mutants have reduced sensitivity to Copper. Phenotypic confirmation of sensitivity phenotypes of wt, m2 mutant and Caf20Δ using spot test after exposure to different concentrations copper sulphate. N = 3 reps

5.3.5 Cycloheximide treatment has no effect on Caf20.

Cycloheximide is an antibiotic that inhibits the translation elongation phase during protein synthesis. It binds the ribosome and prevents eEF2-mediated translocation (Poehlsgaard and Douthwaite, 2005). It is been reported that cycloheximide allows only one cycle of translocation before inhibiting subsequent elongation steps (Pestova and Hellen, 2003). Cycloheximide has been used in most ribosome studies, it can stabilize the ribosome without significant disrupting polysome profiles (Schneider-Poetsch et al., 2010). It freezes ribosomes onto the mRNA in the second codon and has been reported to have a binding pocket at the proximity of the E-site of the 60S ribosome associating within the vicinities of the C3993 base of the hairpin 88 of the 28S rRNA and the ribosomal proteins L28 and L41 in yeast (Schneider-Poetsch et al., 2010). So, cycloheximide prevents translation elongation by binding to the E-site together with the E-site tRNA leading to an arrest of the ribosome on the second or any subsequent codon and prevents its dissociation into component ribosomes.

To test the effects cycloheximide have on cells bearing altered Caf20 status, drug disc containing different concentrations of cycloheximide were placed on lawns of the three strains (Caf20wt, Caf20m2 and caf20Δ), as was performed with clioquinol and paromomycin above, and the diameter of zone of inhibition was calculated with ImageJ software. The result of the tests showed that cycloheximide greatly inhibited yeast growth (**Fig 5.7A**). The drug zone of inhibition increased proportionally with

increasing concentration (**Fig 5.7B**). All the strains responded equally to the treatment and there were no significant differences ($p<0.05$) among the three strains at each cycloheximide concentration (**Fig 5.7B**). The minimum inhibitory concentrations (MIC) for cycloheximide in yeast falls below 0.01 to 0.004 mg/ml (10-4 µg/ml) (**Fig 5.7A,** labelled 4 and 5).

In a separate experiment, the 0.1 OD strains were treated with different concentrations of cycloheximide and allowed to grow in the same SCD-L plus cycloheximide growth medium at 30℃ for 6 days to ensure that even the lowest concentration of cycloheximide exihibits its effect on the yeast cultures. After which 2 µl of each of the strain's neat culture were spotted on a SCD-L plate without cycloheximide to assess how quickly the strains overcome the drug inhibitory effects. Cycloheximide concentrations 10, 2, 1, 0.5 and 0.25 µg/ml were tested. Cultures of low cycloheximide concentrations grew however cultures at higher concentrations appeared not have grown. It was found that none of the strains survived the treatment at 10 µg/ml (**Fig 5.8,** spots lane 2). However at 2 µg/ml cycloheximide treatment, Caf20wt recovered the quickest after 2 days, followed by Caf20m2 and then caf20 which was greatly inhibited by the drug (spots lane 3) when compared to the control in lane 1. At other lower concentrations, there was no clear difference among the strains tested. In conclusion, **Figs 5.7** and **5.8** suggested that cycloheximide sensitivity is not altered by Caf20 mutants, but the presence of Caf20 may enable cells to more quickly recover from the inhibitory effects of cycloheximide once it is removed.

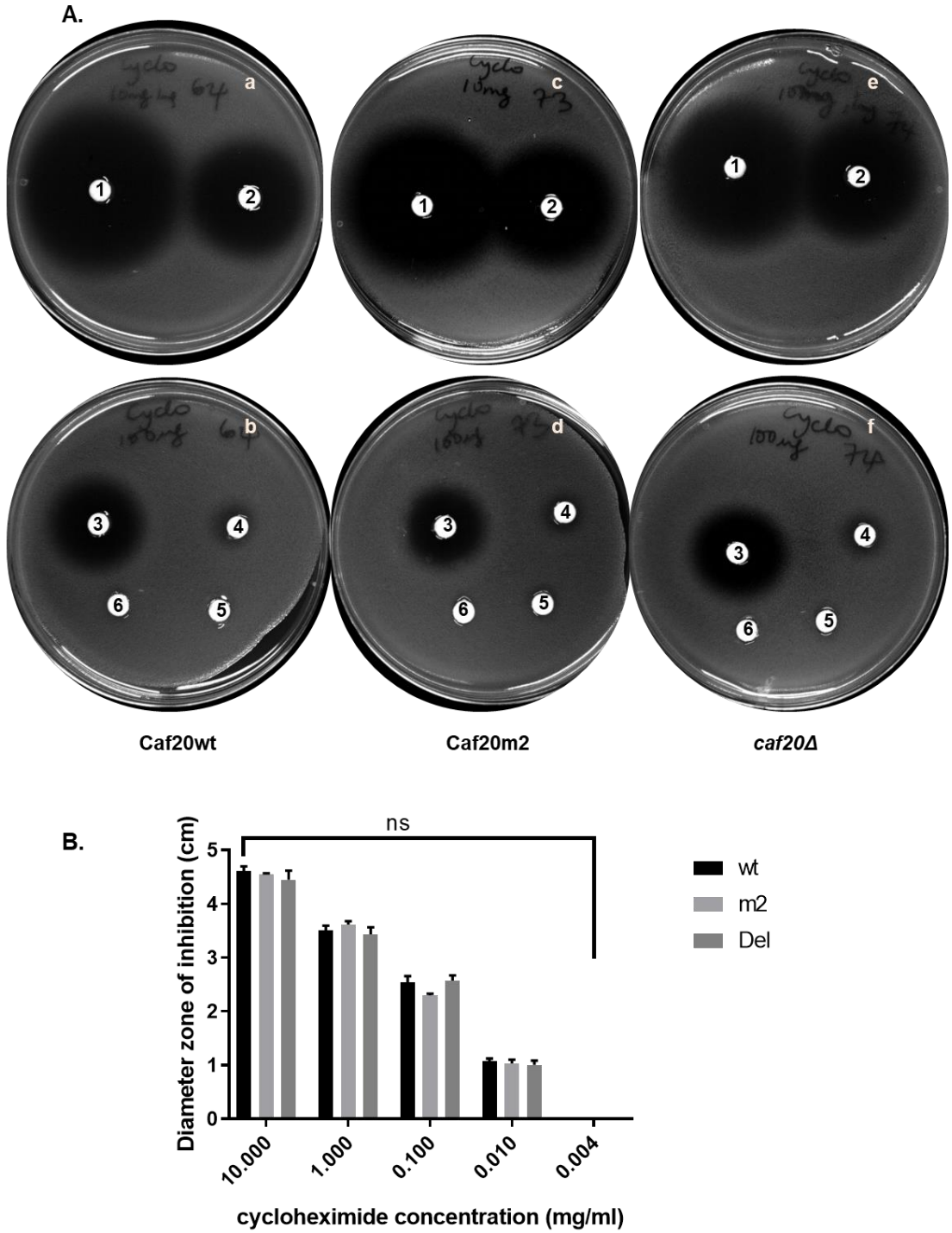

Figure 5.7. Inhibitory effects of Cycloheximide. **A.** Filter disc tests of cycloheximide were performed by adding 5 µl of cycloheximide at different concentration as numbered **1**=10.0 mg/ml, **2**=1.0 mg/ml, **3**=0.1 mg/ml, **4**=0.01 mg/ml, **5**=0.004 mg/ml and **6**=0.002 mg/ml concentrations on approx. 0.65 cm filter discs on lawn of each strain as described in section 2.2.5.1. **B.** Quantification of zone of inhibition in the three strains (Caf20wt, Caf20m2 and caf20Δ) from cycloheximide treatment. The diameter zone of inhibition was estimated on ImageJ software and it was plotted against the drug concentration. There was no statistical difference ($p<0.05$) among the strains to cycloheximide treatment determined by one way ANOVA. N = 3 reps

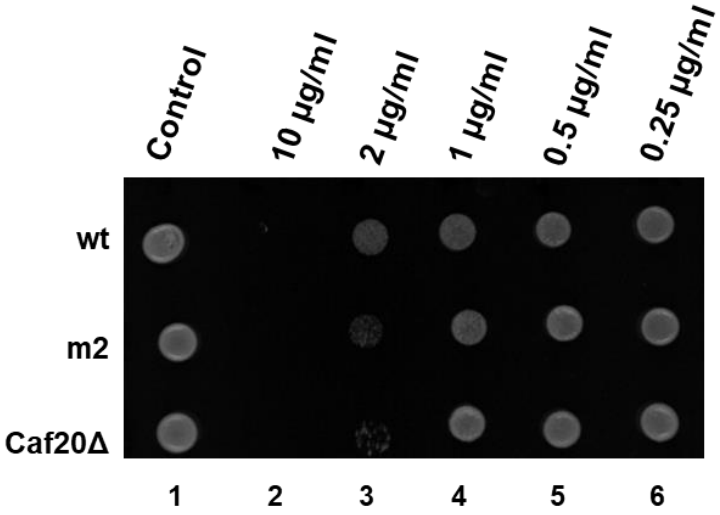

Figure 5.8. Recovery effects to cycloheximide treatment. Strains were grown in liquid media plus cycloheximide of concentrations 10, 2, 1, 0.5 and 0.25 µg/ml for 6 days at 30℃. 2 µl of each strain was spotted on minimal media, SD + His +lys + Ura plate and grown for 2 days at 30℃. Caf20wt recovered quickest, followed by caf20m2 then *caf20*Δ. Note: spots lane **1** is for strains grown without any cycloheximide, spots lanes **2-6** are for strains treated with cycloheximide at 10, 2, 1, 0.5 and 0.25 µg/ml respectively. N=3 reps

Taken all together, Table 5.4 compare the inhibitory effects of the tested drugs to the growth rates to Caf20wt, Caf20m^2 and *caf20Δ*. Caf20wt showed a remarkable difference in general to the other two strains, differing in sensitivity to paromomycin, clioquinol and recovery to cycloheximide treatment. Caf20m2 showed difference to the caf20 only in the recovery effects to cycloheximide treatment. In conclusion, Caf20 control mechanisms in the yeast is directed towards copper utilisation, clioquinol metabolism, in control of defective protein synthesis by paromomycin and in recovery from cycloheximide stress; it's not a target of the TOR pathway and cycloheximide activities. .

Table 5.4. Effects of different drugs on Caf20 growth rates in spots

Drug	Concentration	wt	m^2	*caf20Δ*
$CuSO_4$	2mM – 4mM	**>1***	**>2**	**>2**
Cycloheximide recovery	Treated before plating- 10, 2, 1, 0.5, 0.25 µg/ml	>2*	>1*	>1
Paromomycin	50 mg/ml	>2*	>1	>1
Rapamycin	5, 50, 100, 200, 1000 nM	>1	ND	>1

>3 = normal growth, >2 = sensitive >1 = highly sensitive 0 = No growth. * = phenotypic difference among the strains

5.4 Genetic interaction between Caf20 and MS-identified ribosomal proteins synergy response to heat stress

In Chapter 4 results of MS experiments are described that indicated that Caf20 interacts with the ribosome and can be cross-linked to specific ribosomal proteins. The chief RP targets were Rps27, Rps24, Rps5, Rpl10, Rpl27 and Rpl30. As was mentioned in the last part of Chapter 4, attempts to cross-validate these MS results using tap-tagged subunits were hindered by non-specific interactions between the tag-'specific' antibodies and the lack of availability specific antibodies to the identified yeast ribosomal proteins from literature searches. A genetic approach was taken to study the interactions between Caf20 and some of the identified ribosomal proteins. It has been reported previously of the temperature-sensitivity negative relationship between Caf20 overexpression from a galactose promoter and some mutants affecting translation initiation factors, eIF4B, eIF4E or eIF4G1 (de la Cruz et al., 1997). It was again shown in **Fig 5.2** that *caf20*Δ is temperature-sensitive in respiratory media. Also coupled to the fact that some of the MS-identified targets of Caf20 are proteins chaperones expressed as a result of heat shock, a heat test was recommended to study the genetic interaction between Caf20 and some selected ribosomal proteins which would elucidate more function for Caf20. This section discusses experiments performed in deleting Caf20 from the TAP tagged strains; in creation of different isogenic Caf20 and Caf20 mutants and in assessing Caf20 and tap-tagged subunits synergetic responses to heat stresses.

5.4.1 Deletion and Creation of isogenic *CAF20* in the TAP tagged strains.

To create a series of strains carrying a specific ribosomal TAP tagged subunit and with deletion of *CAF20*, PCR-based gene deletion was performed to delete the entire coding region of *CAF20* and replace it with the standard KanMX disruption cassette as described in section 2.3.3. Although the *CAF20* gene was difficult to delete in these TAP-tagged strains, after series of method optimisations, *CAF20* was successfully deleted and replaced with the G418 resistance cassette in three separate RP-TAP strains (Rps27A, Rps27B and Rpl27A). All strains grew cell on YPD medium. Western blotting of the transformed strains in **Fig 5.9** showed successful deletion of *CAF20* in some candidate clones of each of the 3 TAP strains. After confirming the deletion, the strains were transformed with either Caf20 (*pCaf20-FLAG*) (*p*AV2421, Table 2.1) or with *LEU2* empty plasmid (pAV1302, Table 2.1). The western blot for the isogenic Caf20 strain and the empty plasmid transformed strains is shown in **Fig 5.10**. In conclusion, the results

suggested stable transformation of the strains creating isogenic *caf20*Δ and Caf20wt in the RP-TAP variants.

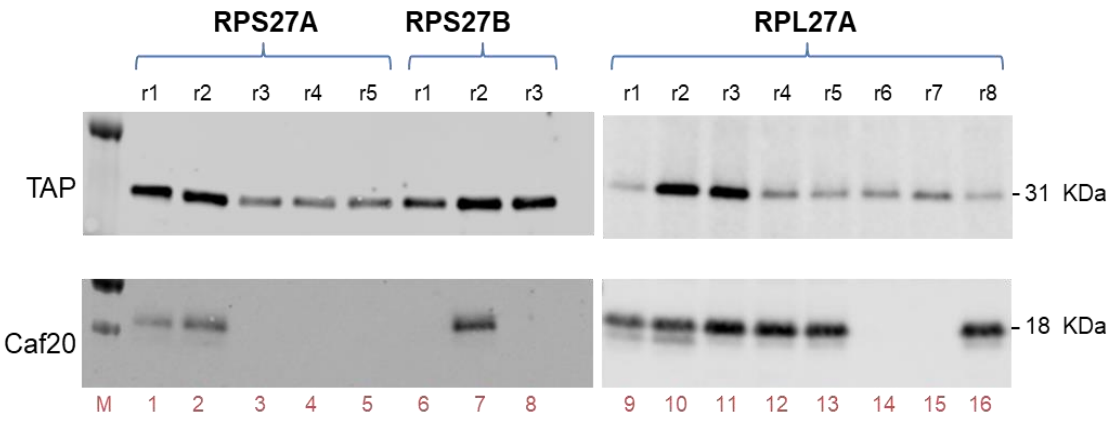

Figure 5.9 Caf20 is knocked out in the TAP strains. Western blotting of total extract of transformed strain of G418 genomic Caf20 deletion. The blots were probed with Caf20 (lower panel) and Protein A (TAP) in the upper panel. The yeast strains in lanes 4, 6 and 14 were assigned GP strain collection numbers GP7838-40 (**Table 2.2**). n = 1 rep

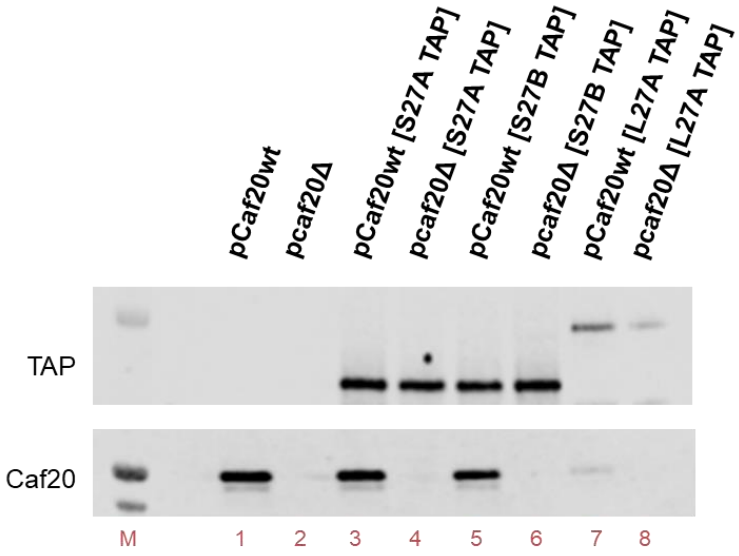

Figure 5.10. Caf20 isogenic strains created in ribosomal TAP –tag protein strains. Western blotting of total extracts of Caf20 knock out of ribosomal proteins TAP tagged strains revealed successful pCaf20-FLAG (pAV2441, Table2.1) and empty LEU2 plasmid (pAV1302) transformations. The yeast strains were assigned GP strain collection numbers GP7841-46 (**Table 2.2**). n=1 rep

5.4.2 Disruption of Caf20 confers temperature sensitivity to Rps27B-TAP and Rpl27A-TAP strains.

The RP-TAP/caf20 strains were screened for genetic synergic effects. The transformed strains were grown to exponential phase and spot tests of the transformed strains were

performed over a range of growth temperatures (16°C, 25°C, 30°C, 33°C, 37°C and 38°C) as described in Methods section **2.2.5.2.**

When the strains were grown in spots at lower, moderate and high temperatures up to 37°C, the results of the heat test showed that most of the strains both the untagged ribosomal proteins, control strains (pCaf20wt and *pcaf20Δ*) and the ribosomal protein-TAP tagged strains had a normal growth rate. The exception was Rpl27A-TAP which had reduced growth when combined only with *caf20Δ* (red box of the spot test plates at 30°C (**Fig 5.11A**).

Out of curiosity, the temperature was raised to 38°C. There was a mild general reduction in the rate of growth of all strains, as expected. Disruption of Caf20 in the both Rpl27A and Rps27B-TAP strains resulted in temperature sensitivity (Rps27B shown in green box, **Fig 5.11B**). Other strains behaved similarly as was observed at lower temperatures. As Caf20wt suppressed the slow-growth, it suggests a genetic interaction between these TAP-tagged forms of Rps27B and Rpl27A and Caf20. This suggests that the TAP-tag is having a modest negative impact on ribosome function that is exacerbated by loss of Caf20. Hence Caf20 is apparently having a positive role in promoting ribosome function.

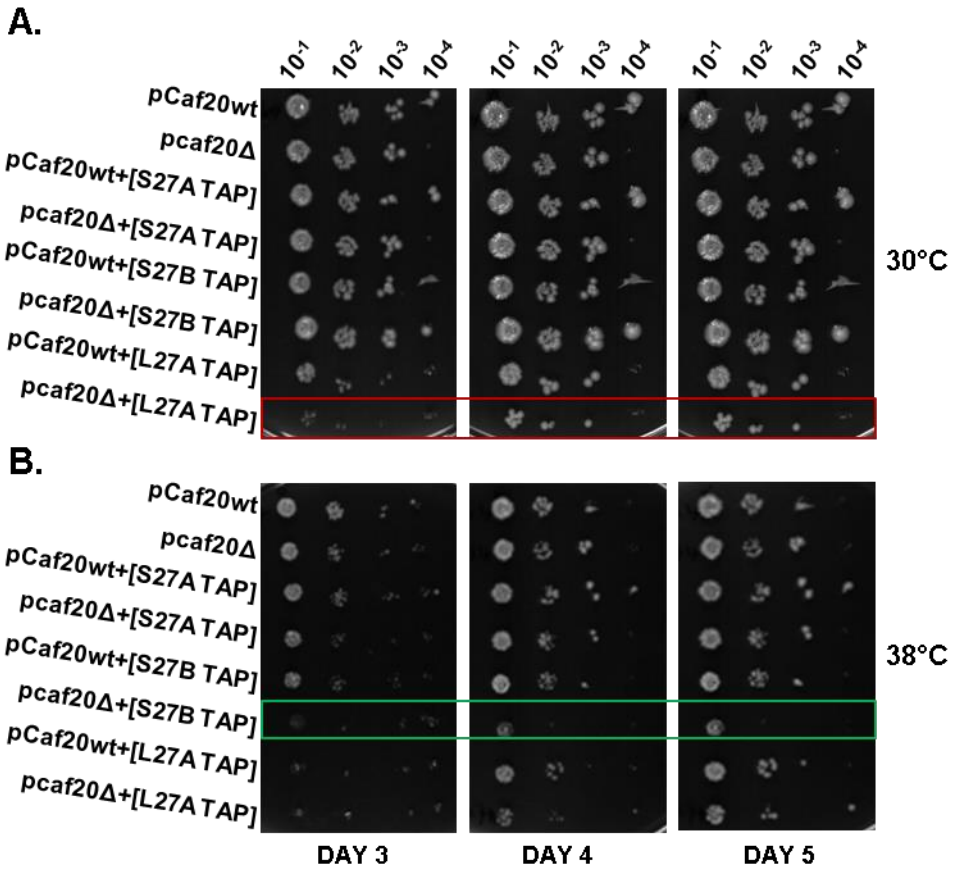

Figure 5.11. Deletion of Caf20 exhibit synthetic semilethality in Rps27B-TAP at 38°C. Strains were grown in SCD-L medium to exponential phase and they were diluted to 0.1 O.D. 2 µl of tenfold dilutions of each strain were spotted on dropout media (SCD-L) plates. **A.** The plate was incubated at 30℃ for a couple of days. All strains had normal growth rate except Rpl27A-TAP, [L27A TAP], strains with the *caf20Δ* strain of Rpl27A-TAP having the least growth (shown in red box). **B.** The plate was incubated at 38℃ for 5 days and images taken. At 38°C, disruption of Caf20 in the Rps27B started to show some synthetic impairment than was observed in the other strains. N=3 reps

5.4.3. Genetic interactions between mutant forms of Caf20 in Rps27B and Rpl27A.

Having identified some genetic interactions between Caf20 and the ribosomal proteins, Rps27B-TAP and Rpl27A-TAP, more genetic studies using different Caf20 mutants generated as described in chapter 3 was undertaken with the aim to establish what region of Caf20 contributes the growth phenotype. Caf20 mutant plasmids that disrupt eIF4E interaction (Caf20^{m2}, Caf20Δ1) as well as those that also impair ribosome binding (Caf20ΔA and Caf20ΔAC) were transformed into the *caf20*Δ TAP strains (Rps 27B and Rpl 27A). The expression of these constructs is shown in **Fig 5.12**. This indicated that each protein is expressed in proportion to what was reported previously (Chapter 3).

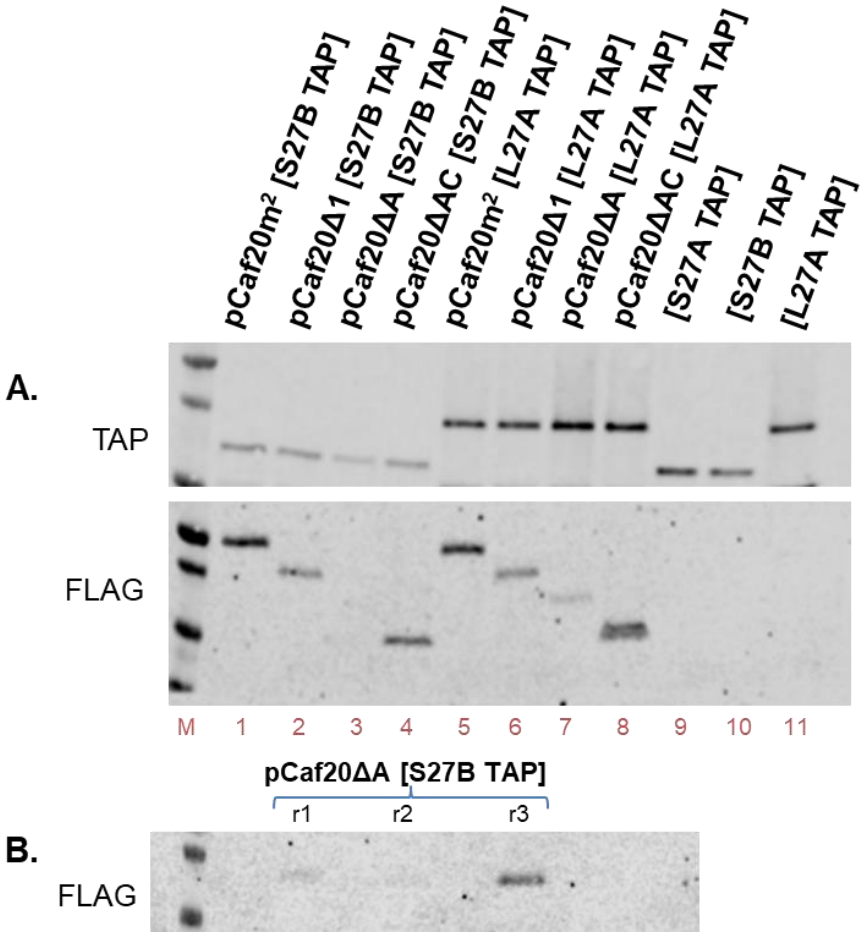

Figure 5.12 Creation of some Caf20 mutants in the Ribosomal TAP Proteins. Western blotting of total extracts of Caf20 knock out of ribosomal proteins TAP tagged strains revealed successful transformation of RPS27B- TAP and RPL27A-TAP with some Caf20 mutants. **A.** Western blot probed for TAP expression (top panel) and FLAG expression (lower panel). **B.** Repeat of western blotting of transformed ***pCaf20A [S27B]*** in triplicate as expression was not visible on the western blot in **A** above. Note: **pCaf20m^2** represents plasmid Caf20m^2-FLAG; **[S27B TAP]** is genomic TAP tagged RPS27B. **M** is the marker lane, Lanes 1-11 are for the total extract input lanes. The yeast strains were assigned GP strain collection numbers GP7847-52 and GP7859-60 (**Table 2.2**). N=1 rep

Spot tests of strains were carried out as described in section 5.4.2 above to determine region of Caf20 contributing to synthetic impairment between caf20 and the ribosomal proteins. The results obtained from the interactions between Caf20 mutants and Rpl27A-TAP suggested that the only Caf20 construct able to complement the growth phenotype at 30C was Caf20ΔA (**Fig 5.13A**). The other Caf20 mutants (Caf20m2, Caf20Δ1 and Caf20ΔAC) had no positive impact and may show some synthetic impairment to the growth rate when compared to either the wildtype Caf20 or the *caf20Δ* alleles. This could mean that both middle and the C-terminal domain or unmodified full length Caf20 is important in interacting with Rpl27A TAP.

On the other hand, in the Rps27B-TAP strain none of the Caf20 mutants suppressed in the growth rate of Rps27B-TAP at 38°C (Fig 5.13B), in addition all mutants were slower growing at 30°C (**Fig 5.13B**). This result suggests that full length Caf20 and hence likely its interaction with eIF4E is important for the genetic interaction with the Rps27B-TAP strain.

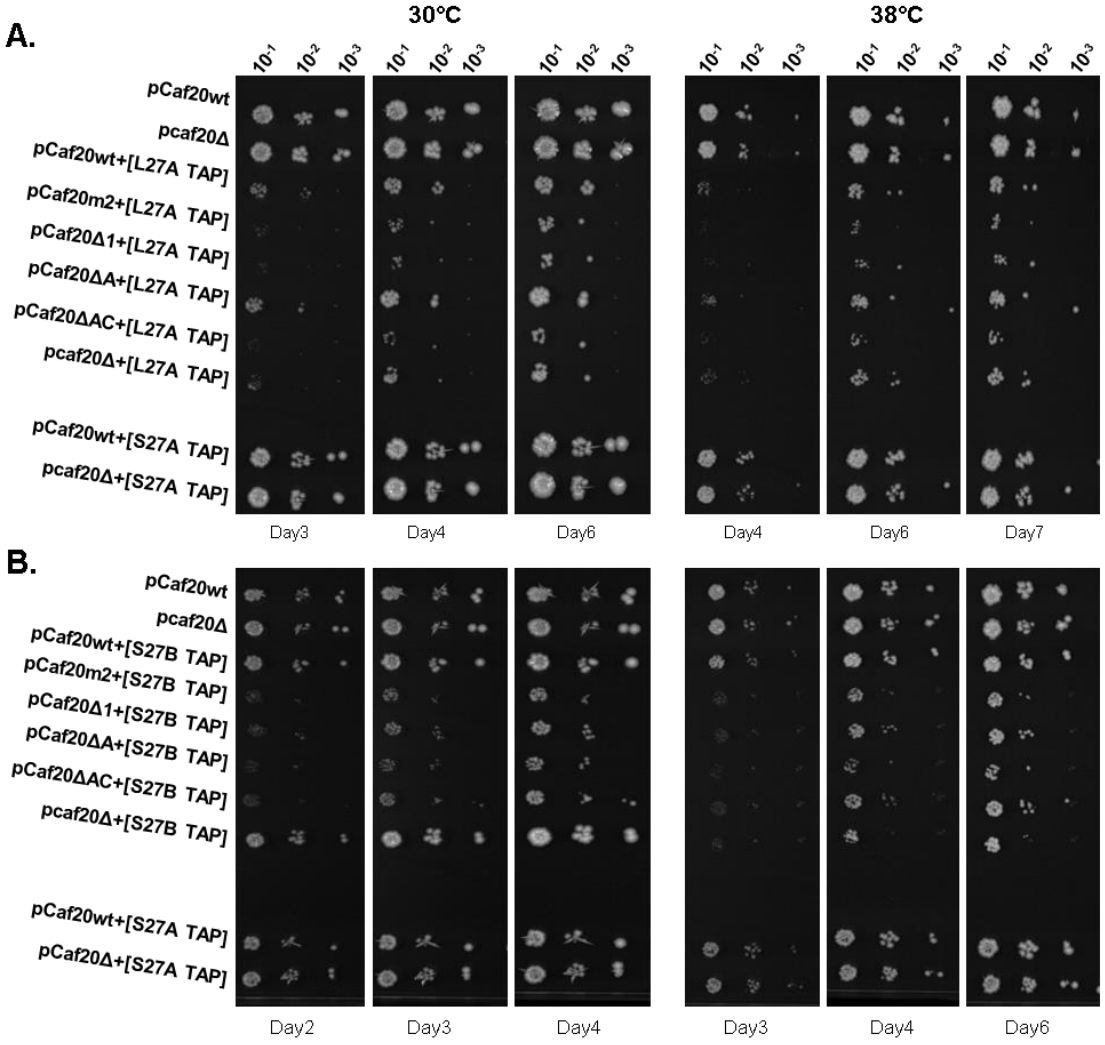

Figure 5.13. Defining regions of Caf20 that complement synthetic impairment between *caf20Δ* and ribosomal proteins Rps27B-TAP and Rpl27A-TAP. Mutant and control strains were grown in SCD-L medium to exponential phase and then diluted to 0.1 O.D. 2 µl of tenfold dilutions of each strain were spotted on dropout media (SCD-L) plates. **A.** The spot plates showing Caf20 mutants transformed into Rps27B –TAP, incubated at 30°C and 38°C for up to 7 days. **B.** The spot plates showing Caf20 mutants transformed into Rpl27A –TAP, incubated at 30°C and 38℃ for up to 4-6 days. N = 3 reps

5.5 Discussion

This chapter describes studies undertaken to define a phenotype associated with loss of Caf20 that may help uncover the function of Caf20-ribosome interaction. Although previous studies in other laboratories have identified some synthetic phenotypes caused by deletion or overexpression of Caf20 (de la Cruz et al., 1997) these may be strain specific as those tested have not been found reproducible in our S288c (BY4741) strains used here (L. Castelli and G. Pavitt, unpublished observations). Hence here a range of different phenotypic characterisations performed for Caf20 comparing wt, caf20Δ and the eIF4E binding mutant m2. The main aim was to assess if any condition could distinguish between *caf20*Δ (no cCaf20) and the m2 mutant that retains ribosome binding, but eliminates eIF4E interaction.

Growth assays were performed for Caf20 in aerobic and anaerobic (respiratory) media. It was shown that there were no differences in the exponential growth phases between Caf20 and *caf20Δ* strains (Tables 5.1 and 5.2) in aerobic and anaerobic media when the strains were first acclimatised in the medium to stationary phase before performing doubling times experiment. However, when there is a switch from aerobic to anaerobic medium as shown in the SCGE spot tests, it results in a delay of growth in Caf20 high copy (wt) isogenic strain which was more pronounced when grown at low temperature of 16°C (Fig 5.2). This could be accounted to a prolonged lag phase to overcome the effects of lack of glucose in Caf20wt strain which was absent with Caf20^{m2} and *caf20*Δ strains. Hence signalling a cold-sensitivity and negative regulatory role of Caf20 to growth in respiratory media. A similar finding has been reported in which deletion of Caf20 was shown to alleviate slow-growth and cold-sensitivity phenotypes caused by mutations in translation initiation factors such as eIF4B, eIF4E or eIF4G1 while overexpression had the opposite effect of enhancing those phenotypes (de la Cruz et al., 1997). As the effect observed was eIF4E-dependent it was not evaluated further.

Caf20wt showed no difference in growth to the *caf20*Δ strain upon rapamycin treatment (**Fig 5.3**) confirming previous report that Caf20 is not a target of Rapamycin (Cosentino et al., 2000). All strains tested were found to be resistant to paromomycin due to the selective KanMX cassette used for *caf20*Δ marker on the plasmid, hence this analysis was not informative (**Fig 5.4B**).

Treatment with clioquinol (a metal chelator of copper, zinc and iron) which had found a revived interest for its use to kill cancer cells (Ding et al., 2005) and in treatment of rare genetic diseases (Cherny et al., 2001; Kaur et al., 2003; Nguyen et al., 2005; Tardiff et al., 2017) found that Caf20wt is more sensitive to clioquinol than either mutant (**Fig 5.5**), a new function to explore for future studies. Likewise, Caf20wt had increased sensitivity to excess $CuS0_4$ (**Fig 5.6**) showing that Caf20 is a target in metal utilisation in yeast of which is coordinated in Caf20-eIF4E dependent manner as the Caf20m2 and *caf20Δ* strains were both more resistant than wt to both treatments. It was also reported that Caf20wt appears to increase cell survival by promoting quicker cell recovery after relief from cycloheximide treatment compared to the *caf20Δ* strain (**Fig 5.8**).

Finally, to examine Caf20-ribosome interactions more directly *CAF20* was deleted in three RP-TAP strains and found to have synthetic growth defects when two strains (Rpl27-TAP and Rps27B-TAP) were grown at different temperatures (**Fig 5.11**). These effects could only be complemented by full length Caf20wt (**Fig 5.13)** indicating again that they are most likely dependent on the eIF4E-Caf20 interaction. It is not clear why a phenotype was observed in the Rps27B-TAP strain and not the Rps27A-TAP strain. Both genes encode Rps27. Paxdb suggests they are approximately equally expressed and western blotting here shows that the TAP-tagged strains are also equally well expressed (Figs. 5.10 and 5.12). Rps27 is 82 residues long and only one position differs between the isoforms, position 62, is isoleucine in Rps27A and valine in Rps27B. It is not known if this conservative change has any impact on ribosome functions.

In conclusion while several mild phenotypes have been identified here and in previous studies e.g. (de la Cruz et al., 1997), all appear to be largely explained by the eIF4E-Caf20 interaction rather than specific for the novel Caf20-ribosome interaction.

Chapter 6

General discussion, conclusion and future work

6.1 Discussion

eIF4E is an important factor for protein synthesis that is controlled to regulate translation initiation. One group of binding proteins, 4E-BPs, associate with eIF4E to regulate its interaction with eIF4G to prevent recruitment of the ribosome. Caf20 is one out of the two known 4E-BPs in yeast which has gained some global interest to study its function.

6.1.1 What was known?

Before the beginning of this research work, it was initially thought that Caf20 was a binding partner of eIF4E when the protein was discovered in yeast, competing with eIF4G to interact with the eIF4E through a canonical motif YXXXXLΦ (Altmann et al., 1989a; Altmann et al., 1997; Lanker et al., 1992). The role of Caf20 was later broadened with the identification of a class of mRNA on polysomes that were altered by *caf20Δ* (Cridge et al., 2010). Using RNA-immunoprecipitation and RNA-sequencing, it was revealed that Caf20 act on specific mRNAs (Castelli et al., 2015). The characteristics of Caf20 regulated mRNA transcript as well as other components of the closed loop complex was reported in which it was shown that Caf20 and another 4E-BP in yeast, Eap1 (Cosentino et al., 2000), showed some overlaps in their mRNA targets and specificity when compared to the other proteins of the closed loop complex (Costello et al., 2015). Their enriched mRNA targets are characterised to having low polyA tail length, low ribosome occupancy and tightly regulated protein products that are dependent on the eIF4F complex and eIF4E repressors (Costello et al., 2015).

Proteins and RNA-binding partners of Caf20 were later identified through TAP and FLAG immunoprecipitations and Mass spectrometry (Castelli et al., 2015). It was revealed from the work that Caf20 interact with two groups of mRNAs which could be distinguished as either eIF4E-dependent or eIF4E-independent; and that Caf20 can associated with translating ribosome which signals translation activation mechanism which is novel as Caf20 was viewed as a repressor protein. Comparison of their structural features indicated that the 4E-Independent mRNAs have longer poly-A tail and half-life, shorter ORFs. There was evidence for a shared AUAUAUAU repeating motif in 3'UTRs. Screening the importance of the 3'UTR in one mRNA *ERS1* showed that it could confer 4E-independent and Caf20-dependent repression to a luciferase reporter gene *in vivo*. However, the mechanism of Caf20 interaction with the ribosome was not known, neither was it clear if Caf20-ribosome interactions is a repression or an activation function.

The 3D structure of Caf20 was unknown and was believed to be unstructured. However, structures from metazoan 4E-BPs (Thor, 4E-T and 4E-BP1) showed that they possess three structural elements common on all metazoan 4E-BPs: an N-terminal α helix formed by the conserved (canonical) motifs which bind to the dorsal surface of the eIF4E; an elbow loop in between that bends the peptide backbone downwards by 90˚ to the lateral surface of the eIF4E and the third structure is a C-terminal (non-canonical) loop formed by the non-canonical motifs. In relation to their competition with eIF4G, 4E-BPs show bipartite binding to the eIF4E. eIF4G and all 4E-BPS can bind to the dorsal surface of eIF4E, while only 4E-BPs also bind to the lateral surface of the eIF4E (Igreja *et al.*, 2014; Peter *et al.*, 2015).

6.1.2 Major research findings from this work

This study focussed on assessing Caf20 interactions with eIF4E and the ribosome; and identifying novel protein-binding partners of Caf20 on the ribosome as a way of contributing to the understanding on translational control in yeast. The major findings from this work so far that has added to the knowledge of Caf20 is summarized in chapters. In Chapter 3, it identified features of Caf20 that are critical for interacting with eIF4E and the ribosome; and structures in Caf20 required to bind itself. Using SDM and other *in vivo* analysis, it was revealed that (i) Caf20 requires a short motif to interact with eIF4E (ii) Caf20 is tightly bound to eIF4E which is difficult to pull apart (iii) Caf20 interaction with the ribosome require multiple elements driven more by an extended region of the N-terminal domain (iv) Caf20 interacts with its binding partners as a monomer rather than a homodimer or other higher order complex. In Chapter 4, it described a crosslinking technique used to determine where on the ribosome Caf20 binds to by identifying Caf20 interacting partners on the ribosome through protein-protein interactions, it was shown that (i) Crosslinking identified proteins from 40S and 60S ribosomes (ii) the crosslinked proteins appear to locate around the interface of the 40S and 60S subunits (iii) it is possible that cysteine in Caf20 could mediate the crosslinking to ribosomal proteins. Results from Chapter 5 that studied the different phenotypic characterisations for Caf20 indicated that (i) Caf20 does not affect growth under normal conditions so far the strain is maintained in either aerobic or anaerobic (respiratory) media (ii) Caf20 can affect growth when there is an immediate switch from glucose to respiratory medium especially at low temperatures of 16°C (iii) Caf20 is not a target of the TOR pathway (iv) Caf20 increases sensitivity to clioquinol drug and excess CuSO4 treatments (v) *CAF20* deletion in three RP-TAP strains was found to have synthetic growth defects when two strains

(Rpl27-TAP and Rps27B-TAP) were grown at different temperatures (vi) mild phenotypes identified in this study all appear to be largely explained by the eIF4E-Caf20 interaction rather than specific for the novel Caf20-ribosome interaction. A simple model is proposed from this study to summarize what was known before, what was found in this study and what is yet to be known (Fig 6.1).

6.1.3 Other Caf20 reports published during the course of this research work

Five papers were published specifically addressing Caf20 since this research work began. The first paper discovered Caf20 as well as Rcn2 and Gga1 proteins as new targets of the cell wall integrity MAPK Slt2 using a quantitative stable isotope labelling of amino acids in cell culture approach. They reported that Slt2 targets Caf20 by phosphorylating it on Thr-102, a putative MAPK-phosphorylation site, though they did not show if the phosphorylation affects Caf20 function (Alonso-Rodriguez et al., 2016). The second paper showed that Caf20 is critical for Ste12 expression and p-body formation. P-bodies are cytoplasmic foci that contain translationally silenced mRNAs together with some decay factors and translation inhibitors (Balagopal and Parker, 2009; Eulalio et al., 2007). In yeast, p-bodies are usually formed under extreme stressful conditions. DEAD-box helicase, Dhh1 and other decapping factors, Dcp1/2 and activators of decapping Lsm1-7, Pat1,Stm1 and 5' – 3' exoribonucleases, Xrn1 are recruited into the p-bodies where repressed mRNAs are deadenylated, decapped through removal of the 5' M^7G cap at the 5'end, and the mRNA degraded by the 5' – 3' exoribonucleases (Balagopal and Parker, 2009; Coller and Parker, 2005; Dunckley and Parker, 1999; Eulalio et al., 2007; Sheth and Parker, 2003). The actual function of p-bodies is not fully understood by it is believe to help to compensate for the limited translation initiation complex available by translating important mRNA under extreme stressful conditions (Balagopal and Parker, 2009). Park et al. (2018) reported that disruption of eIF4E-Caf20 binding reduces p-body accumulation and *caf20Δ* greatly reduces Ste12 expression and the number of p-bodies formed but there was no indication of what loss of p-bodies do to the cell or mechanism that cause loss of p-bodies.

The third paper (Gay et al., 2018) relevant to this work discussed a mediator complex 2 protein, Mad2, known to be involved in spindle checkpoint during mitotic cell cycle and a physical interactor of Caf20 (Castelli et al., 2015). Mad2 was reported to enhance cell survival to stress response and improve cyclin (Clb5) protein translation. Mad2 was found to co-sediment with polysomes and to modulate the association of the

4E-BP, Caf20 by reducing association of Caf20 with the translation machinery while increasing Caf20 association with eIF4E (Gay et al., 2018). This seems important to this work as it suggests that it is possible to alter how much Caf20 is bound to ribosomes vs eIF4E through the Mad2. The last two papers very relevant to my work reported the properties of the ternary complex formed by eIF4E, Caf20 and mRNA (Arndt et al., 2018) and report structures of the yeast 4E-BPs, Caf20 and Eap1 bound to eIF4E (Gruner et al., 2018).

6.1.3.1 Caf20 relationship with eIF4E/mRNA and ribosome.

Arndt et al. (2018) reported that (i) Caf20 binds directly to mRNA via central RRR and HHH motifs (residues 55-57 and 60-62) (ii) Caf20/eIF4E complexes with mRNAs are more stable compared to eIF4E-mRNA alone eIF4E binding to Caf20 forms a stable ternary complex with capped mRNAs in which the eIF4E binds the cap and the Caf20 both bind to the mRNA (iii) *caf20Δ* in a pseudohyphal forming strain results in temperature sensitivity at 37°C but not at 30°C which was rescued only when a genomic Caf20 was integrated back into the strain. (iv) They proposed that Caf20/eIF4E complexes perform two roles – one inhibiting the translation of uncapped mRNA and another promoting capped mRNA translation.

Arndt and colleagues showed that the presence of Caf20 prevents otherwise slow growth in the pseudohyphal strain sigma strain, Σ1278b. This enhancement of growth was interpreted as suggesting that Caf20 can enhance rather than repress translation (Arndt et al., 2018). A similar synthetic growth defect was uncovered in this current study where genetic interaction between Caf20 and ribosomal proteins, Rps27B-TAP and Rpl27A-TAP was observed (Figs 5.11 and 5.13). Arndt argued that the loss of Caf20 and mutant phenotype could be part of a physiological response where in wt cells Caf20 binding to eIF4E normally helps to prevent the translation of uncapped mRNAs during mRNA degradation. Consequently in the absence of Caf20 this model suggests that aberrant translation causes the temperature sensitive phenotype.

The eIF4E/Caf20/mRNA ternary complex is so stable that it cannot be displaced by eIF4E/eIF4G or eIF4E/eIF4A complexes (Arndt et al., 2018). This same observation was found in this present study in which at 1M KCl salt, a strong interaction between eIF4E and Caf20 is maintained. The interaction is so stable that it will require a high force to disrupt the association. It is proposed that treating simultaneously with high salt and

detergent may force separation and some evidence to support this was found during experiments to identify Caf20 cross-linking proteins (Figure not shown).

Caf20 can likely interact with the eIF4E and mRNA probably via distinct protein sequence elements. It is shown in this current study that the ribosome interaction motif is overlapping with eIF4E motif but not the mRNA RRR and HHH motifs as suggested by Arndt et al. (2018). However Caf20 is highly charged throughout. 30/161 or 18.6 % of its residues are acidic D/E and 33 (20.5 %) are K/R/H basic residues. This is likely one reason why there complete disruption of Caf20 from the ribosome was not possible. Arndt et al. (2018) reported Caf20 interaction with the mRNA required RRR and HHH residues 55-57 and 60-62. They also reported that the region of Caf20 (similar to Caf20Δ1) inhibited translation of capped mRNAs but do not affect the interaction with mRNA. As 80S ribosomes have significant rRNA at their surfaces it remains feasible that Caf20 binds to the ribosome via a region that can also interact with mRNA. It could be suggested then that Caf20 interaction with the ribosome may be a form of inhibitory control to translation.

6.1.3.2 The structure of 4E BP, Caf20

The structures of fungal and yeast eIF4E in complex with eIF4G or 4E-BPs (Caf20 and Eap1) revealed a bipartite binding motif in the 4E-BPs comprising both canonical (YXXXXLΦ) and adjacent non-canonical elements that enable the high-affinity interaction of each 4E-BP with both the dorsal and lateral surfaces of eIF4E that are highly similar to metazoan homologs (Gruner et al., 2018). The eIF4E-binding regions on the Caf20 form two alpha helical structures, with the first helical structure falling within residues 6 and 12 of the canonical region (1-17), a connecting linker between residues 12 and 24, and the second helix (residues 24-41) of the non-canonical region (18-49). They showed that though Caf20 can bind to the lateral and dorsal surfaces of eIF4E, disruption of the lateral surface interaction does not affect its association with eIF4E. This was also obtained in this study that Caf20 require only a short canonical motif to interact with eIF4E as Caf20 mutant, Caf20Δ2 (Δ23-42) is synonymous with the deleted eIF4E lateral interacting surface. Here it was found that Caf20Δ2 associated with eIF4E as well as wt Caf20 (Fig 3.4B, lane 3). However we found that the region covered in Caf20Δ2 was important for binding to the 80S ribosome, making it likely that both non-canonical and canonical elements are both important for 80S ribosome binding.

6.1.4 What remains unknown?

A simple model is proposed from this study (**Fig 6.1**) to summarize what was known before, what was found in this study and what is yet to be known. In active translation condition, the eIF4E at the mRNA cap associates with eIF4G, a scaffolding protein, which in turn interact with other proteins including the poly A binding protein (PAB) to recruit the ribosome unto the mRNA and initiate translation. It is only when the mRNA is in this closed loop complex can it recruit the 40S ribosome to initiate translation (Fig 6.1A). However, when 4E-BP such as Caf20 displaces eIF4G through their shared eIF4E-binding site, the closed loop complex dissociates and translation is repressed (Fig 6.1A).

Caf20 has two known modes of regulating translation, through eIF4E-dependent and eIF4E-independent mechanisms (Castelli et al., 2015). As evident in this study, Caf20 associates with eIF4E and ribosomes. In carrying out its repressive role, it could bind directly on eIF4E to regulated its associated proteins (4E- dependent) or bind to the ribosome to regulate the association eIF4E and eIF4G in eIF4E-independent manner (evident with mutants, Caf20m2 and Caf20Δ1 that lost interaction with eIF4E but still associate with the ribosome). We have not yet addressed whether a single wt Caf20 molecule can bind to both the ribosome and eIF4E at the same time (Fig 6.1B). This study identified extended N-region of Caf20 as a major contributing factor to ribosome association.

The role of Caf20 interaction with the ribosome is not fully elucidated. Whether it is acting as a repressor or an activator or involved in another mechanism? Arndt et al. (2018) showed that Caf20 binding to eIF4E and capped mRNA stabilizes the ternary complex and facilitates the translation of the capped mRNA. The only evidence obtained from this present study that may indicate a translation activation role is the genetic interaction studies described in Chapter 5, which showed growth enhancement in the presence of Caf20. This could indicate that Caf20 association with some ribosomal proteins on the ribosome could be activating translation rather than repressing it.

What could be a role for Caf20 in translational activation? Caf20 could be associating with the ribosome to assist with the scanning process in the recognition of the initiator codon, AUG (Fig 6.1C). Caf20 could be binding with the eIF4E to create a stable capped mRNA until when the mRNA is ready to undergo translation initiation. In which case the 40S ribosome in complex with eIF4F or the eIF4F complex alone would displace

Caf20 from the eIF4E and the Caf20 then binds the ribosome for the initiator complex to scan for AUG codon and initiate translation. It is not clear if eIF4E and eIF4G remain associated with each other during scanning. A so-called ‘cap-severed’ model for scanning has been suggested (Shirokikh and Preiss, 2018) and is supported from experiments in which the eIF4F complex could be disrupted from the ribosome in high salt washes but never from cytosolic polysome-free fractions (Duncan et al., 1987; Hershey et al., 1979). If eIF4E and eIF4G interaction is broken during scanning, Caf20 could have a role in binding eIF4E following the release of eIF4G, to prevent a second incoming ribosome attaching until the current initiating ribosome has completed its action. Caf20 binding to the ribosome here would provide a convenient ‘holding point’ during this transition. As such is Caf20 stabilizing the eIF4E-mRNA in preparation for another round of translation initiation.

Alternatively Caf20 could have a more generic role, stabilizing ribosome mRNA interactions during multiple stages of translation by interacting with both mRNA and the ribosomes. Caf20 association with the ribosome and eIF4E could also act as a modifier of the mRNA decay processes (Fig 6.1D). mRNA in yeast is primarily decayed by polyA tail shortening and then 5’decapping and exonucleotytic decay. Caf20 has been shown to be involved in p-bodies recruitment (Blewett and Goldstrohm, 2012; Ibrahimo et al., 2006; Park et al., 2018) and interact with protein Dhh1 involved in mRNA deadenylation and decapping (Coller et al., 2001; Ka et al., 2008). What Caf20’s role here is, is currently not clear.

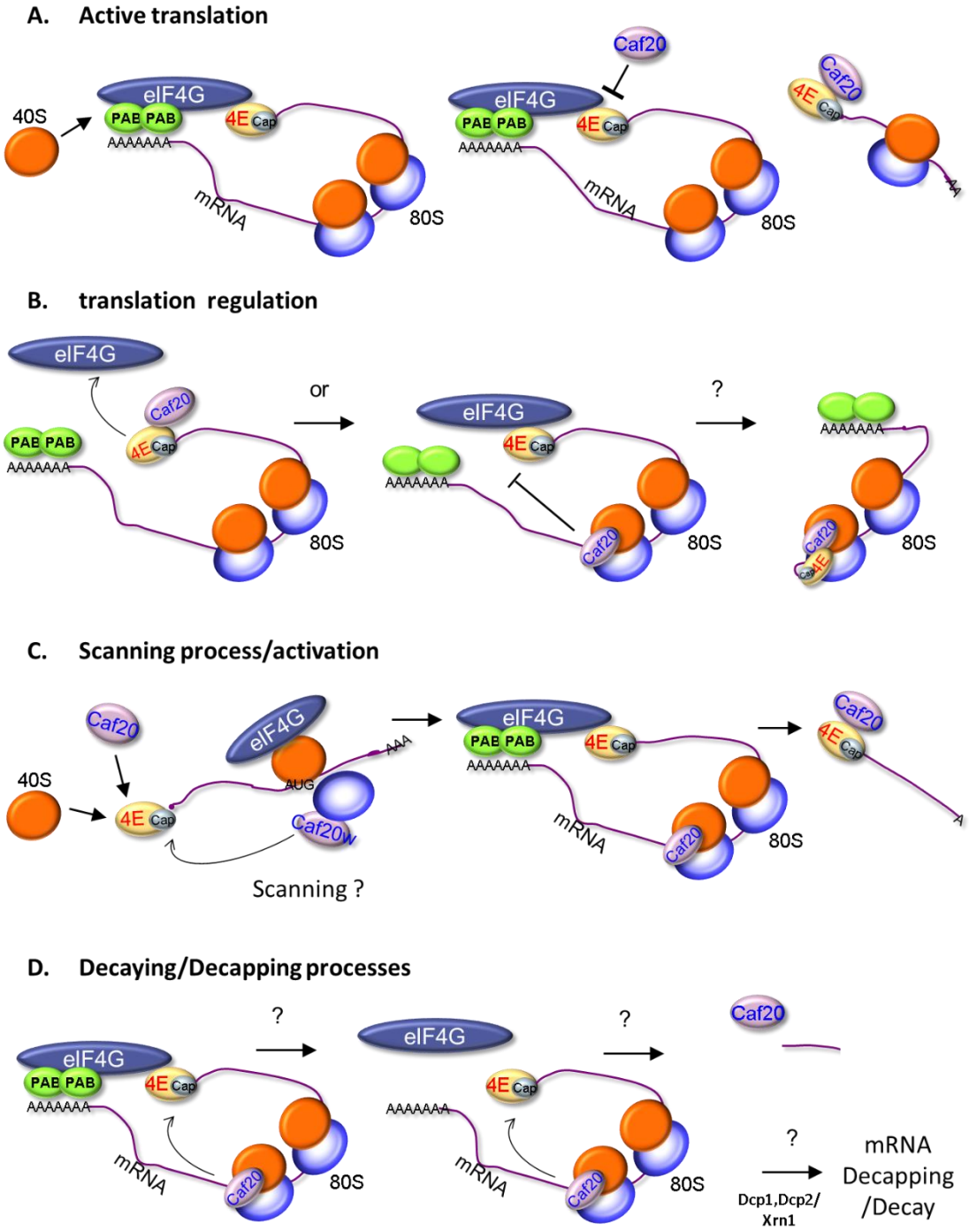

Figure 6.1. Models for Caf20 translation regulation. A. Active translation. mRNA is bound by eIF4E at 5'cap, eIF4G and poly A tail binding protein (PAB) to form a closed loop complex which enables ribosome recruitment. Caf20 comes in to displace eIF4G from eIF4E and disrupts the closed loop association. **B.** Modes of Caf20 translation regulation. It could be 4E-dependent translation control through interaction of Caf20 with eIF4E or eIF4E-independent control through binding to the ribosome or it may be Caf20 binding both the eIF4E and the ribosome at the same time. **C.** Caf20 may be regulate scanning process. Caf20 could bind with the eIF4e. 40S ribosome in complex with eIF4F or the eIF4F complex alone would displace Caf20 from the eIF4E and Caf20 binds the ribosome for the initiator complex to scan for AUG codon and initiate translation. Caf20 on the ribosome may bind to eIF4E and displace eIF4G to repress translation. D. Caf20 may be involved in mRNA decay or decapping processes by working with the decapping enzymes such Dcp1, Dcp2 and decay factors, Xrn1 or could impede decapping.

6.2 Future work

Due to time constraint, not all experiments/objectives were accomplished. Aspects of disrupting Caf20-eIF4E interactions has already been assessed by another PhD student in Pavitt's lab and to perform nucleotide competitive binding assays of eIF4G and Caf20 to eIF4E. Some experiments were not completed and as such were not be reported in this study. Caf20 interaction with RNAs using quantitative reverse transcription PCR has been initiated, so far reverse transcription primers has been designed and ordered. The RNA isolation protocol, first strand cDNA generation and real-Time PCR (qPCR) has been optimised in other to assess microarrays in steady state. This work will be completed and be reported some other time.

Future works would study Caf20-protein interactions on the ribosome using another technique, BioID proximity labelling, which uses a promiscuous biotin ligase enzyme (called birA*) to bind proteins closest to the protein to which it is tagged and to add biotin to available surface amine groups. The bound proteins could be isolated, purified via the strong avidin-biotin interaction and identified through mass spectrometry. Experiments to explore Caf20-interactions with elements in the 3'UTRs of mRNAs would also be undertaken. This is one of the properties for mRNAs under Caf20 eIF4E-independent regulation reported in previous publication (Castelli et al., 2015). By identifying specific elements important for Caf20-mediated control it will allow a clearer understanding of Caf20 functions and may identify elements that can be transferable to other mRNAs.

Finally by purifying the proteins involved in scanning (eIF4E, eIF4G, PAB) 40S and mRNA it may be possible to set up *in vtiro* reactions to determine the impact of adding Caf20 and its mutant forms. This type of approach has been hindered previously because Caf20 is typically not soluble. However the recent structural work shows it is feasible to purify the Caf20 amino-terminal region (Gruner et al., 2018).

6.3 Conclusion

This work showed that Caf20 could interact with ribosome as well as eIF4E and elements required to interact with the ribosome were identified. Through crosslinking techniques, Mass spectrometry and other biochemical assays, ribosome-interacting partners of Caf20 were discovered of which were mostly ribosomal proteins of 40S and 60S subunits. More

physiological functions were characterised for Caf20. This work broadens the classical understanding of Caf20 regulation beyond its usual eIF4E-interactions.

References

Acker, M.G., Shin, B.S., Dever, T.E., and Lorsch, J.R. (2006). Interaction between eukaryotic initiation factors 1A and 5B is required for efficient ribosomal subunit joining. *The Journal of Biological Chemistry 281*, 8469-8475.

Acker, M.G., Shin, B.S., Nanda, J.S., Saini, A.K., Dever, T.E., and Lorsch, J.R. (2009). Kinetic analysis of late steps of eukaryotic translation initiation. *Journal of Molecular Biology 385*, 491-506.

Adomavicius, T., Guaita, M., Zhou, Y., Jennings, M.D., Latif, Z., Roseman, A.M., and Pavitt, G.D. (2019). The structural basis of translational control by eIF2 phosphorylation. *Nature Communications 10*, 2136.

Ajore, R., Raiser, D., McConkey, M., Joud, M., Boidol, B., Mar, B., Saksena, G., Weinstock, D.M., Armstrong, S., Ellis, S.R., *et al.* (2017). Deletion of ribosomal protein genes is a common vulnerability in human cancer, especially in concert with TP53 mutations. *EMBO Mol Med 9*, 498-507.

Albuquerque, C.P., Smolka, M.B., Payne, S.H., Bafna, V., Eng, J., and Zhou, H. (2008). A multidimensional chromatography technology for in-depth phosphoproteome analysis. *Molecular & Cellular Proteomics : MCP 7*, 1389-1396.

Algire, M.A., Maag, D., and Lorsch, J.R. (2005). Pi release from eIF2, not GTP hydrolysis, is the step controlled by start-site selection during eukaryotic translation initiation. *Molecular Cell 20*, 251-262.

Alhebshi, A., Sideri, T.C., Holland, S.L., and Avery, S.V. (2012). The essential iron-sulfur protein Rli1 is an important target accounting for inhibition of cell growth by reactive oxygen species. *Molecular Biology of the Cell 23*, 3582-3590.

Alonso-Rodriguez, E., Fernandez-Pinar, P., Sacristan-Reviriego, A., Molina, M., and Martin, H. (2016). An Analog-sensitive Version of the Protein Kinase Slt2 Allows Identification of Novel Targets of the Yeast Cell Wall Integrity Pathway. *The Journal of Biological Chemistry 291*, 5461-5472.

Altmann, M., Krieger, M., and Trachsel, H. (1989a). Nucleotide sequence of the gene encoding a 20 kDa protein associated with the cap binding protein eIF-4E from Saccharomyces cerevisiae. *Nucleic Acids Research 17*, 7520.

Altmann, M., Schmitz, N., Berset, C., and Trachsel, H. (1997). A novel inhibitor of cap-dependent translation initiation in yeast: p20 competes with eIF4G for binding to eIF4E. *The EMBO Journal 16*, 1114-1121.

Altmann, M., Sonenberg, N., and Trachsel, H. (1989b). Translation in Saccharomyces cerevisiae: initiation factor 4E-dependent cell-free system. *Molecular and Cellular Biology 9*, 4467-4472.

Altmann, M., and Trachsel, H. (1989). Altered mRNA cap recognition activity of initiation factor 4E in the yeast cell cycle division mutant cdc33. *Nucleic Acids Research 17*, 5923-5931.

Arndt, N., Ross-Kaschitza, D., Kojukhov, A., Komar, A.A., and Altmann, M. (2018). Properties of the ternary complex formed by yeast eIF4E, p20 and mRNA. *Scientific Reports 8*, 6707.

Ashe, M.P., De Long, S.K., and Sachs, A.B. (2000). Glucose depletion rapidly inhibits translation initiation in yeast. *Molecular Biology of the Cell 11*, 833-848.

Ashe, M.P., Slaven, J.W., De Long, S.K., Ibrahimo, S., and Sachs, A.B. (2001). A novel eIF2B-dependent mechanism of translational control in yeast as a response to fusel alcohols. *The EMBO Journal 20*, 6464-6474.

Aylett, C.H., Boehringer, D., Erzberger, J.P., Schaefer, T., and Ban, N. (2015). Structure of a yeast 40S-eIF1-eIF1A-eIF3-eIF3j initiation complex. *Nature Structural & Molecular Biology 22*, 269-271.

Bah, A., Vernon, R.M., Siddiqui, Z., Krzeminski, M., Muhandiram, R., Zhao, C., Sonenberg, N., Kay, L.E., and Forman-Kay, J.D. (2015). Folding of an intrinsically disordered protein by phosphorylation as a regulatory switch. *Nature 519*, 106-109.

Balagopal, V., and Parker, R. (2009). Stm1 modulates mRNA decay and Dhh1 function in Saccharomyces cerevisiae. *Genetics 181*, 93-103.

Bandmann, O., Weiss, K.H., and Kaler, S.G. (2015). Wilson's disease and other neurological copper disorders. *The Lancet Neurology 14*, 103-113.

Barbet, N.C., Schneider, U., Helliwell, S.B., Stansfield, I., Tuite, M.F., and Hall, M.N. (1996). TOR controls translation initiation and early G1 progression in yeast. *Molecular Biology of the Cell 7*, 25-42.

Baudin-Baillieu, A., Tollervey, D., Cullin, C., and Lacroute, F. (1997). Functional analysis of Rrp7p, an essential yeast protein involved in pre-rRNA processing and ribosome assembly. *Molecular and cellular biology 17*, 5023-5032.

Bellodi, C., Kopmar, N., and Ruggero, D. (2010a). Deregulation of oncogene-induced senescence and p53 translational control in X-linked dyskeratosis congenita. *The EMBO Journal 29*, 1865-1876.

Bellodi, C., Krasnykh, O., Haynes, N., Theodoropoulou, M., Peng, G., Montanaro, L., and Ruggero, D. (2010b). Loss of function of the tumor suppressor DKC1 perturbs p27 translation control and contributes to pituitary tumorigenesis. *Cancer research 70*, 6026-6035.

Ben-Shem, A., Garreau de Loubresse, N., Melnikov, S., Jenner, L., Yusupova, G., and Yusupov, M. (2011). The structure of the eukaryotic ribosome at 3.0 A resolution. *Science 334*, 1524-1529.

Ben-Shem, A., Jenner, L., Yusupova, G., and Yusupov, M. (2010). Crystal structure of the eukaryotic ribosome. *Science 330*, 1203-1209.

Beretta, L., Gingras, A.C., Svitkin, Y.V., Hall, M.N., and Sonenberg, N. (1996). Rapamycin blocks the phosphorylation of 4E-BP1 and inhibits cap-dependent initiation of translation. *The EMBO Journal 15*, 658-664.

Bidinosti, M., Ran, I., Sanchez-Carbente, M.R., Martineau, Y., Gingras, A.C., Gkogkas, C., Raught, B., Bramham, C.R., Sossin, W.S., Costa-Mattioli, M., *et al.* (2010). Postnatal deamidation of 4E-BP2 in brain enhances its association with raptor and alters kinetics of excitatory synaptic transmission. *Molecular Cell 37*, 797-808.

Blank, H.M., Perez, R., He, C., Maitra, N., Metz, R., Hill, J., Lin, Y., Johnson, C.D., Bankaitis, V.A., Kennedy, B.K., *et al.* (2017). Translational control of lipogenic enzymes in the cell cycle of synchronous, growing yeast cells. *The EMBO Journal 36*, 487-502.

Blewett, N.H., and Goldstrohm, A.C. (2012). A eukaryotic translation initiation factor 4E-binding protein promotes mRNA decapping and is required for PUF repression. *Molecular and Cellular Biology 32*, 4181-4194.

Brachmann, C.B., Davies, A., Cost, G.J., Caputo, E., Li, J., Hieter, P., and Boeke, J.D. (1998). Designer deletion strains derived from Saccharomyces cerevisiae S288C: a useful set of strains and plasmids for PCR-mediated gene disruption and other applications. *Yeast 14*, 115-132.

Bradford, M.M. (1976). A rapid and sensitive method for the quantitation of microgram quantities of protein utilizing the principle of protein-dye binding. *Anal Biochem 72*, 248-254.

Briggs, J.W., and Dinman, J.D. (2017). Subtractional Heterogeneity: A Crucial Step toward Defining Specialized Ribosomes. *Molecular Cell 67*, 3-4.

Brunn, G.J., Hudson, C.C., Sekulic, A., Williams, J.M., Hosoi, H., Houghton, P.J., Lawrence, J.C., Jr., and Abraham, R.T. (1997). Phosphorylation of the

translational repressor PHAS-I by the mammalian target of rapamycin. *Science 277*, 99-101.

Campbell, S.G., Hoyle, N.P., and Ashe, M.P. (2005). Dynamic cycling of eIF2 through a large eIF2B-containing cytoplasmic body: implications for translation control. *The Journal of Cell Biology 170*, 925-934.

Castelli, L.M., Talavera, D., Kershaw, C.J., Mohammad-Qureshi, S.S., Costello, J.L., Rowe, W., Sims, P.F., Grant, C.M., Hubbard, S.J., Ashe, M.P., *et al.* (2015). The 4E-BP Caf20p Mediates Both eIF4E-Dependent and Independent Repression of Translation. *PLoS Genetics 11*, e1005233.

Cawley, A., and Warwicker, J. (2012). eIF4E-binding protein regulation of mRNAs with differential 5'-UTR secondary structure: a polyelectrostatic model for a component of protein-mRNA interactions. *Nucleic Acids Research 40*, 7666-7675.

Cherkasova, V.A., and Hinnebusch, A.G. (2003). Translational control by TOR and TAP42 through dephosphorylation of eIF2alpha kinase GCN2. *Genes & Development 17*, 859-872.

Cherny, R.A., Atwood, C.S., Xilinas, M.E., Gray, D.N., Jones, W.D., McLean, C.A., Barnham, K.J., Volitakis, I., Fraser, F.W., Kim, Y., *et al.* (2001). Treatment with a copper-zinc chelator markedly and rapidly inhibits beta-amyloid accumulation in Alzheimer's disease transgenic mice. *Neuron 30*, 665-676.

Chiu, W.L., Wagner, S., Herrmannova, A., Burela, L., Zhang, F., Saini, A.K., Valasek, L., and Hinnebusch, A.G. (2010). The C-terminal region of eukaryotic translation initiation factor 3a (eIF3a) promotes mRNA recruitment, scanning, and, together with eIF3j and the eIF3b RNA recognition motif, selection of AUG start codons. *Molecular and Cellular Biology 30*, 4415-4434.

Choo, A.Y., Yoon, S.O., Kim, S.G., Roux, P.P., and Blenis, J. (2008). Rapamycin differentially inhibits S6Ks and 4E-BP1 to mediate cell-type-specific repression of mRNA translation. *Proceedings of the National Academy of Sciences of the United States of America 105*, 17414-17419.

Christiano, R., Nagaraj, N., Frohlich, F., and Walther, T.C. (2014). Global proteome turnover analyses of the Yeasts S. cerevisiae and S. pombe. *Cell Reports 9*, 1959-1965.

Christianson, T.W., Sikorski, R.S., Dante, M., Shero, J.H., and Hieter, P. (1992). Multifunctional yeast high-copy-number shuttle vectors. *Gene 110*, 119-122.

Cigan, A.M., Feng, L., and Donahue, T.F. (1988). tRNAi(met) functions in directing the scanning ribosome to the start site of translation. *Science 242*, 93-97.

Coller, J., and Parker, R. (2005). General translational repression by activators of mRNA decapping. *Cell 122*, 875-886.

Coller, J.M., Tucker, M., Sheth, U., Valencia-Sanchez, M.A., and Parker, R. (2001). The DEAD box helicase, Dhh1p, functions in mRNA decapping and interacts with both the decapping and deadenylase complexes. *RNA 7*, 1717-1727.

Cosentino, G.P., Schmelzle, T., Haghighat, A., Helliwell, S.B., Hall, M.N., and Sonenberg, N. (2000). Eap1p, a novel eukaryotic translation initiation factor 4E-associated protein in Saccharomyces cerevisiae. *Molecular and Cellular Biology 20*, 4604-4613.

Costello, J., Castelli, L.M., Rowe, W., Kershaw, C.J., Talavera, D., Mohammad-Qureshi, S.S., Sims, P.F., Grant, C.M., Pavitt, G.D., Hubbard, S.J., *et al.* (2015). Global mRNA selection mechanisms for translation initiation. *Genome Biology 16*, 10.

Crawford, R.A., and Pavitt, G.D. (2019). Translational regulation in response to stress in Saccharomyces cerevisiae. *Yeast 36*, 5-21.

Cridge, A.G., Castelli, L.M., Smirnova, J.B., Selley, J.N., Rowe, W., Hubbard, S.J., McCarthy, J.E., Ashe, M.P., Grant, C.M., and Pavitt, G.D. (2010). Identifying eIF4E-binding protein translationally-controlled transcripts reveals links to mRNAs bound by specific PUF proteins. *Nucleic Acids Research 38*, 8039-8050.

Cuchalova, L., Kouba, T., Herrmannova, A., Danyi, I., Chiu, W.L., and Valasek, L. (2010). The RNA recognition motif of eukaryotic translation initiation factor 3g (eIF3g) is required for resumption of scanning of posttermination ribosomes for reinitiation on GCN4 and together with eIF3i stimulates linear scanning. *Molecular and Cellular Biology 30*, 4671-4686.

Cullen, P.J., and Sprague, G.F., Jr. (2002). The roles of bud-site-selection proteins during haploid invasive growth in yeast. *Molecular Biology of the Cell 13*, 2990-3004.

Cullen, P.J., and Sprague, G.F., Jr. (2012). The regulation of filamentous growth in yeast. *Genetics 190*, 23-49.

Danaie, P., Altmann, M., Hall, M.N., Trachsel, H., and Helliwell, S.B. (1999). CLN3 expression is sufficient to restore G1-to-S-phase progression in Saccharomyces cerevisiae mutants defective in translation initiation factor eIF4E. *The Biochemical Journal 340 (Pt 1)*, 135-141.

De Benedetti, A., and Harris, A.L. (1999). eIF4E expression in tumors: its possible role in progression of malignancies. *The International Journal of Biochemistry & Cell Biology 31*, 59-72.

de la Cruz, J., Iost, I., Kressler, D., and Linder, P. (1997). The p20 and Ded1 proteins have antagonistic roles in eIF4E-dependent translation in Saccharomyces cerevisiae. *Proceedings of the National Academy of Sciences of the United States of America 94*, 5201-5206.

Deloche, O., de la Cruz, J., Kressler, D., Doere, M., and Linder, P. (2004). A membrane transport defect leads to a rapid attenuation of translation initiation in Saccharomyces cerevisiae. *Molecular Cell 13*, 357-366.

des Georges, A., Dhote, V., Kuhn, L., Hellen, C.U., Pestova, T.V., Frank, J., and Hashem, Y. (2015). Structure of mammalian eIF3 in the context of the 43S preinitiation complex. *Nature 525*, 491-495.

des Georges, A., Hashem, Y., Unbehaun, A., Grassucci, R.A., Taylor, D., Hellen, C.U., Pestova, T.V., and Frank, J. (2014). Structure of the mammalian ribosomal pre-termination complex associated with eRF1.eRF3.GDPNP. *Nucleic Acids Research 42*, 3409-3418.

Dever, T.E., Kinzy, T.G., and Pavitt, G.D. (2016). Mechanism and Regulation of Protein Synthesis in Saccharomyces cerevisiae. *Genetics 203*, 65-107.

Ding, W.Q., Liu, B., Vaught, J.L., Yamauchi, H., and Lind, S.E. (2005). Anticancer activity of the antibiotic clioquinol. *Cancer Research 65*, 3389-3395.

Dmitriev, S.E., Terenin, I.M., Andreev, D.E., Ivanov, P.A., Dunaevsky, J.E., Merrick, W.C., and Shatsky, I.N. (2010). GTP-independent tRNA delivery to the ribosomal P-site by a novel eukaryotic translation factor. *The Journal of Biological Chemistry 285*, 26779-26787.

Doerfel, L.K., Wohlgemuth, I., Kothe, C., Peske, F., Urlaub, H., and Rodnina, M.V. (2013). EF-P is essential for rapid synthesis of proteins containing consecutive proline residues. Science *339*, 85-88.

Dolezal, J.M., Dash, A.P., and Prochownik, E.V. (2018). Diagnostic and prognostic implications of ribosomal protein transcript expression patterns in human cancers. *BMC Cancer 18*, 275.

Donahue, T.F. (2000). *In* Translational control of gene expression (eds. Sonenberg, N. Hershey, J. W. B. Mathews, M) 487-502, 2nd edn (Cold Spring Harbor, NY: Cold Spring Harbor Laboratory Press).

Duncan, R., Milburn, S.C., and Hershey, J.W. (1987). Regulated phosphorylation and low abundance of HeLa cell initiation factor eIF-4F suggest a role in translational control. Heat shock effects on eIF-4F. *The Journal of Biological Chemistry 262*, 380-388.

Dunckley, T., and Parker, R. (1999). The DCP2 protein is required for mRNA decapping in Saccharomyces cerevisiae and contains a functional MutT motif. *The EMBO Journal 18*, 5411-5422.

Elantak, L., Wagner, S., Herrmannova, A., Karaskova, M., Rutkai, E., Lukavsky, P.J., and Valasek, L. (2010). The indispensable N-terminal half of eIF3j/HCR1 cooperates with its structurally conserved binding partner eIF3b/PRT1-RRM and with eIF1A in stringent AUG selection. *Journal Of Molecular Biology 396*, 1097-1116.

Eulalio, A., Behm-Ansmant, I., and Izaurralde, E. (2007). P bodies: at the crossroads of post-transcriptional pathways. *Nature Reviews Molecular Cell Biology 8*, 9-22.

Fancy, D.A., Melcher, K., Johnston, S.A., and Kodadek, T. (1996). New chemistry for the study of multiprotein complexes: the six-histidine tag as a receptor for a protein crosslinking reagent. *Chem Biol 3*, 551-559.

Fletcher, C.M., McGuire, A.M., Gingras, A.C., Li, H., Matsuo, H., Sonenberg, N., and Wagner, G. (1998). 4E binding proteins inhibit the translation factor eIF4E without folded structure. *Biochemistry 37*, 9-15.

Gancedo, J.M. (2001). Control of pseudohyphae formation in Saccharomyces cerevisiae. *FEMS Microbiology Reviews 25*, 107-123.

Gay, S., Piccini, D., Bruhn, C., Ricciardi, S., Soffientini, P., Carotenuto, W., Biffo, S., and Foiani, M. (2018). A Mad2-Mediated Translational Regulatory Mechanism Promoting S-Phase Cyclin Synthesis Controls Origin Firing and Survival to Replication Stress. *Molecular Cell 70*, 628-638 e625.

GIMP (2019). GNU Image Manipulation Program (GIMP) version 2.2.10. .

Gingras, A.C., Gygi, S.P., Raught, B., Polakiewicz, R.D., Abraham, R.T., Hoekstra, M.F., Aebersold, R., and Sonenberg, N. (1999a). Regulation of 4E-BP1 phosphorylation: a novel two-step mechanism. *Genes & Development 13*, 1422-1437.

Gingras, A.C., Raught, B., Gygi, S.P., Niedzwiecka, A., Miron, M., Burley, S.K., Polakiewicz, R.D., Wyslouch-Cieszynska, A., Aebersold, R., and Sonenberg, N. (2001). Hierarchical phosphorylation of the translation inhibitor 4E-BP1. Genes & development *15*, 2852-2864.

Gingras, A.C., Raught, B., and Sonenberg, N. (1999b). eIF4 initiation factors: effectors of mRNA recruitment to ribosomes and regulators of translation. *Annual Review of Biochemistry 68*, 913-963.

Gkogkas, C.G., Khoutorsky, A., Ran, I., Rampakakis, E., Nevarko, T., Weatherill, D.B., Vasuta, C., Yee, S., Truitt, M., Dallaire, P., *et al.* (2013). Autism-related deficits via dysregulated eIF4E-dependent translational control. *Nature 493*, 371-377.

Gordiyenko, Y., Schmidt, C., Jennings, M.D., Matak-Vinkovic, D., Pavitt, G.D., and Robinson, C.V. (2014). eIF2B is a decameric guanine nucleotide exchange factor with a gamma2epsilon2 tetrameric core. *Nature Communications 5*, 3902.

Gosselin, P., Oulhen, N., Jam, M., Ronzca, J., Cormier, P., Czjzek, M., and Cosson, B. (2011). The translational repressor 4E-BP called to order by eIF4E: new structural insights by SAXS. *Nucleic Acids Research 39*, 3496-3503.

Goudarzi, K.M., and Lindstrom, M.S. (2016). Role of ribosomal protein mutations in tumor development (Review). *Int J Oncol 48*, 1313-1324.

Goyer, C., Altmann, M., Lee, H.S., Blanc, A., Deshmukh, M., Woolford, J.L., Jr., Trachsel, H., and Sonenberg, N. (1993). TIF4631 and TIF4632: two yeast genes

encoding the high-molecular-weight subunits of the cap-binding protein complex (eukaryotic initiation factor 4F) contain an RNA recognition motif-like sequence and carry out an essential function. *Molecular and Cellular Biology 13*, 4860-4874.

Graduateway (2017). The Effect of Temperature on the Rate of Yeast Respiration Essay. [Online]. Available at:https://graduateway.com/the-effect-of-temperature-on-the-rate-of-yeast-respiration-essay-5228-essay/[Accessed: 13 Apr. 2020].

Gross, J.D., Moerke, N.J., von der Haar, T., Lugovskoy, A.A., Sachs, A.B., McCarthy, J.E., and Wagner, G. (2003). Ribosome loading onto the mRNA cap is driven by conformational coupling between eIF4G and eIF4E. *Cell 115*, 739-750.

Gruner, S., Peter, D., Weber, R., Wohlbold, L., Chung, M.Y., Weichenrieder, O., Valkov, E., Igreja, C., and Izaurralde, E. (2016). The Structures of eIF4E-eIF4G Complexes Reveal an Extended Interface to Regulate Translation Initiation. *Molecular Cell 64*, 467-479.

Gruner, S., Weber, R., Peter, D., Chung, M.Y., Igreja, C., Valkov, E., and Izaurralde, E. (2018). Structural motifs in eIF4G and 4E-BPs modulate their binding to eIF4E to regulate translation initiation in yeast. *Nucleic Acids Research 46*, 6893-6908.

Gu, W., Deng, Y., Zenklusen, D., and Singer, R.H. (2004). A new yeast PUF family protein, Puf6p, represses ASH1 mRNA translation and is required for its localization. *Genes & development 18*, 1452-1465.

Gupta, N., Lorsch, J.R., and Hinnebusch, A.G. (2018). Yeast Ded1 promotes 48S translation pre-initiation complex assembly in an mRNA-specific and eIF4F-dependent manner. *eLife 7*.

Hao, Q., Wang, J., Chen, Y., Wang, S., Cao, M., Lu, H., and Zhou, X. (2020). Dual regulation of p53 by the ribosome maturation factor SBDS. *Cell Death Dis 11*, 197.

Harnpicharnchai, P., Jakovljevic, J., Horsey, E., Miles, T., Roman, J., Rout, M., Meagher, D., Imai, B., Guo, Y., Brame, C.J., *et al.* (2001). Composition and functional characterization of yeast 66S ribosome assembly intermediates. *Molecular cell 8*, 505-515.

Heck, T., Faccio, G., Richter, M., and Thony-Meyer, L. (2013). Enzyme-catalyzed protein crosslinking. Applied microbiology and biotechnology *97*, 461-475.

Heitman, J., Movva, N.R., and Hall, M.N. (1991). Targets for cell cycle arrest by the immunosuppressant rapamycin in yeast. *Science 253*, 905-909.

Hershey, J.W., Sonenberg, N., and Mathews, M.B. (2012). Principles of translational control: an overview. *Cold Spring Harbor Perspectives in Biology 4*.

Hershey, J.W., Yanov, J., and Fakunding, J.L. (1979). Purification of protein synthesis initiation factors IF-1, IF-2, and IF-3 from Escherichia coli. *Methods in Enzymology 60*, 3-11.

Hill, T. (2005). Bioedit for Biological sequence alignment editor v.7.0.5. http://www.mbio.ncsu.edu/BioEdit/bioedit.html.

Hinnebusch, A.G. (2005). Translational regulation of GCN4 and the general amino acid control of yeast. *Annual Review Of Microbiology 59*, 407-450.

Hinnebusch, A.G. (2006). eIF3: a versatile scaffold for translation initiation complexes. *Trends in Biochemical Sciences 31*, 553-562.

Hinnebusch, A.G., and Lorsch, J.R. (2012). The mechanism of eukaryotic translation initiation: new insights and challenges. *Cold Spring Harbor Perspectives in Biology 4*.

Holt, L.J., Tuch, B.B., Villen, J., Johnson, A.D., Gygi, S.P., and Morgan, D.O. (2009). Global analysis of Cdk1 substrate phosphorylation sites provides insights into evolution. *Science 325*, 1682-1686.

Hu, C., Pang, S., Kong, X., Velleca, M., and Lawrence, J.C., Jr. (1994). Molecular cloning and tissue distribution of PHAS-I, an intracellular target for insulin and growth factors. *Proceedings of the National Academy of Sciences of the United States of America 91*, 3730-3734.

Hussain, T., Llacer, J.L., Fernandez, I.S., Munoz, A., Martin-Marcos, P., Savva, C.G., Lorsch, J.R., Hinnebusch, A.G., and Ramakrishnan, V. (2014). Structural changes enable start codon recognition by the eukaryotic translation initiation complex. *Cell 159*, 597-607.

Ibrahimo, S., Holmes, L.E., and Ashe, M.P. (2006). Regulation of translation initiation by the yeast eIF4E binding proteins is required for the pseudohyphal response. *Yeast 23*, 1075-1088.

Igreja, C., Peter, D., Weiler, C., and Izaurralde, E. (2014). 4E-BPs require non-canonical 4E-binding motifs and a lateral surface of eIF4E to repress translation. *Nature Communications 5*, 4790.

Inge-Vechtomov, S., Zhouravleva, G., and Philippe, M. (2003). Eukaryotic release factors (eRFs) history. *Biology of the Cell / under the Auspices of the European Cell Biology Organization 95*, 195-209.

Ingolia, N.T., Lareau, L.F., and Weissman, J.S. (2011). Ribosome profiling of mouse embryonic stem cells reveals the complexity and dynamics of mammalian proteomes. *Cell 147*, 789-802.

Interactions/Cross-linking, P.P.-P. (2011). *Wikibooks*, The Free Textbook Project. .

Irie, K., Tadauchi, T., Takizawa, P.A., Vale, R.D., Matsumoto, K., and Herskowitz, I. (2002). The Khd1 protein, which has three KH RNA-binding motifs, is required for proper localization of ASH1 mRNA in yeast. *The EMBO Journal 21*, 1158-1167.

Jack, K., Bellodi, C., Landry, D.M., Niederer, R.O., Meskauskas, A., Musalgaonkar, S., Kopmar, N., Krasnykh, O., Dean, A.M., Thompson, S.R., *et al.* (2011). rRNA pseudouridylation defects affect ribosomal ligand binding and translational fidelity from yeast to human cells. *Molecular Cell 44*, 660-666.

Jackson, R.J. (1991). The ATP requirement for initiation of eukaryotic translation varies according to the mRNA species. *Eur J Biochem 200*, 285-294.

Jackson, R.J. (2013). The current status of vertebrate cellular mRNA IRESs. Cold Spring Harbor perspectives in biology *5*.

Jackson, R.J., Hellen, C.U., and Pestova, T.V. (2010). The mechanism of eukaryotic translation initiation and principles of its regulation. *Nature Reviews Molecular Cell Biology 11*, 113-127.

Jenner, L., Melnikov, S., Garreau de Loubresse, N., Ben-Shem, A., Iskakova, M., Urzhumtsev, A., Meskauskas, A., Dinman, J., Yusupova, G., and Yusupov, M. (2012). Crystal structure of the 80S yeast ribosome. *Curr Opin Struct Biol 22*, 759-767.

Jennings, M.D., Kershaw, C.J., Adomavicius, T., and Pavitt, G.D. (2017). Fail-safe control of translation initiation by dissociation of eIF2alpha phosphorylated ternary complexes. *eLife 6*.

Jennings, M.D., Kershaw, C.J., White, C., Hoyle, D., Richardson, J.P., Costello, J.L., Donaldson, I.J., Zhou, Y., and Pavitt, G.D. (2016). eIF2beta is critical for eIF5-mediated GDP-dissociation inhibitor activity and translational control. *Nucleic Acids Research 44*, 9698-9709.

Jennings, M.D., and Pavitt, G.D. (2010a). eIF5 has GDI activity necessary for translational control by eIF2 phosphorylation. *Nature 465*, 378-381.

Jennings, M.D., and Pavitt, G.D. (2010b). eIF5 is a dual function GAP and GDI for eukaryotic translational control. *Small GTPases 1*, 118-123.

Jennings, M.D., and Pavitt, G.D. (2014). A new function and complexity for protein translation initiation factor eIF2B. *Cell cycle 13*, 2660-2665.

Jennings, M.D., Zhou, Y., Mohammad-Qureshi, S.S., Bennett, D., and Pavitt, G.D. (2013). eIF2B promotes eIF5 dissociation from eIF2*GDP to facilitate guanine nucleotide exchange for translation initiation. Genes & Development *27*, 2696-2707.

Ka, M., Park, Y.U., and Kim, J. (2008). The DEAD-box RNA helicase, Dhh1, functions in mating by regulating Ste12 translation in Saccharomyces cerevisiae. *Biochemical and Biophysical Research Communications 367*, 680-686.

Kamenska, A., Lu, W.T., Kubacka, D., Broomhead, H., Minshall, N., Bushell, M., and Standart, N. (2014). Human 4E-T represses translation of bound mRNAs and enhances microRNA-mediated silencing. *Nucleic Acids Research 42*, 3298-3313.

Kapp, L.D., and Lorsch, J.R. (2004). GTP-dependent recognition of the methionine moiety on initiator tRNA by translation factor eIF2. *Journal of Molecular Biology 335*, 923-936.

Kashiwagi, K., Takahashi, M., Nishimoto, M., Hiyama, T.B., Higo, T., Umehara, T., Sakamoto, K., Ito, T., and Yokoyama, S. (2016). Crystal structure of eukaryotic translation initiation factor 2B. *Nature 531*, 122-125.

Kaul, G., Pattan, G., and Rafeequi, T. (2011). Eukaryotic elongation factor-2 (eEF2): its regulation and peptide chain elongation. *Cell Biochemistry and Function 29*, 227-234.

Kaur, D., Yantiri, F., Rajagopalan, S., Kumar, J., Mo, J.Q., Boonplueang, R., Viswanath, V., Jacobs, R., Yang, L., Beal, M.F., *et al.* (2003). Genetic or pharmacological iron chelation prevents MPTP-induced neurotoxicity in vivo: a novel therapy for Parkinson's disease. *Neuron 37*, 899-909.

Kinkelin, K., Veith, K., Grunwald, M., and Bono, F. (2012). Crystal structure of a minimal eIF4E-Cup complex reveals a general mechanism of eIF4E regulation in translational repression. *RNA 18*, 1624-1634.

Klinge, S., Voigts-Hoffmann, F., Leibundgut, M., Arpagaus, S., and Ban, N. (2011). Crystal structure of the eukaryotic 60S ribosomal subunit in complex with initiation factor 6. *Science 334*, 941-948.

Komar, A.A., Gross, S.R., Barth-Baus, D., Strachan, R., Hensold, J.O., Goss Kinzy, T., and Merrick, W.C. (2005). Novel characteristics of the biological properties of the yeast Saccharomyces cerevisiae eukaryotic initiation factor 2A. *The Journal of Biological Chemistry 280*, 15601-15611.

Komili, S., Farny, N.G., Roth, F.P., and Silver, P.A. (2007). Functional specificity among ribosomal proteins regulates gene expression. *Cell 131*, 557-571.

Kousar, R. (2013). Regulation of eIF2B by phosphorylation. In Division of Molecular and Cellular Function, Life Sciences (https://www.research.manchester.ac.uk/portal/en/theses/regulation-of-eif2b-by-phosphorylation(82439f9a-9ed1-4708-a87f-f0bcc6f4b64e).html: The University of Manchester), pp. 236.

Kozak, M. (1991). Structural features in eukaryotic mRNAs that modulate the initiation of translation. *The Journal of Biological Chemistry 266*, 19867-19870.

Kozak, M. (1992). Regulation of translation in eukaryotic systems. *Annual Review of Cell Biology 8*, 197-225.

Kozak, M. (1993). Identifying Aug Initiator Codons - a Citation-Classic Commentary on Point Mutations Define a Sequence Flanking the Aug Initiator Codon That Modulates Translation by Eukaryotic Ribosomes - and on an Analysis of 5' Noncoding Sequences from 699 Vertebrate Messenger-Rnas by Kozak,M. Cc/Life Sci, 9-9.

Kozak, M. (1995). Adherence to the first-AUG rule when a second AUG codon follows closely upon the first. *Proceedings of the National Academy of Sciences of the United States of America 92*, 2662-2666.

Kozak, M. (1999). Initiation of translation in prokaryotes and eukaryotes. Gene *234*, 187-208.

Kozak, M. (2002). Pushing the limits of the scanning mechanism for initiation of translation. *Gene 299*, 1-34.

Kron, S.J., Styles, C.A., and Fink, G.R. (1994). Symmetric cell division in pseudohyphae of the yeast Saccharomyces cerevisiae. *Molecular Biology of the Cell 5*, 1003-1022.

Kulak, N.A., Pichler, G., Paron, I., Nagaraj, N., and Mann, M. (2014). Minimal, encapsulated proteomic-sample processing applied to copy-number estimation in eukaryotic cells. *Nature Methods 11*, 319-324.

Kumar, P. (2017). 33 - Pharmacology of Specific Drug Groups: Antibiotic Therapy∗∗The author wishes to recognize Dr. Thomas J. Pallasch for his past contributions to this chapter. In Pharmacology and Therapeutics for Dentistry (Seventh Edition), F.J. Dowd, B.S. Johnson, and A.J. Mariotti, eds. (Mosby), pp. 457-487.

Lai, M.C., Lee, Y.H., and Tarn, W.Y. (2008). The DEAD-box RNA helicase DDX3 associates with export messenger ribonucleoproteins as well as tip-associated protein and participates in translational control. *Molecular biology of the Cell 19*, 3847-3858.

Lanker, S., Muller, P.P., Altmann, M., Goyer, C., Sonenberg, N., and Trachsel, H. (1992). Interactions of the eIF-4F subunits in the yeast Saccharomyces cerevisiae. *The Journal of Biological Chemistry 267*, 21167-21171.

LeFebvre, A.K., Korneeva, N.L., Trutschl, M., Cvek, U., Duzan, R.D., Bradley, C.A., Hershey, J.W., and Rhoads, R.E. (2006). Translation initiation factor eIF4G-1 binds to eIF3 through the eIF3e subunit. *The Journal of Biological Chemistry 281*, 22917-22932.

Li, C., Wang, J., and Zhou, B. (2010). The metal chelating and chaperoning effects of clioquinol: insights from yeast studies. Journal of Alzheimer's disease : *JAD 21*, 1249-1262.

Li, D., Wei, T., Abbott, C.M., and Harrich, D. (2013). The unexpected roles of eukaryotic translation elongation factors in RNA virus replication and pathogenesis. Microbiology and molecular biology reviews : *MMBR 77*, 253-266.

Liang, Q., and Zhou, B. (2007). Copper and manganese induce yeast apoptosis via different pathways. *Molecular Biology of the Cell 18*, 4741-4749.

Llacer, J.L., Hussain, T., Marler, L., Aitken, C.E., Thakur, A., Lorsch, J.R., Hinnebusch, A.G., and Ramakrishnan, V. (2015). Conformational Differences between Open and Closed States of the Eukaryotic Translation Initiation Complex. *Molecular Cell 59*, 399-412.

Lobel, J.H., Tibble, R.W., and Gross, J.D. (2019). Pat1 activates late steps in mRNA decay by multiple mechanisms. *Proceedings of the National Academy of Sciences of the United States of America 116*, 23512-23517.

Lomakin, I.B., Kolupaeva, V.G., Marintchev, A., Wagner, G., and Pestova, T.V. (2003). Position of eukaryotic initiation factor eIF1 on the 40S ribosomal subunit determined by directed hydroxyl radical probing. *Genes & Developmen*t *17*, 2786-2797.

Lynch, B.A., and Koshland, D.E., Jr. (1991). Disulfide cross-linking studies of the transmembrane regions of the aspartate sensory receptor of Escherichia coli. *Proceedings of the National Academy of Sciences of the United States of America 88*, 10402-10406.

Ma, X.M., and Blenis, J. (2009). Molecular mechanisms of mTOR-mediated translational control. *Nature Reviews Molecular Cell Biology 10*, 307-318.

Maag, D., Fekete, C.A., Gryczynski, Z., and Lorsch, J.R. (2005). A conformational change in the eukaryotic translation preinitiation complex and release of eIF1 signal recognition of the start codon. *Molecular Cell 17*, 265-275.

Mader, S., Lee, H., Pause, A., and Sonenberg, N. (1995). The translation initiation factor eIF-4E binds to a common motif shared by the translation factor eIF-4 gamma and the translational repressors 4E-binding proteins. *Molecular and Cellular Biology 15*, 4990-4997.

Madhani, H.D., Galitski, T., Lander, E.S., and Fink, G.R. (1999). Effectors of a developmental mitogen-activated protein kinase cascade revealed by expression signatures of signaling mutants. *Proceedings of the National Academy of Sciences of the United States of America 96*, 12530-12535.

Mangus, D.A., Evans, M.C., and Jacobson, A. (2003). Poly(A)-binding proteins: multifunctional scaffolds for the post-transcriptional control of gene expression. *Genome Biology 4*, 223.

Marcotrigiano, J., Gingras, A.C., Sonenberg, N., and Burley, S.K. (1999). Cap-dependent translation initiation in eukaryotes is regulated by a molecular mimic of eIF4G. *Molecular Cell 3*, 707-716.

Marintchev, A., Edmonds, K.A., Marintcheva, B., Hendrickson, E., Oberer, M., Suzuki, C., Herdy, B., Sonenberg, N., and Wagner, G. (2009). Topology and regulation of the human eIF4A/4G/4H helicase complex in translation initiation. *Cell 136*, 447-460.

Martineau, Y., Azar, R., Bousquet, C., and Pyronnet, S. (2013). Anti-oncogenic potential of the eIF4E-binding proteins. *Oncogene 32*, 671-677.

Mascarenhas, C., Edwards-Ingram, L.C., Zeef, L., Shenton, D., Ashe, M.P., and Grant, C.M. (2008). Gcn4 is required for the response to peroxide stress in the yeast Saccharomyces cerevisiae. Molecular biology of the cell *19*, 2995-3007.

Mathews, M., Sonenberg, N., and Hershey, J.W.B. (2007). Translational control in biology and medicine, 3rd edn (Cold Spring Harbor, N.Y.: Cold Spring Harbor Laboratory Press).

Mauro, V.P., and Edelman, G.M. (2007). The ribosome filter redux. *Cell Cycle 6*, 2246-2251.

Merrick, W.C. (2010). Eukaryotic protein synthesis: still a mystery. *The Journal of Biological Chemistry 285*, 21197-21201.

Metsalu, T., and Vilo, J. (2015). ClustVis: a web tool for visualizing clustering of multivariate data using Principal Component Analysis and heatmap. *Nucleic Acids Research 43*, W566-570.

Montanaro, L., Calienni, M., Bertoni, S., Rocchi, L., Sansone, P., Storci, G., Santini, D., Ceccarelli, C., Taffurelli, M., Carnicelli, D., *et al.* (2010). Novel dyskerin-mediated mechanism of p53 inactivation through defective mRNA translation. *Cancer Research 70*, 4767-4777.

Mosch, H.U., Roberts, R.L., and Fink, G.R. (1996). Ras2 signals via the Cdc42/Ste20/mitogen-activated protein kinase module to induce filamentous growth in Saccharomyces cerevisiae. *Proceedings of the National Academy of Sciences of the United States of America 93*, 5352-5356.

Mothe-Satney, I., Yang, D., Fadden, P., Haystead, T.A., and Lawrence, J.C., Jr. (2000). Multiple mechanisms control phosphorylation of PHAS-I in five (S/T)P sites that govern translational repression. *Molecular and Cellular Biology 20*, 3558-3567.

Napoli, I., Mercaldo, V., Boyl, P.P., Eleuteri, B., Zalfa, F., De Rubeis, S., Di Marino, D., Mohr, E., Massimi, M., Falconi, M., *et al.* (2008). The fragile X syndrome protein

represses activity-dependent translation through CYFIP1, a new 4E-BP. *Cell 134*, 1042-1054.

Nelson, M.R., Leidal, A.M., and Smibert, C.A. (2004). Drosophila Cup is an eIF4E-binding protein that functions in Smaug-mediated translational repression. *The EMBO Journal 23*, 150-159.

Nguyen, T., Hamby, A., and Massa, S.M. (2005). Clioquinol down-regulates mutant huntingtin expression in vitro and mitigates pathology in a Huntington's disease mouse model. *Proceedings of the National Academy of Sciences of the United States of America 102*, 11840-11845.

Nissan, T.A., Bassler, J., Petfalski, E., Tollervey, D., and Hurt, E. (2002). 60S pre-ribosome formation viewed from assembly in the nucleolus until export to the cytoplasm. *The EMBO Journal 21*, 5539-5547.

Ogle, J.M., Brodersen, D.E., Clemons, W.M., Jr., Tarry, M.J., Carter, A.P., and Ramakrishnan, V. (2001). Recognition of cognate transfer RNA by the 30S ribosomal subunit. *Science 292*, 897-902.

Oliveros, J.C. (2007-2015). Venny 2.1. An interactive tool for comparing lists with Venn's diagrams.

Opitz, N., Schmitt, K., Hofer-Pretz, V., Neumann, B., Krebber, H., Braus, G.H., and Valerius, O. (2017). Capturing the Asc1p/Receptor for Activated C Kinase 1 (RACK1) Microenvironment at the Head Region of the 40S Ribosome with Quantitative BioID in Yeast. *Molecular & Cellular Proteomics : MCP 16*, 2199-2218.

Paku, K.S., Umenaga, Y., Usui, T., Fukuyo, A., Mizuno, A., In, Y., Ishida, T., and Tomoo, K. (2012). A conserved motif within the flexible C-terminus of the translational regulator 4E-BP is required for tight binding to the mRNA cap-binding protein eIF4E. *The Biochemical Journal 441*, 237-245.

Palam, L.R., Baird, T.D., and Wek, R.C. (2011). Phosphorylation of eIF2 facilitates ribosomal bypass of an inhibitory upstream ORF to enhance CHOP translation. *The Journal of Biological Chemistry 286*, 10939-10949.

Pan, X., and Heitman, J. (2002). Protein kinase A operates a molecular switch that governs yeast pseudohyphal differentiation. *Molecular and Cellular Biology 22*, 3981-3993.

Papadopoulos, E., Jenni, S., Kabha, E., Takrouri, K.J., Yi, T., Salvi, N., Luna, R.E., Gavathiotis, E., Mahalingam, P., Arthanari, H., *et al.* (2014). Structure of the eukaryotic translation initiation factor eIF4E in complex with 4EGI-1 reveals an allosteric mechanism for dissociating eIF4G. *Proceedings of the National Academy of Sciences of the United States of America 111*, E3187-3195.

Park, K., Lee, Y.S., Jung, D., and Kim, J. (2018). Roles of eIF4E-binding protein Caf20 in Ste12 translation and P-body formation in yeast. J Microbiol *56*, 744-747.

Park, Y.U., Hur, H., Ka, M., and Kim, J. (2006). Identification of translational regulation target genes during filamentous growth in Saccharomyces cerevisiae: regulatory role of Caf20 and Dhh1. *Eukaryotic Cell 5*, 2120-2127.

Parsyan, A., Shahbazian, D., Martineau, Y., Petroulakis, E., Alain, T., Larsson, O., Mathonnet, G., Tettweiler, G., Hellen, C.U., Pestova, T.V., *et al.* (2009). The helicase protein DHX29 promotes translation initiation, cell proliferation, and tumorigenesis. *Proceedings of the National Academy of Sciences of the United States of America 106*, 22217-22222.

Passmore, L.A., Schmeing, T.M., Maag, D., Applefield, D.J., Acker, M.G., Algire, M.A., Lorsch, J.R., and Ramakrishnan, V. (2007). The eukaryotic translation initiation factors eIF1 and eIF1A induce an open conformation of the 40S ribosome. *Molecular Cell 26*, 41-50.

Paulin, F.E., Campbell, L.E., O'Brien, K., Loughlin, J., and Proud, C.G. (2001). Eukaryotic translation initiation factor 5 (eIF5) acts as a classical GTPase-activator protein. *Current Biology: CB 11*, 55-59.

Pavitt, G.D. (2005). eIF2B, a mediator of general and gene-specific translational control. *Biochemical Society Transactions 33*, 1487-1492.

Pavitt, G.D., and Proud, C.G. (2009). Protein synthesis and its control in neuronal cells with a focus on vanishing white matter disease. *Biochemical Society Transactions 37*, 1298-1310.

Pavitt, G.D., and Ron, D. (2012). New insights into translational regulation in the endoplasmic reticulum unfolded protein response. Cold Spring Harbor perspectives in biology *4*.

Perez, F. (2013). Serial Cloner 2.6.1. In Serial Cloner 261.

Perreault, A., Bellemer, C., and Bachand, F. (2008). Nuclear export competence of pre-40S subunits in fission yeast requires the ribosomal protein Rps2. *Nucleic Acids Research 36*, 6132-6142.

Pestova, T.V., Borukhov, S.I., and Hellen, C.U. (1998). Eukaryotic ribosomes require initiation factors 1 and 1A to locate initiation codons. *Nature 394*, 854-859.

Pestova, T.V., and Hellen, C.U. (2003). Translation elongation after assembly of ribosomes on the Cricket paralysis virus internal ribosomal entry site without initiation factors or initiator tRNA. *Genes & Development 17*, 181-186.

Pestova, T.V., Hellen, C.U., and Shatsky, I.N. (1996). Canonical eukaryotic initiation factors determine initiation of translation by internal ribosomal entry. *Molecular and Cellular Biology 16*, 6859-6869.

Pestova, T.V., Lomakin, I.B., Lee, J.H., Choi, S.K., Dever, T.E., and Hellen, C.U. (2000). The joining of ribosomal subunits in eukaryotes requires eIF5B. *Nature 403*, 332-335.

Pestova, T.V., Lorsch, J.R., and hellen, C.U. (2007). *In* Translational control in biology and medicine (Mathews, M. Sonenberg, N. Hershey, J. W. B.) 87-128, 3rd edn (Cold Spring Harbor, N.Y.: Cold Spring Harbor Laboratory Press).

Peter, D., Igreja, C., Weber, R., Wohlbold, L., Weiler, C., Ebertsch, L., Weichenrieder, O., and Izaurralde, E. (2015). Molecular architecture of 4E-BP translational inhibitors bound to eIF4E. *Molecular Cell 57*, 1074-1087.

Planta, R.J., and Mager, W.H. (1998). The list of cytoplasmic ribosomal proteins of Saccharomyces cerevisiae. *Yeast 14*, 471-477.

Poehlsgaard, J., and Douthwaite, S. (2005). The bacterial ribosome as a target for antibiotics. *Nat Rev Microbiol 3*, 870-881.

Prevot, D., Darlix, J.L., and Ohlmann, T. (2003). Conducting the initiation of protein synthesis: the role of eIF4G. *Biology of the Cell / Under the Auspices of the European Cell Biology Organization 95*, 141-156.

Ptushkina, M., von der Haar, T., Vasilescu, S., Frank, R., Birkenhager, R., and McCarthy, J.E. (1998). Cooperative modulation by eIF4G of eIF4E-binding to the mRNA 5' cap in yeast involves a site partially shared by p20. *The EMBO Journal 17*, 4798-4808.

Rajkowitsch, L., Vilela, C., Berthelot, K., Ramirez, C.V., and McCarthy, J.E. (2004). Reinitiation and recycling are distinct processes occurring downstream of translation termination in yeast. *Journal of Molecular Biology 335*, 71-85.

Raught, B., and Gingras, A.C. (1999). eIF4E activity is regulated at multiple levels. *The International Journal of Biochemistry & Cell Biology 31*, 43-57.

Richter, J.D., and Sonenberg, N. (2005). Regulation of cap-dependent translation by eIF4E inhibitory proteins. *Nature 433*, 477-480.

Ross, D., and Altmann, M. (2016). eIF4Es and Their Interactors from Yeast Species. *In: Hernández G., Jagus R. (eds)* Evolution of the Protein Synthesis Machinery and Its Regulation. (Springer, Cham).

Ross, D., Saxena, M., and Altmann, M. (2012). eIF4E is an important determinant of adhesion and pseudohyphal growth of the yeast S. cerevisiae. *PloS One 7*, e50773.

Sachs, A.B. (2000). Physical and functional interaction between the mRNA cap structure and the poly(A) tail. *In:* Translational Control of Gene Expression. (eds. Sonenberg, N. Hershey, J. W. B. Mathews, M.), 2nd edn (Cold Spring Harbor, NY Cold Spring Harbor Laboratory Press p. 447-65).

Scheper, G.C., van Kollenburg, B., Hu, J., Luo, Y., Goss, D.J., and Proud, C.G. (2002). Phosphorylation of eukaryotic initiation factor 4E markedly reduces its affinity for capped mRNA. *The Journal of Biological Chemistry 277*, 3303-3309.

Schmeing, T.M., and Ramakrishnan, V. (2009). What recent ribosome structures have revealed about the mechanism of translation. *Nature 461*, 1234-1242.

Schneider-Poetsch, T., Ju, J., Eyler, D.E., Dang, Y., Bhat, S., Merrick, W.C., Green, R., Shen, B., and Liu, J.O. (2010). Inhibition of eukaryotic translation elongation by cycloheximide and lactimidomycin. *Nature Chemical Biology 6*, 209-217.

Schneider, C.A., Rasband, W.S., and Eliceiri, K.W. (2012). NIH Image to ImageJ: 25 years of image analysis. *Nature Methods 9*, 671-675.

Schuler, M., Connell, S.R., Lescoute, A., Giesebrecht, J., Dabrowski, M., Schroeer, B., Mielke, T., Penczek, P.A., Westhof, E., and Spahn, C.M. (2006). Structure of the ribosome-bound cricket paralysis virus IRES RNA. *Nature Structural & Molecular Biology 13*, 1092-1096.

Searfoss, A., Dever, T.E., and Wickner, R. (2001). Linking the 3' poly(A) tail to the subunit joining step of translation initiation: relations of Pab1p, eukaryotic translation initiation factor 5b (Fun12p), and Ski2p-Slh1p. *Molecular and Cellular Biology 21*, 4900-4908.

Shenoy, N., Kessel, R., Bhagat, T.D., Bhattacharyya, S., Yu, Y., McMahon, C., and Verma, A. (2012). Alterations in the ribosomal machinery in cancer and hematologic disorders. *J Hematol Oncol 5*, 32.

Sheth, U., and Parker, R. (2003). Decapping and decay of messenger RNA occur in cytoplasmic processing bodies. *Science 300*, 805-808.

Shi, Z., Fujii, K., Kovary, K.M., Genuth, N.R., Rost, H.L., Teruel, M.N., and Barna, M. (2017). Heterogeneous Ribosomes Preferentially Translate Distinct Subpools of mRNAs Genome-wide. Molecular cell *67*, 71-83 e77.

Shirokikh, N.E., and Preiss, T. (2018). Translation initiation by cap-dependent ribosome recruitment: Recent insights and open questions. Wiley Interdiscip Rev RNA *9*, e1473.

Siridechadilok, B., Fraser, C.S., Hall, R.J., Doudna, J.A., and Nogales, E. (2005). Structural roles for human translation factor eIF3 in initiation of protein synthesis. *Science 310*, 1513-1515.

Slavov, N., Semrau, S., Airoldi, E., Budnik, B., and van Oudenaarden, A. (2015). Differential Stoichiometry among Core Ribosomal Proteins. *Cell Reports 13*, 865-873.

Sonenberg, N. (1988). Cap-binding proteins of eukaryotic messenger RNA: functions in initiation and control of translation. *Progress in Nucleic Acid Research and Molecular Biology 35*, 173-207.

Sonenberg, N., Morgan, M.A., Merrick, W.C., and Shatkin, A.J. (1978). A polypeptide in eukaryotic initiation factors that crosslinks specifically to the 5'-terminal cap in mRNA. *Proceedings of the National Academy of Sciences of the United States of America 75*, 4843-4847.

Song, Q., and Kumar, A. (2012). An Overview of Autophagy and Yeast Pseudohyphal Growth: Integration of Signaling Pathways during Nitrogen Stress. *Cells 1*, 263-283.

Soulard, A., Cremonesi, A., Moes, S., Schutz, F., Jeno, P., and Hall, M.N. (2010). The rapamycin-sensitive phosphoproteome reveals that TOR controls protein kinase A toward some but not all substrates. *Molecular Biology of the Cell 21*, 3475-3486.

Stebbins-Boaz, B., Cao, Q., de Moor, C.H., Mendez, R., and Richter, J.D. (1999). Maskin is a CPEB-associated factor that transiently interacts with elF-4E. *Molecular Cell 4*, 1017-1027.

Sulima, S.O., Hofman, I.J.F., De Keersmaecker, K., and Dinman, J.D. (2017). How Ribosomes Translate Cancer. *Cancer Discovery 7*, 1069-1087.

Sun, J., Yang, Y., Wan, K., Mao, N., Yu, T.Y., Lin, Y.C., DeZwaan, D.C., Freeman, B.C., Lin, J.J., Lue, N.F., *et al.* (2011). Structural bases of dimerization of yeast telomere protein Cdc13 and its interaction with the catalytic subunit of DNA polymerase alpha. *Cell Res 21*, 258-274.

Sun, M., Samir, P., Shen, B., Li, W., Browne, C.M., Frank, J., and Link, A.J.J.b. (2018). Identification of changing ribosome protein compositions using cryo-EM and mass spectrometry. *271833*.

Svitkin, Y.V., Pause, A., Haghighat, A., Pyronnet, S., Witherell, G., Belsham, G.J., and Sonenberg, N. (2001). The requirement for eukaryotic initiation factor 4A (elF4A) in translation is in direct proportion to the degree of mRNA 5' secondary structure. *RNA 7*, 382-394.

Swaney, D.L., Beltrao, P., Starita, L., Guo, A., Rush, J., Fields, S., Krogan, N.J., and Villen, J. (2013). Global analysis of phosphorylation and ubiquitylation cross-talk in protein degradation. *Nature Methods 10*, 676-682.

Tamas, M.J., Sharma, S.K., Ibstedt, S., Jacobson, T., and Christen, P. (2014). Heavy metals and metalloids as a cause for protein misfolding and aggregation. *Biomolecules 4*, 252-267.

Tardiff, D.F., Brown, L.E., Yan, X., Trilles, R., Jui, N.T., Barrasa, M.I., Caldwell, K.A., Caldwell, G.A., Schaus, S.E., and Lindquist, S. (2017). Dihydropyrimidine-Thiones and Clioquinol Synergize To Target beta-Amyloid Cellular Pathologies through a Metal-Dependent Mechanism. *ACS Chem Neurosci 8*, 2039-2055.

Tavares, M.R., Pavan, I.C., Amaral, C.L., Meneguello, L., Luchessi, A.D., and Simabuco, F.M. (2015). The S6K protein family in health and disease. *Life Sci 131*, 1-10.

Tertoolen, L.G., Blanchetot, C., Jiang, G., Overvoorde, J., Gadella, T.W., Jr., Hunter, T., and den Hertog, J. (2001). Dimerization of receptor protein-tyrosine phosphatase alpha in living cells. *BMC Cell Biol 2*, 8.

Thompson, M.K., Rojas-Duran, M.F., Gangaramani, P., and Gilbert, W.V. (2016). The ribosomal protein Asc1/RACK1 is required for efficient translation of short mRNAs. *eLife 5*.

Trakselis, M.A., Alley, S.C., and Ishmael, F.T. (2005). Identification and mapping of protein-protein interactions by a combination of cross-linking, cleavage, and proteomics. *Bioconjug Chem 16*, 741-750.

Tsubaki, T., Honma, Y., and Hoshi, M. (1971). Neurological syndrome associated with clioquinol. *Lancet 1*, 696-697.

Tsukumo, Y., Alain, T., Fonseca, B.D., Nadon, R., and Sonenberg, N. (2016). Translation control during prolonged mTORC1 inhibition mediated by 4E-BP3. *Nature Communications 7*, 11776.

Tuxworth, W.J., Jr., Saghir, A.N., Spruill, L.S., Menick, D.R., and McDermott, P.J. (2004). Regulation of protein synthesis by eIF4E phosphorylation in adult

cardiocytes: the consequence of secondary structure in the 5'-untranslated region of mRNA. *The Biochemical Journal 378*, 73-82.

Valasek, L.S. (2012). 'Ribozoomin'--translation initiation from the perspective of the ribosome-bound eukaryotic initiation factors (eIFs). *Curr Protein Pept Sci 13*, 305-330.

Vallieres, C., and Avery, S.V. (2017). Metal-Based Combinations That Target Protein Synthesis by Fungi. *Adv Microb Physiol 70*, 105-121.

Vattem, K.M., and Wek, R.C. (2004). Reinitiation involving upstream ORFs regulates ATF4 mRNA translation in mammalian cells. *Proceedings of the National Academy of Sciences of the United States of America 101*, 11269-11274.

Ventoso, I., Sanz, M.A., Molina, S., Berlanga, J.J., Carrasco, L., and Esteban, M. (2006). Translational resistance of late alphavirus mRNA to eIF2alpha phosphorylation: a strategy to overcome the antiviral effect of protein kinase PKR. *Genes & Development 20*, 87-100.

Villa, N., Do, A., Hershey, J.W., and Fraser, C.S. (2013). Human eukaryotic initiation factor 4G (eIF4G) protein binds to eIF3c, -d, and -e to promote mRNA recruitment to the ribosome. *The Journal of Biological Chemistry 288*, 32932-32940.

von der Haar, T. (2008). A quantitative estimation of the global translational activity in logarithmically growing yeast cells. *BMC Syst Biol 2*, 87.

von der Haar, T., Gross, J.D., Wagner, G., and McCarthy, J.E. (2004). The mRNA cap-binding protein eIF4E in post-transcriptional gene expression. *Nature Structural & Molecular Biology 11*, 503-511.

Wang, R., Yoshida, K., Toki, T., Sawada, T., Uechi, T., Okuno, Y., Sato-Otsubo, A., Kudo, K., Kamimaki, I., Kanezaki, R., *et al.* (2015). Loss of function mutations in RPL27 and RPS27 identified by whole-exome sequencing in Diamond-Blackfan anaemia. *Br J Haematol 168*, 854-864.

Wortham, N.C., Martinez, M., Gordiyenko, Y., Robinson, C.V., and Proud, C.G. (2014). Analysis of the subunit organization of the eIF2B complex reveals new insights into its structure and regulation. *FASEB Journal : official publication of the Federation of American Societies for Experimental Biology 28*, 2225-2237.

Xue, S., and Barna, M. (2012). Specialized ribosomes: a new frontier in gene regulation and organismal biology. *Nature Reviews Molecular Cell Biology 13*, 355-369.

Young, D.J., Guydosh, N.R., Zhang, F., Hinnebusch, A.G., and Green, R. (2015). Rli1/ABCE1 Recycles Terminating Ribosomes and Controls Translation Reinitiation in 3'UTRs In Vivo. *Cell 162*, 872-884.

Yu, G., Wang, L.G., Han, Y., and He, Q.Y. (2012). clusterProfiler: an R package for comparing biological themes among gene clusters. *OMICS 16*, 284-287.

Yu, Y., Marintchev, A., Kolupaeva, V.G., Unbehaun, A., Veryasova, T., Lai, S.C., Hong, P., Wagner, G., Hellen, C.U., and Pestova, T.V. (2009). Position of eukaryotic translation initiation factor eIF1A on the 40S ribosomal subunit mapped by directed hydroxyl radical probing. *Nucleic Acids Research 37*, 5167-5182.

Appendix – Supplementary Materials

Appendix I- Pairwise algorithm (NCBI BLASTN) of mutants 1-8 sequencing Results

Mutant Δ1/ 3'UTR: Sequence ID: lcl|Query_185857Length: 558Number of Matches: 3
Range 1: 65 to 558GraphicsNext MatchPrevious Match

Score	Expect	Identities	Gaps	Strand
913 bits(494)	0.0	494/494(100%)	0/494(0%)	Plus/Plus

```
Query  21   TCGATGCGGTGGAATTTAGAGCCATCATTGAAAAAGTTAAGCAATTGCAACACTTGAAAG  80
            ||||||||||||||||||||||||||||||||||||||||||||||||||||||||||||
Sbjct  65   TCGATGCGGTGGAATTTAGAGCCATCATTGAAAAAGTTAAGCAATTGCAACACTTGAAAG  124

Query  81   AGGAAGAGTTTAACAGTCATCATGTTGGTCATTTCGGTCGTAGAAGATCTTCCCACCATC  140
            ||||||||||||||||||||||||||||||||||||||||||||||||||||||||||||
Sbjct  125  AGGAAGAGTTTAACAGTCATCATGTTGGTCATTTCGGTCGTAGAAGATCTTCCCACCATC  184

Query  141  ATGGTAGACCAAAGATTAAGCACAACAAGCCTAAGGTTACAACCGATTCAGATGGTTGGT  200
            ||||||||||||||||||||||||||||||||||||||||||||||||||||||||||||
Sbjct  185  ATGGTAGACCAAAGATTAAGCACAACAAGCCTAAGGTTACAACCGATTCAGATGGTTGGT  244

Query  201  GCACATTTGAAGCCAAGAAGAAGGGTAGTGGAGAAGATGATGAAGAAGAAACAGAAACCA  260
            ||||||||||||||||||||||||||||||||||||||||||||||||||||||||||||
Sbjct  245  GCACATTTGAAGCCAAGAAGAAGGGTAGTGGAGAAGATGATGAAGAAGAAACAGAAACCA  304

Query  261  CACCAACTTCTACTGTGCCAGTTGCTACCATTGCCCAAGAAACTTTAAAAGTCAAGCCAA  320
            ||||||||||||||||||||||||||||||||||||||||||||||||||||||||||||
Sbjct  305  CACCAACTTCTACTGTGCCAGTTGCTACCATTGCCCAAGAAACTTTAAAAGTCAAGCCAA  364

Query  321  ATAACAAAAATATTTCTTCCAACAGACCTGCTGATACCAGAGATATTGTTGCGGACAAGC  380
            ||||||||||||||||||||||||||||||||||||||||||||||||||||||||||||
Sbjct  365  ATAACAAAAATATTTCTTCCAACAGACCTGCTGATACCAGAGATATTGTTGCGGACAAGC  424

Query  381  CAATTCTTGGTTTCAACGCATTTGCTGCTTTGGAAAGTGAAGACGAAGACGACGAAGCAT  440
            ||||||||||||||||||||||||||||||||||||||||||||||||||||||||||||
Sbjct  425  CAATTCTTGGTTTCAACGCATTTGCTGCTTTGGAAAGTGAAGACGAAGACGACGAAGCAT  484

Query  441  CCGGAGACTACAAGGACGACGATGACAAAGATATCACCGGAGACTACAAGGACGACGATG  500
            ||||||||||||||||||||||||||||||||||||||||||||||||||||||||||||
Sbjct  485  CCGGAGACTACAAGGACGACGATGACAAAGATATCACCGGAGACTACAAGGACGACGATG  544

Query  501  ACAAAACCGGATAA  514
            ||||||||||||||
Sbjct  545  ACAAAACCGGATAA  558
```

Mutant Δ2/ 3'UTR: Sequence ID: lcl|Query_22925Length: 558Number of Matches: 4
Range 1: 127 to 558GraphicsNext MatchPrevious Match

Score	Expect	Identities	Gaps	Strand
798 bits(432)	0.0	432/432(100%)	0/432(0%)	Plus/Plus

```
Query  74   GAAGAGTTTAACAGTCATCATGTTGGTCATTTCGGTCGTAGAAGATCTTCCCACCATCAT  133
            ||||||||||||||||||||||||||||||||||||||||||||||||||||||||||||
Sbjct  127  GAAGAGTTTAACAGTCATCATGTTGGTCATTTCGGTCGTAGAAGATCTTCCCACCATCAT  186

Query  134  GGTAGACCAAAGATTAAGCACAACAAGCCTAAGGTTACAACCGATTCAGATGGTTGGTGC  193
            ||||||||||||||||||||||||||||||||||||||||||||||||||||||||||||
Sbjct  187  GGTAGACCAAAGATTAAGCACAACAAGCCTAAGGTTACAACCGATTCAGATGGTTGGTGC  246

Query  194  ACATTTGAAGCCAAGAAGAAGGGTAGTGGAGAAGATGATGAAGAAGAAACAGAAACCACA  253
            ||||||||||||||||||||||||||||||||||||||||||||||||||||||||||||
Sbjct  247  ACATTTGAAGCCAAGAAGAAGGGTAGTGGAGAAGATGATGAAGAAGAAACAGAAACCACA  306

Query  254  CCAACTTCTACTGTGCCAGTTGCTACCATTGCCCAAGAAACTTTAAAAGTCAAGCCAAAT  313
            ||||||||||||||||||||||||||||||||||||||||||||||||||||||||||||
Sbjct  307  CCAACTTCTACTGTGCCAGTTGCTACCATTGCCCAAGAAACTTTAAAAGTCAAGCCAAAT  366

Query  314  AACAAAAATATTTCTTCCAACAGACCTGCTGATACCAGAGATATTGTTGCGGACAAGCCA  373
            ||||||||||||||||||||||||||||||||||||||||||||||||||||||||||||
Sbjct  367  AACAAAAATATTTCTTCCAACAGACCTGCTGATACCAGAGATATTGTTGCGGACAAGCCA  426

Query  374  ATTCTTGGTTTCAACGCATTTGCTGCTTTGGAAAGTGAAGACGAAGACGACGAAGCATCC  433
            ||||||||||||||||||||||||||||||||||||||||||||||||||||||||||||
Sbjct  427  ATTCTTGGTTTCAACGCATTTGCTGCTTTGGAAAGTGAAGACGAAGACGACGAAGCATCC  486
```

```
Query  434  GGAGACTACAAGGACGACGATGACAAAGATATCACCGGAGACTACAAGGACGACGATGAC  493
            ||||||||||||||||||||||||||||||||||||||||||||||||||||||||||||
Sbjct  487  GGAGACTACAAGGACGACGATGACAAAGATATCACCGGAGACTACAAGGACGACGATGAC  546
Query  494  AAAACCGGATAA  505
            ||||||||||||
Sbjct  547  AAAACCGGATAA  558
```

Range 2: 1 to 68GraphicsNext MatchPrevious MatchFirst Match

Score	Expect	Identities	Gaps	Strand
106 bits(57)	6e-27	64/68(94%)	2/68(2%)	Plus/Plus

```
Query  10  ATGATC-NGTATACTATCGATGAGCTTTTTN-ACTGAAGCCAAGTTTAACTTTGGAAGTT  67
           ||||||  ||||||||||||||||||||||  ||||||||||||||||||||||||||||
Sbjct  1   ATGATCAAGTATACTATCGATGAGCTTTTTCAACTGAAGCCAAGTTTAACTTTGGAAGTT  60

Query  68  AATTTCGA  75
           ||||||||
Sbjct  61  AATTTCGA  68
```

Mutant Δ3/ 3'UTR: Sequence ID: lcl|Query_170549Length: 558Number of Matches: 4
Range 1: 187 to 558GraphicsNext MatchPrevious Match

Score	Expect	Identities	Gaps	Strand
688 bits(372)	0.0	372/372(100%)	0/372(0%)	Plus/Plus

```
Query  130  GGTAGACCAAAGATTAAGCACAACAAGCCTAAGGTTACAACCGATTCAGATGGTTGGTGC  189
            ||||||||||||||||||||||||||||||||||||||||||||||||||||||||||||
Sbjct  187  GGTAGACCAAAGATTAAGCACAACAAGCCTAAGGTTACAACCGATTCAGATGGTTGGTGC  246

Query  190  ACATTTGAAGCCAAGAAGAAGGGTAGTGGAGAAGATGATGAAGAAGAAACAGAAACCACA  249
            ||||||||||||||||||||||||||||||||||||||||||||||||||||||||||||
Sbjct  247  ACATTTGAAGCCAAGAAGAAGGGTAGTGGAGAAGATGATGAAGAAGAAACAGAAACCACA  306

Query  250  CCAACTTCTACTGTGCCAGTTGCTACCATTGCCCAAGAAACTTTAAAAGTCAAGCCAAAT  309
            ||||||||||||||||||||||||||||||||||||||||||||||||||||||||||||
Sbjct  307  CCAACTTCTACTGTGCCAGTTGCTACCATTGCCCAAGAAACTTTAAAAGTCAAGCCAAAT  366

Query  310  AACAAAAATATTTCTTCCAACAGACCTGCTGATACCAGAGATATTGTTGCGGACAAGCCA  369
            ||||||||||||||||||||||||||||||||||||||||||||||||||||||||||||
Sbjct  367  AACAAAAATATTTCTTCCAACAGACCTGCTGATACCAGAGATATTGTTGCGGACAAGCCA  426

Query  370  ATTCTTGGTTTCAACGCATTTGCTGCTTTGGAAAGTGAAGACGAAGACGACGAAGCATCC  429
            ||||||||||||||||||||||||||||||||||||||||||||||||||||||||||||
Sbjct  427  ATTCTTGGTTTCAACGCATTTGCTGCTTTGGAAAGTGAAGACGAAGACGACGAAGCATCC  486

Query  430  GGAGACTACAAGGACGACGATGACAAAGATATCACCGGAGACTACAAGGACGACGATGAC  489
            ||||||||||||||||||||||||||||||||||||||||||||||||||||||||||||
Sbjct  487  GGAGACTACAAGGACGACGATGACAAAGATATCACCGGAGACTACAAGGACGACGATGAC  546

Query  490  AAAACCGGATAA  501
            ||||||||||||
Sbjct  547  AAAACCGGATAA  558
```

Range 2: 9 to 127GraphicsNext MatchPrevious MatchFirst Match

Score	Expect	Identities	Gaps	Strand
213 bits(115)	3e-59	118/119(99%)	1/119(0%)	Plus/Plus

```
Query  13   GTATACTATCGATGAGCTTTTTC-ACTGAAGCCAAGTTTAACTTTGGAAGTTAATTTCGA  71
           ||||||||||||||||||||||| ||||||||||||||||||||||||||||||||||||
Sbjct  9    GTATACTATCGATGAGCTTTTTCAACTGAAGCCAAGTTTAACTTTGGAAGTTAATTTCGA  68

Query  72   TGCGGTGGAATTTAGAGCCATCATTGAAAAAGTTAAGCAATTGCAACACTTGAAAGAGG  130
           ||||||||||||||||||||||||||||||||||||||||||||||||||||||||||||
Sbjct  69   TGCGGTGGAATTTAGAGCCATCATTGAAAAAGTTAAGCAATTGCAACACTTGAAAGAGG  127
```

Mutant Δ4/ 3'UTR: Sequence ID: lcl|Query_43019Length: 558Number of Matches: 4
Related Information
Range 1: 247 to 558GraphicsNext MatchPrevious Match

Score	Expect	Identities	Gaps	Strand
577 bits(312)	1e-168	312/312(100%)	0/312(0%)	Plus/Plus

```
Query  178  ACATTTGAAGCCAAGAAGAAGGGTAGTGGAGAAGATGATGAAGAAGAAACAGAAACCACA  237
            ||||||||||||||||||||||||||||||||||||||||||||||||||||||||||||
Sbjct  247  ACATTTGAAGCCAAGAAGAAGGGTAGTGGAGAAGATGATGAAGAAGAAACAGAAACCACA  306

Query  238  CCAACTTCTACTGTGCCAGTTGCTACCATTGCCCAAGAAACTTTAAAAGTCAAGCCAAAT  297
            ||||||||||||||||||||||||||||||||||||||||||||||||||||||||||||
```

```
Sbjct  307  CCAACTTCTACTGTGCCAGTTGCTACCATTGCCCAAGAAACTTTAAAAGTCAAGCCAAAT  366


Query  298  AACAAAAATATTTCTTCCAACAGACCTGCTGATACCAGAGATATTGTTGCGGACAAGCCA  357
            ||||||||||||||||||||||||||||||||||||||||||||||||||||||||||||
Sbjct  367  AACAAAAATATTTCTTCCAACAGACCTGCTGATACCAGAGATATTGTTGCGGACAAGCCA  426

Query  358  ATTCTTGGTTTCAACGCATTTGCTGCTTTGGAAAGTGAAGACGAAGACGACGAAGCATCC  417
            ||||||||||||||||||||||||||||||||||||||||||||||||||||||||||||
Sbjct  427  ATTCTTGGTTTCAACGCATTTGCTGCTTTGGAAAGTGAAGACGAAGACGACGAAGCATCC  486

Query  418  GGAGACTACAAGGACGACGATGACAAAGATATCACCGGAGACTACAAGGACGACGATGAC  477
            ||||||||||||||||||||||||||||||||||||||||||||||||||||||||||||
Sbjct  487  GGAGACTACAAGGACGACGATGACAAAGATATCACCGGAGACTACAAGGACGACGATGAC  546

Query  478  AAAACCGGATAA  489
            ||||||||||||
Sbjct  547  AAAACCGGATAA  558
```

Range 2: 9 to 186Graphics Next Match Previous Match First Match

Score	Expect	Identities	Gaps	Strand
322 bits(174)	5e-92	177/178(99%)	1/178(0%)	Plus/Plus

```
Query  1    GTATACTATCGATGAGCTTTTTC-ACTGAAGCCAAGTTTAACTTTGGAAGTTAATTTCGA  59
            ||||||||||||||||||||||| ||||||||||||||||||||||||||||||||||||
Sbjct  9    GTATACTATCGATGAGCTTTTTCAACTGAAGCCAAGTTTAACTTTGGAAGTTAATTTCGA  68

Query  60   TGCGGTGGAATTTAGAGCCATCATTGAAAAAGTTAAGCAATTGCAACACTTGAAAGAGGA  119
            ||||||||||||||||||||||||||||||||||||||||||||||||||||||||||||
Sbjct  69   TGCGGTGGAATTTAGAGCCATCATTGAAAAAGTTAAGCAATTGCAACACTTGAAAGAGGA  128

Query  120  AGAGTTTAACAGTCATCATGTTGGTCATTTCGGTCGTAGAAGATCTTCCCACCATCAT  177
            ||||||||||||||||||||||||||||||||||||||||||||||||||||||||||
Sbjct  129  AGAGTTTAACAGTCATCATGTTGGTCATTTCGGTCGTAGAAGATCTTCCCACCATCAT  186
```

Mutant Δ5/ 3'UTR: Sequence ID: lcl|Query_212353Length: 558Number of Matches: 4
Related Information
Range 1: 247 to 558Graphics Next Match Previous Match

Score	Expect	Identities	Gaps	Strand
577 bits(312)	1e-168	312/312(100%)	0/312(0%)	Plus/Plus

```
Query  178  ACATTTGAAGCCAAGAAGAAGGGTAGTGGAGAAGATGATGAAGAAGAAACAGAAACCACA  237
            ||||||||||||||||||||||||||||||||||||||||||||||||||||||||||||
Sbjct  247  ACATTTGAAGCCAAGAAGAAGGGTAGTGGAGAAGATGATGAAGAAGAAACAGAAACCACA  306

Query  238  CCAACTTCTACTGTGCCAGTTGCTACCATTGCCCAAGAAACTTTAAAAGTCAAGCCAAAT  297
            ||||||||||||||||||||||||||||||||||||||||||||||||||||||||||||
Sbjct  307  CCAACTTCTACTGTGCCAGTTGCTACCATTGCCCAAGAAACTTTAAAAGTCAAGCCAAAT  366

Query  298  AACAAAAATATTTCTTCCAACAGACCTGCTGATACCAGAGATATTGTTGCGGACAAGCCA  357
            ||||||||||||||||||||||||||||||||||||||||||||||||||||||||||||
Sbjct  367  AACAAAAATATTTCTTCCAACAGACCTGCTGATACCAGAGATATTGTTGCGGACAAGCCA  426

Query  358  ATTCTTGGTTTCAACGCATTTGCTGCTTTGGAAAGTGAAGACGAAGACGACGAAGCATCC  417
            ||||||||||||||||||||||||||||||||||||||||||||||||||||||||||||
Sbjct  427  ATTCTTGGTTTCAACGCATTTGCTGCTTTGGAAAGTGAAGACGAAGACGACGAAGCATCC  486

Query  418  GGAGACTACAAGGACGACGATGACAAAGATATCACCGGAGACTACAAGGACGACGATGAC  477
            ||||||||||||||||||||||||||||||||||||||||||||||||||||||||||||
Sbjct  487  GGAGACTACAAGGACGACGATGACAAAGATATCACCGGAGACTACAAGGACGACGATGAC  546

Query  478  AAAACCGGATAA  489
            ||||||||||||
Sbjct  547  AAAACCGGATAA  558
```

Range 2: 9 to 186Graphics Next Match Previous Match First Match

Score	Expect	Identities	Gaps	Strand
322 bits(174)	5e-92	177/178(99%)	1/178(0%)	Plus/Plus

```
Query  1    GTATACTATCGATGAGCTTTTTC-ACTGAAGCCAAGTTTAACTTTGGAAGTTAATTTCGA  59
            ||||||||||||||||||||||| ||||||||||||||||||||||||||||||||||||
Sbjct  9    GTATACTATCGATGAGCTTTTTCAACTGAAGCCAAGTTTAACTTTGGAAGTTAATTTCGA  68

Query  60   TGCGGTGGAATTTAGAGCCATCATTGAAAAAGTTAAGCAATTGCAACACTTGAAAGAGGA  119
            ||||||||||||||||||||||||||||||||||||||||||||||||||||||||||||
Sbjct  69   TGCGGTGGAATTTAGAGCCATCATTGAAAAAGTTAAGCAATTGCAACACTTGAAAGAGGA  128
```

```
Query  120  AGAGTTTAACAGTCATCATGTTGGTCATTTCGGTCGTAGAAGATCTTCCCACCATCAT  177
            ||||||||||||||||||||||||||||||||||||||||||||||||||||||||||
Sbjct  129  AGAGTTTAACAGTCATCATGTTGGTCATTTCGGTCGTAGAAGATCTTCCCACCATCAT  186
```

Mutant Δ6/ 3'UTR:

Sequence ID: lcl|Query_149539Length: 558Number of Matches: 4

Related Information

Range 1: 9 to 306GraphicsNext MatchPrevious Match

Score	Expect	Identities	Gaps	Strand
551 bits(298)	6e-161	298/298(100%)	0/298(0%)	Plus/Plus

```
Query  1    GTATACTATCGATGAGCTTTTTCAACTGAAGCCAAGTTTAACTTTGGAAGTTAATTTCGA  60
            ||||||||||||||||||||||||||||||||||||||||||||||||||||||||||||
Sbjct  9    GTATACTATCGATGAGCTTTTTCAACTGAAGCCAAGTTTAACTTTGGAAGTTAATTTCGA  68

Query  61   TGCGGTGGAATTTAGAGCCATCATTGAAAAAGTTAAGCAATTGCAACACTTGAAAGAGGA  120
            ||||||||||||||||||||||||||||||||||||||||||||||||||||||||||||
Sbjct  69   TGCGGTGGAATTTAGAGCCATCATTGAAAAAGTTAAGCAATTGCAACACTTGAAAGAGGA  128

Query  121  AGAGTTTAACAGTCATCATGTTGGTCATTTCGGTCGTAGAAGATCTTCCCACCATCATGG  180
            ||||||||||||||||||||||||||||||||||||||||||||||||||||||||||||
Sbjct  129  AGAGTTTAACAGTCATCATGTTGGTCATTTCGGTCGTAGAAGATCTTCCCACCATCATGG  188

Query  181  TAGACCAAAGATTAAGCACAACAAGCCTAAGGTTACAACCGATTCAGATGGTTGGTGCAC  240
            ||||||||||||||||||||||||||||||||||||||||||||||||||||||||||||
Sbjct  189  TAGACCAAAGATTAAGCACAACAAGCCTAAGGTTACAACCGATTCAGATGGTTGGTGCAC  248

Query  241  ATTTGAAGCCAAGAAGAAGGGTAGTGGAGAAGATGATGAAGAAGAAACAGAAACCACA  298
            ||||||||||||||||||||||||||||||||||||||||||||||||||||||||||
Sbjct  249  ATTTGAAGCCAAGAAGAAGGGTAGTGGAGAAGATGATGAAGAAGAAACAGAAACCACA  306
```

Range 2: 367 to 558GraphicsNext MatchPrevious MatchFirst Match

Score	Expect	Identities	Gaps	Strand
355 bits(192)	5e-102	192/192(100%)	0/192(0%)	Plus/Plus

```
Query  299  AACAAAAATATTTCTTCCAACAGACCTGCTGATACCAGAGATATTGTTGCGGACAAGCCA  358
            ||||||||||||||||||||||||||||||||||||||||||||||||||||||||||||
Sbjct  367  AACAAAAATATTTCTTCCAACAGACCTGCTGATACCAGAGATATTGTTGCGGACAAGCCA  426

Query  359  ATTCTTGGTTTCAACGCATTTGCTGCTTTGGAAAGTGAAGACGAAGACGACGAAGCATCC  418
            ||||||||||||||||||||||||||||||||||||||||||||||||||||||||||||
Sbjct  427  ATTCTTGGTTTCAACGCATTTGCTGCTTTGGAAAGTGAAGACGAAGACGACGAAGCATCC  486

Query  419  GGAGACTACAAGGACGACGATGACAAAGATATCACCGGAGACTACAAGGACGACGATGAC  478
            ||||||||||||||||||||||||||||||||||||||||||||||||||||||||||||
Sbjct  487  GGAGACTACAAGGACGACGATGACAAAGATATCACCGGAGACTACAAGGACGACGATGAC  546

Query  479  AAAACCGGATAA  490
            ||||||||||||
Sbjct  547  AAAACCGGATAA  558
```

Mutant Δ7/ 3'UTR: Sequence ID: lcl|Query_116751Length: 558Number of Matches: 4

Related Information

Range 1: 2 to 367GraphicsNext MatchPrevious Match

Score	Expect	Identities	Gaps	Strand
669 bits(362)	0.0	365/366(99%)	1/366(0%)	Plus/Plus

```
Query  10   TGATC-AGTATACTATCGATGAGCTTTTTCAACTGAAGCCAAGTTTAACTTTGGAAGTTA  68
            ||||| ||||||||||||||||||||||||||||||||||||||||||||||||||||||
Sbjct  2    TGATCAAGTATACTATCGATGAGCTTTTTCAACTGAAGCCAAGTTTAACTTTGGAAGTTA  61

Query  69   ATTTCGATGCGGTGGAATTTAGAGCCATCATTGAAAAAGTTAAGCAATTGCAACACTTGA  128
            ||||||||||||||||||||||||||||||||||||||||||||||||||||||||||||
Sbjct  62   ATTTCGATGCGGTGGAATTTAGAGCCATCATTGAAAAAGTTAAGCAATTGCAACACTTGA  121

Query  129  AAGAGGAAGAGTTTAACAGTCATCATGTTGGTCATTTCGGTCGTAGAAGATCTTCCCACC  188
            ||||||||||||||||||||||||||||||||||||||||||||||||||||||||||||
Sbjct  122  AAGAGGAAGAGTTTAACAGTCATCATGTTGGTCATTTCGGTCGTAGAAGATCTTCCCACC  181

Query  189  ATCATGGTAGACCAAAGATTAAGCACAACAAGCCTAAGGTTACAACCGATTCAGATGGTT  248
            ||||||||||||||||||||||||||||||||||||||||||||||||||||||||||||
Sbjct  182  ATCATGGTAGACCAAAGATTAAGCACAACAAGCCTAAGGTTACAACCGATTCAGATGGTT  241

Query  249  GGTGCACATTTGAAGCCAAGAAGAAGGGTAGTGGAGAAGATGATGAAGAAGAAACAGAAA  308
            ||||||||||||||||||||||||||||||||||||||||||||||||||||||||||||
Sbjct  242  GGTGCACATTTGAAGCCAAGAAGAAGGGTAGTGGAGAAGATGATGAAGAAGAAACAGAAA  301

Query  309  CCACACCAACTTCTACTGTGCCAGTTGCTACCATTGCCCAAGAAACTTTAAAAGTCAAGC  368
```

```
            ||||||||||||||||||||||||||||||||||||||||||||||||||||||||||||||||
Sbjct  302  CCACACCAACTTCTACTGTGCCAGTTGCTACCATTGCCCAAGAAACTTTAAAAGTCAAGC  361

Query  369  CAAATA  374
            ||||||
Sbjct  362  CAAATA  367
```

Range 2: 427 to 558Graphics Next Match Previous Match First Match

Score	Expect	Identities	Gaps	Strand
244 bits(132)	1e-68	132/132(100%)	0/132(0%)	Plus/Plus

```
Query  374  ATTCTTGGTTTCAACGCATTTGCTGCTTTGGAAAGTGAAGACGAAGACGACGAAGCATCC  433
            ||||||||||||||||||||||||||||||||||||||||||||||||||||||||||||||||
Sbjct  427  ATTCTTGGTTTCAACGCATTTGCTGCTTTGGAAAGTGAAGACGAAGACGACGAAGCATCC  486

Query  434  GGAGACTACAAGGACGACGATGACAAAGATATCACCGGAGACTACAAGGACGACGATGAC  493
            ||||||||||||||||||||||||||||||||||||||||||||||||||||||||||||||||
Sbjct  487  GGAGACTACAAGGACGACGATGACAAAGATATCACCGGAGACTACAAGGACGACGATGAC  546

Query  494  AAAACCGGATAA  505
            ||||||||||||
Sbjct  547  AAAACCGGATAA  558
```

Mutant Δ8/ 3'UTR: Sequence ID: lcl|Query_54031Length: 558Number of Matches: 4
Related Information
Range 1: 8 to 426Graphics Next Match Previous Match

Score	Expect	Identities	Gaps	Strand
767 bits(415)	0.0	418/419(99%)	1/419(0%)	Plus/Plus

```
Query  16   AGTATACTATCGATGAGCTTTTTC-ACTGAAGCCAAGTTTAACTTTGGAAGTTAATTTCG  74
            ||||||||||||||||||||||| ||||||||||||||||||||||||||||||||||||
Sbjct  8    AGTATACTATCGATGAGCTTTTTCAACTGAAGCCAAGTTTAACTTTGGAAGTTAATTTCG  67

Query  75   ATGCGGTGGAATTTAGAGCCATCATTGAAAAAGTTAAGCAATTGCAACACTTGAAAGAGG  134
            ||||||||||||||||||||||||||||||||||||||||||||||||||||||||||||||||
Sbjct  68   ATGCGGTGGAATTTAGAGCCATCATTGAAAAAGTTAAGCAATTGCAACACTTGAAAGAGG  127

Query  135  AAGAGTTTAACAGTCATCATGTTGGTCATTTCGGTCGTAGAAGATCTTCCCACCATCATG  194
            ||||||||||||||||||||||||||||||||||||||||||||||||||||||||||||||||
Sbjct  128  AAGAGTTTAACAGTCATCATGTTGGTCATTTCGGTCGTAGAAGATCTTCCCACCATCATG  187

Query  195  GTAGACCAAAGATTAAGCACAACAAGCCTAAGGTTACAACCGATTCAGATGGTTGGTGCA  254
            ||||||||||||||||||||||||||||||||||||||||||||||||||||||||||||||||
Sbjct  188  GTAGACCAAAGATTAAGCACAACAAGCCTAAGGTTACAACCGATTCAGATGGTTGGTGCA  247

Query  255  CATTTGAAGCCAAGAAGAAGGGTAGTGGAGAAGATGATGAAGAAGAAACAGAAACCACAC  314
            ||||||||||||||||||||||||||||||||||||||||||||||||||||||||||||||||
Sbjct  248  CATTTGAAGCCAAGAAGAAGGGTAGTGGAGAAGATGATGAAGAAGAAACAGAAACCACAC  307

Query  315  CAACTTCTACTGTGCCAGTTGCTACCATTGCCCAAGAAACTTTAAAAGTCAAGCCAAATA  374
            ||||||||||||||||||||||||||||||||||||||||||||||||||||||||||||||||
Sbjct  308  CAACTTCTACTGTGCCAGTTGCTACCATTGCCCAAGAAACTTTAAAAGTCAAGCCAAATA  367

Query  375  ACAAAAATATTTCTTCCAACAGACCTGCTGATACCAGAGATATTGTTGCGGACAAGCCA  433
            ||||||||||||||||||||||||||||||||||||||||||||||||||||||||||||||||
Sbjct  368  ACAAAAATATTTCTTCCAACAGACCTGCTGATACCAGAGATATTGTTGCGGACAAGCCA  426
```

Range 2: 475 to 558Graphics Next Match Previous Match First Match

Score	Expect	Identities	Gaps	Strand
145 bits(78)	1e-38	83/85(98%)	2/85(2%)	Plus/Plus

```
Query  425  GAC-AAGCCATCCGGAGACTACAAGGACGACGATGACAAAGATATCACCGGAGACTACAA  483
            ||| ||| ||||||||||||||||||||||||||||||||||||||||||||||||||||||||
Sbjct  475  GACGAAG-CATCCGGAGACTACAAGGACGACGATGACAAAGATATCACCGGAGACTACAA  533

Query  484  GGACGACGATGACAAAACCGGATAA  508
            |||||||||||||||||||||||||
Sbjct  534  GGACGACGATGACAAAACCGGATAA  558
```

Appendix II – Tables of Mass Spectrometry identified proteins of total extract crosslinking and GO Analysis

			XL WT	XL WT		XL Δ4	XL Δ4		XL M2	XL M2		XL ΔAC	XL ΔAC		no.XL		
		Identified proteins	No. of Peptides	**log2 XL/nXL**	**se**	No of Peptides	**Log Δ4/WT**	**se**	No of Peptides	Log2 M2/WT	se	No of Peptidea	Log2 AC/WT	se	No of Peptides	no.X L-WT	Groups
1	SVF1	Svf1p OS=Saccharomyces cerevisiae YJM993 GN=SVF1 PE=4 SV=1	28	**8.1**	0.33	0.1	**-8.1**	0.00	13	-1.11	1.20	36	0.36	0.00	0.1	-8.1	group I
2	CKA1	**Cka1p OS=Saccharomyces cerevisiae YJM993 GN=CKA1 PE=3 SV=1**	25	**8.0**	0.33	0.1	**-8.0**	0.00	37	0.57	2.91	9	-1.47	1.50	0.1	-8.0	group I
3	SKY1	Sky1p OS=Saccharomyces cerevisiae YJM320 GN=SKY1 PE=4 SV=1	22	**7.8**	2.33	0.1	**-7.8**	0.00	9	-1.29	0.58	59	1.42	2.40	0.1	-7.8	group I
4	IDP1	Isocitrate dehydrogenase [NADP] OS=Saccharomyces cerevisiae YJM993 GN=IDP1 PE=3 SV=1	20	**7.6**	1.45	0.1	**-7.6**	0.00	19	-0.07	0.33	37	0.89	2.60	0.1	-7.6	group I
5	PDI1	Pdi1p OS=Saccharomyces cerevisiae YJM993 GN=PDI1 PE=4 SV=1	19	**7.6**	1.45	7	**-1.4**	0.33	39	1.04	1.00	75	1.98	1.00	0.1	-7.6	group I
6	CPS1	Cps1p OS=Saccharomyces cerevisiae YJM1083 GN=CPS1 PE=4 SV=1	18	**7.5**	1.15	0.1	**-7.5**	0.00	25	0.47	1.33	15	-0.26	1.15	0.1	-7.5	group I
7	CKA2	Cka2p OS=Saccharomyces cerevisiae YJM993 GN=CKA2 PE=3 SV=1	18	**7.5**	1.53	0.1	**-7.5**	0.00	24	0.42	0.58	2	-3.17	0.00	0.1	-7.5	group I
8	TOM1	**Tom1p OS=Saccharomyces cerevisiae YJM326 GN=TOM1 PE=4 SV=1**	14	**7.1**	0.33	0.1	**-7.1**	0.00	10	-0.49	1.33	14	0.00	0.88	0.1	-7.1	group I
9	YGR017W	Uncharacterized protein OS=Saccharomyces cerevisiae YJM689 GN=H769_YJM689G00273 PE=4 SV=1(SYNTHEMATIC NAME= YGR017W)	12	**6.9**	0.00	0.1	**-6.9**	0.00	2	-2.58	0.00	17	0.50	0.33	0.1	-6.9	group I
10	CUB1	Uncharacterized protein OS=Saccharomyces cerevisiae YJM993 GN=H779_YJM993P00020 PE=4 SV=1 (gn = CUB1 OR YPL260W)	12	**6.9**	0.00	0.1	**-6.9**	0.00	0.1	-6.91	0.00	0.1	-6.91	0.00	0.1	-6.9	group I
11	DHH1	Dhh1p OS=Saccharomyces cerevisiae YJM993 GN=DHH1 PE=3 SV=1	11	**6.8**	2.50	5	**-1.1**	0.50	21	0.93	1.00	9	-0.29	0.58	0.1	-6.8	group I
12	SEC2	Sec2p OS=Saccharomyces cerevisiae YJM1460 GN=SEC2 PE=4 SV=1	11	**6.8**	0.67	0.1	**-6.8**	0.00	2	-2.46	0.00	11	0.00	0.33	0.1	-6.8	group I
13	Tps1	Alpha,alpha-trehalose-phosphate synthase (UDP-forming) OS=Saccharomyces cerevisiae P301 GN=Tps1 PE=3 SV=1	10	**6.6**	1.33	0.1	**-6.6**	0.00	5	-1.00	0.50	5	-1.00	0.50	0.1	-6.6	group I
14	GLC7	Serine/threonine-protein phosphatase OS=Saccharomyces cerevisiae YJM1078 GN=GLC7 PE=3 SV=1	10	**6.6**	1.00	2	**-2.3**	0.00	8	-0.32	0.67	13	0.38	0.88	0.1	-6.6	group I
15	UBP1	Ubp1p OS=Saccharomyces cerevisiae YJM993 GN=UBP1 PE=4 SV=1	10	**6.6**	0.88	0.1	**-6.6**	0.00	2	-2.32	0.00	12	0.26	1.15	0.1	-6.6	group I

16	TUF1	Elongation factor Tu OS=Saccharomyces cerevisiae (strain FostersB) GN=FOSTERSB_4483 PE=3 SV=1	9	**6.5**	2.50	0.1	**-6.5**	0.00	2	-2.17	0.00	0.1	-6.49	0.00	0.1	-6.5	group I
17	HRK1	Hrk1p OS=Saccharomyces cerevisiae YJM1252 GN=HRK1 PE=4 SV=1	9	**6.5**	0.00	0.1	**-6.5**	0.00	12	0.42	0.58	4	-1.17	0.00	0.1	-6.5	group I
18	PRO1	Pro1p OS=Saccharomyces cerevisiae YJM993 GN=PRO1 PE=3 SV=1	8	**6.3**	2.00	2	**-2.0**	0.00	0.1	-6.32	0.00	6	-0.42	0.00	0.1	-6.3	group I
19	PRO2	Pro2p OS=Saccharomyces cerevisiae YJM993 GN=PRO2 PE=3 SV=1	8	**6.3**	1.00	3	**-1.4**	0.00	7	-0.19	0.50	11	0.46	0.88	0.1	-6.3	group I
20	ESS1	Peptidyl-prolyl cis-trans isomerase ESS1 OS=Saccharomyces cerevisiae (strain ATCC 204508 / S288c) GN=ESS1 PE=1 SV=3	8	**6.3**	1.00	0.1	**-6.3**	0.00	7	-0.19	0.50	16	1.00	1.33	0.1	-6.3	group I
21	SRM1	Srm1p OS=Saccharomyces cerevisiae YJM993 GN=SRM1 PE=4 SV=1	8	**6.3**	1.00	0.1	**-6.3**	0.00	0.1	-6.32	0.00	11	0.46	0.88	0.1	-6.3	group I
22	Spt6	Spt6p OS=Saccharomyces cerevisiae (strain CEN.PK113-7D) GN=CENPK1137D_3083 PE=4 SV=1	7	**6.1**	1.50	3	**-1.2**	0.00	8	0.19	0.33	2	-1.81	0.00	0.1	-6.1	group I
23	YDJ1	Mitochondrial protein import protein MAS5 OS=Saccharomyces cerevisiae (strain ATCC 204508 / S288c) GN=YDJ1 PE=1 SV=1	7	**6.1**	1.50	3	**-1.2**	0.00	9	0.36	0.58	2	-1.81	0.00	0.1	-6.1	group I
24	DRE2	Fe-S cluster assembly protein DRE2 OS=Saccharomyces cerevisiae YJM1083 GN=DRE2 PE=3 SV=1	7	**6.1**	0.50	0.1	**-6.1**	0.00	0.1	-6.13	0.00	23	1.72	0.67	0.1	-6.1	group I
25	HYP2	Eukaryotic translation initiation factor 5A OS=Saccharomyces cerevisiae YJM993 GN=HYP2 PE=3 SV=1	7	**6.1**	0.33	8	**0.2**	0.33	10	0.51	0.33	11	0.65	0.33	0.1	-6.1	group I
26	Ncl1	Ncl1p OS=Saccharomyces cerevisiae (strain Zymaflore VL3) GN=VL3_0138 PE=4 SV=1	7	**6.1**	0.50	2	**-1.8**	0.00	6	-0.22	0.00	15	1.10	1.53	0.1	-6.1	group I
27	VAS1	Vas1p OS=Saccharomyces cerevisiae YJM993 GN=VAS1 PE=3 SV=1	6	**5.9**	1.00	2	**-1.6**	0.00	16	1.42	0.88	13	1.12	0.88	0.1	-5.9	group I
28	Zpr1	Zpr1p OS=Saccharomyces cerevisiae (strain Lalvin QA23) GN=QA23_1952 PE=4 SV=1	6	**5.9**	1.00	3	**-1.0**	0.00	11	0.87	0.33	12	1.00	0.58	0.1	-5.9	group I
29	RPS10B	Rps10bp OS=Saccharomyces cerevisiae YJM993 GN=RPS10B PE=4 SV=1	6	**5.9**	1.00	8	**0.4**	0.33	7	0.22	0.33	0.1	-5.91	0.00	0.1	-5.9	group I
30	Wrs1	Wrs1p OS=Saccharomyces cerevisiae P301 GN=Wrs1 PE=3 SV=1	6	**5.9**	1.00	4	**-0.6**	0.00	5	-0.26	0.50	0.1	-5.91	0.00	0.1	-5.9	group I
31	RPN5	Rpn5p OS=Saccharomyces cerevisiae YJM993 GN=RPN5 PE=4 SV=1	6	**5.9**	1.00	5	**-0.3**	0.50	2	-1.58	0.00	0.1	-5.91	0.00	0.1	-5.9	group I
32	ILV1	Threonine dehydratase OS=Saccharomyces cerevisiae YJM993 GN=ILV1 PE=3 SV=1	6	**5.9**	1.00	3	**-1.0**	0.00	2	-1.58	0.00	0.1	-5.91	0.00	0.1	-5.9	group I

33	PRS3	Prs3p OS=Saccharomyces cerevisiae YJM993 GN=PRS3 PE=4 SV=1	6	**5.9**	0.00	6	**0.0**	0.00	2	-1.58	0.00	0.1	-5.91	0.00	0.1	-5.9	group I
34	TRP2	Trp2p OS=Saccharomyces cerevisiae YJM993 GN=TRP2 PE=4 SV=1	5	**5.6**	0.50	3	**-0.7**	0.00	5	0.00	0.50	16	1.68	0.88	0.1	-5.6	group I
35	SUI2	Sui2p OS=Saccharomyces cerevisiae YJM993 GN=SUI2 PE=4 SV=1	5	**5.6**	0.50	3	**-0.7**	0.00	8	0.68	0.33	2	-1.32	0.00	0.1	-5.6	group I
36	ASP1	Asp1p OS=Saccharomyces cerevisiae YJM993 GN=ASP1 PE=3 SV=1	5	**5.6**	0.50	2	**-1.3**	0.00	9	0.85	1.00	15	1.58	1.15	0.1	-5.6	group I
37	PRS1	Prs1p OS=Saccharomyces cerevisiae YJM993 GN=PRS1 PE=4 SV=1	5	**5.6**	0.50	0.1	**-5.6**	0.00	9	0.85	0.00	3	-0.74	0.00	0.1	-5.6	group I
38	GVP36	Gvp36p OS=Saccharomyces cerevisiae YJM1078 GN=GVP36 PE=4 SV=1	5	**5.6**	0.50	2	**-1.3**	0.00	8	0.68	0.67	5	0.00	0.50	0.1	-5.6	group I
39	SAM2	S-adenosylmethionine synthase OS=Saccharomyces cerevisiae YJM993 GN=SAM2 PE=3 SV=1	5	**5.6**	0.50	5	**0.0**	0.50	6	0.26	1.00	2	-1.32	0.00	0.1	-5.6	group I
40	SNF4	Snf4p OS=Saccharomyces cerevisiae YJM993 GN=SNF4 PE=4 SV=1	5	**5.6**	0.50	2	**-1.3**	0.00	12	1.26	0.58	10	1.00	0.33	0.1	-5.6	group I
41	SBA1	Sba1p OS=Saccharomyces cerevisiae YJM193 GN=SBA1 PE=4 SV=1	5	**5.6**	0.50	0.1	**-5.6**	0.00	0.1	-5.64	0.00	11	1.14	0.33	0.1	-5.6	group I
42	DET1	Det1p OS=Saccharomyces cerevisiae YJM993 GN=DET1 PE=4 SV=1	5	**5.6**	0.50	0.1	**-5.6**	0.00	0.1	-5.64	0.00	13	1.38	0.88	0.1	-5.6	group I
43	ILS1	Ils1p OS=Saccharomyces cerevisiae YJM1401 GN=ILS1 PE=3 SV=1	41	**3.8**	4.06	48	**0.2**	2.65	63	0.62	1.15	47	0.20	2.19	3	-3.8	group II
44	MMS1	E3 ubiquitin-protein ligase linker protein MMS1 OS=Saccharomyces cerevisiae (strain ATCC 204508 / S288c) GN=MMS1 PE=1 SV=1	17	**3.1**	3.18	0.1	**-7.4**	0.00	29	0.77	0.88	0.1	-7.41	0.00	2	-3.1	group II
45	RPL1B	Ribosomal protein OS=Saccharomyces cerevisiae YJM993 GN=RPL1B PE=3 SV=1	16	**3.0**	1.20	16	**0.0**	0.33	14	-0.19	0.88	5	-1.68	0.50	2	-3.0	group II
46	BMH1	Bmh1p OS=Saccharomyces cerevisiae YJM993 GN=BMH1 PE=3 SV=1	13	**2.7**	0.67	10	**-0.4**	0.33	19	0.55	0.88	35	1.43	1.76	2	-2.7	group II
47	ARG1	Arg1p OS=Saccharomyces cerevisiae YJM993 GN=ARG1 PE=3 SV=1	17	**2.5**	2.50	17	**0.0**	0.67	22	0.37	0.88	23	0.44	1.45	3	-2.5	group II
48	PAB1	Polyadenylate-binding protein OS=Saccharomyces cerevisiae YJM993 GN=PAB1 PE=3 SV=1	11	**2.5**	1.20	8	**-0.5**	0.00	14	0.35	0.88	10	-0.14	0.33	2	-2.5	group II
49	PSA1	Psa1p OS=Saccharomyces cerevisiae YJM993 GN=PSA1 PE=4 SV=1	10	**2.3**	3.00	11	**0.1**	0.50	13	0.38	1.45	4	-1.32	0.00	2	-2.3	group II
50	Snf1	Snf1p OS=Saccharomyces cerevisiae (strain FostersO) GN=FOSTERSO_0987 PE=4 SV=1	10	**2.3**	0.33	0.1	**-6.6**	0.00	22	1.14	0.67	20	1.00	0.88	2	-2.3	group II
51	ILV3	Ilv3p OS=Saccharomyces cerevisiae YJM993 GN=ILV3 PE=3 SV=1	10	**2.3**	0.67	0.1	**-6.6**	0.00	5	-1.00	0.50	22	1.14	0.33	2	-2.3	group II

52	GRS1	Grs1p OS=Saccharomyces cerevisiae YJM993 GN=GRS1 PE=4 SV=1	13	**2.1**	2.50	3	**-2.1**	0.00	19	0.55	1.33	14	0.11	0.33	3	-2.1	group II
53	GND1	6-phosphogluconate dehydrogenase, decarboxylating 1 OS=Saccharomyces cerevisiae (strain ATCC 204508 / S288c) GN=GND1 PE=1 SV=1	16	**2.0**	2.40	7	**-1.2**	0.50	18	0.17	0.58	21	0.39	2.00	4	-2.0	group II
54	RNA1	Rna1p OS=Saccharomyces cerevisiae YJM993 GN=RNA1 PE=4 SV=1	8	**2.0**	1.00	15	**0.9**	0.00	10	0.32	0.33	4	-1.00	0.00	2	-2.0	group II
55	GGA2	Gga2p OS=Saccharomyces cerevisiae YJM993 GN=GGA2 PE=4 SV=1	8	**2.0**	1.00	2	**-2.0**	0.00	2	-2.00	0.00	0.1	-6.32	0.00	2	-2.0	group II
56	IMD3	Inosine-5'-monophosphate dehydrogenase OS=Saccharomyces cerevisiae YJM993 GN=IMD3 PE=3 SV=1	8	**2.0**	0.00	14	**0.8**	0.88	27	1.75	0.00	16	1.00	1.76	2	-2.0	group II
57	THR1	Thr1p OS=Saccharomyces cerevisiae YJM993 GN=THR1 PE=3 SV=1	8	**2.0**	0.67	5	**-0.7**	0.50	9	0.17	0.58	0.1	-6.32	0.00	2	-2.0	group II
58	NSR1	Nsr1p OS=Saccharomyces cerevisiae YJM1383 GN=NSR1 PE=4 SV=1	30	**1.9**	2.52	0.1	**-8.2**	0.00	32	0.09	1.45	21	-0.51	3.21	8	-1.9	group II
59	ADE12	Adenylosuccinate synthetase OS=Saccharomyces cerevisiae (strain FostersB) GN=FOSTERSB_3936 PE=3 SV=1 (GN = ADE12, system name =YNL220W)	7	**1.8**	1.50	6	**-0.2**	0.00	7	0.00	0.33	0.1	-6.13	0.00	2	-1.8	group II
60	GLY1	Gly1p OS=Saccharomyces cerevisiae YJM993 GN=GLY1 PE=4 SV=1	7	**1.8**	0.33	3	**-1.2**	0.00	2	-1.81	0.00	13	0.89	0.33	2	-1.8	group II
61	SCP160	Scp160p OS=Saccharomyces cerevisiae YJM993 GN=SCP160 PE=4 SV=1	20	**1.7**	7.00	5	**-2.0**	0.50	14	-0.51	0.33	7	-1.51	0.50	6	-1.7	group II
62	UGP1	Ugp1p OS=Saccharomyces cerevisiae YJM993 GN=UGP1 PE=4 SV=1	58	**1.6**	3.93	20	**-1.5**	0.67	68	0.23	2.33	102	0.81	3.06	19	-1.6	group II
63	YKT6	Ykt6p OS=Saccharomyces cerevisiae YJM993 GN=YKT6 PE=4 SV=1	9	**1.6**	2.50	12	**0.4**	4.00	13	0.53	0.50	8	-0.17	0.33	3	-1.6	group II
64	ARO8	Aro8p OS=Saccharomyces cerevisiae YJM326 GN=ARO8 PE=4 SV=1	9	**1.6**	1.50	6	**-0.6**	0.00	14	0.64	0.67	29	1.69	0.88	3	-1.6	group II
65	PYC2	Pyruvate carboxylase OS=Saccharomyces cerevisiae YJM993 GN=PYC2 PE=4 SV=1	9	**1.6**	1.00	9	**0.0**	2.50	16	0.83	0.33	18	1.00	1.73	3	-1.6	group II
66	TIF34	Eukaryotic translation initiation factor 3 subunit I OS=Saccharomyces cerevisiae YJM993 GN=TIF34 PE=3 SV=1	12	**1.6**	0.58	8	**-0.6**	0.33	11	-0.13	0.88	11	-0.13	0.67	4	-1.6	group II
67	RPN3	Rpn3p OS=Saccharomyces cerevisiae YJM693 GN=RPN3 PE=4 SV=1	6	**1.6**	1.00	6	**0.0**	0.00	12	1.00	1.53	0.1	-5.91	0.00	2	-1.6	group II
68	ATP2	ATP synthase subunit beta OS=Saccharomyces cerevisiae YJM993 GN=ATP2 PE=3 SV=1	6	**1.6**	1.00	8	**0.4**	0.33	9	0.58	0.58	2	-1.58	0.00	2	-1.6	group II

69	TSA1	Tsa1p OS=Saccharomyces cerevisiae YJM993 GN=TSA1 PE=4 SV=1	6	**1.6**	0.00	10	**0.7**	0.88	9	0.58	1.50	15	1.32	1.15	2	-1.6	group II
70	RPL19A	Ribosomal protein L19 OS=Saccharomyces cerevisiae YJM993 GN=RPL19A PE=3 SV=1	6	**1.6**	0.00	5	**-0.3**	0.50	10	0.74	0.33	2	-1.58	0.00	2	-1.6	group II
71	GSP2	Gsp2p OS=Saccharomyces cerevisiae YJM993 GN=GSP2 PE=4 SV=1	6	**1.6**	1.00	2	**-1.6**	0.00	8	0.42	0.33	0.1	-5.91	0.00	2	-1.6	group II
72	SPT5	Transcription elongation factor SPT5 OS=Saccharomyces cerevisiae YJM1388 GN=SPT5 PE=3 SV=1	6	**1.6**	0.00	0.1	**-5.9**	0.00	3	-1.00	0.00	0.1	-5.91	0.00	2	-1.6	group II
73	GDH1	Glutamate dehydrogenase OS=Saccharomyces cerevisiae YJM993 GN=GDH1 PE=3 SV=1	8	**1.4**	0.33	4	**-1.0**	0.00	14	0.81	0.67	29	1.86	1.33	3	-1.4	group II
74	SSZ1	Ssz1p OS=Saccharomyces cerevisiae YJM1615 GN=SSZ1 PE=3 SV=1	29	**1.4**	3.18	20	**-0.5**	1.20	29	0.00	2.03	16	-0.86	0.67	11	-1.4	group II
75	Gpd2	Glycerol-3-phosphate dehydrogenase [NAD(+)] OS=Saccharomyces cerevisiae R103 GN=Gpd2 PE=3 SV=1	13	**1.4**	1.20	9	**-0.5**	0.58	17	0.39	1.20	9	-0.53	0.58	5	-1.4	group II
76	EFT2	Eft1p OS=Saccharomyces cerevisiae YJM993 GN=EFT2 PE=4 SV=1	100	**1.4**	4.63	82	**-0.3**	0.33	150	0.58	0.00	135	0.43	0.00	39	-1.4	group II
77	ALD6	Ald6p OS=Saccharomyces cerevisiae YJM993 GN=ALD6 PE=3 SV=1	25	**1.3**	0.88	21	**-0.3**	1.53	25	0.00	1.20	63	1.33	1.53	10	-1.3	group II
78	GCD6	Gcd6p OS=Saccharomyces cerevisiae YJM993 GN=GCD6 PE=4 SV=1	10	**1.3**	3.00	3	**-1.7**	0.00	9	-0.15	0.58	7	-0.51	0.33	4	-1.3	group II
79	ASC1	Asc1p OS=Saccharomyces cerevisiae YJM993 GN=ASC1 PE=4 SV=1	10	**1.3**	0.00	10	**0.0**	1.33	14	0.49	1.00	14	0.49	0.33	4	-1.3	group II
80	PRS5	Prs5p OS=Saccharomyces cerevisiae YJM993 GN=PRS5 PE=4 SV=1	5	**1.3**	0.50	5	**0.0**	0.50	10	1.00	0.67	5	0.00	0.50	2	-1.3	group II
81	RPT4	Rpt4p OS=Saccharomyces cerevisiae YJM993 GN=RPT4 PE=3 SV=1	5	**1.3**	0.50	2	**-1.3**	0.00	4	-0.32	0.00	2	-1.32	0.00	2	-1.3	group II
82	RTF1	Rtf1p OS=Saccharomyces cerevisiae YJM993 GN=RTF1 PE=4 SV=1	5	**1.3**	0.50	2	**-1.3**	0.00	7	0.49	1.50	0.1	-5.64	0.00	2	-1.3	group II
83	RPN6	Rpn6p OS=Saccharomyces cerevisiae YJM993 GN=RPN6 PE=4 SV=1	5	**1.3**	0.50	2	**-1.3**	0.00	4	-0.32	0.00	2	-1.32	0.00	2	-1.3	group II
84	LEU2	3-isopropylmalate dehydrogenase OS=Saccharomyces cerevisiae YJM993 GN=LEU2 PE=4 SV=1	40	**1.2**	2.60	42	**0.1**	0.58	54	0.43	1.15	47	0.23	1.86	17	-1.2	group III
85	FBA1	Fba1p OS=Saccharomyces cerevisiae YJM993 GN=FBA1 PE=4 SV=1	35	**1.2**	2.33	26	**-0.4**	0.67	31	-0.18	1.45	47	0.43	1.20	15	-1.2	group III
86	PFK26	6-phosphofructo-2-kinase 1 OS=Saccharomyces cerevisiae (strain ATCC 204508 / S288c) GN=PFK26 PE=1 SV=1	7	**1.2**	0.33	0.1	**-6.1**	0.00	9	0.36	0.50	0.1	-6.13	0.00	3	-1.2	group III

87	SEC23	Sec23p OS=Saccharomyces cerevisiae YJM993 GN=SEC23 PE=4 SV=1	9	**1.2**	2.50	2	**-2.2**	0.00	8	-0.17	0.00	17	0.92	1.20	4	-1.2	group III
88	SHM2	Serine hydroxymethyltransferase OS=Saccharomyces cerevisiae YJM993 GN=SHM2 PE=3 SV=1	40	**1.2**	2.60	20	**-1.0**	1.20	45	0.17	3.21	69	0.79	0.58	18	-1.2	group III
89	HSP104	Hsp104p OS=Saccharomyces cerevisiae YJM993 GN=HSP104 PE=3 SV=1	20	**1.2**	4.18	11	**-0.9**	0.67	17	-0.23	0.88	12	-0.74	1.53	9	-1.2	group III
90	Ura7	CTP synthase OS=Saccharomyces cerevisiae P301 GN=Ura7 PE=3 SV=1	13	**1.1**	1.33	13	**0.0**	0.50	16	0.30	1.45	12	-0.12	0.58	6	-1.1	group III
91	ACS2	Acetyl-coenzyme A synthetase OS=Saccharomyces cerevisiae YJM993 GN=ACS2 PE=3 SV=1	30	**1.1**	2.52	32	**0.1**	1.76	32	0.09	1.76	32	0.09	1.20	14	-1.1	group III
92	THS1	Ths1p OS=Saccharomyces cerevisiae YJM1307 GN=THS1 PE=3 SV=1	25	**1.1**	2.03	20	**-0.3**	0.88	27	0.11	0.58	30	0.26	1.53	12	-1.1	group III
93	ACC1	Acetyl-CoA carboxylase OS=Saccharomyces cerevisiae (strain ATCC 204508 / S288c) GN=ACC1 PE=1 SV=2	66	**1.0**	7.55	37	**-0.8**	3.48	70	0.08	2.19	47	-0.49	1.20	33	-1.0	group III
94	VPS1	Vps1p OS=Saccharomyces cerevisiae YJM993 GN=VPS1 PE=3 SV=1	16	**1.0**	5.00	7	**-1.2**	1.50	9	-0.83	1.50	9	-0.83	0.58	8	-1.0	group III
95	GPM1	Gpm1p OS=Saccharomyces cerevisiae YJM993 GN=GPM1 PE=3 SV=1	18	**1.0**	1.73	10	**-0.8**	1.00	14	-0.36	0.88	6	-1.58	1.00	9	-1.0	group III
96	DBP5	Dbp5p OS=Saccharomyces cerevisiae YJM993 GN=DBP5 PE=3 SV=1	16	**1.0**	1.45	8	**-1.0**	1.00	11	-0.54	0.33	6	-1.42	1.00	8	-1.0	group III
97	CHC1	Clathrin heavy chain OS=Saccharomyces cerevisiae YJM993 GN=CHC1 PE=3 SV=1	10	**1.0**	3.00	5	**-1.0**	0.50	7	-0.51	0.50	7	-0.51	0.33	5	-1.0	group III
98	SER1	Phosphoserine aminotransferase OS=Saccharomyces cerevisiae YJM195 GN=SER1 PE=3 SV=1	8	**1.0**	2.00	7	**-0.2**	0.50	9	0.17	0.50	0.1	-6.32	0.00	4	-1.0	group III
99	CDC60	Cdc60p OS=Saccharomyces cerevisiae YJM993 GN=CDC60 PE=4 SV=1	8	**1.0**	1.00	4	**-1.0**	0.00	12	0.58	0.58	14	0.81	0.67	4	-1.0	group III
100	FUR1	Fur1p OS=Saccharomyces cerevisiae YJM993 GN=FUR1 PE=4 SV=1	6	**1.0**	1.00	7	**0.2**	0.50	16	1.42	0.33	13	1.12	0.67	3	-1.0	group III
101	Rpl8b	Rpl8bp OS=Saccharomyces cerevisiae P301 GN=Rpl8b PE=4 SV=1	8	**1.0**	0.00	10	**0.3**	0.67	8	0.00	0.00	5	-0.68	0.50	4	-1.0	group III
102	NOP58	Nop58p OS=Saccharomyces cerevisiae YJM1342 GN=NOP58 PE=4 SV=1	6	**1.0**	1.00	3	**-1.0**	0.00	6	0.00	1.00	0.1	-5.91	0.00	3	-1.0	group III
103	HIS4	His4p OS=Saccharomyces cerevisiae YJM1417 GN=HIS4 PE=3 SV=1	4	**1.0**	0.00	0.1	**-5.3**	0.00	6	0.58	0.00	19	2.25	2.03	2	-1.0	group III
104	ARP2	Arp2p OS=Saccharomyces cerevisiae YJM993 GN=ARP2 PE=3 SV=1	4	**1.0**	0.00	0.1	**-5.3**	0.00	9	1.17	0.58	2	-1.00	0.00	2	-1.0	group III

105	VMA1	Vma1p OS=Saccharomyces cerevisiae YJM450 GN=VMA1 PE=4 SV=1	71	**0.9**	2.60	49	**-0.5**	2.60	73	0.04	1.86	92	0.37	3.33	37	-0.9	group III
106	CCT3	T-complex protein 1 subunit gamma OS=Saccharomyces cerevisiae YJM993 GN=CCT3 PE=3 SV=1	21	**0.9**	1.15	14	**-0.6**	0.33	21	0.00	0.58	4	-2.39	0.00	11	-0.9	group III
107	UBA1	Uba1p OS=Saccharomyces cerevisiae YJM193 GN=UBA1 PE=3 SV=1	26	**0.9**	3.38	34	**0.4**	3.18	32	0.30	0.67	36	0.47	2.31	14	-0.9	group III
108	RPN2	Rpn2p OS=Saccharomyces cerevisiae YJM993 GN=RPN2 PE=4 SV=1	13	**0.9**	4.50	4	**-1.7**	0.00	21	0.69	0.58	10	-0.38	1.33	7	-0.9	group III
109	ARO1	Pentafunctional AROM polypeptide OS=Saccharomyces cerevisiae YJM993 GN=ARO1 PE=3 SV=1	38	**0.8**	4.67	30	**-0.3**	2.52	54	0.51	2.08	45	0.24	1.53	22	-0.8	group III
110	GCD11	Gcd11p OS=Saccharomyces cerevisiae YJM993 GN=GCD11 PE=4 SV=1	19	**0.8**	2.33	16	**-0.2**	1.20	17	-0.16	1.76	16	-0.25	0.33	11	-0.8	group III
111	SAC6	Sac6p OS=Saccharomyces cerevisiae YJM993 GN=SAC6 PE=4 SV=1	17	**0.8**	1.76	17	**0.0**	1.67	20	0.23	1.76	9	-0.92	0.58	10	-0.8	group III
112	DED81	Ded81p OS=Saccharomyces cerevisiae YJM993 GN=DED81 PE=3 SV=1	15	**0.7**	4.50	13	**-0.2**	0.88	19	0.34	0.33	17	0.18	0.67	9	-0.7	group III
113	RPL12B	Rpl12bp OS=Saccharomyces cerevisiae YJM993 GN=RPL12B PE=3 SV=1	15	**0.7**	0.58	15	**0.0**	1.00	15	0.00	1.53	13	-0.21	0.33	9	-0.7	group III
114	Ptc3	Ptc3p OS=Saccharomyces cerevisiae P301 GN=Ptc3 PE=3 SV=1	5	**0.7**	0.50	2	**-1.3**	0.00	12	1.26	0.58	4	-0.32	0.00	3	-0.7	group III
115	AHP1	Ahp1p OS=Saccharomyces cerevisiae YJM993 GN=AHP1 PE=4 SV=1	5	**0.7**	0.50	0.1	**-5.6**	0.00	2	-1.32	0.00	10	1.00	0.33	3	-0.7	group III
116	CCT2	Cct2p OS=Saccharomyces cerevisiae YJM993 GN=CCT2 PE=3 SV=1	26	**0.7**	2.73	24	**-0.1**	1.73	41	0.66	1.76	32	0.30	1.45	16	-0.7	group III
117	SUP35	Sup35p OS=Saccharomyces cerevisiae GN=SUP35 PE=4 SV=1	8	**0.7**	0.00	7	**-0.2**	0.33	13	0.70	0.33	10	0.32	1.33	5	-0.7	group III
118	TRP5	Trp5p OS=Saccharomyces cerevisiae YJM993 GN=TRP5 PE=3 SV=1	35	**0.7**	4.63	33	**-0.1**	2.52	34	-0.04	2.03	25	-0.49	0.67	22	-0.7	group III
119	YHR020W	Uncharacterized protein OS=Saccharomyces cerevisiae YJM1383 GN=H804_YJM1383H00074 PE=3 SV=1 (Gene=YHR020W, Prolyl-tRNA synthetase)	33	**0.7**	2.65	19	**-0.8**	1.67	39	0.24	1.53	39	0.24	0.58	21	-0.7	group III
120	AHA1	Aha1p OS=Saccharomyces cerevisiae YJM993 GN=AHA1 PE=4 SV=1	14	**0.6**	1.20	10	**-0.5**	0.33	9	-0.64	0.00	3	-2.22	0.00	9	-0.6	group III
121	SPT16	Spt16p OS=Saccharomyces cerevisiae YJM555 GN=SPT16 PE=4 SV=1	14	**0.6**	1.45	0.1	**-7.1**	0.00	14	0.00	0.00	10	-0.49	1.33	9	-0.6	group III
122	ACT1	Act1p OS=Saccharomyces cerevisiae YJM993 GN=ACT1 PE=3 SV=1	48	**0.6**	2.89	50	**0.1**	1.67	49	0.03	1.33	41	-0.23	1.76	31	-0.6	group III

123	Cys4	Cystathionine beta-synthase OS=Saccharomyces cerevisiae P301 GN=Cys4 PE=3 SV=1	15	**0.6**	3.50	25	**0.7**	2.96	31	1.05	1.45	24	0.68	1.53	10	-0.6	group III
124	VMA13	Vma13p OS=Saccharomyces cerevisiae YJM993 GN=VMA13 PE=4 SV=1	15	**0.6**	1.53	12	**-0.3**	1.15	18	0.26	0.58	6	-1.32	1.00	10	-0.6	group III
125	SEC31	Sec31p OS=Saccharomyces cerevisiae YJM1342 GN=SEC31 PE=4 SV=1	12	**0.6**	1.00	11	**-0.1**	0.33	15	0.32	0.58	9	-0.42	0.58	8	-0.6	group III
126	MES1	Mes1p OS=Saccharomyces cerevisiae YJM993 GN=MES1 PE=3 SV=1	6	**0.6**	1.00	4	**-0.6**	0.00	12	1.00	1.00	6	0.00	1.00	4	-0.6	group III
127	GUA1	Gua1p OS=Saccharomyces cerevisiae YJM993 GN=GUA1 PE=3 SV=1	22	**0.6**	2.33	20	**-0.1**	0.67	25	0.18	1.45	18	-0.29	0.58	15	-0.6	group III
128	Eno2	Eno2p OS=Saccharomyces cerevisiae R103 GN=Eno2 PE=3 SV=1	19	**0.5**	2.40	18	**-0.1**	1.15	25	0.40	1.20	19	0.00	1.20	13	-0.5	group IV
129	TCP1	Tcp1p OS=Saccharomyces cerevisiae YJM993 GN=TCP1 PE=3 SV=1	32	**0.5**	2.60	28	**-0.2**	0.88	37	0.21	0.33	25	-0.36	1.45	22	-0.5	group IV
130	KAP123	Kap123p OS=Saccharomyces cerevisiae YJM993 GN=KAP123 PE=4 SV=1	32	**0.5**	0.88	32	**0.0**	2.03	44	0.46	1.76	42	0.39	0.58	22	-0.5	group IV
131	MAE1	Malic enzyme OS=Saccharomyces cerevisiae YJM1078 GN=MAE1 PE=3 SV=1	16	**0.5**	1.45	11	**-0.5**	0.67	16	0.00	0.88	12	-0.42	0.00	11	-0.5	group IV
132	GCN1	Gcn1p OS=Saccharomyces cerevisiae YJM682 GN=GCN1 PE=4 SV=1	23	**0.5**	5.67	15	**-0.6**	0.00	24	0.06	1.73	19	-0.28	1.45	16	-0.5	group IV
133	TDH3	Glyceraldehyde-3-phosphate dehydrogenase OS=Saccharomyces cerevisiae YJM1443 GN=TDH3 PE=3 SV=1	33	**0.5**	1.53	35	**0.1**	0.88	42	0.35	0.58	39	0.24	1.53	23	-0.5	group IV
134	Sse1	Sse1p OS=Saccharomyces cerevisiae P301 GN=Sse1 PE=3 SV=1	30	**0.5**	4.51	19	**-0.7**	1.45	24	-0.32	1.15	20	-0.58	0.67	21	-0.5	group IV
135	DED1	Ded1p OS=Saccharomyces cerevisiae YJM326 GN=DED1 PE=3 SV=1	27	**0.5**	2.00	23	**-0.2**	1.86	35	0.37	0.88	26	-0.05	1.20	19	-0.5	group IV
136	NEW1	New1p OS=Saccharomyces cerevisiae YJM993 GN=NEW1 PE=4 SV=1	17	**0.5**	3.18	13	**-0.4**	0.33	25	0.56	1.45	13	-0.39	0.88	12	-0.5	group IV
137	TEF2	Elongation factor 1-alpha OS=Saccharomyces cerevisiae YJM993 GN=TEF2 PE=3 SV=1	65	**0.5**	1.86	59	**-0.1**	1.45	69	0.09	1.15	68	0.07	2.33	46	-0.5	group IV
138	HSP60	Hsp60p OS=Saccharomyces cerevisiae YJM993 GN=HSP60 PE=3 SV=1	35	**0.5**	4.41	35	**0.0**	1.33	48	0.46	1.00	46	0.39	1.67	25	-0.5	group IV
139	BAT1	Branched-chain-amino-acid aminotransferase OS=Saccharomyces cerevisiae YJM993 GN=BAT1 PE=3 SV=1	11	**0.5**	0.88	6	**-0.9**	1.00	8	-0.46	0.33	19	0.79	0.88	8	-0.5	group IV
140	SAM1	S-adenosylmethionine synthase OS=Saccharomyces cerevisiae YJM993 GN=SAM1 PE=3 SV=1	26	**0.5**	2.91	31	**0.3**	2.19	38	0.55	0.88	28	0.11	1.20	19	-0.5	group IV

141	CCT4	T-complex protein 1 subunit delta OS=Saccharomyces cerevisiae YJM993 GN=CCT4 PE=3 SV=1	23	**0.4**	0.67	12	**-0.9**	1.00	31	0.43	0.88	15	-0.62	0.58	17	-0.4	group IV
142	CDC19	Pyruvate kinase OS=Saccharomyces cerevisiae YJM993 GN=CDC19 PE=3 SV=1	89	**0.4**	3.53	82	**-0.1**	3.38	87	-0.03	2.65	95	0.09	2.19	66	-0.4	group IV
143	VMA5	Vma5p OS=Saccharomyces cerevisiae YJM993 GN=VMA5 PE=4 SV=1	12	**0.4**	1.00	11	**-0.1**	1.50	14	0.22	0.67	4	-1.58	0.00	9	-0.4	group IV
144	CCT7	T-complex protein 1 subunit eta OS=Saccharomyces cerevisiae (strain ATCC 204508 / S288c) GN=CCT7 PE=1 SV=1	21	**0.4**	2.08	20	**-0.1**	0.88	36	0.78	1.15	14	-0.58	1.45	16	-0.4	group IV
145	RPS2	Rps2p OS=Saccharomyces cerevisiae YJM993 GN=RPS2 PE=3 SV=1	17	**0.4**	1.45	15	**-0.2**	0.00	14	-0.28	0.88	13	-0.39	0.67	13	-0.4	group IV
146	SUB2	Sub2p OS=Saccharomyces cerevisiae YJM450 GN=SUB2 PE=4 SV=1	26	**0.4**	1.67	20	**-0.4**	2.60	31	0.25	0.33	15	-0.79	0.58	20	-0.4	group IV
147	Ilv2	Acetolactate synthase OS=Saccharomyces cerevisiae P301 GN=Ilv2 PE=3 SV=1	31	**0.4**	2.60	24	**-0.4**	1.73	27	-0.20	1.00	21	-0.56	1.15	24	-0.4	group IV
148	CCT6	Cct6p OS=Saccharomyces cerevisiae YJM270 GN=CCT6 PE=3 SV=1	18	**0.4**	1.00	15	**-0.3**	1.15	23	0.35	0.67	9	-1.00	0.00	14	-0.4	group IV
149	TEF4	Tef4p OS=Saccharomyces cerevisiae YJM993 GN=TEF4 PE=4 SV=1	23	**0.4**	1.33	25	**0.1**	0.67	28	0.28	0.88	19	-0.28	0.88	18	-0.4	group IV
150	SUP45	Sup45p OS=Saccharomyces cerevisiae YJM993 GN=SUP45 PE=4 SV=1	14	**0.3**	2.19	10	**-0.5**	1.33	15	0.10	1.15	14	0.00	0.88	11	-0.3	group IV
151	LEU1	3-isopropylmalate dehydratase OS=Saccharomyces cerevisiae (strain ATCC 204508 / S288c) GN=LEU1 PE=1 SV=3	81	**0.3**	5.03	79	**0.0**	2.60	83	0.04	2.03	63	-0.36	2.52	64	-0.3	group IV
152	RPS4B	40S ribosomal protein S4 OS=Saccharomyces cerevisiae YJM993 GN=RPS4B PE=3 SV=1	15	**0.3**	1.00	22	**0.6**	0.33	19	0.34	1.20	14	-0.10	0.88	12	-0.3	group IV
153	RPS1B	40S ribosomal protein S1 OS=Saccharomyces cerevisiae YJM993 GN=RPS1B PE=3 SV=1	10	**0.3**	0.33	8	**-0.3**	0.67	9	-0.15	0.58	8	-0.32	0.33	8	-0.3	group IV
154	ARC35	Arc35p OS=Saccharomyces cerevisiae YJM993 GN=ARC35 PE=4 SV=1	5	**0.3**	0.50	2	**-1.3**	0.00	4	-0.32	0.00	2	-1.32	0.00	4	-0.3	group IV
155	RPN1	Rpn1p OS=Saccharomyces cerevisiae YJM1078 GN=RPN1 PE=4 SV=1	17	**0.3**	0.67	14	**-0.3**	0.88	22	0.37	0.33	39	1.20	0.58	14	-0.3	group IV
156	LYS21	Lys21p OS=Saccharomyces cerevisiae YJM271 GN=LYS21 PE=3 SV=1	17	**0.3**	1.45	26	**0.6**	1.86	24	0.50	1.15	17	0.00	0.33	14	-0.3	group IV
157	COP1	Coatomer subunit alpha OS=Saccharomyces cerevisiae YJM271 GN=COP1 PE=4 SV=1	23	**0.3**	4.67	9	**-1.4**	1.50	18	-0.35	0.58	18	-0.35	0.58	19	-0.3	group IV
158	RPT3	Rpt3p OS=Saccharomyces cerevisiae YJM993 GN=RPT3 PE=3 SV=1	6	**0.3**	1.00	6	**0.0**	1.00	6	0.00	0.00	2	-1.58	0.00	5	-0.3	group IV
159	ADH1	Adh1p OS=Saccharomyces cerevisiae YJM1078 GN=ADH1 PE=3 SV=1	49	**0.3**	2.19	54	**0.1**	1.00	60	0.29	2.00	77	0.65	0.33	41	-0.3	group IV

160	RNR1	Ribonucleoside-diphosphate reductase OS=Saccharomyces cerevisiae YJM993 GN=RNR1 PE=3 SV=1	19	**0.2**	0.33	16	**-0.2**	1.76	17	-0.16	1.20	16	-0.25	0.67	16	-0.2	group IV
161	PDC1	Pdc1p OS=Saccharomyces cerevisiae YJM993 GN=PDC1 PE=3 SV=1	51	**0.2**	1.15	49	**-0.1**	0.33	59	0.21	0.67	48	-0.09	1.00	43	-0.2	group IV
162	DBP2	Dbp2p OS=Saccharomyces cerevisiae YJM993 GN=DBP2 PE=3 SV=1	7	**0.2**	1.50	5	**-0.5**	0.50	6	-0.22	1.00	3	-1.22	0.00	6	-0.2	group IV
163	SAR1	Sar1p OS=Saccharomyces cerevisiae YJM993 GN=SAR1 PE=3 SV=1	7	**0.2**	0.50	6	**-0.2**	1.00	5	-0.49	0.50	8	0.19	0.33	6	-0.2	group IV
164	RNR4	Rnr4p OS=Saccharomyces cerevisiae YJM993 GN=RNR4 PE=4 SV=1	16	**0.2**	2.00	18	**0.2**	0.58	20	0.32	1.20	11	-0.54	1.67	14	-0.2	group IV
165	ILV5	Ketol-acid reductoisomerase, mitochondrial OS=Saccharomyces cerevisiae YJM993 GN=ILV5 PE=3 SV=1	24	**0.2**	2.08	19	**-0.3**	0.67	27	0.17	1.53	42	0.81	0.58	21	-0.2	group IV
166	Gus1	Gus1p OS=Saccharomyces cerevisiae (strain Lalvin QA23) GN=QA23_1564 PE=3 SV=1	16	**0.2**	0.88	16	**0.0**	1.33	26	0.70	1.76	19	0.25	1.33	14	-0.2	group IV
167	RPS7B	Rps7bp OS=Saccharomyces cerevisiae YJM993 GN=RPS7B PE=4 SV=1	8	**0.2**	2.00	5	**-0.7**	0.50	14	0.81	0.33	9	0.17	0.00	7	-0.2	group IV
168	GFA1	Gfa1p OS=Saccharomyces cerevisiae YJM993 GN=GFA1 PE=4 SV=1	25	**0.2**	2.33	21	**-0.3**	1.53	35	0.49	2.40	24	-0.06	1.00	22	-0.2	group IV
169	ARB1	Arb1p OS=Saccharomyces cerevisiae YJM993 GN=ARB1 PE=4 SV=1	26	**0.2**	1.76	28	**0.1**	0.88	45	0.79	1.00	30	0.21	0.58	23	-0.2	group IV
170	**RPP0**	60S acidic ribosomal protein P0 OS=Saccharomyces cerevisiae (strain FostersB) GN=FOSTERSB_3338 PE=3 SV=1	**18**	**0.2**	1.15	24	**0.4**	0.58	20	0.15	2.03	20	0.15	1.76	16	-0.2	group IV
171	NOP56	Nop56p OS=Saccharomyces cerevisiae YJM993 GN=NOP56 PE=4 SV=1	9	**0.2**	1.00	0.1	**-6.5**	0.00	16	0.83	0.88	2	-2.17	0.00	8	-0.2	group IV
172	RPL17A	Rpl17ap OS=Saccharomyces cerevisiae YJM993 GN=RPL17A PE=3 SV=1	9	**0.2**	0.58	10	**0.2**	0.33	10	0.15	0.33	9	0.00	0.58	8	-0.2	group IV
173	Get3	ATPase GET3 OS=Saccharomyces cerevisiae R103 GN=Get3 PE=3 SV=1	10	**0.2**	2.00	8	**-0.3**	0.67	5	-1.00	0.50	7	-0.51	0.33	9	-0.2	group IV
174	OLA1	Obg-like ATPase 1 OS=Saccharomyces cerevisiae YJM993 GN=OLA1 PE=3 SV=1	25	**0.1**	1.86	17	**-0.6**	1.45	24	-0.06	1.00	20	-0.32	0.33	23	-0.1	group IV
175	FAS1	Fas1p OS=Saccharomyces cerevisiae YJM993 GN=FAS1 PE=4 SV=1	53	**0.1**	4.33	28	**-0.9**	2.03	75	0.50	3.21	68	0.36	0.33	49	-0.1	group IV
176	RVB1	RuvB-like helicase OS=Saccharomyces cerevisiae YJM993 GN=RVB1 PE=3 SV=1	15	**0.1**	2.00	16	**0.1**	1.76	12	-0.32	0.00	5	-1.58	0.50	14	-0.1	group IV
177	RPS6B	40S ribosomal protein S6 OS=Saccharomyces cerevisiae YJM993 GN=RPS6B PE=3 SV=1	15	**0.1**	1.00	18	**0.3**	1.00	19	0.34	0.67	13	-0.21	0.67	14	-0.1	group IV
178	YEF3	Yef3p OS=Saccharomyces cerevisiae YJM1083 GN=YEF3 PE=4 SV=1	86	**0.1**	4.41	85	**0.0**	1.86	115	0.42	0.88	103	0.26	2.91	81	-0.1	group IV

179	RPL20A	60S ribosomal protein L20 OS=Saccharomyces cerevisiae YJM993 GN=RPL20A PE=3 SV=1	20	**0.1**	1.00	15	**-0.4**	1.15	18	-0.15	1.53	13	-0.62	0.88	19	-0.1	group IV
180	CPA2	Cpa2p OS=Saccharomyces cerevisiae YJM993 GN=CPA2 PE=4 SV=1	26	**0.1**	2.96	39	**0.6**	2.31	48	0.88	2.52	29	0.16	0.88	25	-0.1	group IV
181	RPS1A	40S ribosomal protein S1 OS=Saccharomyces cerevisiae YJM993 GN=RPS1A PE=3 SV=1	26	**0.1**	2.03	28	**0.1**	1.45	31	0.25	1.33	24	-0.12	2.00	25	-0.1	group IV
182	Cdc33	Cdc33p OS=Saccharomyces cerevisiae (strain FostersO) GN=FOSTERSO_4174 PE=3 SV=1	74	**0.0**	1.20	73	**0.0**	1.20	25	-1.57	1.20	18	-2.04	2.00	73	0.0	group IV
183	HSC82	Hsc82p OS=Saccharomyces cerevisiae YJM320 GN=HSC82 PE=3 SV=1	54	**0.0**	5.86	69	**0.4**	1.00	63	0.22	2.08	54	0.00	0.58	54	0.0	group IV
184	RPG1	Eukaryotic translation initiation factor 3 subunit A OS=Saccharomyces cerevisiae YJM1418 GN=RPG1 PE=3 SV=1	21	**0.0**	2.52	17	**-0.3**	0.88	21	0.00	1.15	16	-0.39	2.33	21	0.0	group IV
185	SEC21	Coatomer subunit gamma OS=Saccharomyces cerevisiae YJM993 GN=SEC21 PE=3 SV=1	17	**0.0**	2.73	15	**-0.2**	0.58	19	0.16	1.45	24	0.50	1.00	17	0.0	group IV
186	ARF1	Arf1p OS=Saccharomyces cerevisiae YJM993 GN=ARF1 PE=3 SV=1	21	**0.0**	1.73	16	**-0.4**	1.45	22	0.07	1.20	16	-0.39	0.67	21	0.0	group IV
187	CDC48	Cdc48p OS=Saccharomyces cerevisiae YJM993 GN=CDC48 PE=3 SV=1	15	**0.0**	2.00	18	**0.3**	0.00	25	0.74	2.33	24	0.68	0.58	15	0.0	group IV
188	RPS18B	Rps18ap OS=Saccharomyces cerevisiae YJM993 GN=RPS18B PE=3 SV=1	16	**0.0**	1.45	16	**0.0**	0.88	22	0.46	0.88	14	-0.19	1.20	16	0.0	group IV
189	RPL7A	Rpl7ap OS=Saccharomyces cerevisiae YJM993 GN=RPL7A PE=3 SV=1	13	**0.0**	1.86	18	**0.5**	1.15	19	0.55	0.88	16	0.30	1.86	13	0.0	group IV
190	RPL11A	Rpl11ap OS=Saccharomyces cerevisiae YJM993 GN=RPL11A PE=3 SV=1	12	**0.0**	2.00	14	**0.2**	0.33	16	0.42	0.67	12	0.00	0.58	12	0.0	group IV
191	ADE5,7	Ade5,7p OS=Saccharomyces cerevisiae YJM993 GN=ADE5,7 PE=3 SV=1	11	**0.0**	0.50	19	**0.8**	0.33	24	1.13	0.58	10	-0.14	1.00	11	0.0	group IV
192	RPL2A	Rpl2ap OS=Saccharomyces cerevisiae YJM993 GN=RPL2A PE=4 SV=1	12	**0.0**	0.00	15	**0.3**	1.00	12	0.00	1.00	7	-0.78	0.50	12	0.0	group IV
193	CAF20	**Cap-associated protein CAF20 OS=Saccharomyces cerevisiae YJM428 GN=CAF20 PE=3 SV=1**	15	**0.0**	1.15	14	**-0.1**	1.45	13	-0.21	0.67	7	-1.10	0.33	15	0.0	group IV
194	RPS12	40S ribosomal protein S12 OS=Saccharomyces cerevisiae YJM993 GN=RPS12 PE=3 SV=1	10	**0.0**	0.88	12	**0.3**	0.00	14	0.49	0.33	13	0.38	0.33	10	0.0	group IV
195	Leu4	Leu4p OS=Saccharomyces cerevisiae P301 GN=Leu4 PE=3 SV=1	8	**0.0**	1.00	12	**0.6**	0.58	13	0.70	1.45	15	0.91	1.15	8	0.0	group IV
196	RPS7A	Rps7ap OS=Saccharomyces cerevisiae YJM993 GN=RPS7A PE=4 SV=1	7	**0.0**	1.50	10	**0.5**	0.33	7	0.00	0.33	11	0.65	0.88	7	0.0	group IV

197	RPT1	Rpt1p OS=Saccharomyces cerevisiae YJM993 GN=RPT1 PE=3 SV=1	8	**0.0**	1.00	14	**0.8**	0.67	9	0.17	1.50	2	-2.00	0.00	8	0.0	group IV
198	SRO9	YCL037Cp-like protein OS=Saccharomyces cerevisiae (strain AWRI1631) GN=AWRI1631_30310 PE=4 SV=1 (SRO9 AND PARALOG SLF1	7	**0.0**	1.50	4	**-0.8**	0.00	8	0.19	1.00	3	-1.22	0.00	7	0.0	group IV
199	RPS31	Rps31p OS=Saccharomyces cerevisiae YJM993 GN=RPS31 PE=4 SV=1	13	**0.0**	0.33	16	**0.3**	0.33	9	-0.53	0.58	3	-2.12	0.00	13	0.0	group IV
200	RPL33A	Rpl33ap OS=Saccharomyces cerevisiae YJM993 GN=RPL33A PE=4 SV=1	6	**0.0**	0.00	9	**0.6**	0.58	7	0.22	0.33	8	0.42	0.00	6	0.0	group IV
201	SSA2	Ssa2p OS=Saccharomyces cerevisiae YJM1387 GN=SSA2 PE=3 SV=1	50	**0.0**	1.67	47	**-0.1**	0.33	55	0.14	0.88	49	-0.03	1.86	51	0.0	group IV
202	Cct8	Cct8p OS=Saccharomyces cerevisiae (strain AWRI796) GN=AWRI796_2623 PE=3 SV=1	25	**-0.1**	1.20	28	**0.2**	1.86	38	0.60	2.03	17	-0.56	1.33	26	0.1	group IV
203	PRT1	Eukaryotic translation initiation factor 3 subunit B OS=Saccharomyces cerevisiae YJM1311 GN=PRT1 PE=3 SV=1	19	**-0.1**	2.40	14	**-0.4**	0.88	24	0.34	1.73	12	-0.66	1.00	20	0.1	group IV
204	TIF1	Tif1p OS=Saccharomyces cerevisiae YJM993 GN=TIF1 PE=3 SV=1	37	**-0.1**	1.45	40	**0.1**	0.88	42	0.18	1.15	39	0.08	1.53	39	0.1	group IV
205	SSB2	Ssb2p OS=Saccharomyces cerevisiae YJM1386 GN=SSB2 PE=3 SV=1	53	**-0.1**	3.93	51	**-0.1**	2.08	78	0.56	3.06	75	0.50	4.16	56	0.1	group IV
206	Rpl14a	Rpl14ap OS=Saccharomyces cerevisiae (strain CEN.PK113-7D) GN=CENPK1137D_1004 PE=4 SV=1	15	**-0.1**	1.53	12	**-0.3**	0.58	20	0.42	0.67	15	0.00	1.15	16	0.1	group IV
207	FAS2	Fas2p OS=Saccharomyces cerevisiae YJM1478 GN=FAS2 PE=3 SV=1	43	**-0.1**	3.48	29	**-0.6**	1.20	55	0.36	3.38	47	0.13	0.67	46	0.1	group IV
208	ILV6	Ilv6p OS=Saccharomyces cerevisiae YJM1133 GN=ILV6 PE=4 SV=1	13	**-0.1**	1.45	16	**0.3**	1.33	15	0.21	0.58	14	0.11	0.88	14	0.1	group IV
209	RPS17B	Rps17bp OS=Saccharomyces cerevisiae YJM993 GN=RPS17B PE=3 SV=1	11	**-0.1**	1.50	10	**-0.1**	0.67	15	0.45	1.00	12	0.13	0.00	12	0.1	group IV
210	SSC1	Ssc1p OS=Saccharomyces cerevisiae YJM993 GN=SSC1 PE=3 SV=1	11	**-0.1**	1.20	7	**-0.7**	0.50	19	0.79	1.86	15	0.45	0.58	12	0.1	group IV
211	PGI1	Glucose-6-phosphate isomerase OS=Saccharomyces cerevisiae YJM993 GN=PGI1 PE=3 SV=1	11	**-0.1**	0.33	5	**-1.1**	0.50	13	0.24	0.50	8	-0.46	0.67	12	0.1	group IV
212	RPL3	Rpl3p OS=Saccharomyces cerevisiae YJM993 GN=RPL3 PE=3 SV=1	20	**-0.1**	2.60	17	**-0.2**	0.88	27	0.43	0.58	20	0.00	0.88	22	0.1	group IV
213	KAR2	Kar2p OS=Saccharomyces cerevisiae YJM993 GN=KAR2 PE=3 SV=1	8	**-0.2**	2.00	9	**0.2**	1.50	20	1.32	0.67	13	0.70	2.50	9	0.2	group IV
214	RPL4A	Rpl4ap OS=Saccharomyces cerevisiae YJM993 GN=RPL4A PE=4 SV=1	22	**-0.2**	2.91	23	**0.1**	0.88	29	0.40	1.86	19	-0.21	2.19	25	0.2	group IV

215	PFK1	ATP-dependent 6-phosphofructokinase OS=Saccharomyces cerevisiae YJM993 GN=PFK1 PE=3 SV=1	35	**-0.2**	2.91	40	**0.2**	1.20	53	0.60	0.33	37	0.08	0.88	40	0.2	group IV
216	ARL1	Arl1p OS=Saccharomyces cerevisiae YJM993 GN=ARL1 PE=3 SV=1	7	**-0.2**	0.33	6	**-0.2**	1.00	7	0.00	0.33	6	-0.22	0.00	8	0.2	group IV
217	VMA2	Vma2p OS=Saccharomyces cerevisiae YJM993 GN=VMA2 PE=3 SV=1	38	**-0.2**	1.86	43	**0.2**	0.88	44	0.21	0.88	34	-0.16	1.20	44	0.2	group IV
218	RPL6A	60S ribosomal protein L6 OS=Saccharomyces cerevisiae YJM993 GN=RPL6A PE=3 SV=1	12	**-0.2**	1.00	16	**0.4**	1.33	18	0.58	0.00	11	-0.13	0.50	14	0.2	group IV
219	PMA1	Plasma membrane ATPase OS=Saccharomyces cerevisiae YJM993 GN=PMA1 PE=3 SV=1	12	**-0.2**	1.00	4	**-1.6**	0.00	7	-0.78	0.50	18	0.58	0.58	14	0.2	group IV
220	Dps1	Dps1p OS=Saccharomyces cerevisiae (strain Zymaflore VL3) GN=VL3_3088 PE=3 SV=1	6	**-0.2**	1.00	0.1	**-5.9**	0.00	8	0.42	1.00	8	0.42	0.33	7	0.2	group IV
221	Sec4	Sec4p OS=Saccharomyces cerevisiae R103 GN=Sec4 PE=3 SV=1	6	**-0.2**	1.00	2	**-1.6**	0.00	5	-0.26	0.50	2	-1.58	0.00	7	0.2	group IV
222	URA2	Ura2p OS=Saccharomyces cerevisiae YJM682 GN=URA2 PE=3 SV=1	42	**-0.3**	4.62	28	**-0.6**	3.18	60	0.51	1.53	44	0.07	1.20	50	0.3	group IV
223	RPS0B	40S ribosomal protein S0 OS=Saccharomyces cerevisiae YJM993 GN=RPS0B PE=3 SV=1	10	**-0.3**	2.00	16	**0.7**	0.33	17	0.77	0.33	14	0.49	1.00	12	0.3	group IV
224	RCK2	Rck2p OS=Saccharomyces cerevisiae YJM993 GN=RCK2 PE=4 SV=1	5	**-0.3**	0.50	0.1	**-5.6**	0.00	6	0.26	1.00	14	1.49	2.00	6	0.3	group IV
225	RPL32	Rpl32p OS=Saccharomyces cerevisiae YJM993 GN=RPL32 PE=4 SV=1	5	**-0.3**	0.50	4	**-0.3**	0.00	4	-0.32	0.00	7	0.49	0.50	6	0.3	group IV
226	TPI1	Triosephosphate isomerase OS=Saccharomyces cerevisiae YJM993 GN=TPI1 PE=3 SV=1	5	**-0.3**	0.50	2	**-1.3**	0.00	6	0.26	0.00	2	-1.32	0.00	6	0.3	group IV
227	RPS14A	Rps14ap OS=Saccharomyces cerevisiae YJM993 GN=RPS14A PE=3 SV=1	14	**-0.3**	0.88	16	**0.2**	0.88	15	0.10	1.73	4	-1.81	0.00	17	0.3	group IV
228	RPS3	Rps3p OS=Saccharomyces cerevisiae YJM993 GN=RPS3 PE=3 SV=1	40	**-0.3**	1.76	49	**0.3**	1.33	53	0.41	0.67	41	0.04	0.67	49	0.3	group IV
229	TUB2	Tub2p OS=Saccharomyces cerevisiae YJM993 GN=TUB2 PE=3 SV=1	20	**-0.3**	2.19	28	**0.5**	1.76	36	0.85	1.00	23	0.20	1.33	25	0.3	group IV
230	Rrp5	Rrp5p OS=Saccharomyces cerevisiae (strain CEN.PK113-7D) GN=CENPK1137D_269 PE=4 SV=1	8	**-0.3**	2.00	2	**-2.0**	0.00	17	1.09	0.33	8	0.00	0.33	10	0.3	group IV
231	RPL25	Rpl25p OS=Saccharomyces cerevisiae YJM993 GN=RPL25 PE=3 SV=1	4	**-0.3**	0.00	6	**0.6**	0.00	9	1.17	0.00	5	0.32	0.50	5	0.3	group IV
232	RPL22A	Rpl22ap OS=Saccharomyces cerevisiae YJM993 GN=RPL22A PE=4 SV=1	4	**-0.3**	0.00	0.1	**-5.3**	0.00	7	0.81	0.33	0.1	-5.32	0.00	5	0.3	group IV

233	PFK2	ATP-dependent 6-phosphofructokinase OS=Saccharomyces cerevisiae YJM993 GN=PFK2 PE=3 SV=1	19	**-0.3**	0.33	20	**0.1**	1.20	23	0.28	0.88	23	0.28	0.67	24	0.3	group IV
234	RPS22B	Rps22bp OS=Saccharomyces cerevisiae YJM993 GN=RPS22B PE=3 SV=1	15	**-0.3**	1.73	14	**-0.1**	0.33	14	-0.10	0.33	19	0.34	0.33	19	0.3	group IV
235	TUB1	Tub1p OS=Saccharomyces cerevisiae YJM993 GN=TUB1 PE=3 SV=1	15	**-0.3**	1.15	19	**0.3**	0.67	31	1.05	1.76	30	1.00	1.53	19	0.3	group IV
236	CCT5	Cct5p OS=Saccharomyces cerevisiae YJM993 GN=CCT5 PE=3 SV=1	7	**-0.4**	1.50	8	**0.2**	1.00	17	1.28	0.33	5	-0.49	0.50	9	0.4	group IV
237	RPL21A	Rpl21ap OS=Saccharomyces cerevisiae YJM993 GN=RPL21A PE=4 SV=1	7	**-0.4**	0.50	9	**0.4**	0.58	16	1.19	0.67	12	0.78	0.58	9	0.4	group IV
238	RPS13	Rps13p OS=Saccharomyces cerevisiae YJM993 GN=RPS13 PE=3 SV=1	12	**-0.4**	0.58	12	**0.0**	0.58	16	0.42	0.33	17	0.50	0.67	16	0.4	group IV
239	SEC53	Phosphomannomutase OS=Saccharomyces cerevisiae YJM993 GN=SEC53 PE=3 SV=1	9	**-0.4**	0.50	10	**0.2**	1.00	18	1.00	1.00	9	0.00	1.50	12	0.4	group IV
240	RPS5	Rps5p OS=Saccharomyces cerevisiae YJM993 GN=RPS5 PE=3 SV=1	20	**-0.4**	0.88	21	**0.1**	1.15	33	0.72	0.58	24	0.26	2.31	27	0.4	group IV
241	PGK1	Phosphoglycerate kinase OS=Saccharomyces cerevisiae YJM993 GN=PGK1 PE=3 SV=1	17	**-0.4**	1.76	13	**-0.4**	0.88	34	1.00	0.67	32	0.91	0.88	23	0.4	group IV
242	SAH1	Adenosylhomocysteinase OS=Saccharomyces cerevisiae YJM993 GN=SAH1 PE=3 SV=1	14	**-0.4**	1.20	22	**0.7**	2.19	30	1.10	2.00	33	1.24	0.58	19	0.4	group IV
243	RPL9A	Rpl9ap OS=Saccharomyces cerevisiae YJM993 GN=RPL9A PE=4 SV=1	14	**-0.4**	1.45	16	**0.2**	0.33	20	0.51	0.33	16	0.19	3.00	19	0.4	group IV
244	SEC27	Sec27p OS=Saccharomyces cerevisiae YJM993 GN=SEC27 PE=4 SV=1	25	**-0.5**	3.18	24	**-0.1**	0.00	33	0.40	1.00	38	0.60	0.88	36	0.5	group IV
245	RPL23A	Rpl23ap OS=Saccharomyces cerevisiae YJM993 GN=RPL23A PE=3 SV=1	9	**-0.5**	1.50	11	**0.3**	0.67	15	0.74	0.58	10	0.15	0.33	13	0.5	group IV
246	Rpl10	Rpl10p OS=Saccharomyces cerevisiae P301 GN=Rpl10 PE=4 SV=1	9	**-0.5**	0.50	13	**0.5**	0.67	16	0.83	0.33	10	0.15	1.00	13	0.5	group IV
247	RPS24A	40S ribosomal protein S24 OS=Saccharomyces cerevisiae YJM993 GN=RPS24A PE=3 SV=1	9	**-0.5**	0.50	8	**-0.2**	0.33	12	0.42	1.00	6	-0.58	1.00	13	0.5	group IV
248	RPS8B	40S ribosomal protein S8 OS=Saccharomyces cerevisiae YJM993 GN=RPS8B PE=3 SV=1	15	**-0.6**	1.00	18	**0.3**	0.58	18	0.26	0.58	17	0.18	1.67	22	0.6	group IV
249	YDR341C	Uncharacterized protein OS=Saccharomyces cerevisiae YJM195 GN=H749_YJM195D00568 PE=3 SV=1 (systematic name = YDR341C)Arginyl-tRNA synthetase	8	**-0.6**	1.00	12	**0.6**	0.58	17	1.09	1.45	7	-0.19	0.50	12	0.6	group IV
250	TPD3	Protein phosphatase PP2A regulatory subunit A OS=Saccharomyces cerevisiae (strain ATCC 204508 / S288c) GN=TPD3 PE=1 SV=3	4	**-0.6**	0.00	4	**0.0**	0.00	0.1	-5.32	0.00	0.1	-5.32	0.00	6	0.6	group IV

251	NIP1	Eukaryotic translation initiation factor 3 subunit C OS=Saccharomyces cerevisiae (strain ATCC 204508 / S288c) GN=NIP1 PE=1 SV=2	15	**-0.6**	1.53	15	**0.0**	1.15	23	0.62	1.86	18	0.26	1.73	23	0.6	group IV
252	RPS9A	Rps9ap OS=Saccharomyces cerevisiae YJM993 GN=RPS9A PE=3 SV=1	18	**-0.6**	1.15	19	**0.1**	0.88	20	0.15	1.45	17	-0.08	0.67	28	0.6	group IV
253	RPL15A	Ribosomal protein L15 OS=Saccharomyces cerevisiae YJM993 GN=RPL15A PE=3 SV=1	5	**-0.7**	0.50	2	**-1.3**	0.00	10	1.00	0.88	4	-0.32	0.00	8	0.7	group IV
254	Rpl16b	Rpl16bp OS=Saccharomyces cerevisiae (strain CEN.PK113-7D) GN=CENPK1137D_2610 PE=3 SV=1	9	**-0.7**	0.50	8	**-0.2**	0.33	11	0.29	0.88	7	-0.36	1.50	15	0.7	group IV
255	RNR2	Rnr2p OS=Saccharomyces cerevisiae YJM1419 GN=RNR2 PE=4 SV=1	9	**-0.7**	1.50	9	**0.0**	0.00	13	0.53	1.20	4	-1.17	0.00	15	0.7	group IV
256	TY1B-ER1	Transposon Ty1-ER1 Gag-Pol polyprotein OS=Saccharomyces cerevisiae (strain ATCC 204508 / S288c) GN=TY1B-ER1 PE=3 SV=1	8	**-0.8**	1.00	2	**-2.0**	0.00	7	-0.19	0.33	11	0.46	0.88	14	0.8	group IV
257	RPS11A	Rps11ap OS=Saccharomyces cerevisiae YJM993 GN=RPS11A PE=3 SV=1	8	**-0.8**	0.00	13	**0.7**	0.67	19	1.25	1.45	11	0.46	0.33	14	0.8	group IV
258	PIL1	Pil1p OS=Saccharomyces cerevisiae YJM993 GN=PIL1 PE=4 SV=1	8	**-0.8**	0.00	15	**0.9**	0.58	12	0.58	1.00	3	-1.42	0.00	14	0.8	group IV
259	RPL5	Rpl5p OS=Saccharomyces cerevisiae YJM993 GN=RPL5 PE=3 SV=1	9	**-0.8**	1.50	14	**0.6**	1.33	16	0.83	1.67	9	0.00	0.58	16	0.8	group IV
260	RPS20	Rps20p OS=Saccharomyces cerevisiae YJM993 GN=RPS20 PE=3 SV=1	5	**-0.8**	0.50	4	**-0.3**	0.00	13	1.38	0.33	6	0.26	1.00	9	0.8	group IV
261	RPS16A	Rps16ap OS=Saccharomyces cerevisiae YJM993 GN=RPS16A PE=3 SV=1	6	**-0.9**	1.00	8	**0.4**	0.33	13	1.12	0.33	13	1.12	1.33	11	0.9	group IV
262	RPB2	DNA-directed RNA polymerase subunit beta OS=Saccharomyces cerevisiae YJM993 GN=RPB2 PE=3 SV=1	4	**-1.0**	0.00	0.1	**-5.3**	0.00	11	1.46	0.33	0.1	-5.32	0.00	8	1.0	group IV

	Cluster	Group	ID	Description	Gene Ratio	BgRatio	pvalue	p.adjust	qvalue	geneID	Count
1	1,2	1,2	GO:0016301	kinase activity	8/41	226/5313	0.000268	0.0375	0.035245	CKA1/SKY1/CKA2/HRK1/PRO1/PRS3/PRS1/SNF4	8
2	3	3	GO:0016874	ligase activity	9/43	109/5313	1.46E-07	1.99E-05	1.55E-05	URA7/ACS2/THS1/ACC1/CDC60/UBA1/DED81/MES1/GUA1	9
3	3	3	GO:0016879	ligase activity, forming carbon-nitrogen bonds	3/43	45/5313	2.63E-05	0.001801	0.001398	URA7/ACS2/ACC1/UBA1/GUA1	5
4	3	3	GO:0004812	aminoacyl-tRNA ligase activity	4/43	34/5313	0.000145	0.004954	0.003844	THS1/CDC60/DED81/MES1	4
5	3	3	GO:0016875	ligase activity, forming carbon-oxygen bonds	4/43	34/5313	0.000145	0.004954	0.003844	THS1/CDC60/DED81/MES1	4
6	3	3	GO:0016462	pyrophosphatase activity	10/43	425/5313	0.001669	0.032668	0.025351	HSP104/VPS1/DBP5/HIS4/ARP2/VMA1/GCD11/SUP35/VMA13/GUA1	10
7	3	3	GO:0016817	hydrolase activity, acting on acid anhydrides	10/43	425/5313	0.001669	0.032668	0.025351	HSP104/VPS1/DBP5/HIS4/ARP2/VMA1/GCD11/SUP35/VMA13/GUA1	10
8	3	3	GO:0016818	hydrolase activity, acting on acid anhydrides, in phosphorus-containing anhydrides	10/43	425/5313	0.001669	0.032668	0.025351	HSP104/VPS1/DBP5/HIS4/ARP2/VMA1/GCD11/SUP35/VMA13/GUA1	10
9	3	3	GO:0016836	hydro-lyase activity	03/43	32/5313	0.00208	0.035622	0.027644	ARO1/TRP5/CYS4	3
10	3	3	GO:0016835	carbon-oxygen lyase activity	03/43	35/5313	0.002699	0.041083	0.031882	ARO1/TRP5/CYS4	3
11	4	4	GO:0003735	structural constituent of ribosome	44/131	234/5313	2.22E-28	3.90E-26	3.24E-26	RPS2/RPS4B/RPS1B/RPS7B/RPP0/RPL17A/RPS6B/RPL20A/RPS1A/RPS18B/RPL7A/RPL11A/RPL2A/RPS12/RPS7A/RPS31/RPL33A/RPL14A/RPS17B/RPL3/RPL4A/RPL6A/RPS0B/RPL32/RPS14A/RPS3/RPL25/RPL22A/RPS22B/RPL21A/RPS13/RPS5/RPL9A/RPL23A/RPL10/RPS24A/RPS8B/RPS9A/RPL15A/RPL16B/RPS11A/RPL5/RPS20/RPS16A	44
12	4	4	GO:0005198	structural molecule activity	50/131	371/5313	1.99E-25	1.75E-23	1.45E-23	RPS2/RPS4B/RPS1B/ARC35/COP1/RPS7B/RPP0/RPL17A/RPS6B/RPL20A/RPS1A/SEC21/RPS18B/RPL7A/RPL11A/RPL2A/RPS12/RPS7A/RPS31/RPL33A/RPL14A/RPS17B/RPL3/RPL4A/RPL6A/RPS0B/RPL32/RPS14A/RPS3/TUB2/RPL25/RPL22A/RPS22B/TUB1/RPL21A/RPS13/RPS5/RPL9A/SEC27/RPL23A/RPL10/RPS24A/RPS8B/RPS9A/RPL15A/RPL16B/RPS11A/RPL5/RPS20/RPS16A	50

13	4	4	GO:0044183	protein binding involved in protein folding	7/131	13/5313	7.16E-09	4.20E-07	3.49E-07	TCP1/HSP60/CCT4/CCT7/CCT6/CCT8/CCT5	7
14	4	4	GO:0019843	rRNA binding	17/131	141/5313	4.35E-08	1.92E-06	1.59E-06	RPS2/RPS4B/RPP0/YEF3/RPS18B/RPL11A/RPL2A/RPS14A/RRP5/RPL25/RPS13/RPS5/RPL9A/RPL23A/RPS9A/RPS11A/RPL5	17
15	4	4	GO:0008135	translation factor activity, RNA binding	11/131	56/5313	7.79E-08	2.43E-06	2.02E-06	DED1/TEF2/TEF4/SUP45/YEF3/CDC33/RPG1/CAF20/PRT1/TIF1/NIP1	11
16	4	4	GO:0017111	nucleoside-triphosphatase activity	29/131	404/5313	9.39E-08	2.43E-06	2.02E-06	DED1/NEW1/TEF2/HSP60/VMA5/SUB2/RPT3/DBP2/SAR1/ARB1/GET3/OLA1/RVB1/YEF3/HSC82/ARF1/CDC48/RPT1/SSA2/TIF1/SSB2/SSC1/KAR2/ARL1/VMA2/PMA1/SEC4/TUB2/TUB1	29
17	4	4	GO:0051082	unfolded protein binding	13/131	84/5313	9.66E-08	2.43E-06	2.02E-06	TCP1/HSP60/CCT4/CCT7/CCT6/GET3/HSC82/SSA2/CCT8/SSB2/SSC1/KAR2/CCT5	13
18	4	4	GO:0016462	pyrophosphatase activity	29/131	425/5313	2.82E-07	4.97E-06	4.13E-06	DED1/NEW1/TEF2/HSP60/VMA5/SUB2/RPT3/DBP2/SAR1/ARB1/GET3/OLA1/RVB1/YEF3/HSC82/ARF1/CDC48/RPT1/SSA2/TIF1/SSB2/SSC1/KAR2/ARL1/VMA2/PMA1/SEC4/TUB2/TUB1	29
19	4	4	GO:0016817	hydrolase activity, acting on acid anhydrides	29/131	425/5313	2.82E-07	4.97E-06	4.13E-06	DED1/NEW1/TEF2/HSP60/VMA5/SUB2/RPT3/DBP2/SAR1/ARB1/GET3/OLA1/RVB1/YEF3/HSC82/ARF1/CDC48/RPT1/SSA2/TIF1/SSB2/SSC1/KAR2/ARL1/VMA2/PMA1/SEC4/TUB2/TUB1	29
20	4	4	GO:0016818	hydrolase activity, acting on acid anhydrides, in phosphorus-containing anhydrides	29/131	425/5313	2.82E-07	4.97E-06	4.13E-06	DED1/NEW1/TEF2/HSP60/VMA5/SUB2/RPT3/DBP2/SAR1/ARB1/GET3/OLA1/RVB1/YEF3/HSC82/ARF1/CDC48/RPT1/SSA2/TIF1/SSB2/SSC1/KAR2/ARL1/VMA2/PMA1/SEC4/TUB2/TUB1	29
21	4	4	GO:0016887	ATPase activity	22/131	294/5313	2.17E-06	3.48E-05	2.89E-05	DED1/NEW1/HSP60/VMA5/SUB2/RPT3/DBP2/ARB1/GET3/OLA1/RVB1/YEF3/HSC82/CDC48/RPT1/SSA2/TIF1/SSB2/SSC1/KAR2/VMA2/PMA1	22
22	4	4	GO:0003743	translation initiation factor activity	7/131	36/5313	2.17E-05	0.000318	0.000265	DED1/CDC33/RPG1/CAF20/PRT1/TIF1/NIP1	7
23	4	4	GO:0003729	mRNA binding	13/131	184/5313	0.000545	0.007382	0.006137	DED1/NEW1/GUS1/NOP56/RPG1/RPS14A/RRP5/PFK2/RPS5/NIP1/RPL16B/RPS20/RPB2	13
24	4	4	GO:0032549	ribonucleoside binding	9/131	103/5313	0.000905	0.011381	0.009461	TEF2/SAR1/OLA1/ARF1/ARL1/SEC4/TUB2/TUB1/RPB2	9
25	4	4	GO:0001882	nucleoside binding	9/131	104/5313	0.000971	0.011389	0.009468	TEF2/SAR1/OLA1/ARF1/ARL1/SEC4/TUB2/TUB1/RPB2	9

26	4	4	GO:0001883	purine nucleoside binding	8/131	100/5313	0.00306	0.026927	0.022385	TEF2/SAR1/OLA1/ARF1/ARL1/SEC4/TUB2/TUB1	8
27	4	4	GO:0005525	GTP binding	8/131	100/5313	0.00306	0.026927	0.022385	TEF2/SAR1/OLA1/ARF1/ARL1/SEC4/TUB2/TUB1	8
28	4	4	GO:0019001	guanyl nucleotide binding	8/131	100/5313	0.00306	0.026927	0.022385	TEF2/SAR1/OLA1/ARF1/ARL1/SEC4/TUB2/TUB1	8
29	4	4	GO:0032550	purine ribonucleoside binding	8/131	100/5313	0.00306	0.026927	0.022385	TEF2/SAR1/OLA1/ARF1/ARL1/SEC4/TUB2/TUB1	8
30	4	4	GO:0032561	guanyl ribonucleotide binding	8/131	100/5313	0.00306	0.026927	0.022385	TEF2/SAR1/OLA1/ARF1/ARL1/SEC4/TUB2/TUB1	8
31	4	4	GO:0003924	GTPase activity	7/131	80/5313	0.003359	0.028151	0.023403	TEF2/SAR1/ARF1/ARL1/SEC4/TUB2/TUB1	7
32	4	4	GO:0003746	translation elongation factor activity	3/131	15/5313	0.005365	0.042917	0.035679	TEF2/TEF4/YEF3	3

Appendix III - Table of Mass Spectrometry identified proteins of ribosome extract crosslinking

		XL 1	XL 2	XL 3	XL 4		No. XL1	No. XL2				
Identified Proteins	**Identified Proteins**	**EM A**	**EM B**	**EM C**	**EM D**	**XL**	**EM E**	**EM F**	**No. XL**	**XL/No .XL**	**Log2 XL/no.XL**	**Groups**
RPS27B	40S ribosomal protein S27 OS=Saccharomyces cerevisiae (strain YJM789) GN=RPS27B PE=3 SV=1	2	2	4	2	5		0.1	0.1	50.00	5.64	group 1
RPL30	Ribosomal 60S subunit protein L30 OS=Saccharomyces cerevisiae GN=RPL30 PE=4 SV=1	4	2	3		4.5		0.1	0.1	45.00	5.49	
RPS2	Ribosomal 40S subunit protein S2 OS=Saccharomyces cerevisiae GN=RPS2 PE=3 SV=1	5		4		4.5		0.1	0.1	45.00	5.49	
RPS24B	40S ribosomal protein S24 OS=Saccharomyces cerevisiae GN=RPS24B PE=3 SV=1	2		3		2.5		0.1	0.1	25.00	4.64	
NPL3	mRNA-binding protein OS=Saccharomyces cerevisiae GN=NPL3 PE=4 SV=1			2	3	2.5		0.1	0.1	25.00	4.64	
RPL27A	60S ribosomal protein L27 OS=Saccharomyces cerevisiae GN=RPL27A PE=3 SV=1	2		2		2		0.1	0.1	20.00	4.32	
RPL10	Ribosomal 60S subunit protein L10 OS=Saccharomyces cerevisiae GN=RPL10 PE=4 SV=1	2		2		2		0.1	0.1	20.00	4.32	
RPS13	Ribosomal 40S subunit protein S13 OS=Saccharomyces cerevisiae GN=RPS13 PE=3 SV=1	5	3	5		6.5		2	2	3.25	1.70	group 11
RPL1A	Ribosomal protein OS=Saccharomyces cerevisiae GN=RPL1A PE=3 SV=1	2	3	4		4.5		2	2	2.25	1.17	
RPL17B	Ribosomal 60S subunit protein L17B OS=Saccharomyces cerevisiae GN=RPL17B PE=3 SV=1	3	2	2		3.5		2	2	1.75	0.81	
RPS17B	Ribosomal 40S subunit protein S17B OS=Saccharomyces cerevisiae GN=RPS17B PE=3 SV=1	3	2	5		5		3	3	1.67	0.74	
RPL28	Ribosomal 60S subunit protein L28 OS=Saccharomyces cerevisiae GN=RPL28 PE=3 SV=1	3		3		3	2		2	1.50	0.58	group 111
RPS18B	Ribosomal 40S subunit protein S18B OS=Saccharomyces cerevisiae GN=RPS18B PE=3 SV=1	3	3	3		4.5		3	3	1.50	0.58	
RPS20	Ribosomal 40S subunit protein S20 OS=Saccharomyces cerevisiae GN=RPS20 PE=3 SV=1	2	2	2	2	4		3	3	1.33	0.42	
RPS1B	40S ribosomal protein S1 OS=Saccharomyces cerevisiae GN=RPS1B PE=3 SV=1	3	2	3		4		3	3	1.33	0.42	
NMD3	60S ribosomal export protein NMD3 OS=Saccharomyces cerevisiae GN=NMD3 PE=3 SV=1	3		8	2	6.5		5	5	1.30	0.38	
RPS1A	40S ribosomal protein S1 OS=Saccharomyces cerevisiae GN=RPS1A PE=3 SV=1	6	2	7		7.5		6	6	1.25	0.32	

STM1	Protein required for optimal translation under nutrient stress OS=Saccharomyces cerevisiae GN=STM1 PE=4 SV=1		2	3		2.5		2	2	1.25	0.32	
RPL20B	60S ribosomal protein L20 OS=Saccharomyces cerevisiae GN=RPL20B PE=3 SV=1	5	2			3.5	3		3	1.17	0.22	
RPL7A	Ribosomal 60S subunit protein L7A OS=Saccharomyces cerevisiae GN=RPL7A PE=4 SV=1	4		5		4.5		4	4	1.13	0.17	
RPL8B	Ribosomal protein L8B OS=Saccharomyces cerevisiae (strain RM11-1a) GN=SCRG_04947 PE=4 SV=1	6	2	9	2	9.5	2	7	9	1.06	0.08	
RPS3	Ribosomal 40S subunit protein S3 OS=Saccharomyces cerevisiae GN=RPS3 PE=3 SV=1	4	8	9		10.5		10	10	1.05	0.07	
RPL14B	Ribosomal 60S subunit protein L14B OS=Saccharomyces cerevisiae GN=RPL14B PE=4 SV=1	3		3		3		3	3	1.00	0.00	
RPL13A	60S ribosomal protein L13 OS=Saccharomyces cerevisiae GN=RPL13A PE=3 SV=1	2		4		3		3	3	1.00	0.00	
RPS5	Ribosomal 40S subunit protein S5 OS=Saccharomyces cerevisiae GN=RPS5 PE=1 SV=1	3	4	5	2	7	2	5	7	1.00	0.00	
RPS6A	40S ribosomal protein S6 OS=Saccharomyces cerevisiae GN=RPS6A PE=3 SV=1	5		3		4	4		4	1.00	0.00	
ADH1	Alcohol dehydrogenase OS=Saccharomyces cerevisiae (strain YJM789) GN=ADH1 PE=3 SV=1	2		4		3		3	3	1.00	0.00	
DBP2	DEAD-box ATP-dependent RNA helicase OS=Saccharomyces cerevisiae GN=DBP2 PE=3 SV=1	2	3	13		9		9	9	1.00	0.00	
TEF1	Elongation factor 1-alpha OS=Saccharomyces cerevisiae GN=TEF1 PE=3 SV=1	4	8	8	3	11.5	3	9	12	0.96	-0.06	group 1V
RPL4A	Ribosomal 60S subunit protein L4A OS=Saccharomyces cerevisiae GN=RPL4A PE=4 SV=1	8	5	10	2	12.5	4	10	14	0.89	-0.16	
RPS9A	Ribosomal 40S subunit protein S9A OS=Saccharomyces cerevisiae GN=RPS9A PE=4 SV=1	3		4		3.5		4	4	0.88	-0.19	
SSB2	Hsp70 family ATPase OS=Saccharomyces cerevisiae GN=SSB2 PE=3 SV=1	7	14	18	17	28	4	29	33	0.85	-0.24	
YMR051C	Conserved protein OS=Saccharomyces cerevisiae (strain YJM789) GN=SCY_0938 PE=4 SV=1	2	2	4		4		5	5	0.80	-0.32	
RPL6B	60S ribosomal protein L6 OS=Saccharomyces cerevisiae GN=RPL6B PE=3 SV=1	4	2	3		4.5	2	4	6	0.75	-0.42	
RPS0B	40S ribosomal protein S0 OS=Saccharomyces cerevisiae GN=RPS0B PE=3 SV=1	2	3	5	3	6.5	3	6	9	0.72	-0.47	
RPP0	60S acidic ribosomal protein P0 OS=Saccharomyces cerevisiae GN=RPP0 PE=3 SV=1			3	2	2.5		4	4	0.63	-0.68	
ASC1	Guanine nucleotide-binding protein subunit beta OS=Saccharomyces cerevisiae GN=ASC1 PE=4 SV=1	3	4	9		8		13	13	0.62	-0.70	
SSZ1	Ssz1p OS=Saccharomyces cerevisiae (strain CEN.PK113-7D) GN=CENPK1137D_5206 PE=3 SV=1		8	8	8	12		20	20	0.60	-0.74	

SSA2	Hsp70 family chaperone OS=Saccharomyces cerevisiae GN=SSA2 PE=3 SV=1		2		4	3		5	5	0.60	-0.74	
RPL3	Ribosomal 60S subunit protein L3 OS=Saccharomyces cerevisiae GN=RPL3 PE=3 SV=1	11		8		9.5	8	8	16	0.59	-0.75	
GCD11	Translation initiation factor eIF2 subunit gamma OS=Saccharomyces cerevisiae GN=GCD11 PE=4 SV=1	2	4	6	2	7		12	12	0.58	-0.78	
UTP15	SnoRNA-binding rRNA-processing protein OS=Saccharomyces cerevisiae GN=UTP15 PE=4 SV=1		2	7		4.5		8	8	0.56	-0.83	
RPL23B	Ribosomal 60S subunit protein L23B OS=Saccharomyces cerevisiae GN=RPL23B PE=3 SV=1	2		2		2		4	4	0.50	-1.00	
RPS8B	40S ribosomal protein S8 OS=Saccharomyces cerevisiae GN=RPS8B PE=3 SV=1	3		2		2.5	5		5	0.50	-1.00	
RPL15B	Ribosomal protein L15 OS=Saccharomyces cerevisiae GN=RPL15B PE=3 SV=1	4		2		3	3	4	7	0.43	-1.22	
RPL12A	Ribosomal 60S subunit protein L12A OS=Saccharomyces cerevisiae GN=RPL12A PE=3 SV=1			2	2	2		5	5	0.40	-1.32	
ZUO1	Zuotin OS=Saccharomyces cerevisiae GN=ZUO1 PE=4 SV=1	2	2	6	2	6	2	13	15	0.40	-1.32	
PDC1	Indolepyruvate decarboxylase 1 OS=Saccharomyces cerevisiae GN=PDC1 PE=3 SV=1			5	2	3.5		9	9	0.39	-1.36	
NOP56	U3 snoRNP protein OS=Saccharomyces cerevisiae (strain YJM789) GN=SIK1 PE=4 SV=1	3	3	4		5	2	11	13	0.38	-1.38	
NOP58	RNA-processing protein OS=Saccharomyces cerevisiae GN=NOP58 PE=4 SV=1	4		4		4	4	8	12	0.33	-1.58	
CDC19	Pyruvate kinase OS=Saccharomyces cerevisiae GN=CDC19 PE=3 SV=1			10	3	6.5		21	21	0.31	-1.69	

	Cluster	Group	ID	Description	GeneRatio	BgRatio	pvalue	p.adjust	qvalue	geneID	Count
1	1, 2, 3	1, 2, 3	GO:0003735	structural constituent of ribosome	21/25	234/5313	1.48E-25	4.45E-24	4.06E-24	RPS27B/RPS2/RPS24B/RPL27A/RPL10/RPS13/RPL1A/RPL17B/RPS17B/RPL28/RPS18B/RPS20/RPS1A/RPL20B/RPL7A/RPL8B/RPS3/RPL14B/RPL13A/RPS5/RPS6A	21
2	1, 2, 3	1, 2, 3	GO:0005198	structural molecule activity	21/25	371/5313	3.02E-21	4.53E-20	4.13E-20	RPS27B/RPS2/RPS24B/RPL27A/RPL10/RPS13/RPL1A/RPL17B/RPS17B/RPL28/RPS18B/RPS20/RPS1A/RPL20B/RPL7A/RPL8B/RPS3/RPL14B/RPL13A/RPS5/RPS6A	21
3	1	1, 2, 3	GO:0019843	rRNA binding	4/25	141/5313	0.003896	0.038964	0.035546	RPS2/RPS13/RPS18B/RPS5	4
4	4	4	GO:0003735	structural constituent of ribosome	10/20	234/5313	2.85E-09	1.20E-07	1.08E-07	RPL4A/RPS9A/RPL6B/RPS0B/RPP0/RPL3/RPL23B/RPS8B/RPL15B/RPL12A	10
5	4	4	GO:0005198	structural molecule activity	10/20	371/5313	2.40E-07	5.04E-06	4.55E-06	RPL4A/RPS9A/RPL6B/RPS0B/RPP0/RPL3/RPL23B/RPS8B/RPL15B/RPL12A	10
6	4	4	GO:0030515	snoRNA binding	3/20	26/5313	0.000112	0.001572	0.001418	UTP15/NOP56/NOP58	3
7	4	4	GO:0019843	rRNA binding	4/20	141/5313	0.001654	0.017367	0.015669	RPS9A/RPP0/RPL23B/RPL12A	4
8	4	4	GO:0051082	unfolded protein binding	3/20	84/5313	0.003579	0.030065	0.027126	SSB2/SSZ1/ZUO1	3